PREDICTING PRESSURE LOSSES IN STRAIGHT-THROUGH DIAPHRAGM VALVES

BAUDOUIN MULUMBA MBIYA

Cape Peninsula
University of Technology

PREDICTING PRESSURE LOSSES IN STRAIGHT-THROUGH DIAPHRAGM VALVES

by

BAUDOUIN MULUMBA MBIYA

Dissertation submitted in fulfilment of the requirements for the degree

DOCTOR TECHNOLOGIAE: Civil Engineering

in the

FACULTY OF ENGINEERING

at the

CAPE PENINSULA UNIVERSITY OF TECHNOLOGY

Supervisor: Dr V. G. Fester
Co-supervisor: Prof P. Slatter

Cape Town
December 2007

Errata

Thesis: predicting Pressure losses in straight-through diaphragm valves

Author: Baudouin Mbiya

The author would like to apologise for some mistakes which made their way to the final copy of the dissertation.

The following mistake must be corrected.

The diameter in Equation 5.30 and 5.31 must be in [dm] instead of [mm] this occurs on pages: 5.40; 5.41; 6.1and 7.4

Figure 5.25 is shown below; note also the change of the unit on the abscissa [dm] instead of mm.

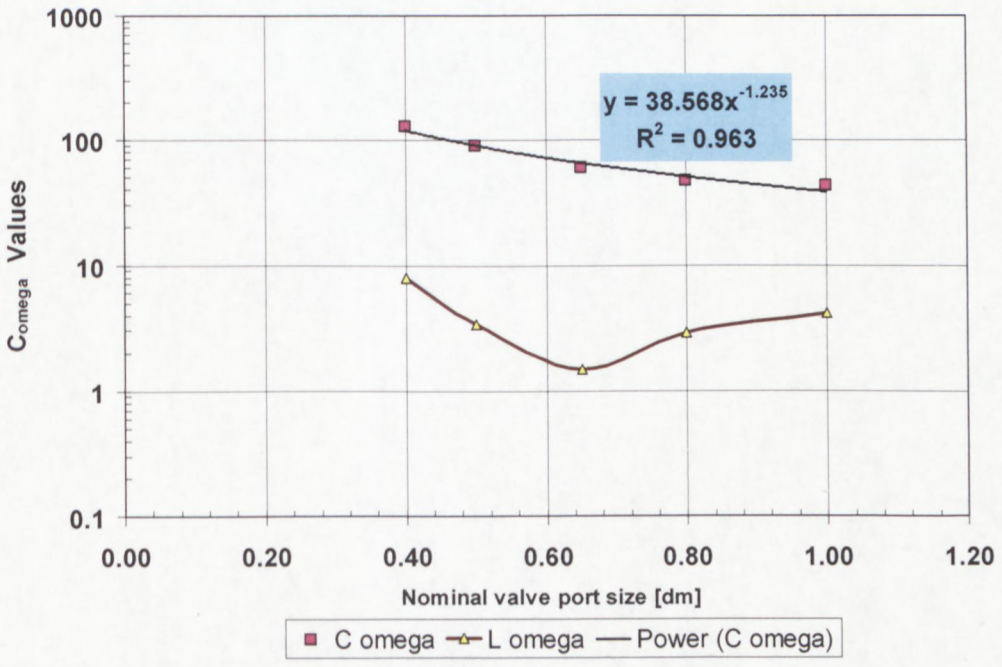

Figure 5.25 : Valve size effect on C_Ω (C omega) and λ_Ω (L omega)

DECLARATION

I, Baudouin Mulumba Mbiya, declare that the contents of this dissertation represent my own unaided work, and that the dissertation has not previously been submitted for academic examination towards any qualification. Furthermore, it represents my own opinions and not necessarily those of the Cape Peninsula University of Technology.

28 MAY 2008

Signed **Date**

PREDICTING PRESSURE LOSSES FOR STRAIGHT-TROUGH DIAPHRAGM VALVES

Baudouin Mbiya
Cape Peninsula University of Technology / Department of Civil Engineering Cape Town Campus PO box 652 Cape Town 8000, South Africa
November, 2007

Abstract

The diaphragm valve traces its origins to ancient Roman and Greek times, where it was used to control water flow and temperature of hot baths (Century-Instruments, 2007). The particularity of this type of valve is the presence of a diaphragm or membrane which controls the flow. Over the years, the design of this type of valve has evolved into two major varieties. The first is the "weir" type, more suitable for less viscous fluids and a second is the "straight-through" type, suitable for suspensions. This study is focused on the straight-through.

With the widespread use of such valves in the mining and mineral processing operations and other industrial applications, although there has been improvement in the selection of the diaphragms and body materials of the valves, as well as actuation methods, improvements were not accompanied by thorough hydraulic investigation to determine the method of calculating the additional head loss caused by the presence of diaphragm valves in pipelines, and in particular for the laminar flow of non-Newtonian fluids. The limited correlations available, such as Hooper's (1981), Perry's (1997) and Miller's (1990) are valid only for Newtonian fluids. Furthermore they are classified as Class 3 (Miller, 1990) which means they are not corroborated in other independent studies.

The aim of this study was to investigate a selection of straight-through diaphragm valves to find correlations which might predict pressure losses. The investigation was a macroscopic approach consisting in the measurement of pressure drop and flow rates.

Experimental data was obtained from a test rig especially built for this study. Five (nominal bore: 40, 50, 65, 80 and 100 mm) straight-through valves obtained from a South African distributor (Natco) were mounted horizontally and tested in the fully, ¾, ½, and ¼ opened positions respectively. These positions were determined using a gravity test. An inspection of the internal sizes revealed the lack of geometrical similarity between valves, which makes a major barrier to obtaining simpler correlation valid for all the valves sizes.

Newtonian fluids: water, glycerol solutions at 99% and 75% (volume / volume) and non-Newtonian fluids: Carboxymethylcellulose (CMC) at 5% and 8% (weight / weight) and kaolin slurries of 10% and 13% (volume / volume) were tested. The Reynolds number range tested was between 0.1 and 140 000.

The contribution and uniqueness of this study is two-fold. Firstly the database of Newtonian and non-Newtonian pressure loss coefficient produced, which might be useful to design engineers and software developers. Secondly, a new predictive correlation for the pressure loss coefficient, named "the two-constant model" was developed after a careful analysis of different correlation schemes.

The comparison between the two-constant model and the few existing models demonstrated that the new model performed well in the respective ranges of applicability and would be useful in practice.

ACKNOWLEDGEMENTS

I wish to thank:

- Dr Veruscha Fester, my supervisor, for her guidance, encouragement, moral support and for having seen my potential.
- Prof Paul Slatter, for his vision and leadership of the Flow Process Research Centre.
- The FPRC staff and students who participated in the experimental programme of this study.
- The Cape Peninsula University of Technology for financial assistance and for giving me an opportunity to complete this degree.
- My family, friends and colleagues in the Foundation Programme, for their love, patience and unstinting support.

The financial assistance of the National Research Foundation towards this research is acknowledged. Opinions expressed in this thesis and the conclusions arrived at, are those of the author, and are not necessarily to be attributed to the National Research Foundation.

DEDICATION

To

Dr Mbula Mamie,

Emmanuel and Andrea

"Your birth is evidence that your purpose is necessary" Dr Myles E Munroe

TABLE OF CONTENTS

CHAPTER 1

CHAPTER 1

INTRODUCTION

1.1 INTRODUCTION

Piping systems in industry consist of straight pipe sections and fittings such as valves, bends, reducers, etc. to regulate flow, change direction and flow velocity. The estimation of pumping pressures normally takes account of geometric heights and frictional losses in straight pipes and fittings. When geometric and flow parameters are known, the selection of loss coefficients is vital. Loss coefficients, therefore, play an important role in practical design (Miller, 1990). The lack of loss coefficient data for non-Newtonian fluids through pipe fittings needs to be addressed.

This study was focused on the determination of pressure losses in straight-through diaphragm valves operating mainly in laminar flow.

The diaphragm valve is commonly used for slurry service because of its features which isolate the fluid from the valve operating mechanism, thus minimising contamination, tear and erosion of the operating mechanism. This type of valve is found in many industrial applications - pharmaceutical, chemical, breweries, dairy, food, petroleum, mining, etc. (Warring, 1982). Moreover, it presents several advantages such as: An

ability to handle solids, a low resistance coefficient; no dead areas where particles may collect, easy maintenance, not requiring the removal of its body from a pipeline, can be used for throttling and is adaptive to automation (Miles, 2000).

Because of water restrictions in many parts of the world and South Africa in particular, the new water law (South Africa, 1998) compels many industries to consider operating mixtures at higher concentrations. This, in turn, is likely to induce laminar flow. The high consistency of most non-Newtonian fluids means that laminar flow occurs more frequently for these mixtures than for Newtonian materials (Skelland, 1967). It is also demonstrated laminar flow can actually offer an economical operating condition (Slatter, 2002).

Although diaphragm valves are in operation throughout industry, there is insufficient loss coefficient data available to predict their pressure losses (Kittredge & Rowley, 1957; Jacobs, 1993; Spence & Nash, 2004). Efficient designs, using, for example, correctly sized pumps, are possible only if reliable loss coefficient data is available. There is limited loss coefficient data available for the prediction of pressure losses in diaphragm valves for Newtonian fluids; and even less for non-Newtonian fluids (Fester, Kazadi, Mbiya and Slatter, 2007).

1.2 STATEMENT OF THE RESEARCH PROBLEM

Most classical books on fluids mechanics or a technical manual, such as Crane (1999), do not provide values or formulae to calculate the loss coefficient inherent to straight-through diaphragm valves. The problem, therefore, is that there is insufficient experimental data and correlations predicting loss coefficients for straight-through diaphragm valves - especially when conveying fluids in the laminar regime.

1.3 OBJECTIVES

The objectives of this study were:

- To design, build and commission an experimental rig to test valves;
- to generate a data base of loss coefficients for straight-through diaphragm valves using both Newtonian and non–Newtonian fluids, with an emphasis on laminar flow and,
- to analyse experimental data in order to produce correlations able to predict loss coefficient values in straight-through diaphragm valves.

1.4 METHODOLOGY

The following steps were undertaken in order to achieve the objectives:

1.4.1 Literature Survey

A comprehensive literature review was conducted regarding issues pertaining to the determination of loss coefficients in valves in general and for straight-through diaphragm valves in particular. Diaphragm valve loss coefficients data available in open literature was reviewed, the works of Hooper (1981), ESDU (2004) and Miller (1990) were found relevant.

1.4.2 Experimental Work

The experimental work was carried out in the FPRC laboratory at CPUT on the "valve test rig" designed and constructed for valve tests.

The rig consists of 6 × 25 m long pipes containing a diaphragm valve in the centre of each pipe. Newtonian and non-Newtonian fluids were tested in four different valves opening positions in order to generate experimental loss coefficients.

1.4.3 Dimensional Analysis

Classical dimensional analysis technique was used to find a functional relationship between loss coefficient and pertinent variables.

1.4.4 Data Analysis

The data generated in the experimental work was scrutinised to retain only the valid data based on pipe friction factors upstream and downstream of the valve.

Classical loss coefficient constants and turbulent loss coefficients were calculated. More elaborate correlations were derived by applying a multiple linear regression analysis and juxtaposition of ranges.

1.5 SCOPE

This study was limited to measuring the loss coefficients of five straight-through diaphragm valves ranging from 40 mm to 100 mm nominal bore. This research was conducted mainly in laminar flow; turbulent data was obtained only with water.

1.6 BENEFITS AND CONTRIBUTIONS

A primary engineering objective is to design and operate at minimum cost, with acceptable safety margins. This work provides the system designer with more accurate experimental data and correlations to predict pressure losses in straight-through diaphragm valves. The results of this study constitute an addition to a relatively small body of information available about straight-through diaphragm valves.

CHAPTER 2

CHAPTER 2

THEORY AND LITERATURE REVIEW

2.1 INTRODUCTION

This study is concerned with pressure losses occurring through diaphragm valves conveying viscous fluids. In this chapter the theory and literature review pertaining to this study is presented.

As diaphragm valves could form an integrated part of pipeline design, the generalities of this chapter comprise fundamental equations of pipe flow, concept of pressure and pressure losses and flow through straight pipes for Newtonian fluids and non-Newtonian fluids, followed by the mechanism of head losses through fittings.

Because of a prevalence of the viscous character of fluids in laminar flow, the rheology of the fluids conveyed is explained and the formulations of Reynolds numbers used in this study, presented.

A summary of the work done on the prediction of pressure drop for industrial diaphragm valves is presented. This chapter ends with the pertinent research topics identified.

2.2 FUNDAMENTAL EQUATIONS OF FLUID FLOW

The fundamental equations governing the mechanics of fluids and solid bodies alike are derived from the principles of conservation as follows:

2.2.1 Conservation of Mass

This principle states that in an isolated system there is never any change (conservation) in the total mass of the system, or otherwise said, the mass flow rate entering a system is equal to the mass rate of storage in that system, plus the mass flow rate leaving the system, this is described in several texts e.g. (Murdock, 1976).

Application of this principle to pipe flow, between two sections (1 and 2), liquids being practically incompressible, i.e. ($\rho_1=\rho_2$) e.g. (Massey, 1975) and if there is no leak between the two sections, gives Equation 2.1 which is known as the continuity equation.

$$A_1V_1 = A_2V_2 = Q \qquad \text{Eq 2.1}$$

This equation is used to calculate the flow velocity by measuring the volumetric flow rate and the pipe internal diameter.

2.2.2 Conservation of Momentum

There is conservation of the total momentum in an isolated system. This is a statement of Newton's Second Law which says: "The rate of change of linear momentum of a body is proportional to the force applied and takes place in the direction of action of that force" this is described in numerous texts e.g. (Douglas *et al.*, 2000) or otherwise said, on a control volume, the change in momentum

is equal to the sum of the impulses of the external forces on the control volume. For an incompressible fluid, assuming a flat velocity profile, the equation is:

$$\rho A_2 V_2^2 - \rho A_1 V^2{}_1 = P_2 A_2 - P_1 A_1 + F_f + F_g \qquad \text{Eq 2.2}$$

Where F_f= friction force and

F_g= gravity force.

2.2.3 Conservation of Energy

This principle says that there is a conservation of total energy in an isolated system. Thus the basic requirement for the satisfaction of this principle may be otherwise stated as: the sum of energy entering a system must be equal to the sum of energy stored and /or work done in the system plus the sum of energy leaving the system e.g. (Murdock, 1976). For ideal flow this principle is known as the Bernoulli Equation or the mechanical energy balance equation. It details the relationship between the velocity, the location and the pressure of fluid particles along a streamline. It should be emphasised that the equation is valid for a steady flow, of incompressible and inviscid fluids. In real fluids, however, there is always a loss of energy due to friction, therefore formulating this equation between two points 1 and 2 and assuming flat velocity profiles gives the results:

$$\frac{P_1}{\rho g} + \frac{V_1^2}{2g} + Z_1 = \frac{P_2}{\rho g} + \frac{V_2^2}{2g} + Z_2 + \text{loss}_{1-2} \qquad \text{Eq 2.3}$$

Where Z is the elevation and $\text{loss}_{1\text{-}2}$ is the sum of losses between sections 1 and 2. Each term in Equation 2.3 represents energy per unit weight, the unit of each term is thus (J/N)

or in metre of fluid (m). This forms the basis for determining the losses through pipe fittings, or diaphragm valves as is the specific aim of this study.

The assumption of flat or uniform velocity profile as portrayed in a stream line is not always valid for real fluid passages. A correction factor α can be applied to the kinetic energy term ($V^2/2g$) in Equation 2.3 to account for the velocity profile. This correction factor is given, for fluids of constant density, by the formula e.g. (Massey, 1975):

$$\alpha = \frac{1}{A}\int_0^A \left(\frac{u}{V}\right)^3 dA \qquad \text{Eq 2. 4}$$

Where u is the velocity profile and V the average velocity in the passage of cross sectional area A. Values of α range from 2 for fully developed laminar pipe flow to nearly unity for turbulent flow. Detailed values of α for viscoplastic fluids pipe laminar flow have been reported by the author (Baudouin *et al.*, 2004)

2.3 CONCEPT OF PRESSURE AND PRESSURE LOSSES

Since pressure is a vital characteristic of a flow field, it is important to have a clear distinction between its different formulations. The atmospheric pressure is the weight per unit area of the air above a reference datum and varies with weather conditions. It has been fixed by international agreement to a value of 101 325 Pa e.g. (Young *et al.*, 1997). Most pressure sensing devices indicate a differential pressure between the absolute pressure and the atmospheric pressure.

When a fluid is in motion, besides kinetic and potential energy, it also possesses pressure. In addition to static pressure, there is also velocity pressure ($\rho V^2/2$). Care must be taken

to account for this pressure when evaluating the total head with Bernoulli Equation. In this regard, the total pressure is synonymous with total head. That explains the terminology: Pressure losses through valves or fitting, this is another way of implying the head loss (Massey, 1975).

2.4 FLOW THROUGH STRAIGHT PIPES

2.4.1 Introduction

It is important to understand flow through straight pipes before considering flow through fittings and valves. Consider a fluid flowing through a pipe of constant diameter, the flow being fully developed and steady[1]. The flow may be laminar or turbulent depending on the value of the Reynolds number. These two types of flow are fundamentally different in several aspects, such as the velocity distribution, and the flow resistance e.g. (Massey, 1975). As shown in the next section, however, the shear distribution presents the same pattern regardless of the flow regime or the viscous nature of the flow.

2.4.2 Shear Stress Distribution in a Pipe

The shear stress distribution can be found by considering a coaxial cylindrical element of length L and radius r in a pipe of radius R over which a pressure difference ΔP exists as shown in Figure 2.1 e.g. (Slatter, 1994). Fluids being practically incompressible e.g.

[1] If the fluid is not full in the pipe, then the flow is treated as an open channel.

(Streeter & Willie, 1975), it can be demonstrated from the forces balance that in a pipe, the shear stress follows a linear law given by Equation 2.5 when the flow is fully developed and steady.

$$\tau = \frac{r}{2}\frac{\Delta P}{L} \qquad \text{Eq 2.5}$$

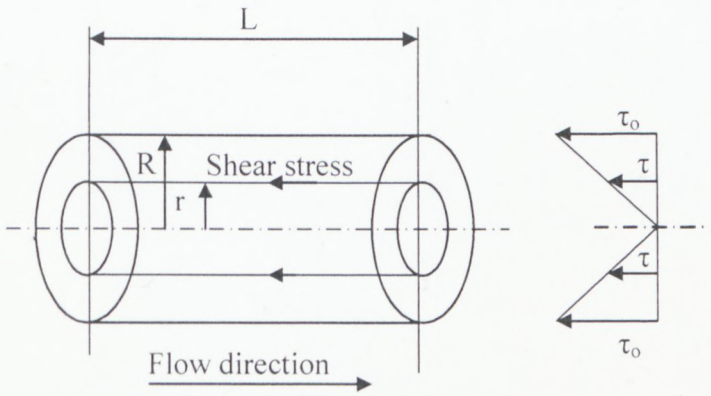

Figure 2.1: Shear stress distribution in a pipe (Slatter, 1994)

The shear stress is zero at the pipe centre and attains the maximum value τ_0 at the pipe wall given by:

$$\tau_o = \frac{D\,\Delta P}{4L} \qquad \text{Eq 2.6}$$

Combining Equations 2.5 and 2.6 yields:

$$\tau = \frac{r}{R}\tau_O \qquad 2.7$$

It should be noted these fundamental relationships are based only on a force balance and the assumption that the fluid is homogeneous, regardless of the viscous nature of the fluids and the type of flow regime e.g. (Chhabra and Richardson, 1999).

2.4.3 Criterion for Transition

Laminar and turbulent flows are widely different in nature and effect. It is of prime importance to know the conditions under which each may be expected. The Reynolds number of flow is widely used as a criterion of transition. It was shown experimentally that with commercial pipes the transition from laminar to turbulent flow occurs at about

Re = 2000 to Re = 4000 e.g. (Finnemore & Franzini, 2002). When predicting the critical velocity, the transitional Reynolds number is often taken as Re = 2100. For fittings, including valves, many researchers such as Beck (1944), Kittredge and Rowley (1957), Jadallah (1980) and Pienaar (1998), have shown transition from viscous flow to turbulent flow appears at much lower Reynolds numbers than in pipe flow, between Reynolds numbers of 30 and 500, depending on the fitting.

2.4.4 Laminar Flow of Newtonian Fluids

In laminar pipe flow of Newtonian fluids, the stress (τ) arising from the shearing of fluid layers is related to the velocity gradient (du/dr) by Equation 2.8 e.g. (Massey, 1975):

$$\tau = \mu\left(-\frac{du}{dr}\right) \qquad \text{Eq 2.8}$$

Where the viscosity (μ) is a fluid property.

The effect of the viscosity is to reduce the velocity of different layers. The maximum velocity is attained at the pipe centre, decreasing gradually toward the pipe wall where it reaches zero.

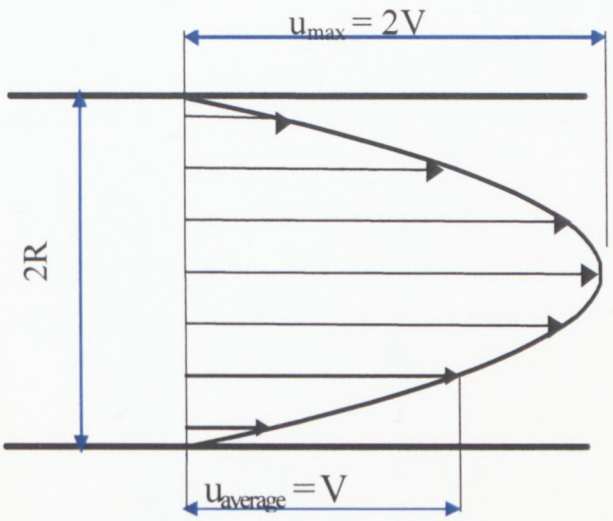

Figure 2.2: Newtonian laminar flow

The velocity distribution follows a parabolic law given by the expression

$$u = u_{max}\left(1 - \frac{r^2}{R^2}\right) \qquad \text{Eq 2.9}$$

where u_{max} is the maximum velocity at the centre of the pipe. The average flow velocity is exactly half the maximum velocity at the pipe centre as portrayed in Figure 2.2. The difference in velocity between layers generates a shear stress, which tends to oppose the relative motion e.g. (Massey, 1975).

The resistance to flow in laminar flow is characterised by the pressure drop being proportional to the first power of the velocity. The discharge through a pipe section of diameter D and length L, where a pressure difference, ΔP exists is, given by Equation 2.10 e.g. (Massey, 1975).

$$Q = \frac{\pi D^4}{128\mu}\frac{\Delta P}{L} \qquad \text{Eq 2.10}$$

This expression is known as the Hagen-Poiseuille Equation.

2.4.5 Laminar Flow of Non-Newtonian Fluids

Laminar flow of non-Newtonian fluids is characterised by the fact that the relationship of the shear stress arising from the friction between layers is not a linear curve starting at zero, as for Newtonian fluids. The relationship between the shear stress and shear rate is more complex and to be described requires more than one parameter. As fluids exhibiting yield stresses will be also tested, the generalised Bingham plastic model, well known as the Herschel-Bulkley Fluids Model, will be considered as a general model to characterise laminar flow.

2.4.5.1 General Approach

The starting point is the constitutive equation, which represents a general rheogram for time-independent fluids:

$$-\frac{du}{dr} = f(\tau) \qquad \text{Eq 2.11}$$

The velocity distribution is obtained by integrating the above equation as follows:

$$du = -f(\tau)dr \qquad \text{Eq 2.12}$$

$$u = \int -f(\tau)dr + C \qquad \text{Eq 2.13}$$

The constant of integration is evaluated using the first boundary condition of no slip at pipe wall.

The flow rate Equation 2.14 can be obtained by integrating the velocity profile over the cross section with respect to the usual boundary conditions for pipe flow:

1. At $r = R$ $u = 0$, (no slip at the wall pipe).
2. At $r = 0$ $du/dr = 0$, the slope of the velocity distribution is zero at the pipe centre line.

$$Q = 2\pi \int_0^R urdr \qquad \text{Eq 2.14}$$

$$Q = \pi \left[ur^2 - \int r^2 \frac{du}{dr} dr \right]_0^R = -\pi \int_0^R r^2 \frac{du}{dr} dr \qquad \text{Eq 2.15}$$

From the force balance over a cylindrical control volume (Figure 2.1) we have:

$$\frac{r}{R} = \frac{\tau}{\tau_o} \qquad \text{Eq 2.16}$$

$$dr = \left(\frac{R}{\tau_o} \right) d\tau \qquad \text{Eq 2.17}$$

$$r^2 = \frac{\tau^2}{\tau_o^2} R^2 \qquad \text{Eq 2.18}$$

Substituting Equations (2.11, 2.17 and 2.18) in Equation 2.15 yields

$$Q = \frac{\pi R^3}{\tau_0^3} \int_0^{\tau_0} \tau^2 f(\tau) d\tau \qquad \text{Eq 2.19}$$

Replacing (R) with (D/2) and (Q) with (VA), one obtains:

$$\frac{32Q}{\pi D^3} = \frac{8V}{D} = \frac{4}{\tau_0^3}\int_0^{\tau_0} \tau^2 f(\tau)d\tau \qquad \text{Eq 2. 20}$$

Equation 2.20 is of fundamental importance e.g. (Chhabra & Richardson, 1999):

- It shows that, in general, the pseudo shear rate (8V/D) is a unique function of the rheogram $f(\tau)$ and the wall shear stress τ_o, provided that there is no time dependency or slip at the wall and the flow is laminar;
- It shows that the relationship between (8V/D) and (τ_o) can be obtained by direct numeric integration using data directly from a rheometer, without using a conventional rheological model.
- Since (8V/D) is a unique function of the rheogram $f(\tau)$ and the wall shear stress (τ_o), it is independent of pipe diameter and can be used for scale-up and design in laminar flow.

2.4.5.2 The Rabinowitsch-Mooney Relation

It can be shown e.g. (Lazarus & Slatter, 1988) that the Rabinowitsch-Mooney relation can be obtained directly by differentiating Equation 2.20 with respect to τ_o and the final form is

$$\left[-\frac{du}{dr}\right]_o = \frac{8V}{D}\left[\frac{3n'+1}{4n'}\right] \qquad \text{Eq 2.21}$$

$$\text{where } n' = \frac{d(\text{Log}\tau_o)}{d\left(\text{Log}\dfrac{8V}{D}\right)} \qquad \text{Eq 2.22}$$

Equation 2.21 relates the nominal or pseudo-shear rate (8V/D) to the true shear rate at the pipe wall ($\dot{\gamma}_0$). This is useful in the rheological characterisation, as it allows converting a pseudo-shear diagram to a true rheogram.

2.4.5.3 The Herschel-Bulkley Fluid Model

The constitutive equation of this model is:

$$\tau = \tau_y + K\left(-\frac{du}{dr}\right)^n \qquad \text{Eq 2. 23}$$

Where K is the fluid consistency index

n is the flow behaviour index.

τ_y is the yield stress.

The shear stress distribution in laminar flow for such a fluid is depicted in Figure 2.3. The flow presents two zones, the core zone where the fluid is unsheared and moves as a solid plug and the annulus zone, where the fluid in sheared. Any integration over the cross section should be undertaken in two parts.

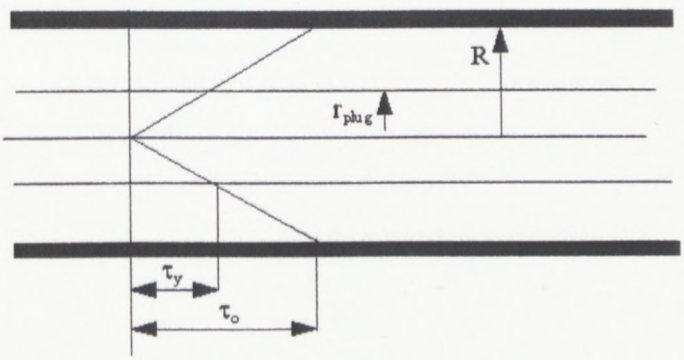

Figure 2.3: Shear stress distribution for non-Newtonian fluid (Herschel-Bulkley fluid model)

The equation for laminar pipe flow is derived by applying the general approach e.g. (Govier & Aziz, 1972).

The velocity distribution can be obtained by integrating the constitutive equation.

For $0 < r < r_{plug}$ the fluid moves as a plug at a uniform plug velocity u_{plug}

$$u_{plug} = \frac{R}{K^{1/n}\tau_0}\frac{n}{n+1}\left[\left(\tau_o - \tau_y\right)^{\frac{n+1}{n}}\right] \qquad \text{Eq 2.24}$$

and for $r > r_{plug}$ the point velocity in the annulus is given by:

$$u = \frac{R}{K^{1/n}\tau_0}\frac{n}{n+1}\left[\left(\tau_o - \tau_y\right)^{\frac{n+1}{n}} - \left(\tau - \tau_y\right)^{\frac{n+1}{n}}\right] \qquad \text{Eq 2. 25}$$

The volumetric discharge and the nominal shear rate are obtained by applying Equation 2.23 into Equation 2.20 and the result is:

$$\frac{32Q}{\pi D^3} = \frac{8V}{D} = \frac{4n}{K^{1/n}\tau^3{}_0}\left(\tau_o - \tau_y\right)^{\frac{n+1}{n}}\left[\frac{\left(\tau_o - \tau_y\right)^2}{1+3n} + \frac{2\tau_y\left(\tau_o - \tau_y\right)}{1+2n} + \frac{\tau_y^2}{1+n}\right] \qquad \text{Eq 2.26}$$

2.4.6 Turbulent flow

Turbulent flow is flow, in which the particles of fluids move in a disorderly manner, occupying different relative position in successive cross-sections. In turbulent flow, the fluid particles move in irregular paths, causing an exchange of momentum from one portion of fluid to another e.g. (Streeter &Wylie, 1975). The paths of individual particles

of fluids are no longer straight, but are random, intertwining and crossing one another in a disorderly manner so that thorough mixing of fluids occurs.

Turbulent flow is complex; an exact mathematical analysis is not yet possible, and there is a need for an empirical approach using information obtainable only from experiments.

In practice the average velocity and pressure over a reasonable time interval remain constant so that the flow can be termed "steady" as shown in Figure 2.4 and the characteristic velocity profile is based on the temporal mean velocity (Streeter &Wylie, 1975).

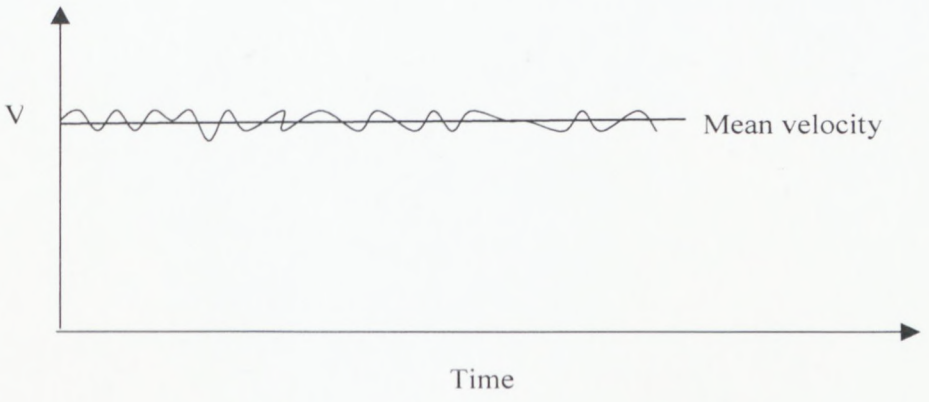

Figure 2.4: Mean velocity in turbulent flow

The velocity distribution for turbulent flow follows a logarithmic law given in Equation 2.27 and shown in Figure 2.5 e.g. (Finnemore & Franzini, 2002):

$$\frac{u_{max} - u}{\sqrt{\left(\frac{\tau_o}{\rho}\right)}} = 5.75 \log \frac{y}{R} \qquad \text{Eq 2.27}$$

Where u is the point velocity and y the distance from the pipe wall and reaches its maximum at the pipe center.

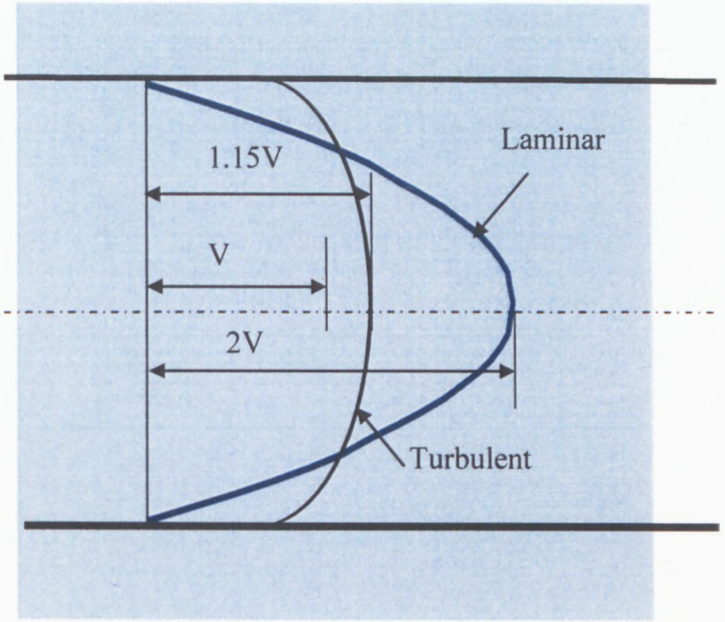

Figure 2.5: Pipe velocity profile for laminar and turbulent flow (Finnemore & Franzini, 2002)

Shear stress in turbulent flow far exceeds that caused by molecular shear alone. The shear stress between adjacent fluid layers is also attributable to momentum exchange between fluid particles moving from one layer to another.

It should be borne in mind that the pressure gradient in turbulent flow is approximately proportional to the second power of the velocity; the friction factor is obtained from various correlations, as it will be explained.

As inertial forces prevail in turbulent flow, there is little difference between the flow of Newtonian and non-Newtonian fluids.

Unlike laminar flow, where resistance is reasonably independent of wall, roughness in turbulent flow is of fundamental importance in the prediction of flow resistance e.g. (Tietjens *et al.*, 1934).

In turbulent flow there is a thin layer at the tube wall called, the laminar sub-layer where viscous forces are far greater than inertial forces. Three different modes of turbulent flow, depending on the relative thickness of sub-layer compared to the roughness of the wall, e.g. (Govier & Aziz, 1972) are distinguishable:

1. Smooth wall turbulent flow: This type of turbulent flow occurs when the viscous sub-layer is thicker than the tube wall roughness.
2. Partially rough wall turbulent flow: This type of turbulent flow occurs when the viscous sub-layer thickness is of similar in magnitude to the tube wall roughness.
3. Fully rough wall turbulent flow: This type of turbulent flow occurs when the viscous sub-layer thickness is significantly smaller than the tube wall roughness.

Various correlations exist to describe all these turbulent flow types, the most common being the Blasius correlation (Equation 2.28) for smooth wall turbulent flow, the Colebrook and White correlation (Equation 2.29) for partially rough wall turbulent flow and the Von Karman and Prandtl correlation (Equation 2.30) for fully rough wall turbulent flow e.g.(Govier & Aziz, 1972) .

$$f = \frac{0.079}{Re^{0.25}} \qquad \text{Eq 2. 28}$$

$$\frac{1}{\sqrt{f}} = -4\log\left[\frac{k}{3.7D} + \frac{1.26}{Re\sqrt{f}}\right] \qquad \text{Eq 2. 29}$$

$$\frac{1}{\sqrt{f}} = -4\log\left[\frac{k}{3.7D}\right] \qquad \text{Eq 2. 30}$$

2.5 HEAD LOSSES IN PIPES AND FITTINGS

2.5.1 Head Losses in Pipes

In pipeline design it is important to predict the loss of available energy or total head. When a fluid flows along a straight pipe, energy is expended in overcoming viscous or turbulent friction. This energy is normally transformed to internal energy, and is regarded as a loss of useful energy as far as fluid transport is concerned. When fully developed flow occurs in a horizontal pipe of constant diameter, the head loss is given by the head difference, ΔH, measured in metres of fluid. This head can be evaluated by the well-known Darcy Equation:

$$\Delta H = \frac{4f\ L}{D}\frac{V^2}{2g} \qquad \text{Eq 2. 31}$$

Where f is the Fanning Friction Factor defined as:

$$f = \frac{2\tau_0}{\rho V^2} \qquad \text{Eq 2. 32}$$

In Equation 2.32, τ_0 is the wall shear stress as defined by Equation 2.6.

In laminar flow, the Fanning friction factor is inversely proportional to the Reynolds number and is given by:

$$f = \frac{16}{Re} \qquad \text{Eq 2. 33}$$

In turbulent flow, the friction factor can be calculated using the Blasius Correlation (Equation 2.28) for the smooth turbulent flow, the Colebrook and White Correlation (Equation 2.29) for the partially rough wall turbulent flow and the Von Karman and

Prandtl correlation (Equation 2.30) for the fully rough wall turbulent flow. All these friction factors can be easily evaluated using the conventional Moody Diagram seen in Figure 2.6.

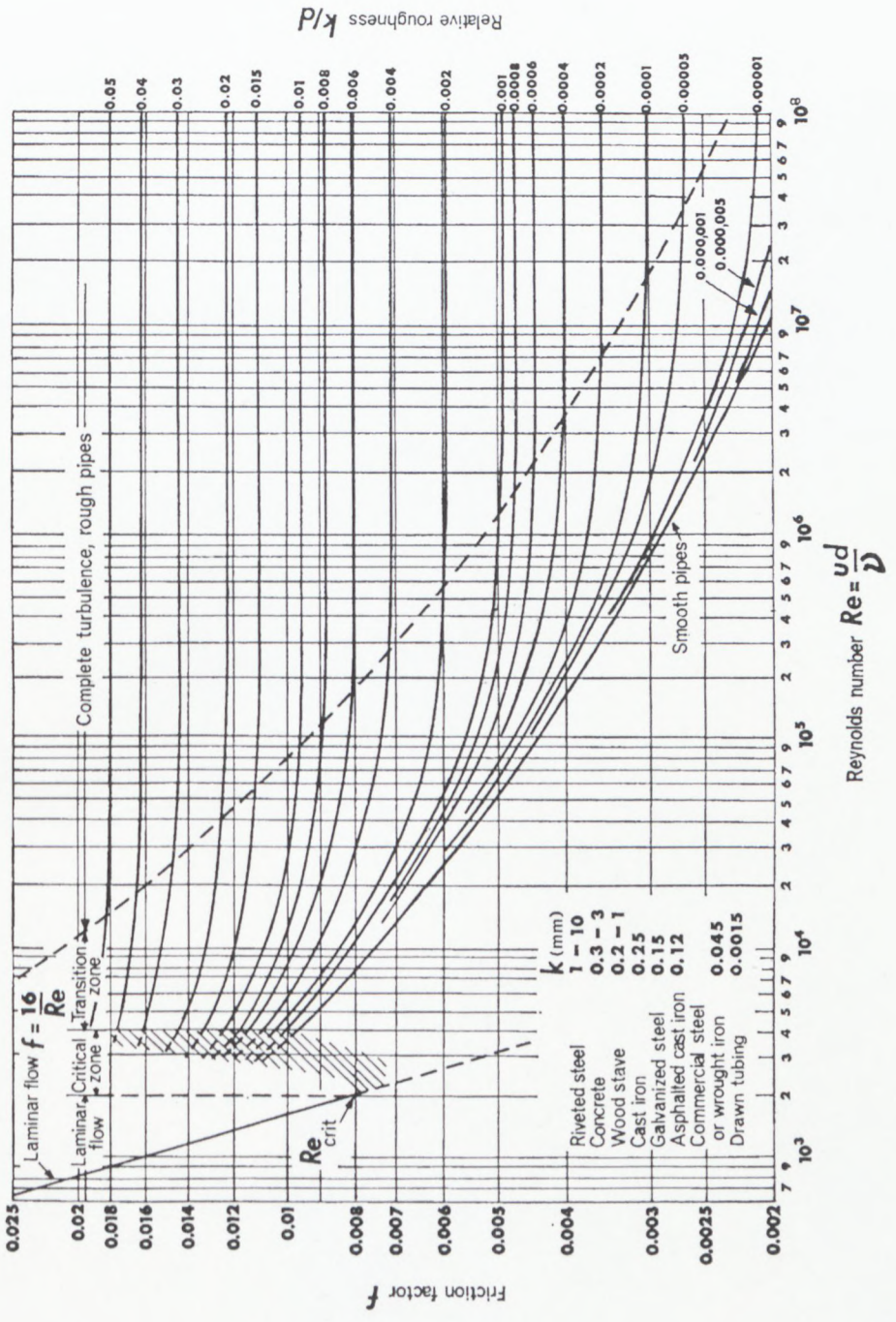

Figure 2.6: Moody Diagram (Massey, 1975)

2.5.2 Head Losses through Valves and Fittings

The head losses through fittings are termed minor losses and the losses from friction in straight pipes, major losses. Minor losses may be ignored when, on average, there is a length of 1000 diameters between each minor loss source (Streeter &Wylie, 1975). In short pipe systems, however, care must be taken as the so-called minor losses may outweigh the major losses (losses in straight pipes) e.g. (Miller, 1990). Since industrial installations usually contain a considerable number of valves and fittings, knowledge of their flow resistance is required to determine the flow characteristic of a complete piping system (Crane, 1999).

At least two mechanisms are involved in head losses through valves (or fittings). One is due to viscous friction, the same as what happens in straight pipes and the second is due to change in flow direction (Turian *et al.*, 1998). This change in direction induces flow separation, or vortices and possibly turbulence, which causes turbulence, and flow recirculation. Energy is expended in maintaining these vortices (Massey, 1975). Depending on the Reynolds number, a considerable portion of the pressure dissipation may take place beyond the fitting (Beck, 1944). This situation is depicted in Figure 2.7.

The curve ST represents the intensity of the disturbance in the fluid introduced by reason of its passage through the fitting. Velocity profiles and the pressure gradients are fully developed at points M and Q which is not the case for a point such as N in the transition zone where the velocity profile and pressure gradients are dependent on location. Pressure measurement to calculate the fitting loss must be made upstream of point M and downstream of point Q.

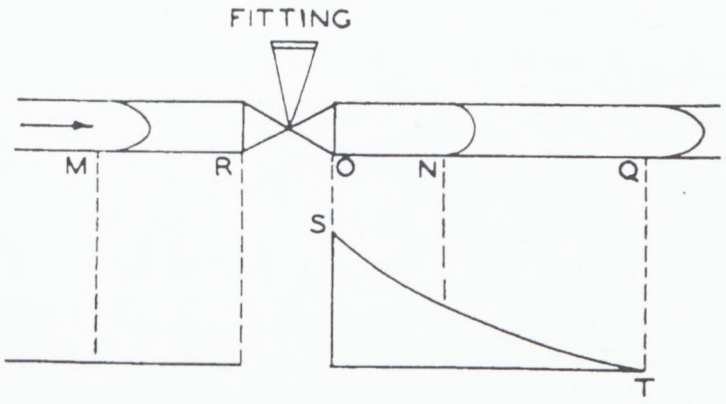

Figure 2.7: Flow distortion due to passage through fittings (Beck, 1944)

To summarise, the loss of pressure produced by a valve or a fitting consists of (Beck, 1944):

- The pressure drop within the valve itself;
- pressure drop in the upstream piping in excess of that which would normally occur if there were no valve in the line. This effect is small and,
- Pressure drop in the downstream piping in excess of that normally occurring if there was no valve in the line. This effect may be comparatively large.

As it is difficult to measure the three items separately, their combined effect, which is the meaningful quantity, should be measured accurately.

There are several ways of quantifying head losses through valves and fitting, as will be explained. But it is important to mention one that is extensively used. It is in the form of the Darcy Equation:

$$H = k_{fitt} \frac{V^2}{2g} \qquad \text{Eq 2. 34}$$

Where k_{fitt} is called the loss coefficient or flow resistance. The loss coefficient, k_{fitt}, is almost constant in turbulent flow. Values of k_{fitt} for various fittings and valves can be found in technical papers e.g. Crane (1999) or ASHRAE (Brooks, 1993). In laminar flow, however, the flow resistance becomes Reynolds number dependant (Edwards *et al.*, 1985). Similar to laminar pipe flow, the resistance coefficient is inversely proportional to the Reynolds number as shown in Equation 2.35.

$$k_{fitt} = \frac{C_{fitt}}{Re} \qquad \text{Eq 2. 35}$$

C_{fitt} is the loss coefficient constant, its numerical value being much higher than 16 (the straight pipe value). Values of C_{fitt} are not yet extensively documented as values of k_{fitt} and are inconsistent, as pointed out by Pienaar (2004). Typical C_{fitt} for various fittings may be found in Pienaar *et al.* (2001).

In this study, the loss coefficient, k_{fitt}, will be replaced by k_v and the loss coefficient constant C_{fitt} by C_v as the fitting, in this case, is a valve.

2.5.3 Dimensional Analysis

Dimensional analysis is a method used extensively in fluid mechanics and other related disciplines that rely on empirical data for solutions. The procedure consists of determining the independent variables, which have an influence on the dependant variable under study

and then enforcing dimensional homogeneity on an assumed power law relationship e.g. (Douglas *et al.*, 2000). There are usually three fundamental dimensions [mass (force), length and time]. If the number of independent variables, X, is greater than the three fundamental dimensions, then (X-3) dimensionless groups will appear in the expression. These groups assist in the interpretation of models studied by ensuring that the conditions under which tests and observations take place at one scale are identical to those on other scales e.g. (Massey, 1975). In addition, dealing with a dimensionless group reduces the number of independent variables in experiments.

There are different techniques for establishing the dimensionless groups involved in a physical problem. The most systematic is probably the Buckingham Π-theorem (Buckingham, 1914) which is found in most fluid mechanics books.

2.5.4 Geometric Similarity

Geometric similarity is the similarity of shape. Two systems or components are geometrically similar if the ratio of any length in one system to the corresponding length in the other system is the same everywhere. This ratio is usually known as the scale factor.

2.5.5 Kinematic Similarity

Kinematic similarity is a similarity of motion. The requirement to have kinematic similarity between two systems is, in addition to geometric similarity, to have similarity of time interval. Therefore the velocities of the corresponding particles must be in a fixed ratio of magnitude at corresponding times. Consequently, the patterns of the streamlines are geometrically similar at the same time in both systems.

2.5.6 Dynamic Similarity

Dynamic similarity is similarity of forces. If two systems are dynamically similar, the magnitudes of forces at similar locations in the two systems are in a fixed ratio. There are numerous types of forces that might be involved in the process, forces such as those due to friction, inertia, gravity, differential pressure, surface tension, elasticity, etc. It could be difficult to satisfy the same ratio to all forces simultaneously. Perfect dynamic similarity, is therefore, seldom obtained.

It should be noted, however, that in general the existence of geometric similarity does not imply dynamic similarity, but geometric similarity is a requirement for dynamic similarity.

In many practical instances, some forces are negligible or do not apply, and so it is possible to consider the similarity of the most important forces. In pipe fluid flow the viscous forces and the inertial forces generally dominate, their ratio forms a dimensionless group, well known as the Reynolds number, which will be used purposely in this study.

2.6 RHEOLOGICAL CHARACTERISATION

2.6.1 Introduction

In non-Newtonian laminar flow, it is important to rheologically characterise the fluids under study. Characterisation usually involves the measurement of the fluid flow properties over an appropriate shear rate (or shear stress) range (Chhabra & Richardson, 1999).

Once a flow curve is available, appropriate relationships may be fitted to the curve to determine the rheological constants. These constants are used in the calculation of the fluid flow parameters, such as the Reynolds number, the volumetric flow rate and the potential frictional pressure loss (knowing the slurry density).

2.6.2 Rheometry

Rheometry encompasses the collection of physical data from tests on a representative sample of fluid under investigation, for the purpose of establishing the relationship between shear stress and shear rate, both qualitatively (identification of the applicable rheological model) and quantitatively (the actual values of the rheological constants in the model) (Chhabra & Richardson, 1999).

The instrument used to measure viscous properties is called a viscometer or rheometer. There are two main types of viscometers: Tube and rotational.

2.6.2.1 Tube Viscometer

A tube or capillary viscometer is a device which forces a sample of fluid to flow at a measured rate in laminar motion under a measured pressure gradient in a precision bore capillary tube of known diameter and length (Govier & Aziz, 1972).

Because of their inherent similarity to many process flows, which typically involve pipes, capillary viscometers are widely employed in process engineering applications (Chhabra & Richardson, 1999).

2.6.2.2 Rotational Viscometer

The rotational viscometer usually consists of a concentric bob and cup, one of which is rotated to produce shear in the test fluid, found in the gap between the bob and the cup. The shear stress is determined by measuring the torque on one of the elements (Chhabra & Richardson, 1999).

2.6.3 Rheological Models

Various rheological models exist to characterise time-independent fluids as well as time dependent fluids. Figure 2.8 depicts idealised curves for the most used models for non-Newtonian slurries. Table 2.1 shows some of the most known rheological models.

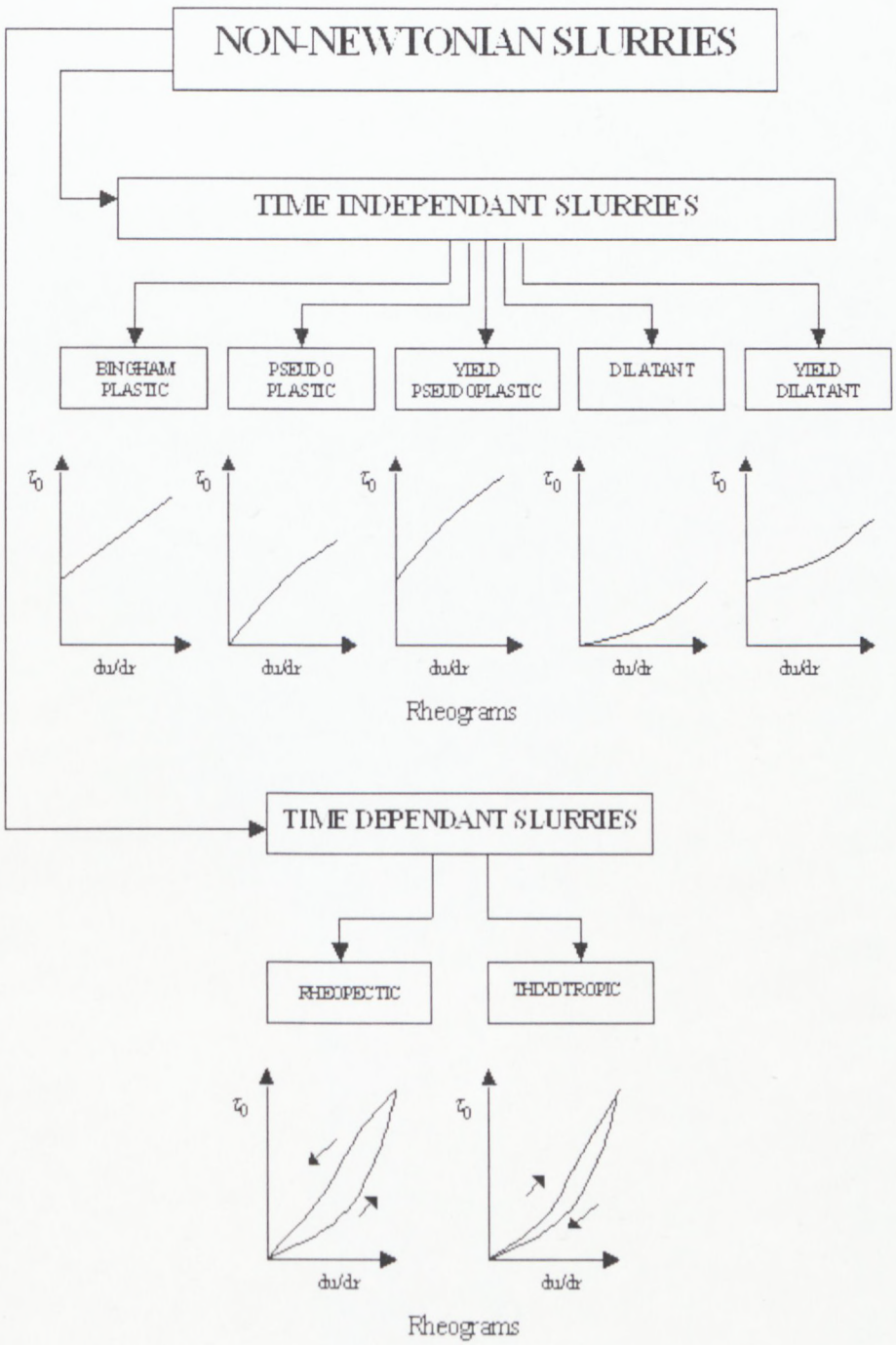

Figure 2.8: Non-Newtonian rheograms (Paterson & Cooke, 1999)

Table 2.1: Rheological models (Chhabra & Richardson, 1999)

Fluid model	Constitutive equation	Number of parameters	Parameters
Newtonian	$\tau = \mu(-\frac{du}{dr})$	1	μ
Bingham plastic	$\tau = \tau_y + K(-\frac{du}{dr})$	2	τ_y and K
Casson	$\sqrt{\tau} = \sqrt{\tau_y} + \sqrt{\mu_c(-\frac{du}{dr})}$	2	τ_y and μ_c
or power-law (pseudoplastic)	$\tau = K(-\frac{du}{dr})^n$	2	K and n
Ellis	$\mu = \frac{\mu_o}{1+(\tau/\tau_{1/2})^{\alpha-1}}$	3	μ_0, α and $\tau_{1/2}$
Herschel-Bulkley	$\tau = \tau_y + K(-\frac{du}{dr})^n$	3	τ_y, n and K
Carreau	$\frac{\mu-\mu_\infty}{\mu_o-\mu_\infty} = \left[1+\left(\lambda(-\frac{du}{dr})\right)^2\right]^{\frac{n-1}{2}}$	4	μ_∞, μ_o, λ and n
Cross	$\frac{\mu-\mu_\infty}{\mu_o-\mu_\infty} = \left[1+\left(\lambda(-\frac{du}{dr})\right)\right]^{\frac{n-1}{2}}$	4	μ_∞, μ_o, λ and n

2.6.4 Procedure for the Analysis of Tube Viscometer Results

The output of a tube viscometer is a set of co-ordinates of average velocity versus pressure drop (V, Δp). These data are plotted as (τ_o) versus (8V/D) on a pseudo shear diagram. The viscous flow data in the laminar region should be coincident for different tubes diameters (Chhabra & Richardson, 1999). If they are not, there is probably a wall slip effect that should first be corrected. The pseudo shear diagram is usually converted to a true rheogram by using the Rabinowitsch-Mooney relation as given in Section 2.4.5.2

The Metzner and Reed (1955) approach is based on the assumption that the apparent flow behaviour index (n') is constant over a wide range, this assumption is not always met for viscoplastic fluids. Since the Herschel-Bulkley model was chosen as it characterises fluids exhibiting yields stress, the following characterisation technique can be used (Lazarus & Slatter, 1988):

For a series of N data points in the laminar region, fixed values of τ_y, K and n can be used in Equation 2.26 to calculate pseudo shear rates $(8V/D)_{i\ calc}$ for each τ_o value. The rheological constants are found by minimising a root mean square error of fit function E defined as (Neill, 1988):

$$E = \sqrt{\frac{\sum_{i=1}^{N}\left[\left(\frac{8V}{D}\right)_{i_{obs}} - \left(\frac{8V}{D}\right)_{i_{calc}}\right]^2}{N-1}} \qquad \text{Eq 2.36}$$

2.7 REYNOLDS NUMBERS

2.7.1 Newtonian Reynolds Number

The Reynolds number is one of the most important dimensionless groups. It is defined as the ratio of the inertial forces to the viscous forces .

$$Re = \frac{\text{Inertial force}}{\text{viscous force}} = \frac{\rho LV}{\mu} \qquad \text{Eq 2. 37}$$

Where L is the characteristic length of the flow. For pipe flow the characteristic length is usually taken as the pipe diameter, therefore, Equation 2.37 becomes:

$$Re = \frac{\rho V D}{\mu} \qquad \text{Eq 2.38}$$

Equation 2.38 was first derived by Osborne Reynolds (1842-1912), an English engineer who developed it analytically and verified it experimentally. The magnitude of the Reynolds numbers will characterise or uniquely define the flow. For this reason it is usually used as a criterion to distinguish the laminar to turbulent transition, as explained earlier. The Reynolds numbers is used for modeling of flow in which viscous force effects are important (Prasuhn, 1980). It has been extended to non-Newtonian fluids using other formulations, as explained in the next section.

2.7.2 Non-Newtonian Reynolds Numbers

As for rheological models, there are various expressions for the Reynolds numbers of non-Newtonian fluids. In the following section, consideration is given to the Reynolds numbers used in this work.

2.7.2.1 Generalised Reynolds Number or Metzner and Reed Reynolds Number

Metzner and Reed (1955) developed a generalised Reynolds number for the correlation of non-Newtonian pipe flow of time-independent fluids as follows:

$$Re_{M-R} = \frac{8\rho V^2}{K'\left(\frac{8V}{D}\right)^{n'}} \qquad \text{Eq 2.39}$$

The above formula may be rewritten as

$$Re_{M-R} = \frac{\rho V^{2-n'} D^{n'}}{8^{n'-1} K'} \qquad \text{Eq 2.40}$$

n' is obtained as the tangent of the double logarithmic plot of τ_o versus (8V/D) at any particular value of τ_o or (8V/D) and Log K' is the intercept on the y-axis (Chhabra & Richardson, 1999).

$$\text{where } n' = \frac{d(\text{Log}\tau_o)}{d\left(\text{Log}\frac{8V}{D}\right)} \qquad \text{Eq 2.22}$$

For the power-law or pseudoplastic fluid model K' is linked to the Metzner-Reed approach by Equation 2.41.

$$K' = K\left(\frac{3n+1}{4n}\right)^n \qquad \text{Eq 2.41}$$

Where n = n'

Thus Equations 2.39 and 2.40 become:

$$Re_{M\text{-}R} = \frac{8\rho V^2}{K\left(\frac{3n+1}{4n}\right)\left(\frac{8V}{D}\right)^n} \qquad \text{Eq 2. 42}$$

$$Re_{M\text{-}R} = \frac{\rho V^{2-n} D^n}{8^{n-1} K\left(\frac{3n+1}{4n}\right)} \qquad \text{Eq 2.43}$$

2.7.2.2 Slatter Reynolds Number

The previous models do not take account of the yield stress. Slatter (1994) developed a Reynolds number that places specific emphasis on the yield stress. The final form of this formulation is as follows:

$$Re_3 = \frac{8\rho V_{ann}^{\ 2}}{\tau_y + K\left(\frac{8V_{ann}}{D_{shear}}\right)^n} \qquad \text{Eq 2.44}$$

In the case where a fluid exhibits a yield stress (such as in kaolin slurries), there is plug flow at the centre of the pipe, starting at distance r_{plug} where the shear stress becomes less than the yield stress.

D_{shear} is the sheared diameter which is calculated as

$$D_{shear} = D - D_{plug} \qquad \text{Eq 2.45}$$

where D_{plug} is the diameter of the plug : $D_{plug} = 2r_{plug}$ and

$$r_{plug} = \frac{\tau_y}{\tau_o} R \qquad \text{Eq 2.46}$$

V_{ann} is the mean velocity in the annulus. It is obtained as follows:

$$V_{ann} = Q_{ann} / A_{ann} \qquad \text{Eq 2.47}$$

where A_{nn} the flow rate in the annulus, and is calculated as:

$$Q_{ann} = Q - Q_{plug} \qquad \text{Eq 2.48}$$

Q_{plug}, the flow rate in the plug, is the product of the plug velocity and the plug area i.e.:

$$Q_{plug} = u_{plug}.A_{plug} \qquad \text{Eq 2.49}$$

$$\text{where } u_{plug} = \frac{D}{2K^{1/n}\tau_o}\left(\frac{n}{n+1}\right)\left(\tau_o - \tau_y\right)^{\frac{n+1}{n}} \qquad \text{Eq 2.50}$$

$$\text{and } A_{plug} = \pi r_{plug}^2 \qquad \text{Eq 2.51}$$

A_{ann} is the area of the sheared annulus and is calculated by:

$$A_{ann} = \pi\ (R^2 - r_{plug}^2) \qquad \text{Eq 2.52}$$

This is a straightforward calculation once the density, the rheological parameters of the fluids (K, n, τ_y) and the flow conditions (D, V, τ_o) are known. The transitional Reynolds number from laminar to turbulent flow in straight pipes is $Re_3 = 2100$. This Reynolds number can accommodate many rheological models by setting:

Newtonian	($\tau_y = 0$, $n = 1$, $K = \mu$)
Yield pseudo plastic	($\tau_y > 0$, $n < 1$, $K > 0$)
Power-law	($\tau_y = 0$, $n < 1$, $K > 0$)
Bingham plastic	($\tau_y > 0$, $n = 1$, $K > 0$)
Dilatant	($\tau_y = 0$, $n > 1$, $K > 0$)
Yield dilatant	($\tau_y > 0$, $n > 1$, $K > 0$)

Flow conditions in this work will be characterised by the Slatter Reynolds number. Its main advantage being the accurate indication of dynamic similarity for yield stress fluids (Slatter, 1999).

2.8 VALVES

2.8.1 Introduction

Although the emphasis of this study is placed on industrial diaphragm valves, it was found worthwhile in this section to mention, in general, the types of valves encountered in industrial applications. The process followed in selecting a valve, the valve flow characteristics and flow resistances.

2.8.2 Types of valves

A valve is a piping component which influences the fluid flow in a process plant by opening, closing, diverting, mixing or partially obstructing the passage through itself (Warring, 1982). Valves may be classified in several ways, e.g. by category (general type), specific type, mode of actuation, purpose or by flow characteristics. Description can also differ slightly in different countries although the main type names are established internationally (Warring, 1982). The main types of valves are given in the following paragraphs.

2.8.2.1 Ball valve

The ball valve is essentially a ported sphere in a housing. Rotation of the sphere by 90° changes the position from fully opened to fully closed. The ball may be of fixed or floating design in full or reduced port. Ball valves are available in a variety of sizes and with a wide choice of actuating mechanisms.

2.8.2.2 Butterfly valve

A typical butterfly valve consists of a disc, which can rotate about a shaft in the housing. The disc closes against a ring seal to close off flow.

2.8.2.3 Gate valve

A gate valve is characterised by a sliding disc or gate, which is moved by the actuator perpendicular to the direction of the flow. There are many variations in seat, stem and bonnet design in gate valves.

2.8.2.4 Globe valve

The three major valves in the globe family are the globe, angle and Y. They are all characterised by a closure member, usually a disc or plug, which is moved by an actuator stem perpendicular to a ring shaped seat. The flow passes from inlet port through the seat to the outlet port. The three types differ mainly in the direction of the seat to the flow direction of the valve. Figure 2.9 illustrates two designs in the seat-plug region of ordinary globe valves.

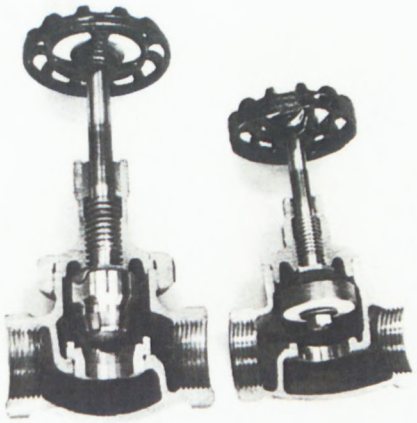

(a) (b)

Figure 2.9: Internal structure of globe valves: (a) with plug (b) with composition disc

2.8.2.5 Pinch valves

Pinch valves are characterised by one or more flexible elements such as diaphragm, rubber tubes, etc., which can be moved together (or against a stop) to pinch off the flow.

2.8.2.6 Poppet valves

The poppet valve is one in which the closure member moves parallel to the fluid flow and perpendicular to the sealing surface. The closure element is usually flat, conical or spherical on the sealing end. It may have many types of actuating elements including spring, screw systems, etc.

2.8.2.7 Swing valve

Swing valves are similar to butterfly valves except they are hinged on one edge rather than along the diameter. They may be actuated by the flow, by torsion springs or by levers. They are used primarily as check valves to block flow in one direction.

2.8.3 Valves Selection

The selection of a valve for a typical service takes into account many parameters, such as the nature of fluid to be handled, the functional requirements of the valve, the operating conditions, the valve flow characteristics and frictional loss and the valve size itself.

2.8.3.1 Fluid handled

The nature of the fluid handled affects the choice of valve and material in which the valve should be constructed. The viscosity or fluidity, particles size distribution, velocity, pressure and the temperature of fluids are among the important parameters to be taken into account. For example, a valve used with a corrosive or an abrasive slurry will be made of more specialised material than a valve required for use with ordinary water.

2.8.3.2 Functional requirement

Whether a valve is used as an on-off device or for a throttling purpose or pressure relief, or as a one-way device, these functions will determine which valve is suitable. Sometimes one type may fulfill many functions. For example a throttling valve may also be used as an on-off device. The answers to such pertinent questions dictate the valve suitable as each suits a particular type of service (Shook and Roco, 1991).

- Is the valve required for high or low pressure /temperature installation?
- Will conditions be moderate or severe?
- What will be the frequency of operation?
- What are the purchase price and maintenance costs?

2.8.3.3 Flow characteristics and frictional loss

Depending on whether the most important parameter is flow control or pressure control, the flow characteristics should be chosen accordingly. Additional losses should be kept under desirable requirements.

2.8.3.4 Valve size

In the design of a fluid handling system, it is usual to first select a pipe size to meet the capacity needed and the permissible frictional pressure losses. The size of valve is therefore dictated by the pipe size. It is important however, to consider the accumulated losses through valves when choosing the optimum pipe size for the system (Shook & Roco, 1991). It should also be noted also that the availability of very large sizes is only limited to a certain type of valve.

2.8.3.5 Mode of Actuation

Valve selection may possibly be subjected to the method of operation. Although the handwheel is the simplest mechanical type of actuation encountered, for reasons of automation and size, operation may be assisted by gear heads, which are operated by mechanical, electrical, hydraulic or pneumatic mechanisms.

2.8.3.6 Material of Construction

There is a wide range of materials available to meet various service conditions. In selecting a valve it is advisable to consider separately the different components (body, bonnet, and trim comprising the closing member, stem mating sets, etc.) to optimise the material specifications to meet the service conditions.

The most used materials are: cast iron, bronze, nickel alloys, copper alloys, steel, stainless steel and sometimes aluminum and titanium (Saundersvalves, 2004). Cast iron and bronze are probably the materials most used in low temperature applications. Plastics valves are being extensively used in place of stainless steel or alloy for systems conveying acids or corrosive chemicals. If the fluid handled is highly corrosive or chemically reacts with metal, precaution must be taken to prevent contamination by fluid. The valve may be lined with ebonite, plastics glass or ceramics.

2.8.4 Diaphragm Valves

2.8.4.1 History

The diaphragm valve traces its origins back to Roman and Greek times, where it was used to control the water flow and temperature of hot baths. With a crude diaphragm that was manually closed over a weir, it was a primitive, but effective, control valve (Centuryinstrument, 2004).

In the early 1900s, P.K. Saunders, a South African mining engineer, whose hobby was history and archeology, aimed to improve the performance of valves used to supply air

and water to mines. In 1928 Saunders developed the first modern diaphragm valve based on the concept of the control valves used in Greco-Roman baths (Saundersvalves, 2004).

In 1931, the Hills McCanna Company became the first licensee to manufacture the Saunders patent diaphragm valve in the United States. In succeeding years other businesses such as Grinell (ITT Dia flow), Dow Chemical, and Arco Winn, were granted a patent to produce Saunders valves (Centuryinstrument, 2004).

With the advent of a variety of advanced polymer and elastomer materials used in the internal construction of the diaphragm valve, its sales growth was notable. However it soon became apparent that a reliable automatic actuator was required. CenturyInstrument became the first to produce a diaphragm type pneumatic operator in 1950. Other actuations such as electric, hydraulic, mechanical were soon also introduced (Centuryinstrument, 2004).

In the early 1950, the straight-through design was introduced in an effort to improve the flow performance of the weir type, which accounted for 90% of the then world diaphragm valves (Waterfield, 1982).

2.8.4.2 Advantages of Diaphragm Valves

Diaphragm valves are preferred because of many advantages they provide against other types of valves, the most obvious being:

- They are extremely clean (Globalspec, 2004), because of the isolating quality of the diaphragm which guarantees the purity of the fluid being conveyed (Warring, 1982);
- They can form a leak-proof seal for tight shut-off (Globalspec, 2004). In addition they present a glandless construction which leads to an absence of seating problems (Warring, 1982);
- They present low cost maintenance as the diaphragm design provides for easy maintenance and repair as it may be replaced with less disturbance to the pipe line (Global spec, 2004).

With such advantages, diaphragm valves are used in many applications. Pharmaceutical industries, chemical processing, breweries, dairies and general foodstuffs factories, gas and petroleum, mining and minerals processing, are some key applications (Warring, 1982).

2.8.4.3 Diaphragm Material

A broad range of elastomer and plastic diaphragms have also been developed to meet the chemical and physical conditions imposed by different valve applications. Table 2.2 presents some of the materials used for diaphragm fabrication.

Table 2.2: Diaphragm Materials (Century instrument, 2004)

MATERIALS	TEMPERATURE RANGE	SIZE RANGE	TYPICAL APPLICATIONS
Natural Rubber	0 to 88 °C	1/2" - 8"	Wet or dry abrasives at moderate temperatures
Neoprene	0 to 93 °C	1/2" - 8"	Acids, alkalies, alcohol and oil
Hypalon*	-34 to 121 °C	1/2" - 8"	Acids, Caustics and Oil
Ethylene Propylene Rubber	-34 to 149 °C	1/2" - 8"	Excellent chemical and abrasive resistance at elevated temperatures
Viton*	-29 to 177 °C	1/2" - 8"	Aggressive chemicals, acids and oil. High temperature service
TFE Faced	-34 to 149 °C	1/2" - 8"	Maximum resistance to aggressive chemicals and solvents at elevated temperatures. Excellent ant-stick properties
Butyl	-26 to 100 °C	1/2" - 8"	Acids and alkalies
White EPR	-34 to 149 °C	1/2" - 8"	Excellent chemical and abrasive resistance at elevated temperatures. Food grade - F.D.A. approved
White Butyl	-26 to 100 °C	1/2" - 8"	Acids and alkalies. Food grade

* Hypalon and Viton are registered trademarks of Dupont Dow Elastomers

2.8.4.4 Different Design of Diaphragm Valves

Although diaphragm valves are made in a number of designs for different types of service there are, however, two basic forms: The weir and straight-through types (Globalspec, 2004).

1. **The weir type**: Referred to by manufactures as Saunders weir Type A. It is the original Saunders diaphragm valve design (Saundersvalves, 2004) It presents a weir or bridge over which the diaphragm is lowered to provide the shutoff. Because of the short distance travel of the diaphragm this design presents an advantage of a long life of the diaphragm. It is best suited for gas, water or fluids containing no solids material of substantial size.
2. **The straight-through type:** Referred to by manufactures as Saunders Type KB. As the name implies, it is a straight-through design without a weir. It presents the advantage of having a low resistance coefficient and can handle a wide range of fluids, including slurries containing solid materials.

There are other non-common types of valves such as:

WFB type: Specialised diaphragm valves with a variety of specialised end connections specifically designed for marine and fire hydrant duties (Saundersvalves, 2004)

The VeeValv: Introduced in 1976. Is a variant of the type KB valve. It is claimed to have the advantage of fewer components, wider manufacturing tolerances and a better flow performance than traditional designs (Waterfield, 1982)

The MEMS diaphragm valves: These are valves found in microelectromechanical systems. These microvalves are habitually operated by compressed air of other fluids. They are inherently smaller, lighter, faster, and usually more precise than their bulk scale counterparts (Yang and Kao, 2000)

Not all these types are studied. This work is concerned with the straight-through or KB type of industrial diaphragm valves usually found in slurry applications. Hence, more details on this valve is given in Chapter 3.

2.8.5 Valve Flow Characteristic and Losses through Valves

2.8.5.1 Losses through Valves

Pressure drop due to changes in the shape of the flow path or due to changes in cross sectional area as produced by fittings such as valves can be evaluated in three ways (Warring, 1982):

1. As a resistance (or loss) coefficient (k_v)

   Additional losses due to a valve are expressed in term of the velocity head as:

$$H = k_v \frac{V^2}{2g} \qquad \text{Eq 2. 53}$$

Where H is the head loss incurred through the valve, the bigger the k_v value is, the more resistant is the valve.

2. As an equivalent length (L/D)

Additional losses from a valve are expressed in term of an equivalent length of the pipe in which there would be an equivalent head loss as incurred by the valve at the same flow rate. This length is usually expressed as a number of pipe diameters in which the valve is installed.

Loss coefficient and equivalent length are linked by the formula:

$$\left(\frac{L}{D}\right) = \frac{k_v}{4f} \qquad \text{Eq 2. 54}$$

Where f is the Fanning friction factor of the pipe and D the diameter of the pipe.

3. As a flow coefficient (C_V or K_V)[2]

The flow coefficient is defined, as the number of cubic metres per hour of water at 20° C, which will flow with a pressure drop of 1 bar. Therefore, the pressure drop on the valve is calculated with the formula:

$$\Delta P = \rho\left(\frac{Q}{C_V}\right)^2 \qquad \text{Eq 2. 55}$$

Where ρ is the specific gravity of the fluid.

The valve flow coefficient (C_V) and the loss coefficient (k_v) are linked by the formula:

([2]) The definition of C_V was originally based on US or UK gallon for flowrate and $1b/in^2$ for pressure. K_V is mostly used in European countries. The relation between them is $K_V = 0853\ C_V$. Until now, there is not yet an agreed international definition for a flow coefficient in terms of SI units (Crane, 1999).

$$C_V = b\frac{D^2}{\sqrt{k_v}} \qquad \text{Eq 2. 56}$$

Where: b is a units conversion factor, and

D is the pipe diameter

In this experimental work, the measured quantities will be the flow rate and the pressure drop. From these measurements an empirical expression of the pressure drop through the valve will be determined. Subsequently the loss coefficient (k_v), the equivalent length (L/D) or the flow coefficient (C_V) can be determined.

2.8.5.2 Valve Flow Characteristic

As a valve can be set in different positions (from fully opened to fully closed) it will present different flow resistances, or conversely, flow capacities. This variation occurs according to the percentage opening of the closing member or the stem travel. Therefore it should be remembered that a value of loss coefficient for a valve must be associated with the percentage opening. That is why it is important to establish the valve flow characteristics. A valve flow characteristic is nothing else but a graph which portrays the relation of the valve capacity to the percentage opening of the valve closing member.

A typical flow characteristic for a diaphragm valve is shown in Figure 2.10 where the opening positions tested are marked.

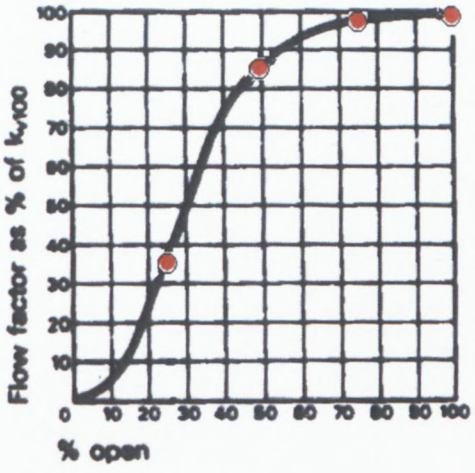

Figure 2.10: Typical diaphragm valve flow characteristics (Warring, 1982)

2.9 PREVIOUS WORK ON PRESSURE LOSSES IN VALVES

The literature on diaphragm valves is limited and studies related to diaphragm valves pressure drop scant. This section, however, gives an overview of previous work related to valves, in general, to establish a background to this work. The aspects of interest were the type and size of valves tested, the nature of fluids used, the type and range of Reynolds numbers used, the correlations obtained and the technique used in the derivation of these correlations.

Beck (1944) developed correlations of an array of fittings which included a gate and a globe valve of port size 88.9 mm for Newtonian laminar flow, with a range of Newtonian Reynolds numbers from 20 up to 1000. He used dimensional analysis to derive a correlation based on the equivalent length method. A four constant functional relationship (Equation 2.57) was derived and the constants were obtained by solving differential equations obtained in the range of Reynolds numbers of 100 to 1000.

$$E = a\,\mathrm{Re}^{h}\,D^{c\log \mathrm{Re}+b} \qquad \text{Eq 2.57}$$

Although the author derived an equation to correlate equivalent length with diameter D and Re, this expression was unable to give a definitive equivalent length as there was always a dependence of E with the location of the downstream tap. This is especially true for valves in the partial opening positions. Moreover, data for the gate valve did not fit this equation. However, this paper gives a plausible explanation of the critical Reynolds numbers found in fittings and valves. Critical Reynolds number has a much lower value than the traditional lower critical Reynolds numbers (Re = 2100) found for straight pipes. Another positive aspect of this correlation is that it includes D which takes into account the valve size.

Kittredge and Rowley (1957) tested kerosene and SAE 10 oil in a variety of fittings and valves of port diameter 12.7 mm. They tested over a wide range of Reynolds numbers including laminar, transitional and turbulent flow. The valves tested included, gate, globe, swing, check, ball, angle and plug valves. No diaphragm valve was tested, although the first one was already developed in 1928. Based on dimensional analysis, they developed a 3 constants functional relationship (Equation 2.58) which included the kinematic viscosities as scaling ratio

$$k_v = C(\mathrm{Re})^{a}\left(\frac{\nu}{\nu_s}\right)^{b} \qquad \text{Eq 2. 58}$$

Where C, a and b are constants.

ν_s is a reference kinematic viscosity

The reference viscosity used was pure water at 15.5 °C. Although this correlation already included the viscous properties of the fluid in the Reynolds number, it still has another factor to account for differences in the viscosity and density of the fluid. In addition this correlation obviously assumes geometric similarity and no scaling factor is given for size.

Some general observations were:

- The existence of an apparent critical Reynolds number which occurs far below Re = 1000 for valves and,
- below the critical Reynolds number the k_v values increase approximately according to Equation 2.59

$$k_v = \frac{C}{Re^a} \qquad \text{Eq 2. 59}$$

Where C and a are constants

The constants C = 203 and a = 0.5 and a critical Reynolds number of 350 were given for globe valves with composition disk.

Hooper (1981) developed a two-k method and provided k-values from literature for both laminar and turbulent flow. The values given for diaphragm valves were C_v = 1000 and k_v = 2. A scaling factor to account for size was introduced with the inclusion of D in his correlation, where D is the valve port diameter in inches.

$$k = \frac{C_v}{Re} + k_v\left(1 + \frac{1}{D}\right) \qquad \text{Eq 2. 60}$$

Edwards *et al.* (1985) tested non-Newtonian fluids in several fittings and valves at low Reynolds numbers. Two sizes (25 mm and 50 mm) of gate and globe valves were tested to evaluate dynamic similarity. For laminar flow, the loss coefficient was correlated with the generalized Metzner and Reed Reynolds number to account for non-Newtonian behaviour. In this study, the constants were provided for these specific valves. The importance of geometric similarity to obtain dynamic similarity was shown in the results obtained from the globe valves that had different seat types, one circular and one plug. They found that the loss coefficient could be meaningfully correlated as plots of loss coefficient versus generalized Reynolds numbers. Also, for any given geometry of fitting, the data for all fluids tested could be correlated by a loss coefficient constant C_v in laminar flow and by a loss coefficient k_v at high Reynolds numbers. For the gate valves tested they found that the loss coefficient constant was 273 for the two sizes, but for globe valve they found loss coefficient constants of 384 for the 50 mm valve and 1460 for the 25 mm valve. These results were not correlated to various openings of the valves. These authors suggested that much more testing was required to obtain results for the wide range of fittings available commercially. The lack of data and improved test methods and equipment such as electronic transducers were also highlighted.

Miller (1990) published a graph of loss coefficients for two types of diaphragm valves for turbulent flow at various openings as shown in Figure 2.11. There is no mention of the valve size.

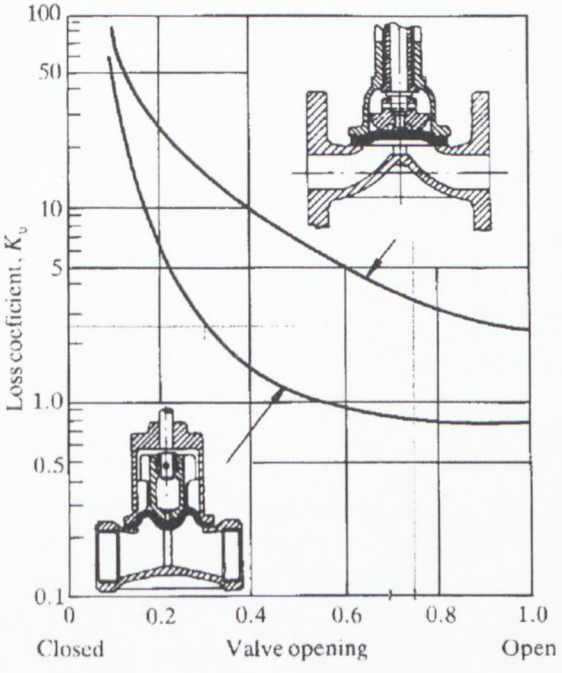

Figure 2.11: Diaphragm valve loss coefficients (Miller, 1990)

Banerjee *et al.* (1994) developed correlations for 12.5 mm gate and globe valves in laminar flow of CMC solutions. As Beck (1944) and Kittredge and Rowley (1957), they used dimensional analysis to derive the correlation. They included a vital factor - the valve opening. From the experimental data they derived the following 3 constant generalised correlations for globe valves.

$$\frac{\Delta P}{\rho V^2} = 8.266 Re^{-0.061 \pm 0.013} \alpha^{-0.797 \pm 0.03} \qquad \text{Eq 2. 61}$$

For gate valves, they found the correlation:

$$\frac{\Delta P}{\rho V^2} = 1.905 Re^{-0.197 \pm 0.046} \alpha^{-0.987 \pm 0.09} \qquad \text{Eq 2. 62}$$

This correlation did not, however, compare well with other experimental results; the shortcomings have been discussed by Pienaar *et al.* (2004).

Turian *et al.* (1998) used the same approach as Edwards *et al.* (1985), but included yield pseudoplastic fluids with the objective of determining the loss coefficient constant in laminar flow and turbulent loss coefficient data for these fluids in turbulent flow for gate and globe valves. The results for gate valves compared well with those obtained by Edwards *et al.* (1985). They could however not obtain laminar flow in the globe valves. An important contribution from this work was the fact that they showed that in turbulent flow the same loss coefficient could be used for both Newtonian and non-Newtonian fluids.

Perry *et al.* (1997) reported values of turbulent loss coefficients for diaphragm valves at various openings as depicted in Table 2.3. In this case, as with Miller (1990), the valve size was not mentioned.

Table 2.3: Loss coefficients of diaphragm valves published by Perry *al*. (1997)

Diaphragm valve opening	Loss coefficient
¼ Open	21
½ Open	4.3
¾ Open	2.6
Fully Open	2.3

Darby (1999) improved the 2–k method of Hooper (1981) by introducing additional constants to accurately account for the non-linear nature of scale-up of valves sizes (Equation 2.63). However, he provided constants for only gate and ball valves in a fully opened position.

$$k = \frac{C_v}{Re} + k_i\left(1 + \frac{k_d}{D^{1..3}}\right) \qquad \text{Eq 2. 63}$$

Where k_i and k_d valve parameters given in Table 2.4

Table 2.4: k_i and k_d values in Equation 2.63

Valve type	k_i [-]	k_d [$m^{0.3}$]
Gate valve, fully opened	0.0114	0.124
Ball valve, fully opened	-0.086	-0.0635

Yang and Kao (2000) studied the deflection of a microvalve diaphragm (Figure 2.12) actuated by air pressure. Based on the linear theory for an elastic thin plate and the Bernoulli equation they derived some modelling equations. Theses equations were non-linear differential equation which was solved numerically using an iterative procedure. The effect of the fluid speed, the outlet diameter, the gap between the valve diaphragm and valve seat and the bending stiffness of the diaphragm were analysed. It was found that for a given size, there was a range of critical air speed within which the diaphragm was unstable. If the air pressure P_o is bigger than the fluid pressure P_f, the diaphragm will move up and make contact with the valve seat to shut off the flow.

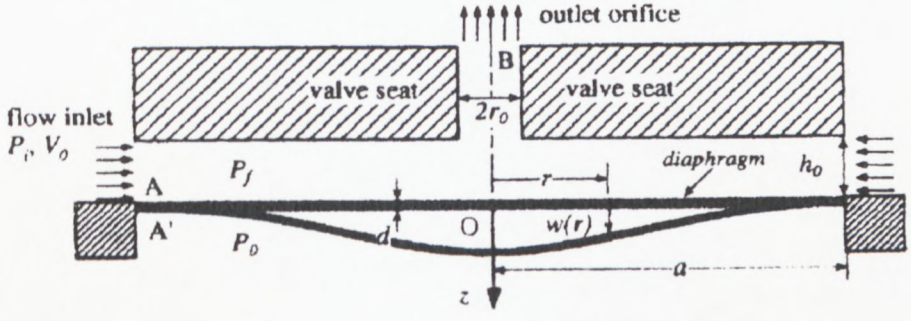

Figure 2.12: Pressure-balanced diaphragm MEMS valve (Yang & Kao, 2000)

ESDU (2004) substantiated the fact that the diaphragm valve loss coefficient is not independent of the valve port diameter as shown in Figure 2.13. The loss coefficient of various diaphragm valves, as estimated by the ESDU (2004), is determined by Equation 2.64 where C'_k is the loss coefficient applicable for the fully opening position and for Reynolds numbers greater than 10^4, to which correction α_1 and α_2 must be applied to account for partial opening and low Reynolds number effects respectively.

$$C_k = C'_k \times \alpha_1 \times \alpha_2 \qquad \text{Eq 2. 64}$$

α_1 and α_2 are given by the graphs in Figure 2.14 and Figure 2.15.

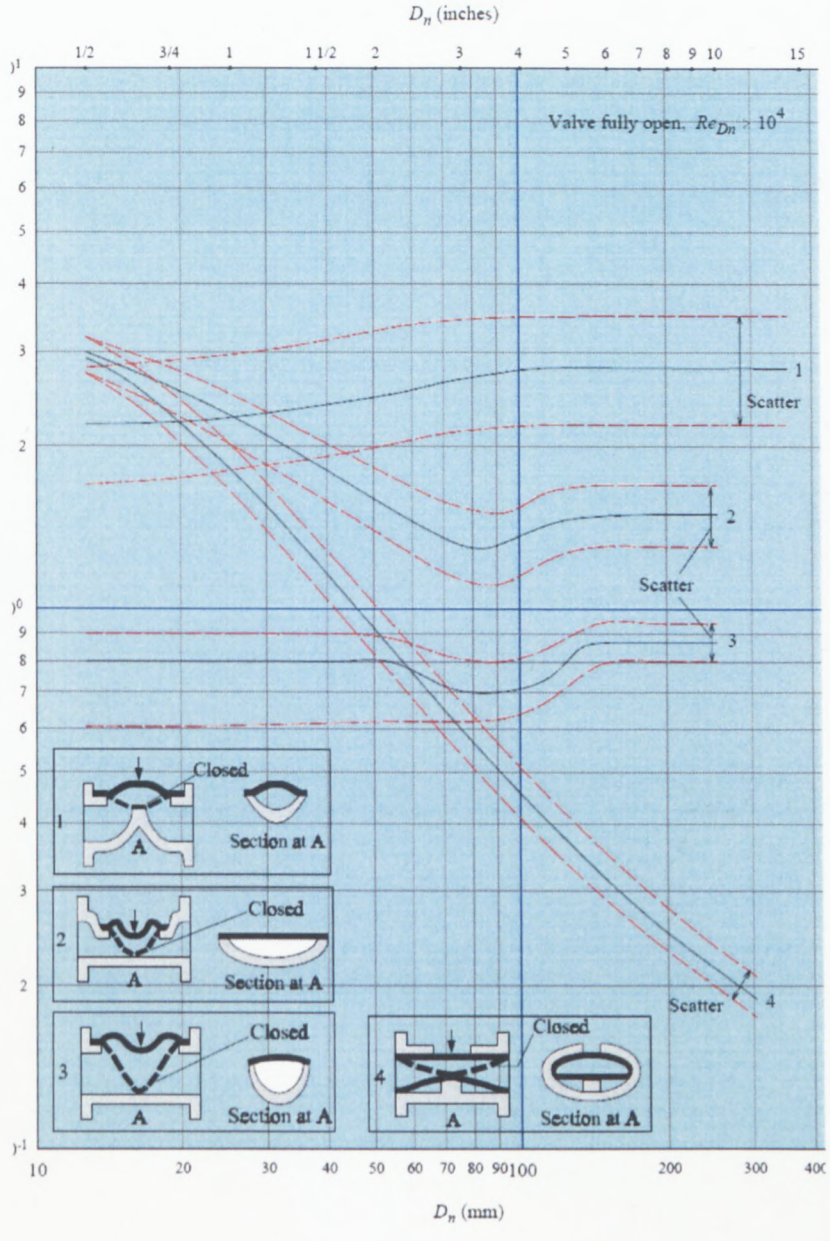

Figure 2.13: C_k' for diaphragm valves (ESDU, 2004)

Although the correlations accounted for both low Reynolds number effects as well as valve opening, no information is available for the Type 2 and Type 4 valves (as given in Figure 2.13), accounting for partial opening effects.

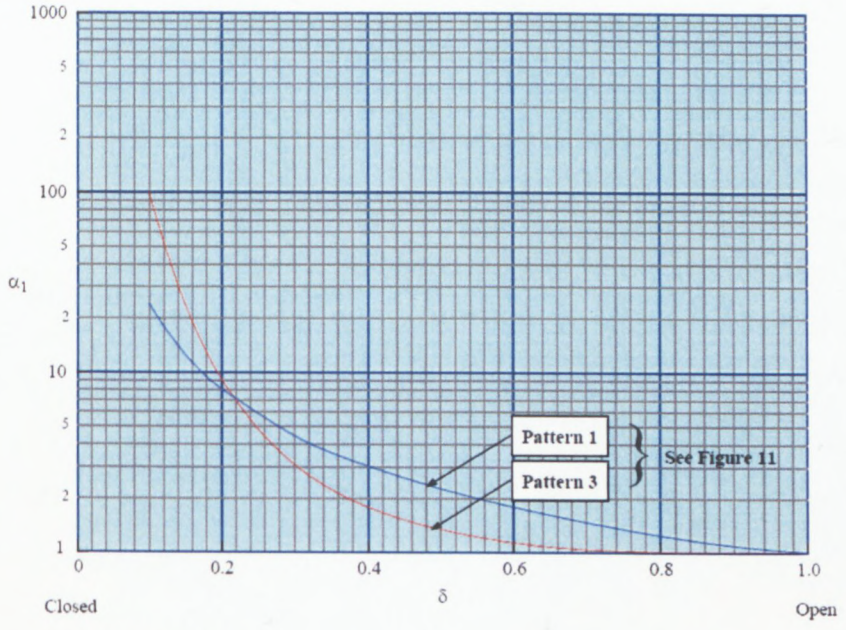

Figure 2.14: Approximate effect of partial opening, diaphragm valves (ESDU, 2004)

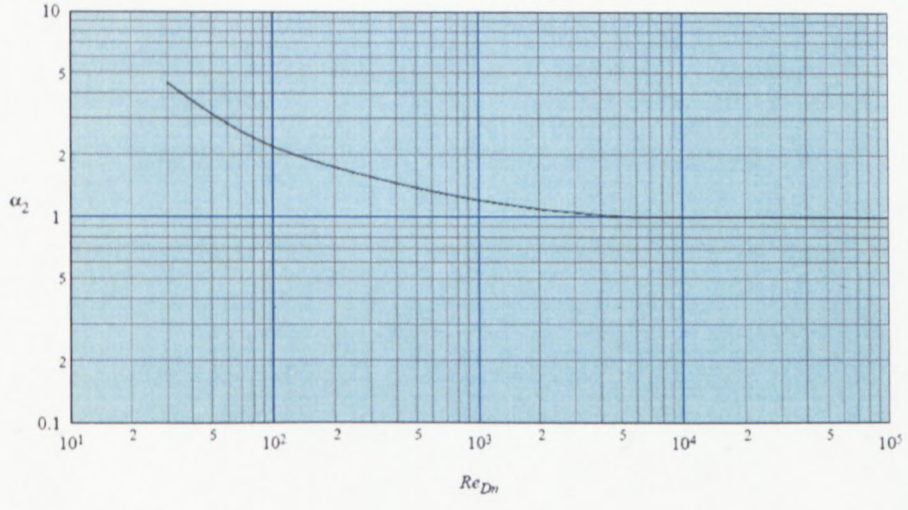

Figure 2.15: Approximate effect of Reynolds number, poppet type and diaphragm valve (ESDU, 2004)

Pienaar *et al.* (2004) gave a comprehensive review of work done on valves and highlighted in particular the lack of experimental data for flow of both Newtonian and non-Newtonian fluids in diaphragm valves. In addition, they evaluated the flow of a non-Newtonian kaolin slurry through globe valves and a 40 mm diaphragm valve. They found that, for the diaphragm valve the preliminary results compared well with Hooper (1981) in laminar flow, and the loss coefficient given by Perry *et al.* (1997) in turbulent flow. They suggested that a full range of valves should be tested to determine if dynamic similarity exists.

Fester *et al.* (2007) conducted initial work on a series of diaphragm valves ranging from 40 mm to 100 mm using both Newtonian and non-Newtonian fluids in laminar flow. They presented their results in the form of C_v for four openings of the diaphragm valves and highlighted the influence of the lack of geometric similarity on the loss coefficients obtained for different valves sizes.

Mbiya *et al.* (2007) presented a 3-constant correlation for a 40 mm diaphragm valve based on the Fester *et al.* (2007) data, by adopting a similar approach as Banerjee *et al.* (1994). This correlation was limited to the laminar region. The shortcoming of this correlation as well as Barnejee *et al.* (1994) was the inadequate fit of the experimental data at very low Reynolds numbers ($Re < 10$) and its restriction to the pipe laminar flow range.

2.10 CONCLUSION

In this chapter, fundamental equations governing the mechanics of fluids have been presented. The concept of pressure and pressure losses has been explained. Because fluids are generally transported through straight pipes, the fluid flow through straight pipes has been revisited. The rheological characterisation and the Reynolds numbers used have been explained since they play a major role in viscous flow of non-Newtonian fluids.

There is an endless list of valves found in industrials applications, in this chapter however, the major types of valve were briefly described. The main aspects of valve selection were explained and different diaphragm valve designs presented. The straight-through type diaphragm valve, the object of this study, is fully described in Chapter 3.

Previous work on pressure losses in valves dating to as far as 1944 was considered. It was apparent globe and gate valves were mostly studied, but little work was conducted on diaphragm valves. Dynamic similarity was found only with gate valves using the generalised Metzner and Reed Reynolds numbers, but not for globe valves (Edwards *et al.*, 1985 & Turian *et al.*, 1998). Pienaar *et al.* (2004) showed, however, that dynamic similarity could be achieved in globe valves using the Slatter Reynolds number.

Most correlations predicting valve loss coefficient were deduced with dimensional analysis and had at least three constants. Hooper (1981) and Darby (1999) alone introduced D in their correlations to account for the valve size. Banerjee *et al.* (1994) and ESDU (2004) introduced a parameter taking the partial valve opening into account. Additional work was unanimously recommended by most researchers.

2.11 RESEARCH ASPECTS IDENTIFIED

From the literature survey undertaken, it is evident that some aspects require further research and are identified as follows:

- A lack of experimental data on pressure losses for the diaphragm valve is apparent and should be remedied as it is of great importance, considering the widespread use of this type of valve;
- laminar flow in valves requires more investigation as it occurs more frequently in slurry applications due to water restriction law (South-Africa, 1998) and higher concentration pumping . Although some work has been done on other types of valves, these were limited to the turbulent flow and tests conducted mostly with Newtonian fluids - water in particular;
- valve size effect should be ascertained and their influence on correlation predicting pressure loss determined;
- losses through partially opened valve should be investigated as valves also operate in intermediate opening positions and,
- correlations for laminar, transition and turbulent losses will be advantageous as would the critical Reynolds number, so that the laminar C_v or turbulent k_v could be applied to determine the pressure losses.

CHAPTER 3

CHAPTER 3

EXPERIMENTAL WORK

3.1 INTRODUCTION

The test work for this project was conducted at the Flow Process Research Centre (FPRC) of the Cape Peninsula University of Technology on Cape Town campus. The experimental test work completed on an exclusively designed and constructed rig.

Prior to the construction of this test facility, another smaller rig tested contraction and expansion fittings. That work was instrumental in the understanding of the experimental procedures for measuring fittings' loss coefficients (Pienaar, 2004 and Baudouin, 2003). The experience gained on that rig was taken into account in the design and building stages of the new valve test rig.

This chapter presents the following aspects of the experimental work:

- Description of the experimental rig;
- instrumentation;
- experimental procedures;
- valves tested;
- materials tested and,
- experimental errors.

3.2 DESCRIPTION OF THE EXPERIMENTAL RIG

The experimental rig is shown in Figure 3.1 and consists of six lines of PVC pipes with diameters ranging from 50 mm to 110 mm. These lines are each 25 m long and contain a test diaphragm valve.

This length was chosen to allow a fully developed flow before and after each test valve.

Test fluids were mixed in a 1.7 m^3 mixing tank, this tank was rubber-lined to avoid chemical reactions of fluid with metal. The fluids were circulated in a continuous loop as follows: From the storage tank, fluids were pumped out with a positive displacement pump before passing through a heat exchanger. After the heat exchanger, two valves coupled in parallel directed the flow either to the high part of the rig (which contained smaller pipe 42 mm and 50 mm ID) or the lower part (which contained bigger pipes, 63 mm, 80 mm and 2x100 mm ID). The two routes were equipped with a flow meter. After the flow meters the fluids could enter any of the 6 test sections. Each test section had 9 pressure tappings, a schematic diagram showing the locations these pressure tapings can be seen in Appendix E. An on/off valve was situated at the beginning of each line for isolation so that only one line was tested at a time. After fluid had passed through a test section it was collected, via a common pipe, and directed to the mixing tank. At the outlet it was possible to send the fluid through a weigh tank used for calibration purposes.

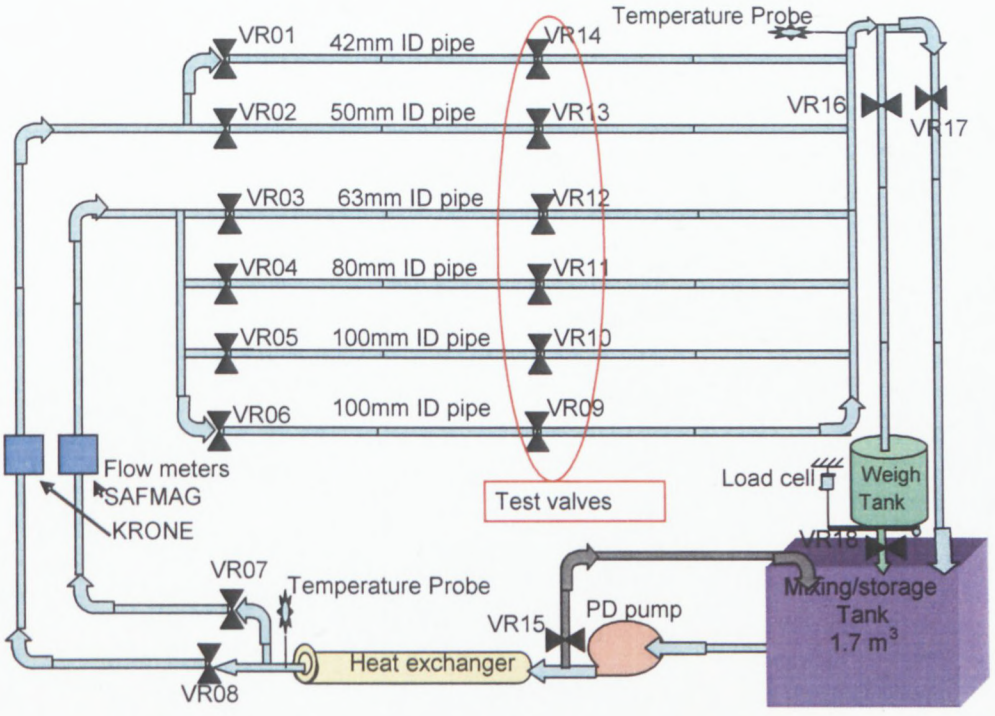

Figure 3.1: Schematic diagram of valve test rig

3.3 INSTRUMENTATION

This section presents all the instruments connected to the rig or used in order to collect experimental data.

3.3.1 Pressure Transducers

Two types of pressure transducer were used to measure the pressure: The point pressure transducer and the differential pressure transducer.

1) Point Pressure Transducers (PPT):

The pressure gradients in the test pipes were measured with 9 point pressure transducers of the type PHPWO1V1-AKAYY-OY [GP] version 25.0 Fuji Electric. These PPT's had a maximum range of 130 kPa with a precision of 0.25 %. The output of these instruments was a DC current ranging from 4 to20 mA, proportional to the pressure applied. The range and span of these instruments were adjusted by a hand held communicator (HHC)

2) Differential Pressure Transducers (DP cell):

Two DP cells of the type IKKW35VI-AKCYYAA [DP] version 25.0 Fuji Electric were used to measure differential pressures. The maximum ranges were 6 kPa and 60 kPa respectively. They had the same characteristics as the PTT i.e. a precision of 0.25 % and could be adjusted with a HHC.

3.3.2 The Hand Held Communicator (HHC)

A Fuji electric hand held communicator, type FXY 10AY A3, was used. This portable instrument was connected to the PPT or DP cell to change parameters such as: data display, range, span, time constant, units, calibration, etc. It was mainly used to change the ranges and to calibrate the transducers.

3.3.3 Data Acquisition Unit (DAU)

A Hewlett Packard (HP) data acquisition unit of the type HP 34970A was connected to a computer. This instrument received through various channels, analogue signals from

different parts of the rig (DP cell, PTT, temperature probes, load cell) and converted them to digital signals compatible with a PC.

3.3.4 Computer

All processes were controlled by a central PC, a Celeron 300. This was coupled with the DAU as an interface and was used to capture and process the experimental data automatically. Test programs were written in Visual Basics 6. The computation of the data was made using pre-programmed Microsoft Excel spreadsheets.

3.3.5 Flow Meters

Two flow meters were used to measure the flow rate of the test fluids, a Safmag flow meter of 80 mm internal diameter was installed to measure flow rate in the bigger pipes (63 mm, 80 mm, 100 mm) and a Khrone flow meter of 42 mm internal diameter was installed to measure flow rate in the smaller pipes (42 mm and 50 mm).

3.3.6 Pumps

A progressive cavity positive displacement pump was used to circulate the fluid in the test loop. This pump was driven by an electric motor of 5.5 kW. It had a maximum capacity of 11 l/s (39.6 m^3/h). A connection to another rig was made in order to have higher flow rates so that sufficient pressure drop could be obtained in larger pipes when pumping water. This rig had two centrifugal pumps of 80 l/s and 140 l/s (288 m^3/h and 504 m^3/h) maximum flow rate, and were driven by a 45 kW and a 90 kW electric motor respectively.

3.3.7 Weigh Tank and Load Cell

These were used to determine the flow rate of the test fluid during the calibration or when running a test at low flow rate. The set-up consisted of a 500 l weigh tank installed above the storage tank. It was suspended to the ceiling via a load cell. The load cell was made of a rectangular piece of stainless steel bar, with strain gauge resistors connected at the point of maximum strain. The resistors were connected to a power supply of 5 V, so that an output voltage varied linearly with an applied force proportional to the weight of fluid retained in the tank. The output voltage was sent to the PC via the DAU.

3.3.8 Heat Exchanger

A double pipe heat exchanger was installed at the inlet of the rig to keep the test fluids at a constant temperature.

3.3.9 Temperature Probes

Two temperature probes were installed to measure the temperature before and after a fluid had entered a test section.

3.3.10 Mixer

A mixer was fitted to the storage tank to mix the test fluids at the preparation stage. At times, the mixer was run during a test to keep the fluid particles suspended. This mixer was driven by a 3 KW electrical motor.

3.3.11 Valves Board and Pressure lines

A switchboard made of small ball valves, as shown in Figure 3.2, was used to select a particular test section and direct their pressure readings to specific pressure transducers so that different test modes could be possible.

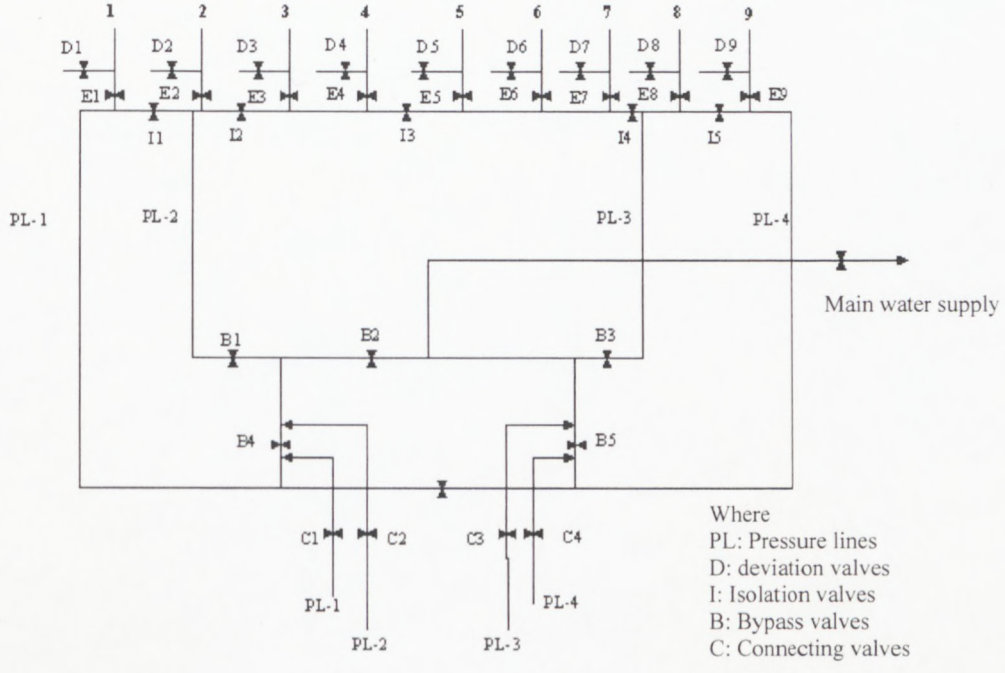

Figure 3.2: Pressure lines board of the valve test rig

Figure 3.2, presents schematically the connection of pressure lines on the valves board. These pressures lines were made of nylon tubes of 3mm internal diameter and filled with water. Deviation valves (D1, D2, ...,D9) were on-off valves giving access to pressure transducers. Pressures lines [(PL1, ..., PL4) and (1,2, ...,9)] were connected to the test sections' pressure tappings via pods filled with water. The purpose of the pods was to collect any solid particles that might come from the test fluid, preventing it from entering the pressure lines. Each pod had a valve on top and at the bottom. The top valve was for flushing away any air bubbles and the bottom valve was used for flushing away any solids particles.

3.4 EXPERIMENTAL PROCEDURES

This section describes the procedure used to gather the experimental data. It consists of the calibration of transducers, load cell and flow meters, measuring the pipe internal diameter, setting the valve positions, measuring the density, running tests to measure the viscous properties of fluids and running tests to measure valve loss coefficients.

3.4.1 Calibration Procedures

The aim of the calibration was two fold: firstly, to ensure that the measuring instrument readings were valid, (normally this is done by double checking the measurement with other devices), and secondly, to ensure that the readings appearing on the PC via the DAU were as close as possible to actual readings.

a) Load Cell

To calibrate the load cell, the weigh tank was emptied. It was ensured that nothing disturbed the tank. The calibration procedure was as follows:

1. Switch on the computer and load the calibration program.
2. Select an appropriate channel on the DAU assigned to capture the voltage induced on the load cell.
3. Divert water flow into the weigh tank and fill it to a certain level.
4. Re-direct the water to the mixing tank.

5. Record the voltage indicated on the DAU and use a bucket to collect all water from the weigh tank and weigh it on the portable scale (Ohaus).
6. Repeat steps 3 to 5 for different water levels and record both voltage and weight.
7. Plot the weight versus the voltage and perform a linear regression to determine the slope and the intercept of the straight line.

The linear relationship of the weight versus the voltage for load cell calibration is given in Figure 3.3.

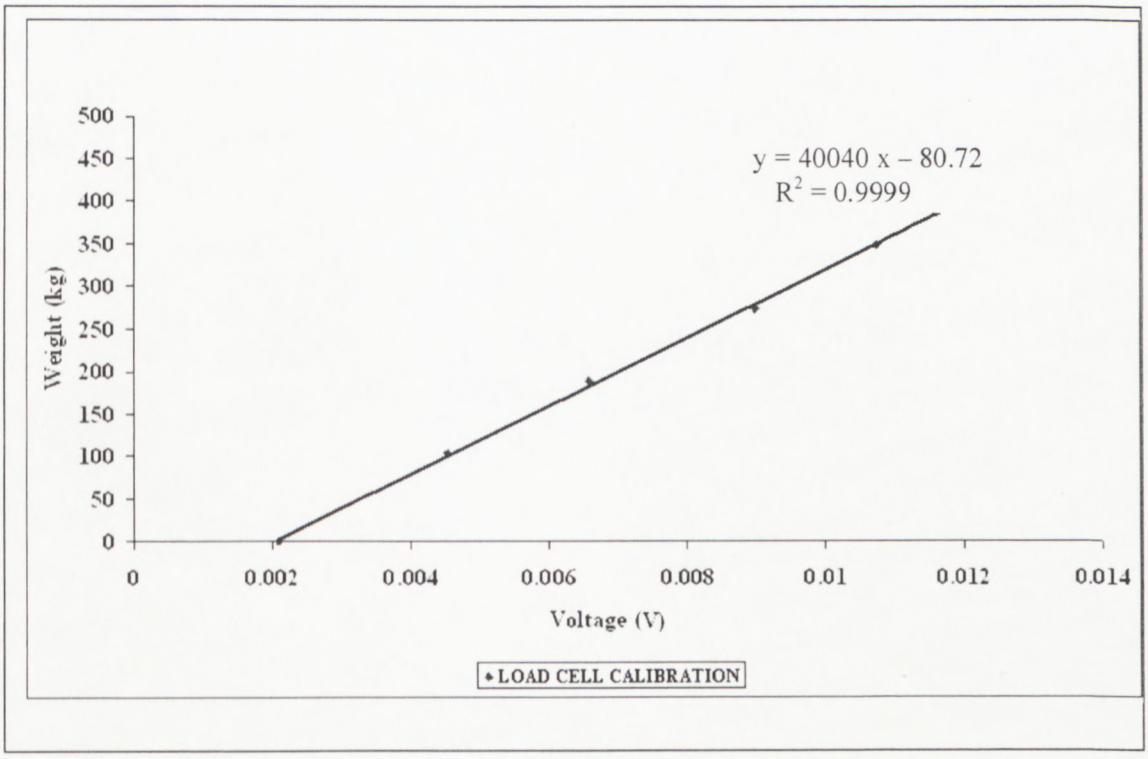

Figure 3.3: Load cell calibration line

b) Flow meters

The flow meters were calibrated using the weigh tank, the load cell, DAU and the computer program. The weigh tank was used to record the mass of water, the DAU was

used to record the voltage induced by the flow meter while the program was used to record both the mass and the time in order to determine the flow rate. The calibration procedure was as follows:

1. Open the computer program and select the appropriate channel on the DAU for the Khrone flow meter.
2. Choose the time interval for which the mass of the tank should be recorded by the computer program.
3. Pump water through the rig and close valves VR07 and VR17 with VR16 open (Figure 3.1) to divert the flow through the Khrone flow meter and the weigh tank.
4. Close valve VR18 at the bottom of the weigh tank to accumulate water in the tank.
5. Start the computer program. Stop it when the tank is almost full.
6. Record the voltage reading on the DAU.
7. Empty the weigh tank by opening valve VR18 at the bottom of the tank.
8. Vary the speed of the pump to change the flow rate of water through the rig.
9. Repeat steps 4 to 8 to record another set of data.
10. Repeat the same procedure to acquire at least five sets of data at differing flow rates.
11. Follow the same procedure to calibrate the Safmag flow meter. Water flow was diverted through the Safmag flow meter by first opening valve VR07 and closing valve VR08.

The mass flow rate through the flow meter was determined as the ratio of the recorded mass of the weigh tank to the time it took to fill. It was converted to the volumetric flow rate by dividing by the density of water at its recorded temperature.

The calibration curves obtained for the Khrone and Safmag flow meters are shown in Figure 3.4 and Figure 3.5 respectively.

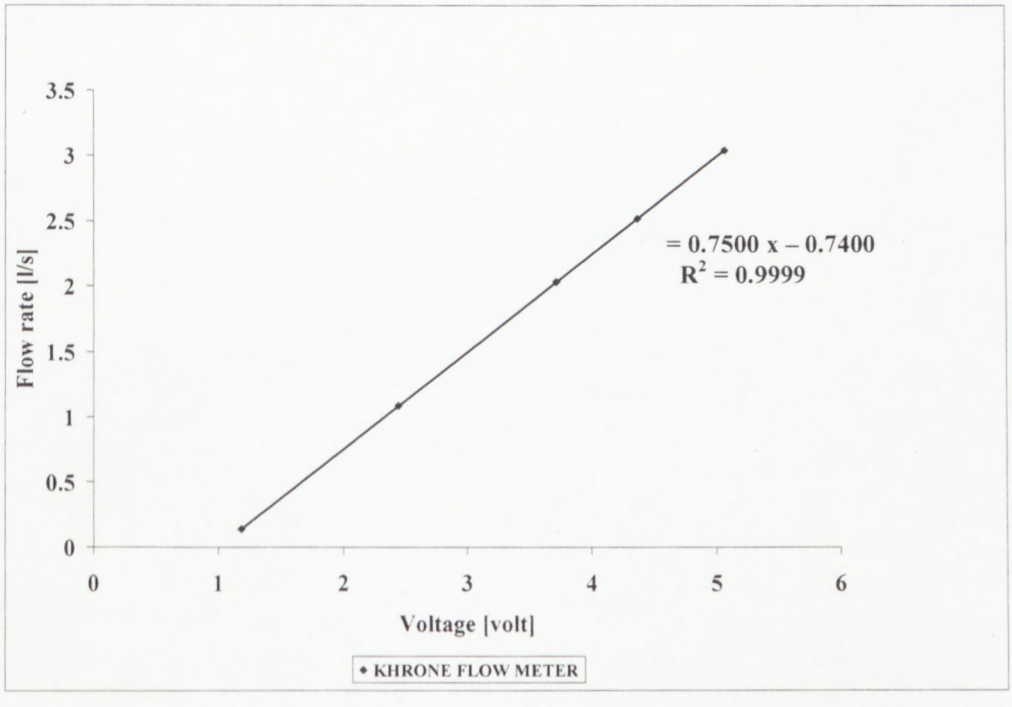

Figure 3.4: Khrone flow meter calibration constants

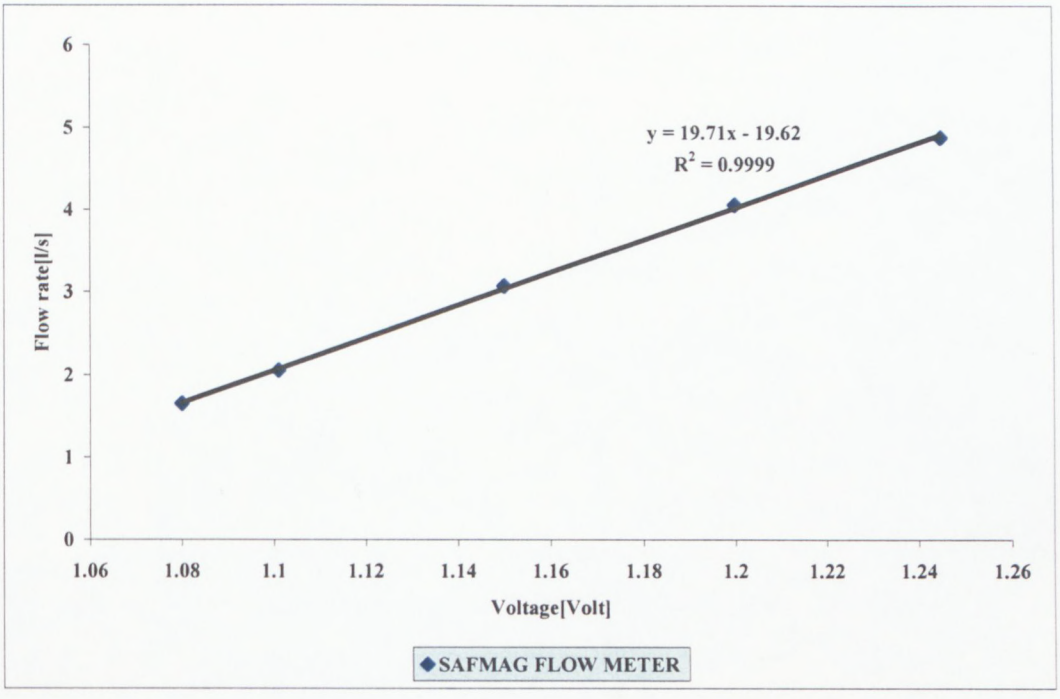

Figure 3.5: Safmag flow meter calibration constants

c) Transducers

The PTT and DP cells were checked using a water/mercury manometer connected to the transducers. A pressure was applied to the transducers. The magnitude of this pressure could be found directly from the manometer by converting the column of water or mercury into pressure.

The procedure is as follows:

1. Open the calibration computer program and switch on the DAU to the appropriate channel.
2. Open the transducer's cap and set it to zero.

3. Open the pressure tap leading to the transducers and expose them to the atmosphere, to release any residual pressure.
4. Connect the manometer to the transducers and switch it on.
5. Set a pressure difference on the manometer.
6. Read the pressure from the manometer and the voltage recorded by the DAU.
7. Continue to increase the pressure on the transducers, recording the pressure and voltage readings to acquire at least six different readings.
8. Plot the pressure readings against the voltage reading to determine the linear relationship between them. The slope and the intercept of this linear relationship were used to relate a pressure applied by the test fluid in the rig to the voltage recorded by the DAU.

Typical calibration curves obtained for point pressure transducers and DP cell are shown in Figure 3.6 and Figure 3.7 respectively.

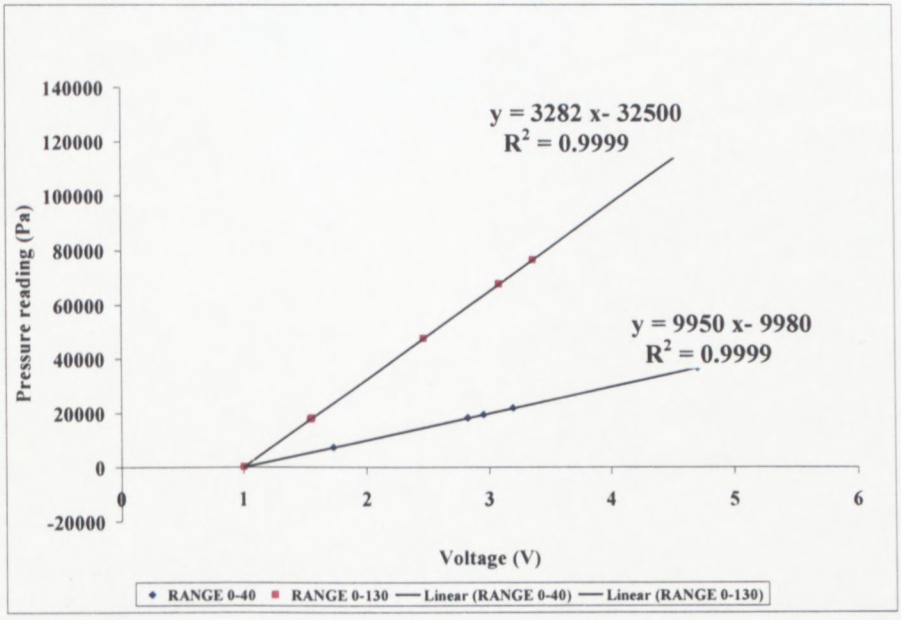

Figure 3.6: Typical calibration curve of Point Pressure Transducer

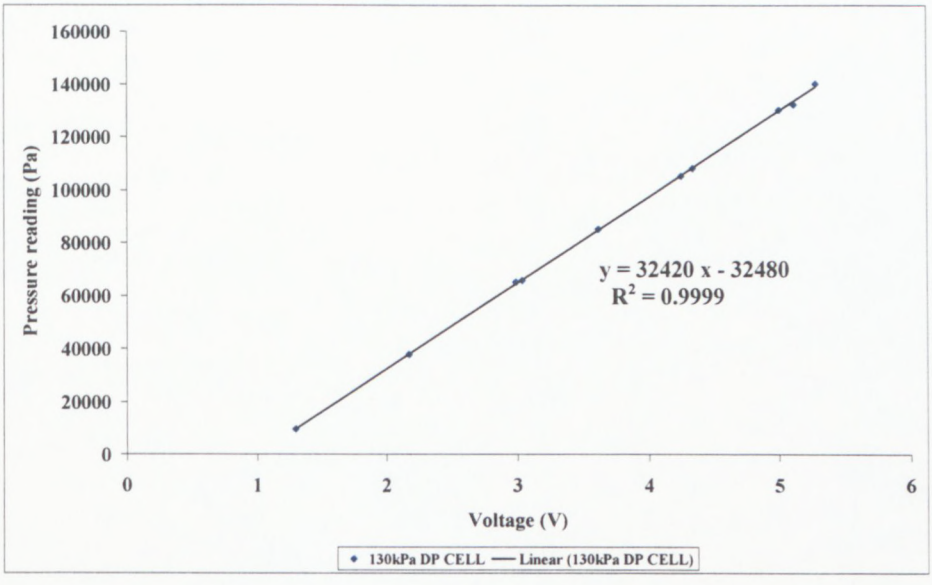

Figure 3.7: Calibration curve of the 130-kPa DP cell

3.4.2 Measuring the Pipe Internal Diameters

It was important to measure the internal diameters of all the pipes used in the test sections, as these values were needed to calculate the velocities in the pipes.

The internal pipe diameters were measured by weighing the mass of water (M_w) filling a known length of pipe (L).The pipe diameter was then calculated from Equation 3.1

$$D = \sqrt{\frac{4M_w}{\pi \rho_w L}} \qquad \text{Eq 3.1}$$

Where ρ_w is the water density

The method used to determine the diameter of the test sections on the valve test rig was as follows:

1. A pipe was unscrewed at the flanges and removed from the rig.

2. The pipe was fitted with a rubber plug or valve (ball valve) mounted on the flanges at one end of the pipe.
3. The pipe was then positioned into an upright position, with a valve at the bottom of the pipe, and filled with water.
4. The next step was to measure the temperature of water and determine its density at that temperature from literature.
5. The water level in the vertically positioned pipe was marked as point A_o.
6. Water was drained out of the pipe to level A_1 by opening the valve at bottom of the pipe. The distance between A_o and A_1 was measured and the water drained was weighed and recorded.
7. Water was again drained to another level, A_2, and the mass of the drained water and the distance of drainage were recorded. This was repeated three more times to obtain a set of five readings of drained mass and the drainage distance.
8. Using the measured mass of water, M_w, drainage length, L, and known water density, Equation 3.1 was applied to determine the internal diameter of the pipe.

The results of all these measurements are shown in Table 3.1. Weighted averages of the test sections have been calculated, the weight being the number of repeated measurements taken.

Table 3.1: Internal pipe diameters of the test sections

Test section Position (Figure 3.1)	F-LHS ID (cm)	LHS ID (cm)	RHS ID (cm)	F-RHS ID (cm)	Weighted Average ID (cm)
Top	4.217	4.209	4.205	4.207	**4.212**
2nd Top	5.299	5.298	5.317	5.215	**5.280**
3rd Top	6.295	6.324	6.299	6.306	**6.308**
4th Top	8.040	8.047	8.045	8.041	**8.043**
2nd Bottom*	9.913	9.919	9.924	9.888	**9.911**
Bottom	9.621	9.925	9.668	9.621	**9.717**

In Table 3.1, F stand for far, LHS and RHS stand for left hand side and right side respectively as shown in Figure 3.8.

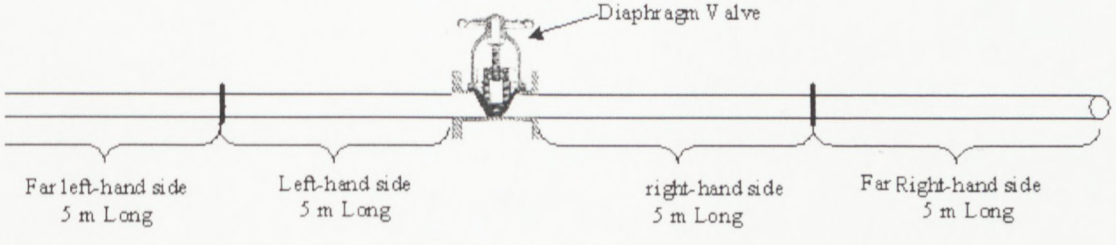

Figure 3.8: Typical test section of the valve test section

* This test section was not part of this study

3.4.3 Setting the Valve Opening Positions

The setting of the valves opening position was conducted using the gravity test as explained in Sections 3.5.2 and 3.5.3

3.4.4 Fluid Relative Density

The fluid relative density was measured from a fluid sample collected from a sampling valve on the rig. About one litre of fluid was collected; half of it was retained and labelled for future reference. The other half was used for the relative density test according to a standard procedure in the FPRC as follows:

1. Three clean, dry volumetric flasks were weighed separately (M1).
2. The fluid was poured in to those flasks (approximately half the volume) and weighed respectively (M2).
3. Water was added up to the graduated mark of the flasks, and each was weighed (M3). Flasks had to be shaken gently to remove any air bubbles.
4. The flasks were emptied and rinsed with water and alcohol to dry. They were filled completely with water to the same graduated mark and each was weighed (M4).

Calculations

Mass of fluid: M2-M1

Mass of water filling the flask: M4-M1

Mass of water filling the space left by the fluid: M3-M2

Mass of water having volume equal to that of the fluid: (M4-M1)-(M3-M2).

Therefore $$RD = \frac{\text{Mass of fluid}}{\text{Mass of equal volume of water}}$$

$$RD = \frac{M2 - M1}{(M4 - M1) - (M3 - M2)} \qquad \text{Eq 3.2}$$

The arithmetic mean of the values obtained from the three flasks (which did not differ appreciably) was taken as the actual RD. A typical example of such a test is given in Appendix A.

3.4.5 Valve Test Procedures

The purpose of a test on the valve test rig was to obtain a set of pressure drops versus flow rates. These were further transformed into a set of k_v versus Reynolds number.

In this section, the general operation mode of the valve test rig is explained step by step. In addition, brief descriptions of the particular modes such as HGL manual mode, HGL automatic mode, DP cell mode or the straight pipe test are also given.

a) General Mode

1. Switch on the computer and open the desired programme of test operation, i.e. the HGL manual mode, automatic mode, DP cell mode or the straight pipe test.
2. In the case of testing a settling slurry, switch on the mixer to mix the slurry evenly.
3. Open fully the by-pass valve VR 15 (Figure 3.1) positioned immediately after the pump, to ensure no build-up of pressure occurs in the rig if all outlet valves were closed.
4. Switch on the pump and set it at the desired speed to achieve a certain flow rate.
5. Open all the diaphragm valves in the system to circulate the test fluid left in the rig.
6. Close the bypass valve and let the rig run for a while to thoroughly mix the test fluid.
7. Select a test section :
    - To conduct a test on the 42 mm or 50 mm ID pipes, ensure that valve VR08 is open and close valve VR07. Then choose either the 42 mm ID pipe or the 50 mm ID pipe by closing either VR01 or VR02, as shown in Figure 3.1;
    - to conduct a test on the 63 mm ID, 80 mm ID or the 100 mm ID pipes, open valve VR07 and close VR08 and,
    - Choose the desired pipe among the four pipes fed though VR07 by opening or closing the appropriate valves among VR03, VR04, VR05 and VR06.
8. Decide on the required pressure tappings on the test section and record their distances in the appropriate columns of the spreadsheet.

9. Flush the pods and the pressure line board and fill them with tap water, ensuring that there are no bubbles in the tubes. Open the ball valves of the pressure tappings leading to the pods
10. Use the HHC to set the pressure range to be used during the test on each transducer.
11. Connect the pressure tapping to the transducers by opening or closing the appropriate valves on the pressure lines board.
12. Take a sample of the fluid and conduct the RD tests as explained in Section 3.4.4 Send another sample to the rheology lab.
13. Record the necessary information on the computer program, i.e. the selected tapping distances, pressure ranges, pipe diameter, fluids density, the type and concentration of fluid, the date and the name of the operator.
14. Start the test
15. Change the flow rate of the fluid by increasing or decreasing the pump speed.
16. Perform the flow stability control test and take a reading only if the flow had stabilised.
17. Repeat steps 15 and 16 until the maximum pressure range or flow rate is reached.

b) HGL Manual mode test

The hydraulic gradeline, manual mode of the valve test rig was used when pressure drops were lower than 1300 Pa, especially when testing the larger pipes. It consisted of recording the static pressure at one, tapping using either one PTT or all nine PPTs together.

c) HGL automatic mode

The hydraulic gradeline, automatic mode of the valve test rig was used when pressure drops were high enough. It consisted of connecting each pressure tap to each PTT separately so that on a click, all the static pressures could be recorded at the same time; this was the default mode.

d) Straight pipe test or rheology mode

The straight pipe test, or rheology mode, was used to measure the viscous properties of the fluids. This test consisted of measuring simultaneously on the upstream and downstream sides of the test valve, pressure drop over a straight part of the test section at least 50 diameters away from the bend or the test valve. The pressure drops were measured with the two DP cells separately, but simultaneously. This test was conducted in at least two different diameter pipes to ensure that there was no slip effect. Only laminar data was used for rheological charcterisation as explained in Section 2.6.4.

e) HGL, DP cell mode

The hydraulic gradeline, DP cell mode, was used when the pressure drops in the test section were too high, especially when testing viscous fluids in the small pipes. This test consisted of obtaining the hydraulic gradeline with a DP cell as follows. The first pressure tap on the test section was chosen as a reference. Then the HGL was obtained by

reading the pressure drop between the first tap and the others eight taps successively, by opening and closing the appropriate valves on the valves board. This test was similar to the manual mode test, the only difference being a DP cell was used instead of the PPT's.

3.5 VALVES TESTED

The valves tested in this study were the straight-through type i.e. without a weir. These valves are suitable for slurry applications. A schematic diagram and a photograph of one these valves are shown in Figure 3.9 and Figure 3.10, respectively. They consist of two principal parts, the bonnet and the base, which are separated by a paraboloidal-shaped flexible rubber band (the diaphragm). The bonnet consists of a hand wheel and the spindle, which together drive the diaphragm down across the flow area to obstruct the flow

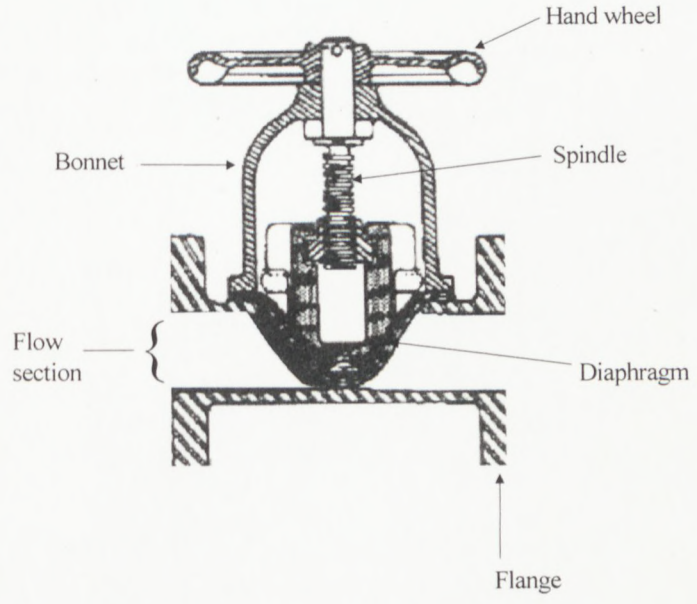

Figure 3.9: Schematic diagram of a Natco diaphragm valve (Warring, 1982)

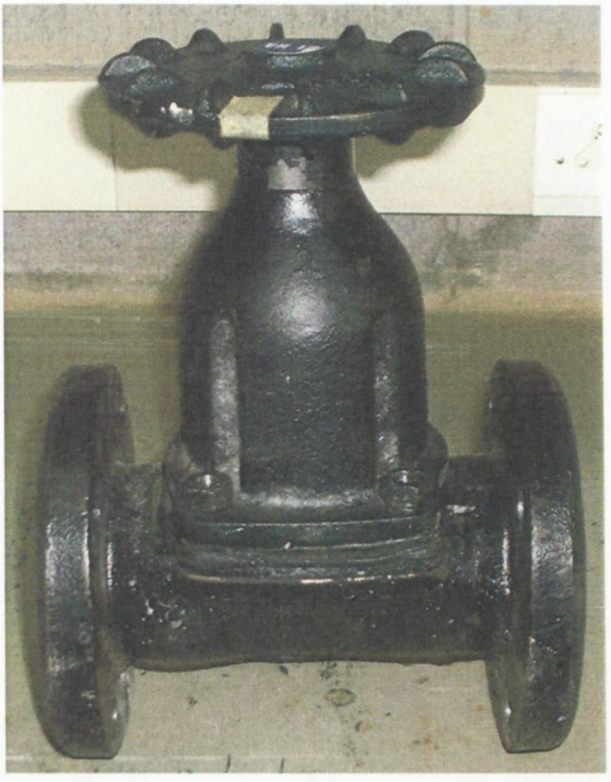

Figure 3.10: Photograph of a Natco diaphragm valve

Five diaphragm valves (from Natco Valves) have been tested during of this study. Additional valves from a different manufacturer (Saunders Valves) have also been tested. The external dimensions of these valves are shown in Table 3.2

Table 3.2: External dimensions of Natco valves

Nominal bore	A	B	C	Safe working Pressure
mm	mm	mm	mm	kPa
40	83	121	159	700
50	140	181	191	700
65	165	200	216	700
80	197	245	254	700
100	254	267	305	700

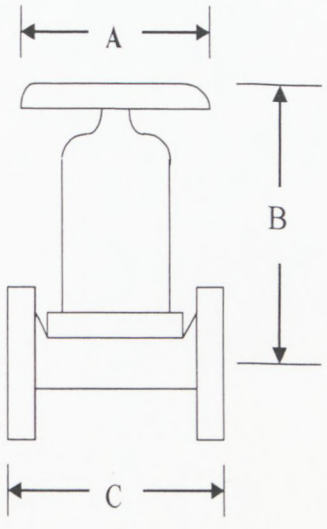

It was unfortunate that the values of dimensions shown in Table 3.2 do not have a geometric similarity, for instance the dimension C, which is the length of the flow path of fluid through the valve, if the 40 mm bore valve is taken as a prototype, all C dimension of other valves are shorter than should be for geometric similarity to be observed. Only the 80 mm valve bore shows an acceptable similarity, on dimension B, with the 40 mm bore valve. From the outset therefore, the external dimensions of the valves do not follow a geometrical similarity. This fact is probably dictated by an economic aspect in the manufacturing process. The next section looks at the internal dimensions of valves.

3.5.1 Internal Dimension of Valves

The valves' internal dimensions were measured after they had been unscrewed. A schematic diagram of the inside dimensions of the valves is shown in Figure 3.11.

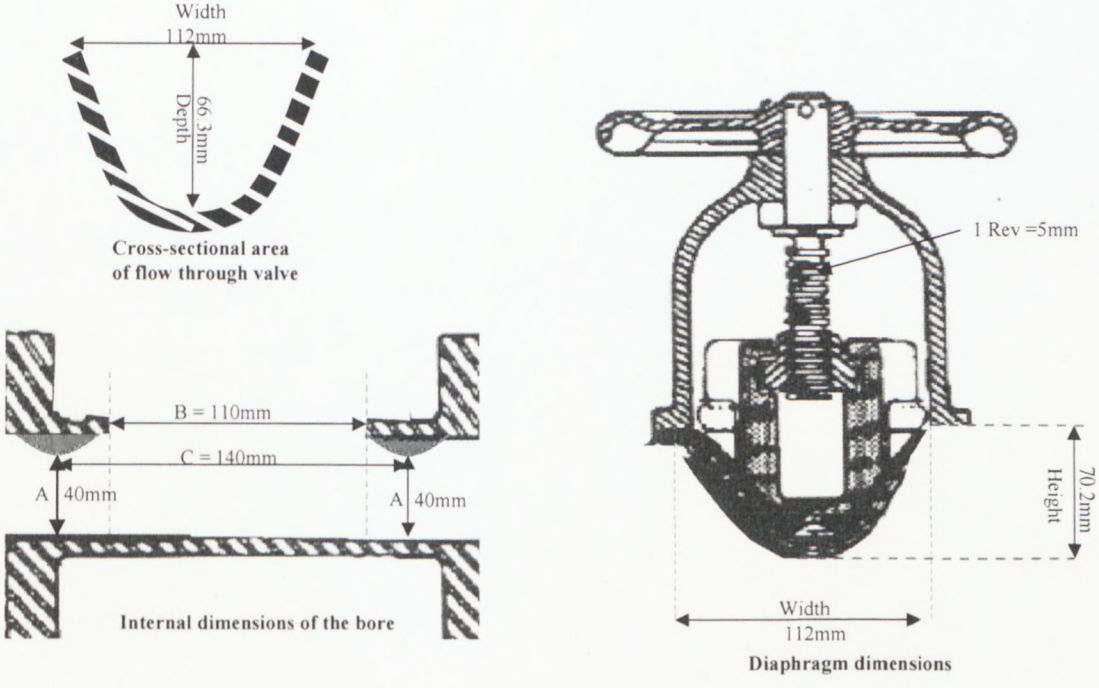

Figure 3.11 Internal dimension of the 80 mm bore diaphragm valve (Pienaar et al., 2006)

The internal measured dimensions for all the Natco valves tested are shown in Table 3.3.

Table 3.3: Internal dimensions of the diaphragm valves (Pienaar *et al*, 2006)

Bore size	Cross section area (mm)		Diaphragm Dimension (mm)			Bore dimension (mm)		
	Depth	Width	Height	Width	Per Rev	A	B	C
40	35.26	42.78	36.00	47.38	4.50	26.18	45.02	65.34
50	46.65	64.26	47.00	66.34	4.27	36.26	66.71	81.00
65	62.42	90.82	63.00	92.14	6.30	40.00	88.00	125.00
80	68.92	112.00	69.00	114.20	6.27	42.26	111.0	140.50
100	74.72	124.46	75.00	129.92	5.36	62.14	128.0	150.40

A close look at the values given in Table 3.3 shows that the measured values also do not portray a geometrical similarity. However, some dimensions such as the depth of the cross sectional area and the height of the diaphragm proved close correlation with the bore dimensions.

3.5.2 Valves Opening setting

Because valves can assume many positions - from fully opened to fully closed - it was necessary to establish a way of determining exactly the percentage opening of the valve so that the position of interest, 100 %, 75 %, 50 % and 25 % opened could be chosen without ambiguity.

A first attempt was made by taking photographs of the cross sections of the valves as the diaphragm was gradually moved down by turning the hand wheel as shown in Figure 3.12. It was expected the flow area would be proportional to the opening pictured on the side view of the valve. Analytic and numeric approaches were used to quantify these areas, to establish a modus operandus of setting positions. This procedure however, was abandoned, because, when a valve was dismantled it became evident the section seen from a side view was a combination of areas not situated in the same plane. Therefore, a new approach, so-called "the gravity test" was introduced and is described in the next section.

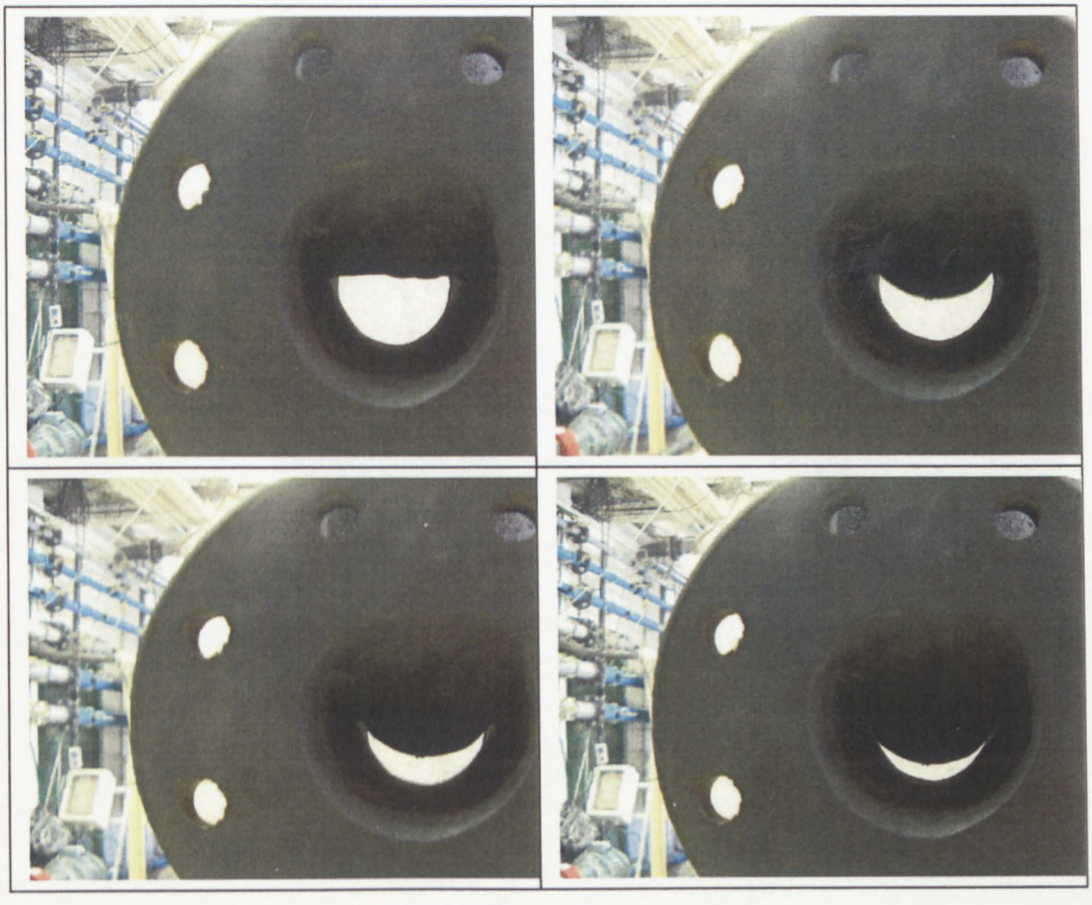

Figure 3.12: Cross-sectional view of the 80 mm bore valve at full, ½, ¾ and ¼, open positions respectively

3.5.3 Gravity Test

In this test, about 3 m^3 of water was stored in a tank (from another rig) as shown in Figure 3.13. The test valve was connected at the end of the exit pipe so that water flowed freely by gravity when the valve was opened. The test valve was causing the major obstruction to the flow of water, therefore the flow depended on the discharge coefficient of the valve and the level of water in the storage tank.

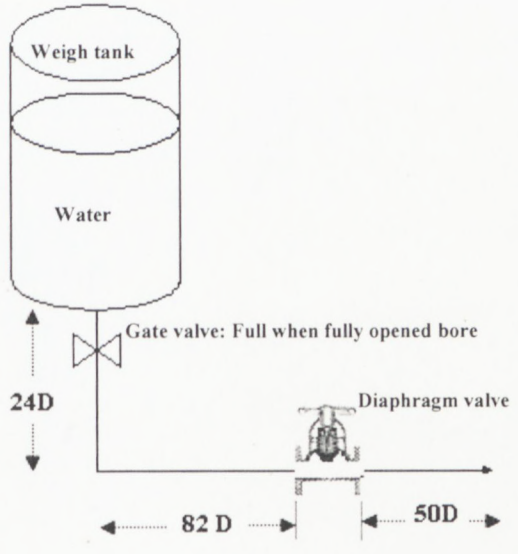

Figure 3.13: Gravity flow system used to determine the valve positions

The procedure was as follows:

1. Open the computer program that records the mass of water within the weigh tank.
2. Fill the weigh tank with water.

3. Set the valve at fully opened position.
4. Select the time interval, for which the mass of water was to be recorded, ideally at 1sec intervals.
5. Start the program to record the mass of water in the tank every second.
6. Open the valve at the bottom of the weigh tank to allow water to run through the valve, recording the change in mass simultaneously.
7. Stop the computer programme once the tank emptied.
8. Close the valve, at the bottom of the tank, and refill it.
9. Set the valve position by revolving the hand-wheel once, (first revolution), towards the closing position.
10. Repeat steps 4 to 8.
11. Set the valve position by revolving the hand-wheel once more. This was a second revolution, towards the closing position.
12. Repeat steps 4 to 8.
13. Conduct the experiment until the valve was fully closed.

Typical results, of such test are shown in Appendix B and the associated graphs are shown in Figure 3.14 where the equation of the 8^{th} revolution is shown. The slope of this line is proportional to the flow rate initiated when the valve is set on the 8^{th} revolution.

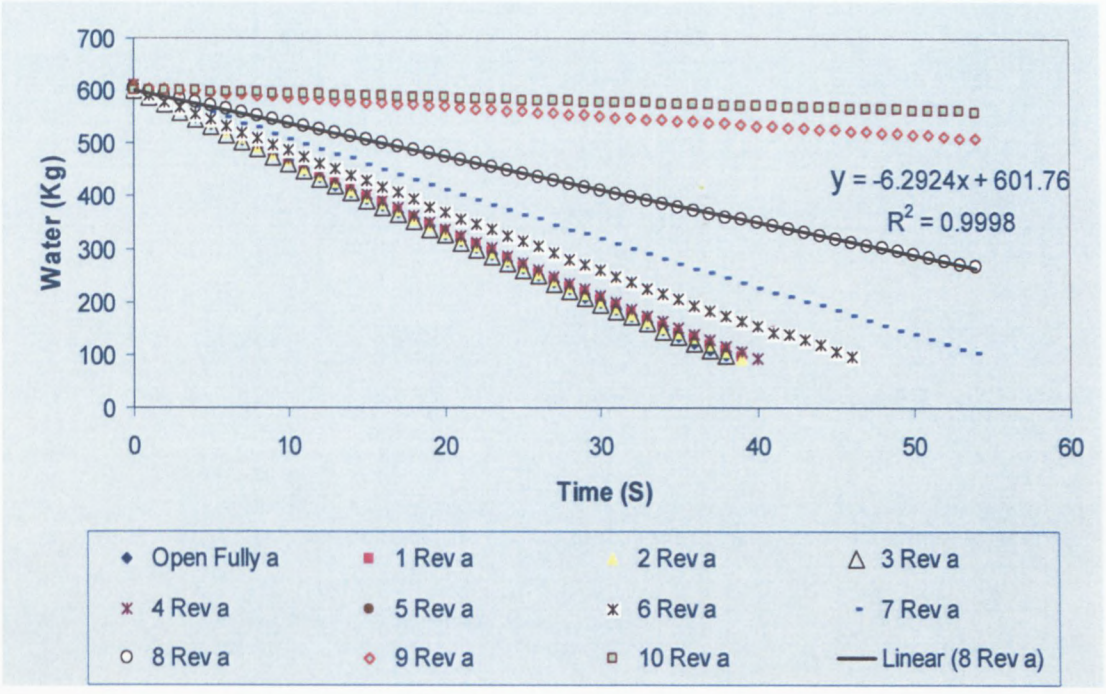

Figure 3.14: Gravity test for 65 mm bore diaphragm valve

From these curves the flow rate was obtained as a first derivative of the curve at a specific height. It was observed however, even taking the gradient over a short linear part of these curves, that results were insignificantly different. As there were many tests to perform, the latter procedure which is faster was used to calculate the flow rate for each valve opening.

The data generated from these tests was used to construct the valve characteristic as shown below.

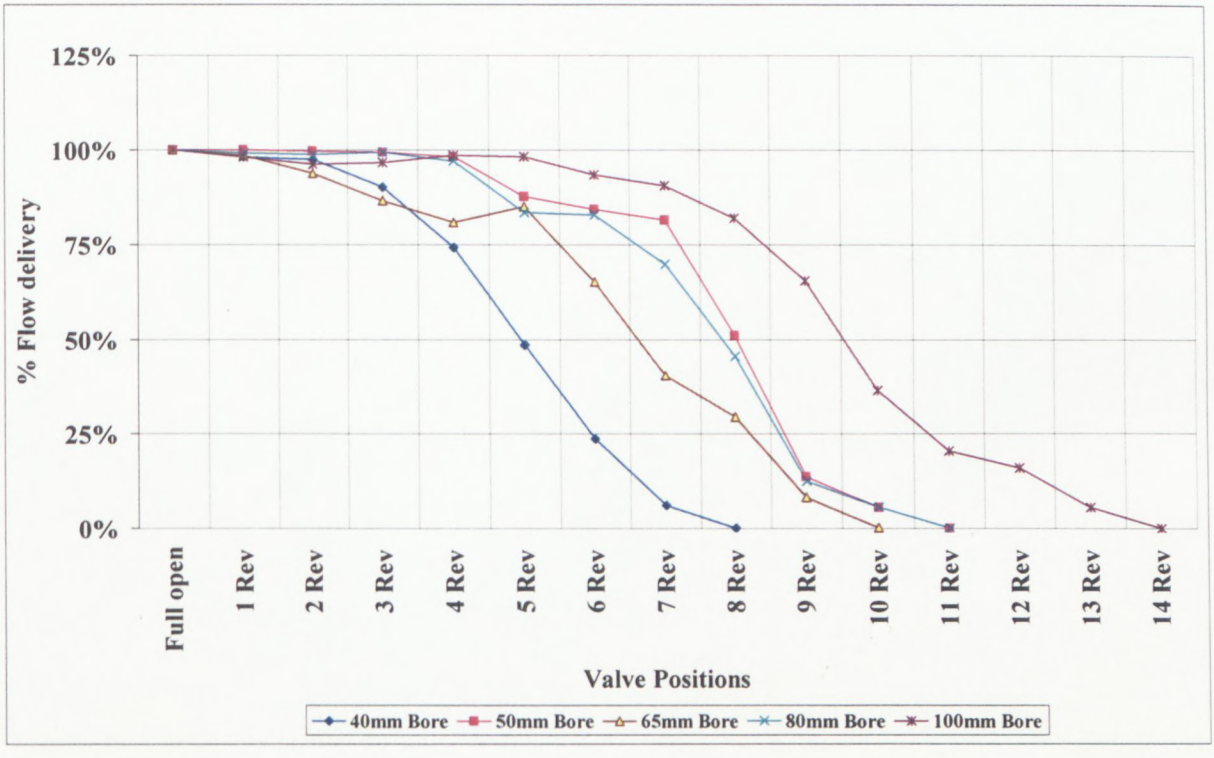

Figure 3.15: Percentage flow delivery at different valve positions

Figure 3.15 was used to determine the valve opening positions. A valve position (θ), in this study, is defined as the ratio of flows discharged under gravity, with the same head, between a particular valve position and the fully opened position.

For example the 40 mm valve is 50 % opened, when the hand wheel is turned 5 revolutions from the fully opened position. Whereas the 50 mm valve would require to be turned 8 revolutions to obtained the same $\theta = 0.5$.

3.6 MATERIAL/FLUID TESTED

Fluids tested were selected to represent a wide range of rheological behaviour associated with industrial slurries, hence experimental fluids were selected to represent typical examples of Newtonian, pseudo plastic, and viscoplastic models fluids. The materials chosen were:

Typical Newtonian fluids: Water and glycerol solutions.

Typical Non-Newtonian fluids: Pseudoplastic: Carboxyl methyl cellulose (CMC)

Viscoplastic: Kaolin slurries

A detailed description of these fluids is given below.

3.6.1 Water

Ordinary municipal tap water was used. This fluid was mainly used for commissioning the experimental rig. It was also used in the mixture to make up other fluids.

The typical properties of this water are as follow: A pH of 9 with a total alkalinity of 35 mg/l as $CaCO_3$ and an ionic strength of less than 0.01 molar scale (Haldenwang, 2003).

3.6.2 Carboxyl Methyl Cellulose (CMC)

The carboxyl methyl cellulose (CMC) was supplied in granular form in bags of 12 kg. This granular CMC dissolves easily in water at low concentration. Solutions of this material at 5% and 8% (weight/weight) were prepared. These were made up by adding CMC powder in the storage tank which contained a prescribed quantity of water. The solutions were then mechanically agitated with the mixer. Care was taken to avoid formation of lumps. The solutions were then mixed for 48 hours before being pumped into

the rig. CMC solutions are stable between 2 ≤ pH ≤10. Below pH 2 precipitation occurs and above pH 10 the viscosity decreases rapidly. The pH of the solutions tested in these experiments was about 9 at 20° Celsius. Typical pseudo shear diagrams obtained online are shown in Figure 3.16. Industrial applications of this fluid include: as a paper glue, drilling mud, protective colloid, resin emulsion and as a stabiliser in foods.

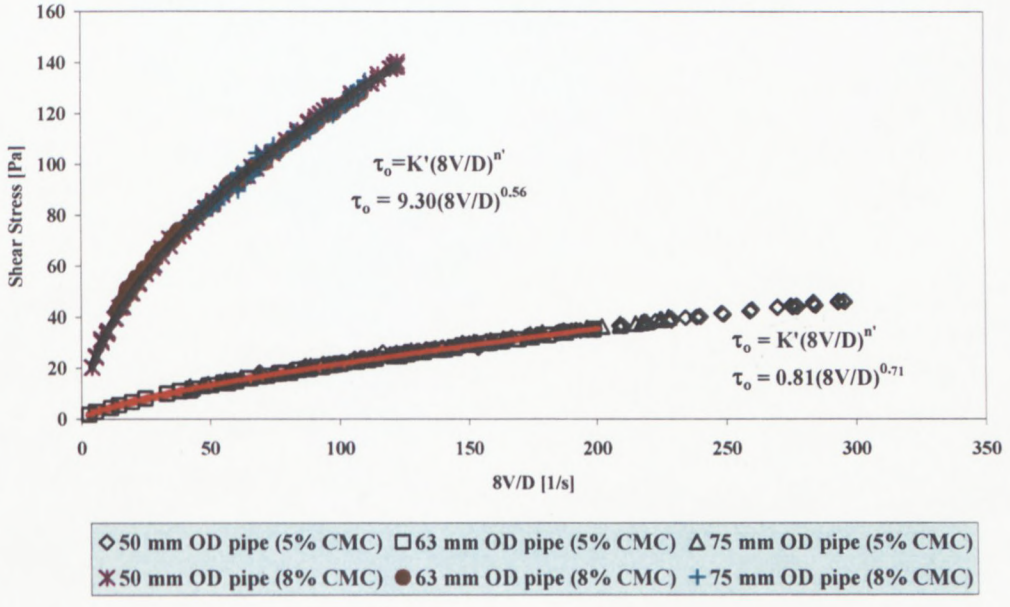

Figure 3.16: Straight pipe test of 5 % and 8 % CMC slurry

3.6.3 Kaolin

Kaolin slurries were prepared by mixing water with kaolin powder. Kaolin powder was supplied by Serina Kaolin (Ltd). This kaolin is mined in the Fish Hoek area near Cape Town. The composition and physical properties of dry kaolin are given in Appendix C.

Kaolin slurries of 10 % and 13 % volumetric concentration were prepared and tested. A typical pseudo shear diagram of this fluid is presented in Figure 3.17.

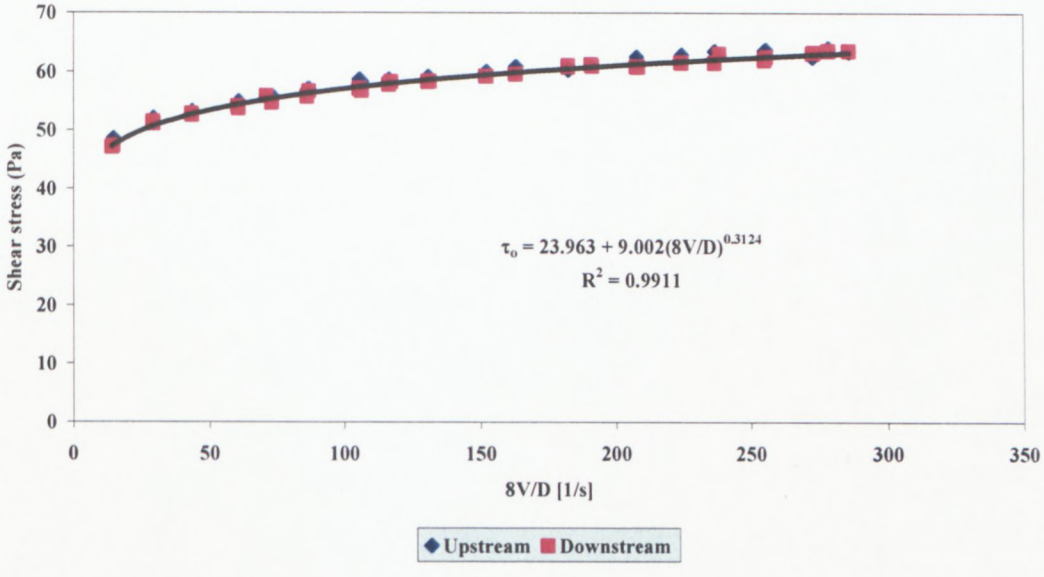

Figure 3. 17: Typical pseudo shear diagram of a 13% kaolin slurry

3.6.4 Glycerine

Pure glycerol was obtained and tested. It was then diluted with tap water to 75 % solution of glycerine in water and tested again. The viscosity of glycerine is very sensitive to changes in temperature, e.g. Perry, (1997) reported values of viscosity with related temperatures as shown in Appendix D.

The cooling system implemented with the double pipe heat exchanger was useful in maintaining the temperature within 1 degree increment from inlet to outlet of the test

section. A typical pseudo shear diagram of this fluid obtained on the rig is shown in Figure 3.18.

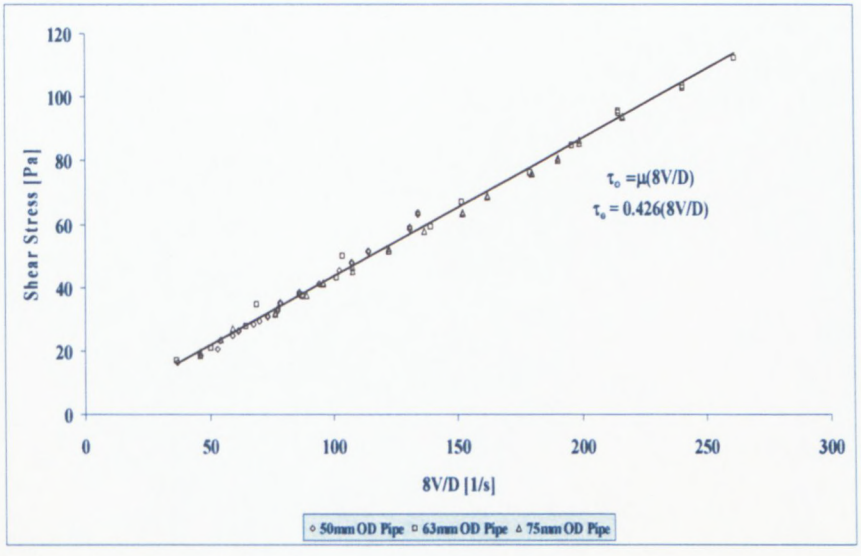

Figure 3.18: Typical pseudo shear diagram of the glycerine

3.7 EXPERIMENTAL ERRORS

The term errors should be seen as the uncertainty associated with an experimental measurement. In research it is of utmost importance to be aware of the sources of errors and to minimise them, especially the systematic errors. But even if care has been taken to eliminate systematic errors, random errors remain in experimental measurements. It is important to know the extent of such uncertainties.

There are two ways to approach the quantification of errors.

1) At the design stage of the experiment, an expression or equation of the experimental errors can be developed and from this expression one should be able to identify which parameters have most influence on the final results. Care should be taken to minimise the errors of these parameters, by choosing an accurate instrument to measure them.

2) A second approach is when the experiment is being performed. The best way to minimise random errors is to take many measurements of one parameter while maintaining constant conditions for the experiment. Use a mean value of these measurements and calculate the uncertainty by using a statistic such the average deviation or the standard deviation. The disadvantage of this approach is that it requires many repeated measurements. Donald (1996) reports that to estimate the uncertainty of an error estimate made from (n) repeated measurements, the following expression can be used.

$$E = \frac{100}{[2(n-1)]^{1/2}} \qquad \text{Eq 3. 3}$$

So based on Equation 3.3, to obtain a 10 % error in the estimation of error one should have to average 51 independent repeated values and for a 1 % error estimate, this number rises to 5001 measurements. Both approaches have been used in this work.

3.7.1 Errors in Measured Variables

The errors in measured variables may be associated with the precision of the instrument used to measure them. Normally an absolute error equivalent to the resolution or the least increment of the instrument can be assumed to occur on any measurement done made.

a) Weight

Samples taken for measuring the density on a daily basis were measured with an electronic balance (Denver Instrument) accurate to ± 0.001 g with a maximum reading of 410 g. Thus a sample of say 100 g would be measured with a relative error of ± 0.001 %. Samples of water taken for measuring the internal diameter or for calibrating the weight tank were measured with an electronic balance (type: Ohaus) accurate at 20 g with a maximum load of 60 kg. A sample of say 10 kg was measured with a relative error of 0.033 %

b) Distances

Tape measures were graduated in mm, thus an absolute error of ± 0.001 m can be assumed on axial distance measured to locate the pressure tapping or drop of water level when measuring the pipe diameter.

c) Flow rate

Flow rates were measured with a Safmag electromagnetic flow meter, according to the manufacturer, the performance specifications are as follows:

- Accuracy: display and frequency output: ± 0.5 % of rate for velocity > 0.5 m/s
  0.025 % of full scale for velocity < 0.5 m/s;

- analog output : above error ± 0.008 mA;
- repeatability ± 0.1 % of rate and,
- Temperature effect ± 0.01 % per degree Celsius.

d) Pressures

Pressure transducers were accurate to 0.25 % of the full range. Care was taken in calibrating the transducers to obtain a correlation coefficient of 0.9999. Such calibration gave rise to an average error of 0.24 %. Thus the overall error in pressure measurement was 0.35 % (quadratic sum of calibration and accuracy errors).

3.7.2 Errors in Computed Variables

When a variable is a result of a computation of other variables with their subsequent errors, the resulting error is the combination of the independent variables errors (quadratic sum of the independents errors). If a variable X is a function of n other variables, i.e., X= F (a, b, c…n), the expected highest error (Brinkworth, 1968) can be calculated from:

$$\left(\frac{\Delta X}{X}\right)^2 = \sum\left(\frac{\partial X}{\partial n}\right)^2\left(\frac{n}{X}\right)^2\left(\frac{\Delta n}{n}\right)^2 \qquad \text{Eq 3. 4}$$

where X is the computed result.

ΔX is the computed result absolute error.

n are the independent variables involved.

Δn are the independent absolute errors.

The reader is referred to Baudouin (2003) where equations of the errors of the major calculated parameters had been derived. However, here, the derivation of the expected error of k_v and Re_3 is shown, as k_v and Re_3 were the final result for the tests.

k_v is obtained from Equation 2.53 as

$$k_v = 2g\, H_v / V^2 \qquad \text{Eq 3. 5}$$

This equation can be simplified to Equation 3.6 by replacing H by ($\Delta P/\rho g$):

$$k_v = 2\Delta P_v/\rho V^2 \qquad \text{Eq 3. 6}$$

Applying Equation 3.4 to Equation 3.6 yields the following result

$$\frac{\Delta k_v}{k_v} = \pm\sqrt{\left(\frac{\Delta(\Delta P_v)}{\Delta P_v}\right)^2 + \left(\frac{\Delta\rho}{\rho}\right)^2 + 4\left(\frac{\Delta V}{V}\right)^2} \qquad \text{Eq 3. 7}$$

As the velocity is also a computed variable obtained from two other independent variables i.e. the flow rate (Q) and the pipe diameter (D), Equation 3.7 can be further developed as:

$$\frac{\Delta k_v}{k_v} = \pm\sqrt{\left(\frac{\Delta(\Delta P_v)}{\Delta P_v}\right)^2 + \left(\frac{\Delta\rho}{\rho}\right)^2 + 4\left(\frac{\Delta Q}{Q}\right)^2 + 16\left(\frac{\Delta D}{D}\right)^2} \qquad \text{Eq 3. 8}$$

The same procedure was applied to Re_3 and the final form is:

$$\left(\frac{\Delta \mathrm{Re}_3}{\mathrm{Re}_3}\right)=\sqrt{\left(\frac{\Delta\rho}{\rho}\right)^2+4\left(\frac{\Delta Q}{Q}\right)^2+\left(\frac{\Delta L}{L}\right)^2+25\left(\frac{\Delta D}{D}\right)^2+\left(\frac{\Delta\Delta P}{\Delta P}\right)^2} \qquad \text{Eq 3.9}$$

It may be seen from Equation 3.8, that the error in diameter will propagate more than the others in the overall error of both k_v and Re_3, followed by the error in flow rate.

3.7.3 Errors Based on Repeated Measurements

A more practical way to reduce random errors is to take many repeated measurements. An approximation of expected error can be deduced from the measurements by using the standard deviation. The absolute error was taken as twice the standard deviation; this is of course assuming a 95 % confidence level.

a) Pipe internal diameter

The errors in pipe diameters have been calculated from the standard deviations of each individual pipe (measured length of 5 m). A weighted average standard deviation has been calculated for each test section. From the weighted average a relative error has been calculated. It should be remembered that the weight was taken as the number of repeated measures. The results are shown in Table 3.4 . Detailed measurements of pipes sections are in Appendix E.

Table 3.4: Pipe internal diameters and their standard deviations

Pipe Position (Figure 3.1)	Average Diameter [mm]	Weighted standard deviation [mm]
1st Top	42.12	0.13
2nd Top	52.80	0.08
3rd Top	63.80	0.19
4th Top	80.43	0.09
2nd Bottom	98.58	0.22
1st Bottom	97.17	0.18

b) Reynolds number, k_v, pressure velocity, shear stress, shear rate and friction factor

100 repeated measurements were taken in order to evaluate the magnitude of errors, thus using Equation 3.3 It can be said these errors were approximated with 7.1% uncertainty. The procedure was to maintain the experimental setting as constant as possible and take repeated measurements in a shorter period of time.

Table 3.5 gives typical errors of the major parameters using the above mentioned approach. The relative errors in other pipes are listed in Appendix F.

Table 3.5: Typical relative errors (42 mm ID pipe)

	Average	Standard Deviation	Error [± %]	95 % Confidence Interval
Re_3	60933.5	159.574	0.52	319.15
k_v	7.52629	0.54933	14.60	1.10
PTT 1 [Pa]	39753.4	634.526	3.19	1269.05
PTT 2 [Pa]	38970.7	177.708	0.91	355.42
PTT 3 [Pa]	37759.4	164.415	0.87	328.83
PTT 4 [Pa]	37114.5	171.158	0.92	342.32
PTT 5 [Pa]	28202.4	126.706	0.90	253.41
PTT 6 [Pa]	26885.9	46.7698	0.35	93.54
PTT 7 [Pa]	25770.7	70.4593	0.55	140.92
PTT 8 [Pa]	24760.2	34.1422	0.28	68.28
PTT 9 [Pa]	23826.8	29.1658	0.24	58.33
Q [l/sec]	2.016	0.00528	0.52	0.01
V [m/s]	1.44685	0.00379	0.52	0.01
τ_o (US)	4.75255	0.15843	6.67	0.32
τ_o (DS)	5.20977	0.20162	7.74	0.40
f (US)	0.00454	0.000151	6.65	0.00
f (DS)	0.00498	0.00019	7.63	0.00

3.8 CONCLUSION

The aspects related to the experimental part of this work and presented in chapter 3 may be summarised as follows:

- An experimental rig was constructed solely for this study, and consisted of six lines of PVC Pipes of diameter ranging from 50 mm to 110 mm. These lines were 25 m long each and contained a test diaphragm valve;
- instrumentation comprised flow meters, electric pressure transducers, temperature probe, data acquisition unit, valves board, etc;
- experimental procedures such as test, calibration, measurement of density and pipe internal diameter, setting of valves positions were explained
- the straight-through diaphragm valve, vital to this study, was described.
- the properties of materials and fluids tested - kaolin slurries, Carboxyl methyl cellulose (CMC), Glycerine and water – were described and,
- experimental errors were analysed, quantified and were within acceptable limits.

The next chapter presents the analysis of the experimental results of data generated in this work.

CHAPTER 4

CHAPTER 4

ANALYSIS OF RESULTS

4.1 INTRODUCTION

In this chapter the procedure followed to obtain the experimental data is explained with the analysis techniques applied to the raw data. The result of the water test in one of the pipes tested is shown to emphasise the precision of the experimental set-up; the manner in which the rheological charcterisation of the fluids tested was obtained is explained, with typical rheological constants given for fluids tested. The output of the experimental work is summarised in plots of loss coefficient versus Reynolds number for each valve at each opening. Furthermore the loss coefficients obtained for each opening are summarised in a table for the Natco Valves.

4.2 ANALYSIS TECHNIQUES

4.2.1 Data capture and analysis

The experimental data was captured via a data acquisition unit (DAU) and processed on the PC. Any mode of test available i.e. rheology test, hydraulic gradeline test with PPT or hydraulic gradeline test with DP cell could have been carried out either manually using one transducer or automatically using many transducers. The conditions of each

test dictated which test mode was appropriate. The explanation given below is related to the hydraulic gradeline test with PPT, which was the default mode.

4.2.2 Pressure Gradeline line

The primary output of the experimental rig was the static pressure at each tap and the flow rate. It was necessary that hydraulic grade lines be linear in order to proceed with test work. The data were, therefore, plotted on a graph which gave the operator from the onset of the test runs an indication of the validity of the tests. Figure 4.1 shows a typical plot of valid pressure gradelines. The distance between data points is related to the distance between pressure tap as shown in the same figure.

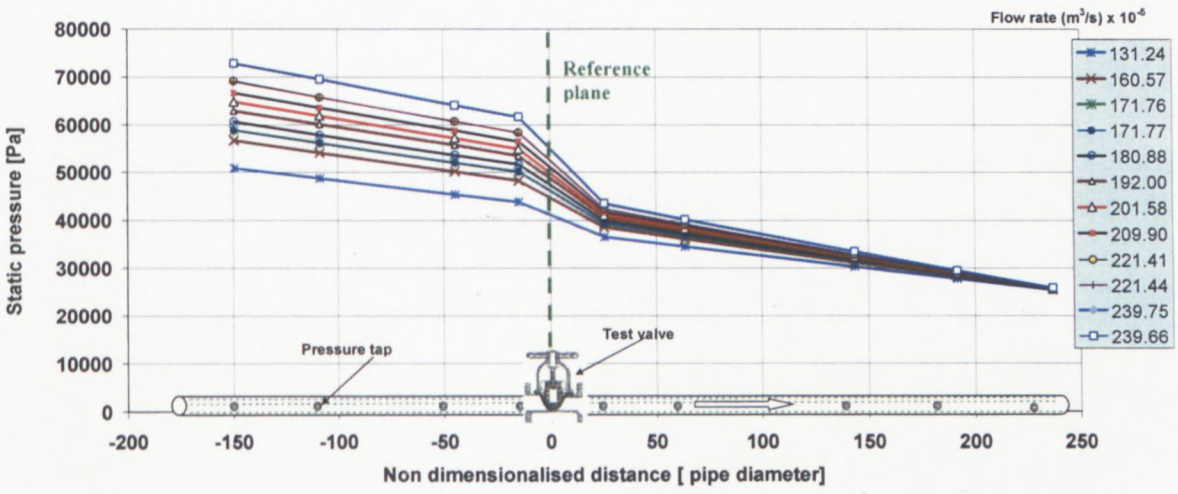

Figure 4.1: Typical pressure gradelines, CMC 5% in 42 mm pipe

4.2.3 Friction factor

Friction factor were measured from experimental measurement of pressure drop and velocity using Equation 4.1. In both sections (upstream and downstream of the test valve) respective wall shear stresses were used in the calculation of the friction factors

$$f = \frac{2\tau_0}{\rho V^2} \qquad \text{Eq 4.1}$$

Theoretical friction factors were calculated using, for laminar flow, the Poiseuille Equation from which, as explained in Section 2.4.4, emanates the friction factor $f = 16/Re$ and in turbulent flow, the Blasius equation: $f = 0.079/Re^{0.25}$. The criterion used for laminar to turbulent flow transition was $Re_3 = 2100$.

4.2.4 Valves Pressures drop

The coordinates of the static pressure versus the tapping distances (measured from the valve centre line as origin) were used to find the slopes and the intercepts of the pressure grade lines upstream and downstream of the valves. Because the abscissa origin was set on the valves, valve pressure drops were found as the difference between the upstream intercept and the downstream intercept, as shown in Figure 4.2. It should be noted that the first three data points and the last four data points only were selected in the linear regression respectively upstream and downstream of the valve. This excluded data points close to the test valve which might be in the region where the flow was distorted by the valve presence. Once the pressure drop across the valve was found, the valve loss coefficient was calculated using Equation 4.2, which is a variant of Equation 2.34 where k_{fitt} is replaced by k_v and the head loss (H) expressed in terms of the total pressure drop.

$$k_v = \frac{\Delta P}{\frac{1}{2}\rho V^2} \qquad \text{Eq 4. 2}$$

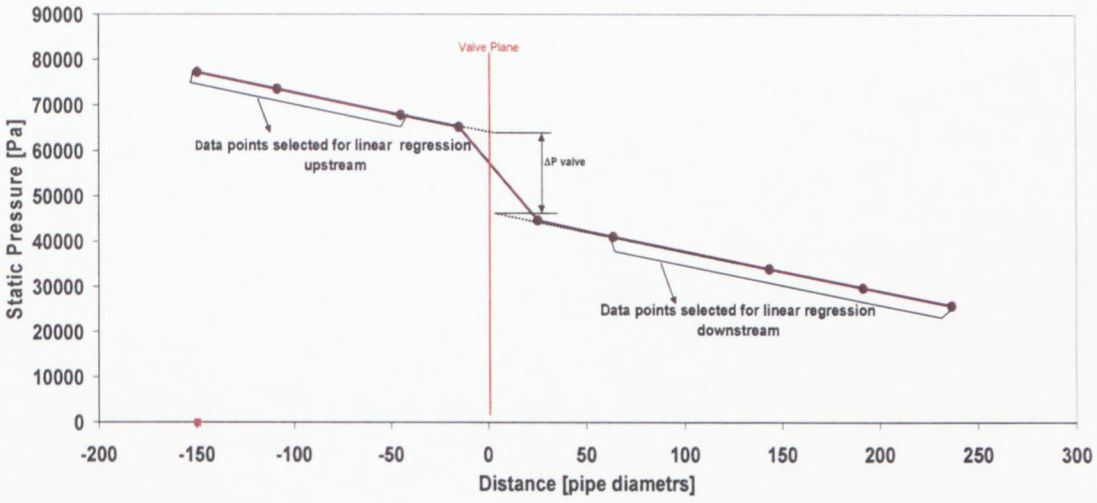

Figure 4.2: Selection of data points for extrapolation of the valve pressure drop(ΔP_{valve})

4.2.5 Flow rate

The flow rate was measured with a flow meter and the velocity was obtained using Equation 4.3. The velocity was used, in turn, to find valve loss coefficient and pseudo shear rate (8V/D), which is important in the rheological characterisation.

$$V = \frac{Q}{\left(\frac{\pi D^2}{4}\right)} \qquad \text{Eq 4.3}$$

4.2.6 Wall shear stress

The wall shear stresses in the upstream and downstream sections were obtained by measuring the pressure drop (ΔP) over a known length L. Given the internal diameter of the pipe tested, the wall shear stress was calculated using Equation 2.12. The length L

was taken between the first and the third pressure taps, about 3 m, and on the downstream side between the sixth and ninth taps, about 3 m, in the largest pipe.

$$\tau = \frac{D\,\Delta P}{4L} \qquad \text{Eq 2.12}$$

4.2.7 Charts

Some charts were used to give a visual check of the test run data, these were:

4.2.7.1 Pressure Gradient Chart

This chart showed plots of pressure readings against tapping distance. A typical example is shown in Figure 4.1. This chart ensured that if something went wrong, the rig operator could immediately see the unfamiliar shape and take corrective action.

4.2.7.2 Pseudo Shear Diagram Chart

This chart showed the plot of the shear stress against the pseudo shear rate during the test. It gives an indication of the viscous properties of the fluids being tested. A typical example is shown in Figure 4.3.

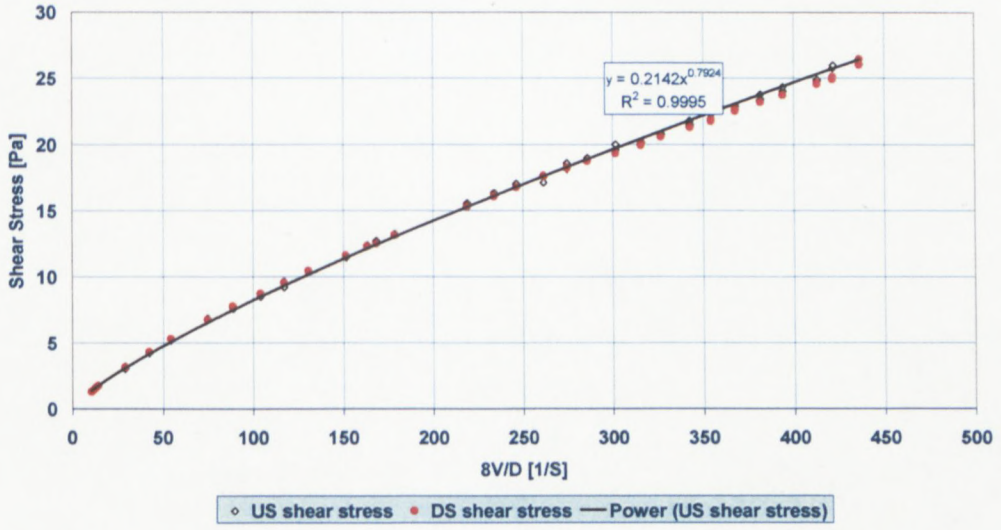

Figure 4.3: Pseudo shear diagram (CMC 5% in 42 mm pipe)

4.2.7.3 Friction Factor Chart

In this chart the theoretical friction factors are plotted with the experimental friction factors against the Reynolds number. This chart was important, as it alerted the operator if something was incorrect (density, pressure ranges, or tapping distances). If everything is set correctly, the experimental friction factors should be within 10 % at worst with the theoretical friction factor. A typical example is given in Figure 4. 4.

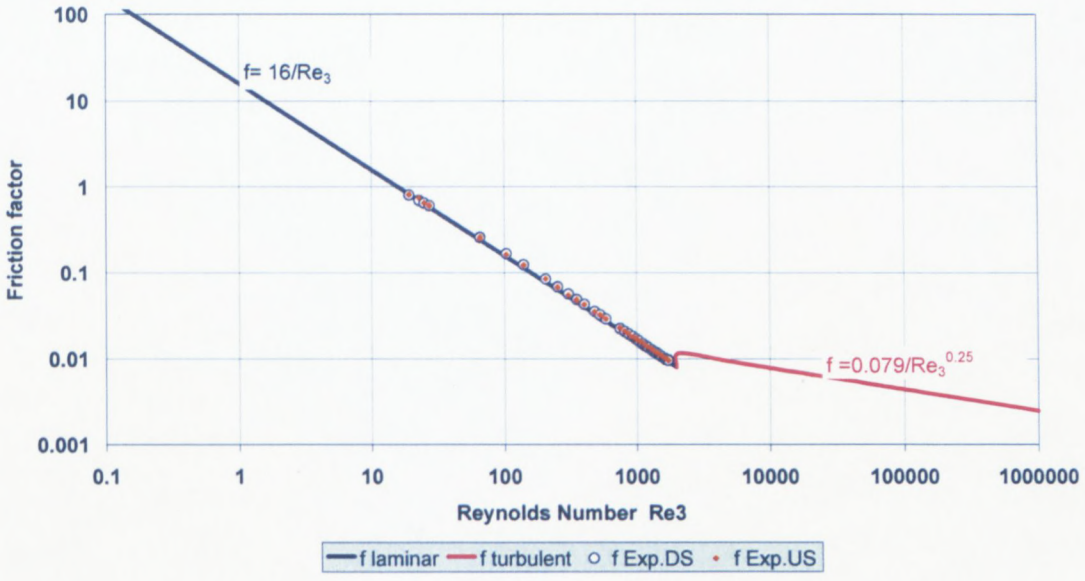

Figure 4. 4: Friction factor chart (CMC 5% in 40mm)

4.2.7.1 Loss Coefficients

The loss coefficients chart, as given in Figure 4.5, was normally considered as the output of the test and shows a plot of the valve loss coefficients against Reynolds number. The chart is acceptable only if the others charts, mentioned before were consistent.

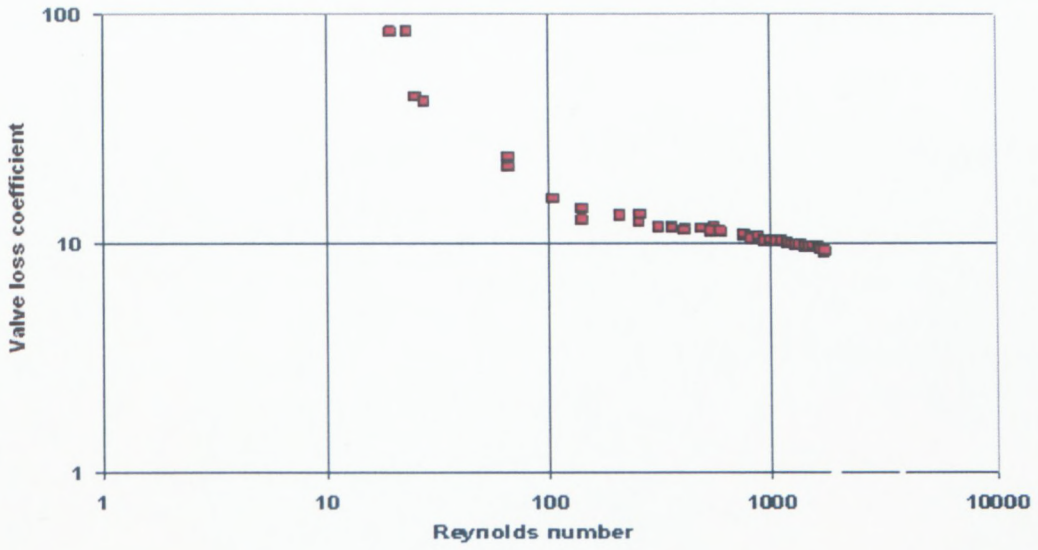

Figure 4.5: Plot of valve loss coefficient against Reynolds number

(CMC 5% in 42 mm)

4.3 WATER TEST

Water tests were conducted in straight pipe sections, to ascertain the credibility of the equipment and the experimental approach. Clear water is a fluid that is well documented (Colebrook, 1939). Good agreement between the water experimental data and the prediction of Equation 2.29 indicates that the instruments (pressure transducers and flow meters) were well calibrated and that the experiment was set up correctly. The experimental data from this test were presented as coordinates of wall shear stress (τ_o) versus mean velocity (V). These data were compared to the equivalent shear stresses obtained with (Equation 2.29 and 2.32) assuming the same velocities.

$$\frac{1}{\sqrt{f}} = -4\log\left[\frac{k}{3.7D} + \frac{1.26}{Re\sqrt{f}}\right] \qquad \text{Eq 2.29}$$

$$\tau_0 = \frac{f\rho V^2}{2} \qquad \text{Eq 2.32}$$

It should be noted that as the friction factor (f) appears on both sides of Equation 2.29, it was found by an iterative method and then used in Equation 2.32 to find the theoretical wall shear stress. A typical water test chart where the experimental shear stresses are compared to the theoretical shear stresses predicted by the Colebrooke & White's equation (Equation 2.29) is shown in Figure 4.6 for the 42 mm pipe.

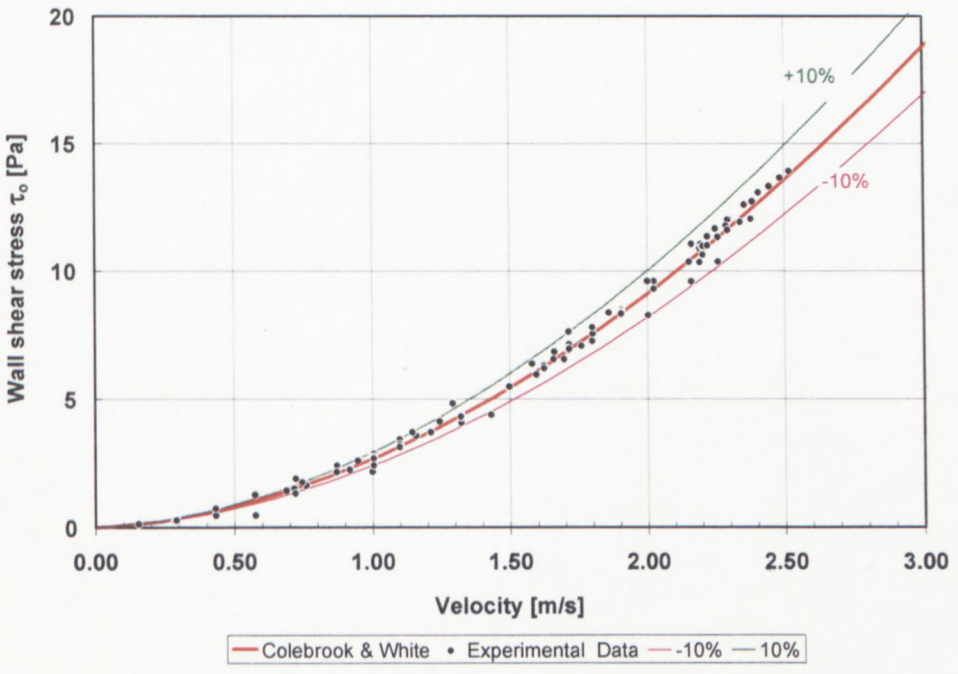

Figure 4.6: Water test comparison with Colebrook & White prediction (42 mm pipe)

4.4 RHEOLOGICAL CHARCTERISATION

Tube viscometry was used in this study. The rheological parameters of the fluids tested were obtained from data gathered from the valve test rig on the straight pipe sections. At least two pipes were combined to find the rheological parameters of the materials tested.

The data consisted of wall shear stress (τ_o) versus pseudo shear rate (8V/D) for both upstream and downstream sections. Turbulent data was excluded from this analysis; only laminar data was considered in the determination of rheological parameters, as explained in Section 2.6.4. A typical pseudo-shear diagram is shown in Figure 4.7. This graph shows coincidental laminar shear stress data for three different pipe diameters, showing that pipe slip effects were unapparent. And this was noticed for all the fluids tested.

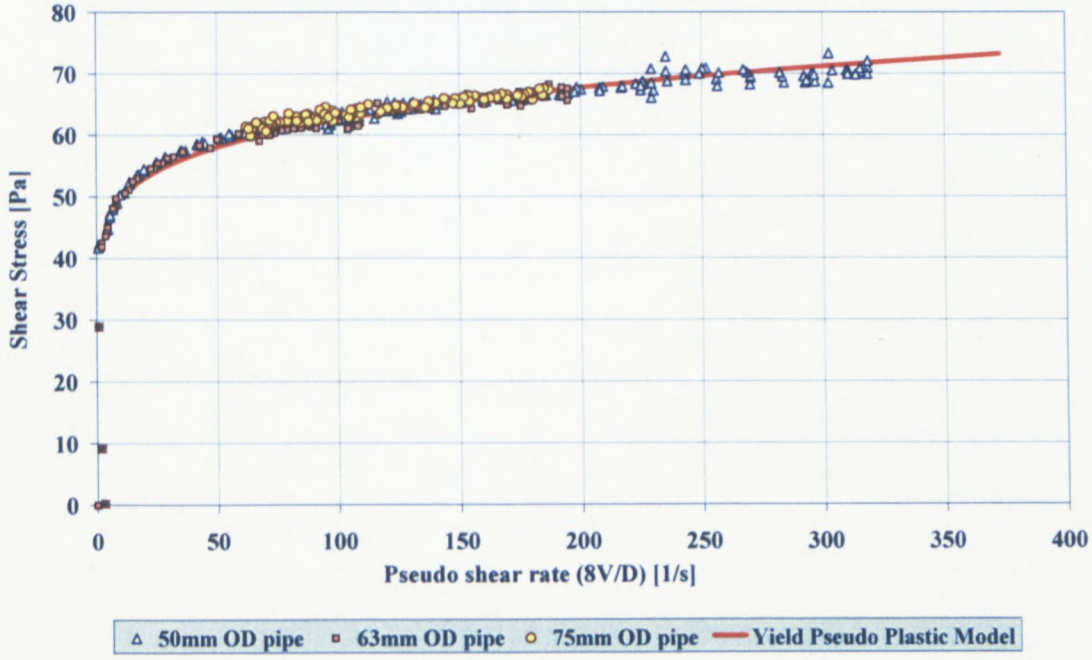

Figure 4.7: Pseudo shear diagram of kaolin 13% showing coincident data of 3 pipes

The rheological parameters of the fluids tested were monitored on a daily basis. Specific rheological parameters obtained for various tests are given in Appendix G. Table 4.1 however, shows representative rheological parameters for fluids tested in this study.

Table 4.1: Density and rheological parameters of fluids tested

Fluid	Density [kg/m^3]	τ_y [Pa]	K [Pa.s^n]	n [-]
Kaolin 10%	1163	3.91	9.34	0.14
Kaolin 13%	1214	15.0	15.04	0.17
CMC 5%	1025	0	0.23	0.79
CMC 8%	1037	0	4.95	0.54
Glycerol 75%	1197	0	0.02	1
Glycerol 99%	1256	0	0.85	1

To highlight the extent to which these constants varied with each test, the rheological parameter of kaolin slurry 10 % were analysed over a period of two years. It was noticed that as a result of using the Herschel Bulkley model, the three rheological constants were varying significantly, as a consequence of a curve fitting exercise. Fluid density was a parameter with the least variation. The extent to which it varied is shown in Table 4.2 as a coefficient of variation, which is the ratio of the standard deviation over the mean value. Although the coefficient of variation of three rheological parameters is quite high separately, their sum however had a very low coefficient of variation as shown in Table 4.2. This fact demonstrates that the three rheological parameters operate together (as a team) to characterise a fluid. To consider separately a parameter without the two others

may not necessary reflect a true physical characteristic of the fluid. For example, taking τ_y, for a true yield stress might be dubious.

Table 4.2: Coefficient of variation of the rheological parameters (kaolin 10%)

Fluid parameter	Average	Standard deviation	Coefficient of variation[%]	N (number of data)
ρ [kg/m^3]	1165	2.35	0.2	24
τ_y [Pa]	6.82	3.77	55	24
K [Pa.s^n]	6.83	2.91	43	24
n	0.22	0.06	29	24
τ_y+K+n	13.9	1.63	12	24

4.5 PRESENTATION OF RESULTS

The experimental study consisted of physically pumping the fluids (as described in section 3.5) through five diaphragm valves mounted horizontally. Each valve had to be tested in four different positions of valve opening.

The schedule of these tests has been carried out according to the matrix shown in Table 4.3. Water was first tested in all the pipes at different valves opening positions, followed respectively by glycerine 100 %, glycerine 75 %, CMC 5 %, CMC 8 %, kaolin 10 % and kaolin 13 %. It should be noted that the Natco set of diaphragms valves were tested first followed by the Saunders diaphragms valves. Few scheduled tests could not be tested due to technical difficulties.

Table 4.3: Schedule of test work

VALVE SIZE	VALVE OPENING	WATER	GLYCEROL		CMC		KAOLIN	
			99%	75%	5%	8%	10%	13%
40 mm	100 %	✔	✔	✔	✔	✔	✔	✔
	75 %	✔	✔	✔	✔	✔	✔	✔
	50 %	✔	✔	✔	✔	✔	✔	✔
	25 %	✔	✔	✔	✔	✔	✔	✔
50 mm	100 %	✔	✔	✔	✔	✔	✔	✔
	75 %	✔	✔	✔	✔	✔	✔	✔
	50 %	✔	✔	✔	✔	✔	✔	✔
	25 %	✔	✔	✔	✔	✔	✔	✔
65 mm	100 %	✔	✔	✔	✔	✔	✔	✔
	75 %	✔	✔	✔	✔	✔	✔	✔
	50 %	✔	✔	✔	✔	✔	✔	✔
	25 %	✔	✔	✔	✔	✔	✔	✔
80 mm	100 %	✔	✔	✔	✔	✔	✔	✔
	75 %	✔	✔	✔	✔	✔	✔	✔
	50 %	✔	✔	✔	✔	✔	✔	✔
	25 %	✔	✔	✔	✔	✔	✔	✔
100 mm	100 %	✔	✔	✔	✔	✔	✔	✔
	75 %	✔	✔	✔	✔	✔	✔	✔
	50 %	✔	✔	✔	✔	✔	✔	✔
	25 %	✔	✔	✔	✔	✔	✔	✔

The detailed pressure data and the subsequent loss coefficients versus Reynolds numbers data are presented in Appendix G. However, the data for the Natco diaphragm valves are illustrated in Figure 4.8 for the full opening valve position. Similar graphs were obtained for other valves at various opening positions. The Slatter Reynolds number, Re_3, was able to achieve dynamic similarity in each valve and these figures show that Re_3 is able to account for the viscous nature of the fluids. The same values of C_v and k_v will apply

to both Newtonian and non-Newtonian fluids for any particular valve as shown in each of these figures.

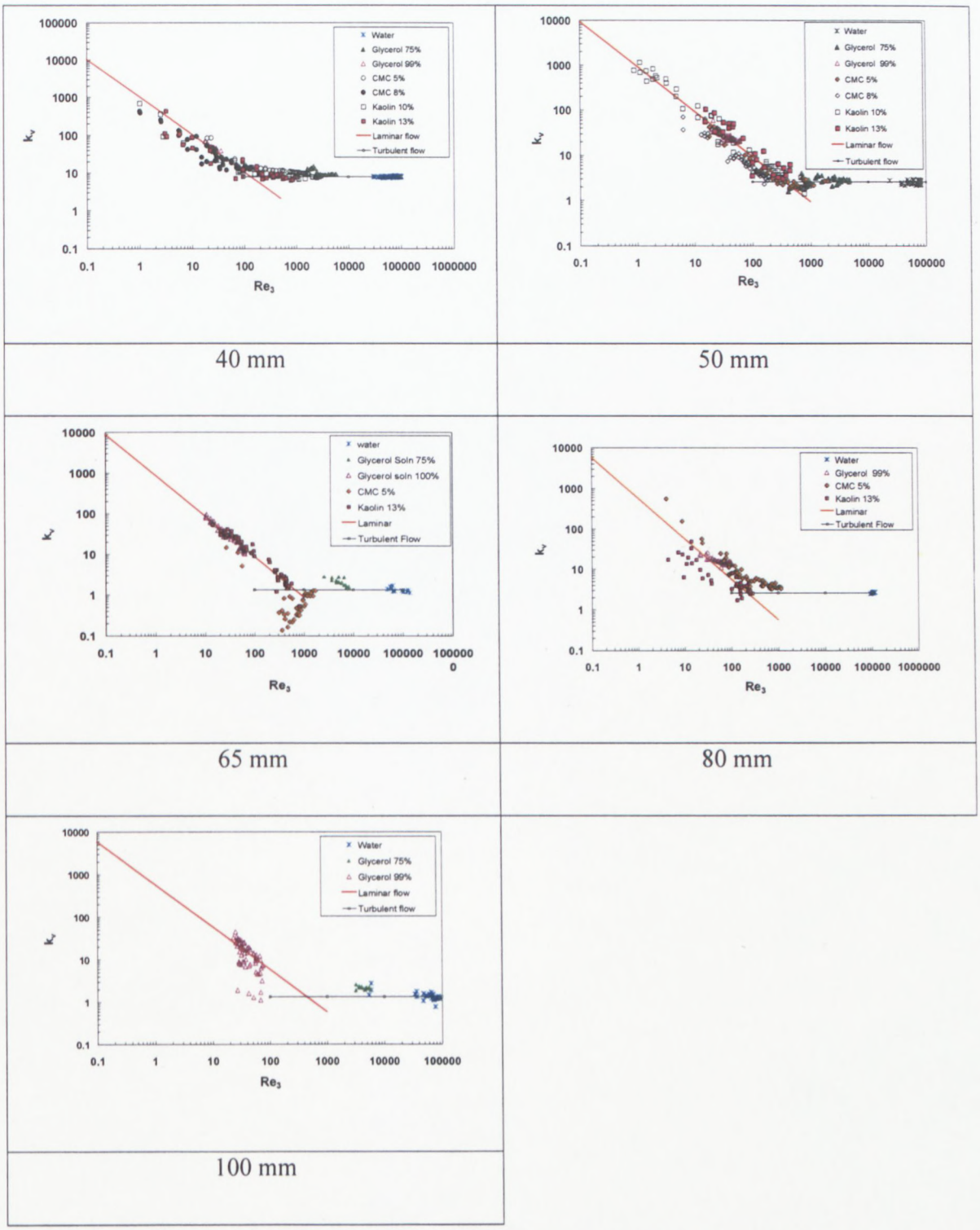

Figure 4.8: Loss coefficient of the Natco diaphragm valve at full opening position

The scatter of data in Figure 4.8 is probably the results of larger uncertainty of the experimental pressure drop measured. Pressure drops were lower in larger pipes and at lower flow rates. The scatter of data is still an unresolved issue for this type of experimental work. Although care was taken to maintain the friction factor error to less than 10 % in the smaller pipes and to less than 20 % in the 80 mm and 100 mm pipes, large scatter was still observed in the calculation of k_v. This occurred most markedly in the transitional zone, which is an indication of regime instability in this region.

The values of loss coefficients constants and turbulent loss coefficients are shown in Table 4.4. The loss coefficient constants (defined as $C_v = k_v\ Re_3$) is obtained by minimizing the logarithmic least square error function E (Equation 4.4) between the calculated and the observed data.

$$E = \sum \left(\ln \frac{C_v}{Re_3} - \ln k_v \right)^2 \qquad \text{Eq 4.4}$$

The turbulent loss coefficients were calculated as the arithmetic mean of the turbulent loss coefficients. It should be noted that the bulk of the turbulent data was obtained with water.

The uncertainty in the calculated C_v and k_v was evaluated in the fully opened position, which is the worst case scenario regarding uncertainties, as the pressure drops are smaller compared to pressure drops in other closure positions. A statistical analysis showed that the uncertainty of the C_V levels up to ± 49 % and the uncertainty of k_v levels up to ± 10 % for the smaller pipes and ± 20 % for larger pipes (80 mm and 100 mm pipes).

Table 4.4: Summary of the diaphragm valve loss coefficient in laminar / turbulent region at ¼, ½ and ¾ and fully open positions

Valve bore size	Diaphragm valve loss coefficients							
	Laminar flow regime (C_v)				Turbulent flow regime (k_v)			
	¼ Open	½ Open	¾ Open	Fully Open	¼ Open	½ Open	¾ Open	Fully Open
40 mm	2020	1834	1076	1200	211	35	18	8.1
50 mm	3920	1313	844	946	85	25	8.1	2.5
65 mm	3511	2133	522	766	63	16	2.8	1.2
80 mm	2942	1505	820	871	67	18	6.8	2.5
100 mm	1554	887	301	585	100	29	10	1.4

Table 4.5 shows the same values as Table 4.4, but in a normalised format, which facilitates a comparison of sizes. The values shown in Table 4.5 are the ratios of the individual loss coefficient constants C_v and loss coefficients k_v divided by $k_{v\ 100\%}$ and $C_{v100\%}$ respectively. Dynamic similarity would be achieved if these ratios were the same for the different openings. Unfortunately there is inconsistency of the ratios obtained, particularly in laminar flow as seen in Figure 4.9. In turbulent flow, however, there is a marked trend with all the curves taking an identical slope. This fact is considered in Chapter 5 to find a scaling factor for loss coefficients in turbulent flow.

Table 4.5: Summary of the diaphragm valve loss coefficients normalised

	Diaphragm valve loss coefficients							
Valve	Laminar flow regime (C_v)				Turbulent flow regime (k_v)			
Opening	25%	50%	75%	100%	25%	50%	75%	100%
40 mm	1.68	1.53	0.90	1	26.05	4.32	2.22	1
50 mm	4.14	1.39	0.89	1	34.00	10.00	3.24	1
65 mm	4.58	2.78	0.68	1	52.50	13.33	2.33	1
80 mm	3.38	1.73	0.94	1	26.80	7.20	2.72	1
100 mm	2.66	1.52	0.51	1	71.43	20.71	7.14	1

From Table 4.4 it can be seen that loss coefficients vary with pipe diameter and increase with valve closure, as one would expect. However, observation of normalised loss coefficients in Table 4.5 reveals that in turbulent flow, the loss coefficients increase rapidly with valve closure compared to laminar flow. In laminar flow, a minimum is obtained for loss coefficient constants at 75% opening position for all the valve sizes, as shown in Figure 4.9.

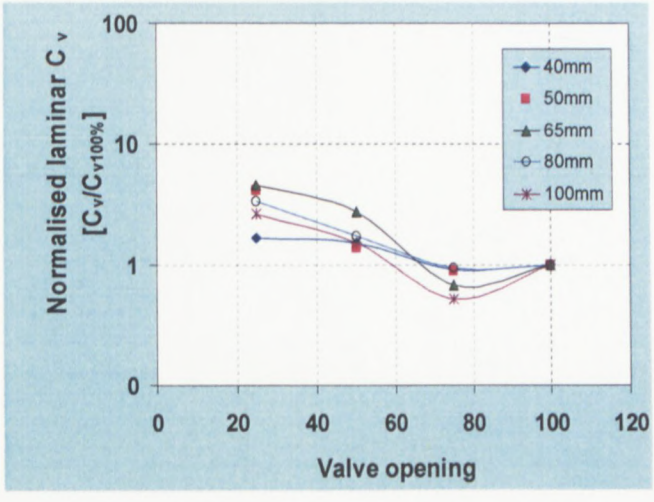

Normalised C_v

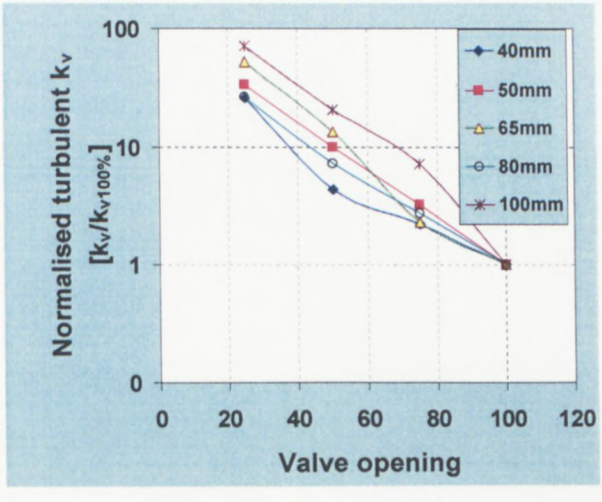

Normalised k_v

Figure 4.9 Plots of normalised C_v and k_v versus valve opening

4.6 CONCLUSION

This chapter presented the ways the experimental data were captured and analysed. These results are summarised in Table 4.4 as values of loss coefficient and loss coefficient constants for the different valve sizes and openings tested.

This traditional, or standard, approach to analysing the data resulted in a C_v value for each valve size and valve opening position for laminar flow and the same for the turbulent flow loss coefficient, k_v. For the five valves tested, 20 values of C_v and 20 values of k_v were obtained. The non-linear nature of the diameter effect is largely responsible for the above situation, which is undoubtedly not desirable for a design engineer.

Although Re_3 was able to achieve dynamic similarity for each valve, the lack of geometrical similarity prevents dynamic similarity across the different valve sizes. It is clear, however that Re_3 is able to account for the viscous nature of the fluids so that the same values of C_v and k_v apply to both Newtonian and non-Newtonian fluids for any particular valve.

The next chapter, however, uses the large database of results obtained in this study, to develop new predictive correlations for laminar, transitional and turbulent flow in straight-through diaphragm valves.

CHAPTER 5

CHAPTER 5

DEVELOPMENT OF NEW CORRELATIONS

5.1 INTRODUCTION

The quest for simpler design equations has led one to consider analysing the experimental data using four approaches; bearing in mind a sound correlation should give an accurate fit to experimental data over a wide range. It should involve a minimum number of constants, which should be readily evaluated and preferably have a physical meaning (Cross, 1964).

Analyses of experimental data were done with the following approaches:

- Dimensional analysis, with pipe Reynolds number;
- analysis of data with valve throat Reynolds number;
- analysis of data according to area ratio and,
- analysis of data in terms of degree of opening equivalent to the same flow ratio.

In the next section, these approaches as well as their related issues are explained. The order in which these approaches are presented is chronological. It is shown that some of the approaches taken were flawed and the reasons of not analysing them further are given, and finally the model developed in this study is presented.

5.2 *Approach One*: DIMENSIONAL ANALYSIS, WITH PIPE REYNOLDS NUMBER

This is the main approach for which the experiments were designed; other approaches are more or less related. The technique of dimensional analysis was applied to the data reduced with the pipe Reynolds number in which the valve was installed. Based solely on dimensional analysis, a functional relationship was derived. The constants of the functional relationship were obtained by applying a linear multiple regression analysis to the experimental data. For simplicity and generality an overall relationship was derived from the individual equations of different valve sizes. Such steps are explained in detail in the following paragraphs.

5.2.1 Dimensional Analysis

The following variables were identified as important in influencing the valve pressure drop in laminar flow: flow rate, pipe diameter, fluid rheology or effective viscosity, fluid density, and the degree of valve opening. This can be written as:

$$\Delta P = f(Q, D, \mu_{eff}, \rho, \theta) \qquad \text{Eq 5. 1}$$

It should be noted that the roughness of the valve wall was omitted as the diaphragm valve is normally rubber lined. Moreover, the bulk of the experimental data were tested in laminar flow, in which roughness does not play a major role.

5.2.2 Functional Relationship

Applying the Buckingham Π-theorem (Buckingham, 1914) to the identified variables (Equation 5.1) gives the following expression between the dimensionless groups:

$$F\left(\frac{D^4\Delta P}{Q^2\rho}, \frac{D\,\mu_{eff}}{Q\rho}, \theta\right) = 0 \qquad \text{Eq 5.2}$$

This can be explicitly formulated in terms of Reynolds numbers as:

$$\frac{\Delta P}{\rho V^2} = c' Re^a \theta^b \qquad \text{Eq 5.3}$$

where c', a and b are constants

Equation 5.3 is more conveniently expressed in terms of the valve loss coefficient or valve resistance coefficient (k_v) by dividing both sides of (Equation 5.3) by ½, resulting in the functional relationship given in Equation 5.4.

$$k_v = c\,Re^a\,\theta^b \qquad \text{Eq 5.4}$$

where $c = 2c'$

Dimensional analysis gives a qualitative relationship between the variables. In most cases, experiments are necessary to obtain the constants to complete the qualitative relationship (Finnemore and Franzini, 2002).

5.2.3 Linear Regression Analysis

To perform the linear regression, Equation 5.4 was first linearised by expressing it in the logarithmic form as:

$$\ln k_v = a \ln Re + b \ln \theta + \ln c \qquad \text{Eq 5.5}$$

In this form the dependant variable becomes ($\ln k_v$) and the independent variables, ($\ln Re$) and ($\ln \theta$), where (θ)is the valve opening. The regression technique consists in finding the constants: $\ln c$, a and b.

Equation 5.5 may be considered as the equation of a least squares plane (Mathews and Fink, 1999).

$$z = Ax + By + C \qquad \text{Eq 5.6}$$

For N points: $\{(x_1, y_1, z_1); \ldots;(x_N, y_N, z_N)\}$, the constants A, B, and C are obtained by minimizing the function E (Equation 5.7), which is the sum of the deviations squared.

$$E(A,B,C) = \sum_{k=1}^{n} \left(Ax_k + By_k + C - z_k\right)^2 \qquad \text{Eq 5.7}$$

This optimisation may be done by setting respectively the partial derivatives $\delta E/\delta A$, $\delta E/\delta B$ and $\delta E/\delta C$ equal to zero and solving these equations simultaneously for A, B and C. This will result in the algebraic equations: Equation 5.8, Equation 5.9 and Equation 5.10. (Mathews and Fink, 1999).

$$\left(\sum_{k=1}^{N} x_k^2\right)A+\left(\sum_{k=1}^{N} x_k y_k\right)B+\left(\sum_{k=1}^{N} x_k\right)C=\sum_{k=1}^{N} z_k x_k \qquad \text{Eq 5.8}$$

$$\left(\sum_{k=1}^{N} x_k y_k\right)A+\left(\sum_{k=1}^{N} y_k^2\right)B+\left(\sum_{k=1}^{N} y_k\right)C=\sum_{k=1}^{N} z_k y_k \qquad \text{Eq 5.9}$$

$$\left(\sum_{k=1}^{N} x_k\right)A+\left(\sum_{k=1}^{N} y_k\right)B+NC=\sum_{k=1}^{N} z_k \qquad \text{Eq 5.10}$$

These normal equations were applied to equations Equation 5.5 and resulted in the system of Equations (5.11, 5.12 and 5.13), which were solved for a, b and $\ln c$ using the data obtained in the experimental work.

$$\left(\sum_{k=1}^{N} (\ln \mathrm{Re}_k)^2\right)a+\left(\sum_{k=1}^{N} \ln \mathrm{Re}_k \ln \theta_k\right)b+\left(\sum_{k=1}^{N} \ln \mathrm{Re}_k\right)\ln c=\sum_{k=1}^{N} \ln kv_k \ln \mathrm{Re}_k \qquad \text{Eq 5.11}$$

$$\left(\sum_{k=1}^{N} \ln \mathrm{Re}_k \ln \theta_k\right)a+\left(\sum_{k=1}^{N} (\ln \theta_k)^2\right)b+\left(\sum_{k=1}^{N} \ln \theta_k\right)\ln c=\sum_{k=1}^{N} kv_k \ln \theta_k \qquad \text{Eq 5.12}$$

$$\left(\sum_{k=1}^{N} \ln \mathrm{Re}_k\right)a+\left(\sum_{k=1}^{N} \ln \theta_k\right)b+N\ln c=\sum_{k=1}^{N} kv_k \qquad \text{Eq 5.13}$$

The results for all the valves tested are shown in Table 5.1. Column (N) has been inserted to show the number of data points used in the computation of constants.

Table 5. 1: Results of the multiple regressions showing the constants in Equation 5. 4 for all the Natco valves tested

Valve bore size	a	b	c	N
40 mm	-0.50	-1.80	224.6	391
50 mm	-0.67	-1.94	246.6	644
65 mm	-0.87	-2.00	403.0	262
80 mm	-0.48	-2.08	64.5	597
100 mm	-0.19	-1.64	28.7	387

The same process has been done for the Saunders Valves and the results are shown in Table 5.2

Table 5.2: Results of the multiple regression showing the constants in Equation 5. 4 for all the Saunders valves tested

Valve bore size	a	b	c	N
40 mm	-0.32	-2.15	30.5	173
50 mm	-0.53	-1.85	30.1	115
65 mm	-0.59	-2.77	48.6	195
80 mm	-0.59	-2.83	47.3	86
100 mm	-0.49	-2.82	30.8	89

A typical plot of these correlations, where k_v is plotted against $Re_3^a \Theta^b$, is shown in Figure 5.1. The large scatter of data is again evident in this figure, and is typical of this type of work. It is usually caused by large uncertainties in the data and a general lack of understanding of the controlling physics.

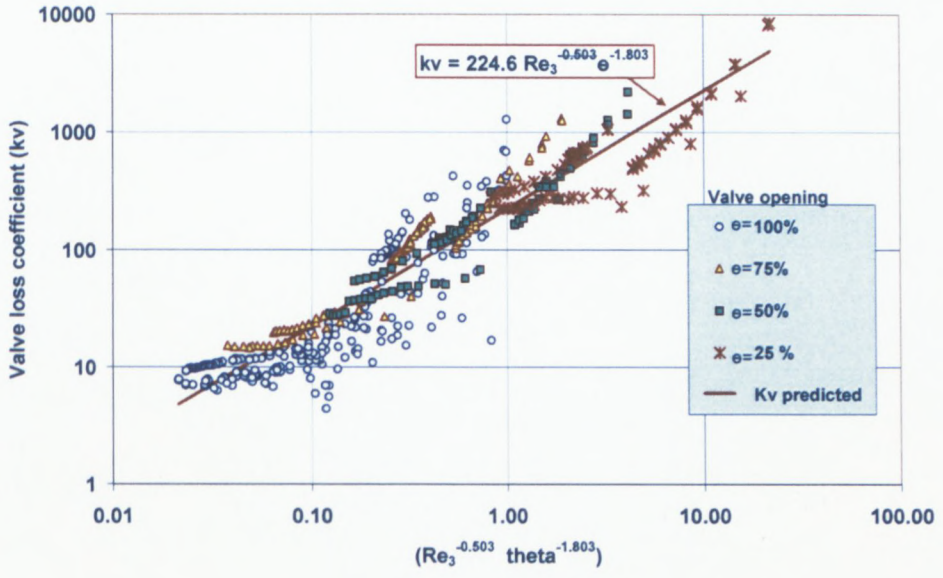

Figure 5.1: Plot of calculated k_v versus $Re_3^a \Theta^b$

5.2.4 Generalised correlation for laminar flow based on pipe Reynolds number

An analysis of the coefficients obtained for the different valves' sizes and manufacturers showed that there is a variability of constants due to valve size and valve manufacturer. However, it was noticed that the coefficients of variation of these constant were smaller for both a and b constants (Table 5.3) by taking average rounded-off values (a = -0.5 and b = -2) the author, thus suggests a generalized correlation of the form:

$$k_v = \frac{C_\Omega}{\sqrt{\mathrm{Re}}\,\theta^2} \qquad \text{Eq 5.14}$$

Table 5.3: Variability of constants for the valves tested

Constants	Average	Standard Deviation	Coefficient of Variation (%)	N
a	-0.53	0.18	34.7	10
b	-2.18	0.45	20.8	10
c	121	136	112	10

With Equation 5.14, only one constant (C_Ω) is needed to predict the loss coefficients in laminar flow for a diaphragm valve for given Reynolds number and degree of valve opening. Table 5.4 shows the constants found for the valves tested in this study.

Table 5.4: C_{Omega} constants for valves tested

Nominal Valve size Natco	C_Ω	Nominal Valve size Saunders	C_Ω
40 mm	200	40 mm	53
50 mm	1146	50 mm	36
65 mm	93	65 mm	95
80 mm	83	80 mm	144
100 mm	45	100 mm	108

5.2.5 Conclusion on Approach 1: Dimensional analysis with pipe Reynolds number

In spite of there being no geometrical similarity between diaphragm valve of different sizes, and that even, for valves of the same size but from different manufacturers, there is no dynamic similarity, an overall expression has been found that requires only one constant (C_Ω) to fully characterise the valve loss coefficient in laminar flow at different degrees of valve opening.

However, there are some short-comings associated with this approach such as:

- a large discrepancy between the predicted and the experimental values at very low Reynolds numbers;
- the model is limited only to laminar flow and,
- the linear form of the model did not fit the data well which show a curvature transiting from the laminar to the turbulent region.

The average absolute deviation between the predicted and experimental k_v was found to be ± 50 % and the root mean square error leveled up to 87 %, therefore other approaches were explored.

5.3 *Approach Two: ANALYSIS WITH VALVE THROAT REYNOLDS NUMBER*

So far the experimental data had been analysed with the pipe Reynolds number i.e. using the pipe diameter, on which the valve was installed, as the characteristic length in the Reynolds number formula. For this approach, however, the throat characteristic length was used, instead of the pipe diameter. The Newtonian Reynolds number is a linear function of its variables and will scale simply with the length dimension, i.e. $Re_{pipe} = \beta\, Re_{throat}$, ($\beta$ is the ratio of the throat length to pipe diameter). However, this is not true for viscoplastic Reynolds numbers (such as Re_3) which are non-linear functions of their

variables and the Reynolds numbers will not scale simply with the length dimension. The rationale behind this approach was possible dynamic similarity might be achieved among valves of different sizes.

5.3.1 Throat length

The throat length was set as the length of the most restricted area i.e. the length between valve invert level and the lower part of the diaphragm as shown in Figure 5.2

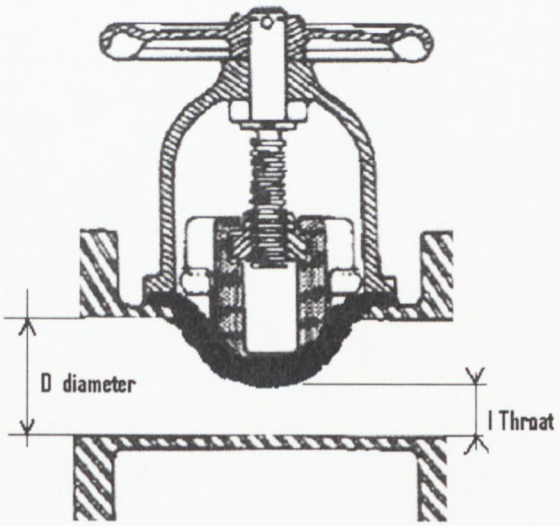

Figure 5.2: Section of a diaphragm valve showing the throat length (l) and the valve port diameter (D)

As the valve positions tested and the valve stem displacement per revolution were known, it was possible to calculate the throat length for each test and recalculate the "so-called" throat Reynolds number for each test. The throat Reynolds number has the same formulation as the normal Reynolds number, the only difference being the pipe diameter had been replaced by the throat length (l).

5.3.2 Loss coefficient based on pipe and throat velocities

Within this approach there were two ways to calculate the valve loss coefficient - using throat velocity or using pipe velocity. The loss coefficients calculated with the throat velocity were obviously much lower than those calculated with pipe velocity as the fluid velocity is much higher in the throat of the valve as seen in Figure 5.3. where the data of the 40 mm valve is shown.

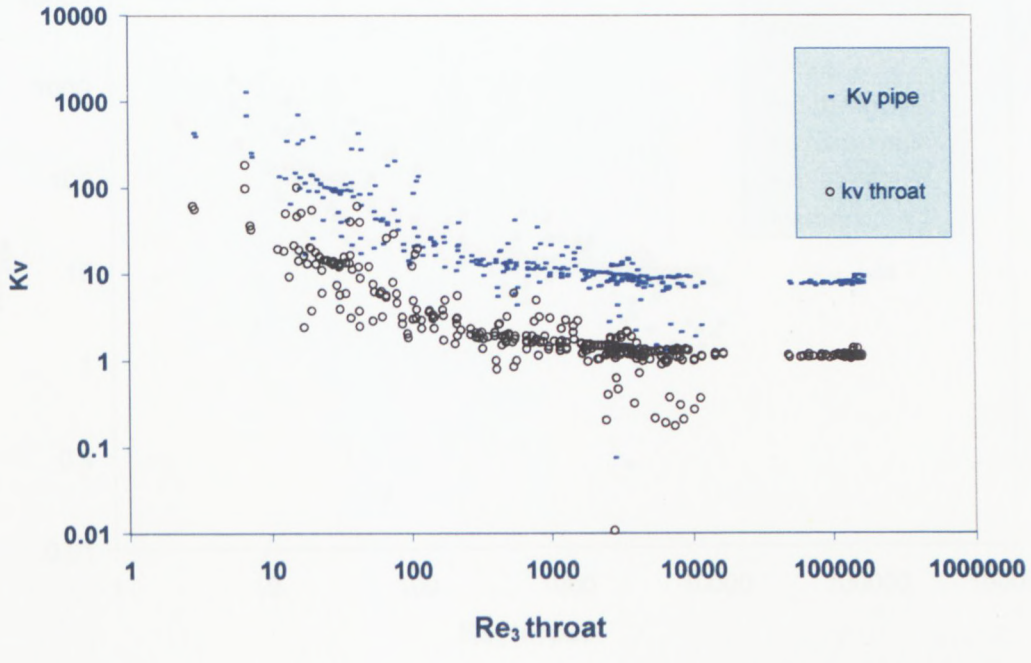

Figure 5.3: 40 mm valve , comparison of kv_{throat} Vs kv_{pipe} for same Re_{throat}

5.3.3 Scatter diagrams

Plotting the loss coefficients (kv_{pipe}), calculated with the fluid pipe velocity for the different fluids tested against the throat Reynolds number offered no advantage over the conventional method of using the pipe diameter, as seen in Figure 5.4.

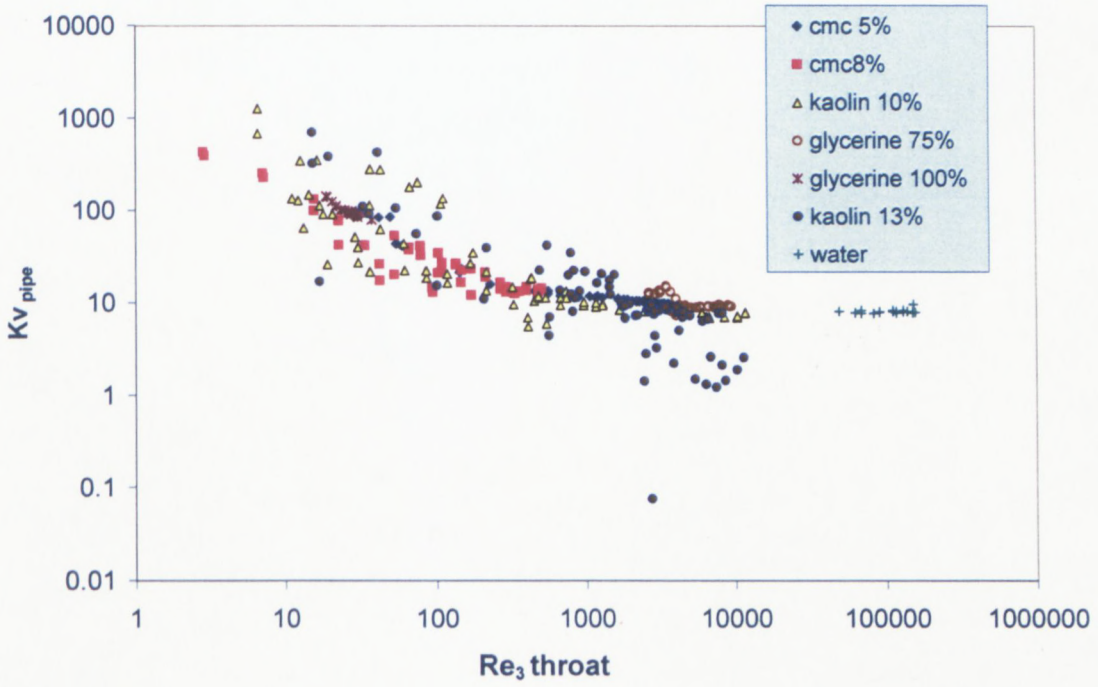

Figure 5.4: 40 mm valve , plot of kv_{pipe} vs $Re_{3throat}$ per fluids

Neither plotting the loss coefficients (kv_{throat}), calculated with the fluid throat velocity for the different fluids tested against the throat Reynolds number, improved the reduction scatter in the data, see Figure 5.5.

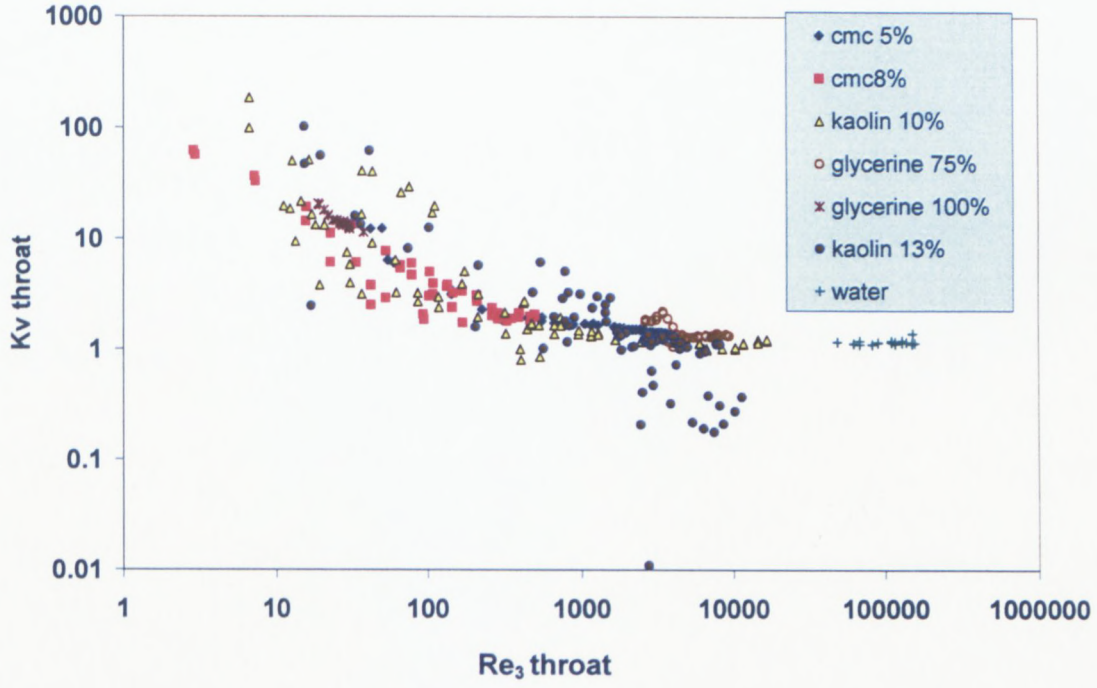

Figure 5.5: 40 mm valve , plot of kv_{throat} vs $Re_{3\ throat}$ per fluids

When plotting kv_{throat} versus throat Reynolds number for different openings of the same valve, the data for all but the 100% open valve seem to collapse onto the same line, see Figure 5.6. Attempting to plot kv_{pipe} versus throat Reynolds number for different openings of the same valve makes matters even worse as the different opening drift away from each other as seen in Figure 5.7.

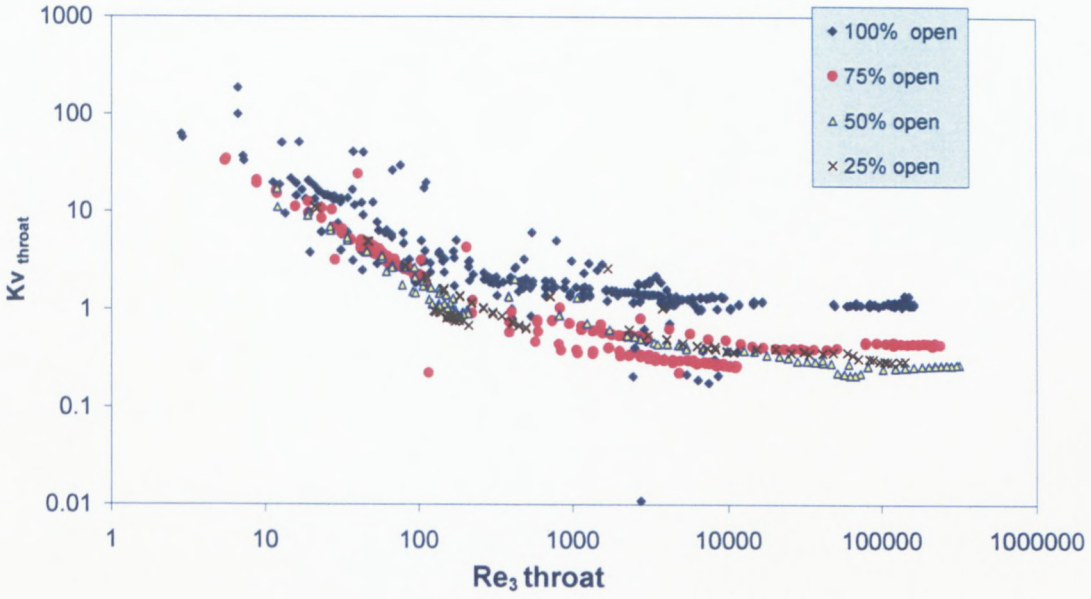

Figure 5.6: 40mm valve , plot of kv_{throat} vs $Re_{3\ throat}$ per valve opening.

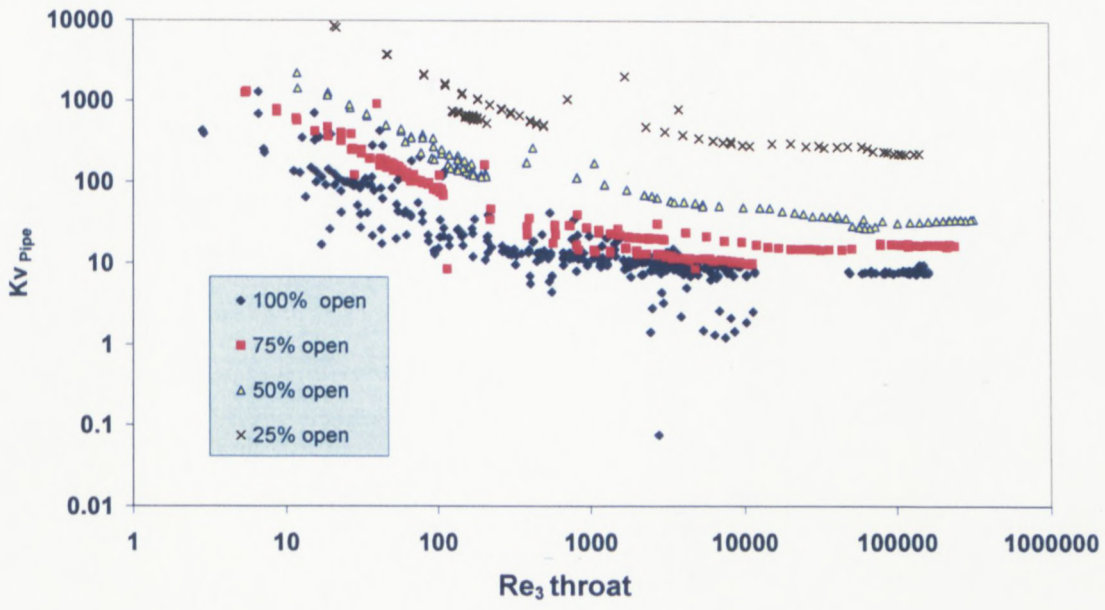

Figure 5.7: 40 mm valve , plot of kv_{pipe} vs $Re_{3\ throat}$ per valve opening.

5.3.4 Conclusion on approach 2

From discussions it is apparent that using the throat as a characteristic length in the Reynolds number or/and incorporating it in the loss coefficient did not present obvious advantage over the k_v and Reynolds number based on the pipe velocity.

5.4 *Approach three*: ANALYSIS OF DATA IN TERMS OF THE SAME VALVE OF AREA RATIO

In this approach the relationships between the valve loss coefficient and the throat area, the most restricted passage in the valve, was examined.

5.4.1 Area ratio

The area ratio was calculated for each valve position as the ratio of the most restricted area passage over the area of the full passage when the diaphragm is fully retracted i.e.

$$Area\,ratio = \frac{area\ B}{area\ A} \qquad \text{Eq 5.15}$$

$$Area\,ratio = \frac{area\ A - area\ D}{area\ A} \qquad \text{Eq 5.16}$$

The passage was idealised with a parabola of width ***a*** and height ***b*** as depicted in Figure 5.8. The total area was calculated with Equation 5.17, an expression that can be found by direct integration.

$$S = \frac{2ab}{3} \qquad \text{Eq 5.17}$$

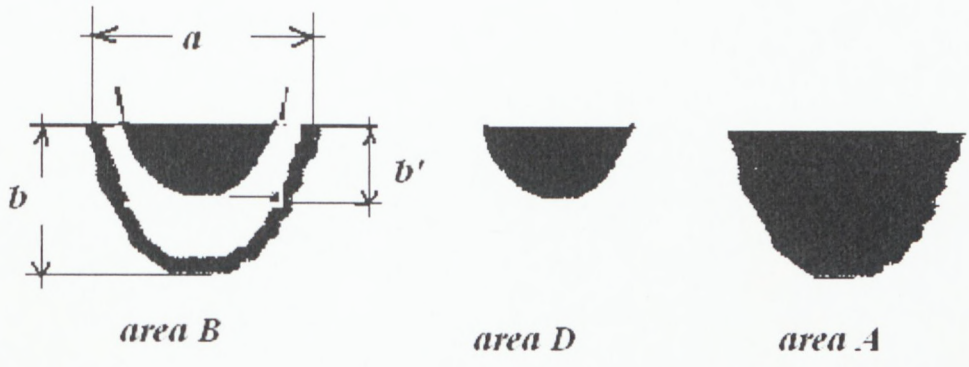

Figure 5.8: Definition of area ratio

The measured values of ***a*** and ***b*** for the valves tested are shown in Table 5.5. The area of the fully opened position is also shown as is the span per revolution of the hand wheel.

Table 5.5: Internal measurement of valves and area of the fully opened position

Valve Nominal size	*a* [mm]	*b* [mm]	Area [mm^2]	span per rev [mm]
40	42.78	35.26	1006	4.50
50	64.26	46.65	1998	4.27
65	90.82	62.42	3779	6.30
80	112.00	68.98	5151	6.27
100	124.46	74.72	6200	5.36

With the assumption that when the valve is closing, the diaphragm is entering with the same passage shape i.e. the parabolic shape. Knowing the span per revolution for each valve, the length ***b***' of the stern displacement was found and used to calculate the area D (see Figure 5.8), and subsequently the area ratio for each opening. Consequently the valve characteristic area of each valve was found and is shown in Figure 5.9.

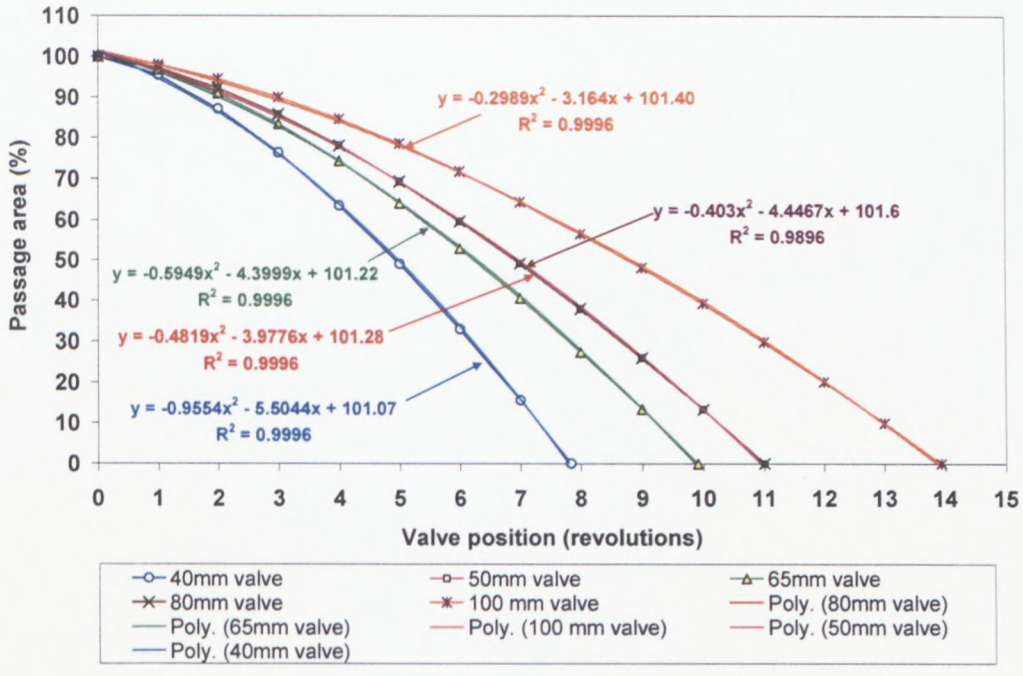

Figure 5.9: Valve position vs most restricted area ratio.

It should be noted that the area of the full passage of each valve was set to 100 % for normalisation purposes. In this way knowledge of the opening revolutions would also determine the area ratios. The area ratios of valve positions tested during the experimental work are shown in Table 5.6

Table 5.6: Area ratio of valves positions tested

Valve size	percentage	Revolutions	area
40 mm	100%	0	1.00
	75%	4	0.64
	50%	5	0.49
	25%	6	0.33
50 mm	100%	0	1.00
	75%	7.4	0.45
	50%	8	0.38
	25%	8.7	0.30
65 mm	100%	0	1.00
	75%	5.5	0.59
	50%	6.7	0.44
	25%	8	0.27
80 mm	100%	0	1.00
	75%	6.7	0.53
	50%	7.8	0.40
	25%	8.7	0.30
100 mm	100%	0	1.00
	75%	8.5	0.52
	50%	9.7	0.42
	25%	10.7	0.33

It is interesting to note that the area ratio differs from the flow ratio, for example in the 80 mm valve, 50% flow ratio is equal to 41% area ratio only.

Table 5.6 has been sorted by order of increasing area ratio to produce Table 5.7. Unfortunately few positions tested presented exactly the same area ratio.

Table 5.7: area ratio of valves position tested / sorted

Valve size	Percentage	Rounds	Area	Identical
65 mm	25%	8	0.27	
80 mm	25%	8.7	0.30	#
50 mm	25%	8.7	0.30	#
100 mm	25%	10.7	0.33	@
40 mm	25%	6	0.33	@
50 mm	50%	8	0.38	
80 mm	50%	7.8	0.40	
100 mm	50%	9.7	0.42	
65 mm	50%	6.7	0.44	
50 mm	75%	7.4	0.45	
40 mm	50%	5	0.49	$
100 mm	75%	8.5	0.52	$
80 mm	75%	6.7	0.53	$
65 mm	75%	5.5	0.59	
40 mm	75%	4	0.64	
40 mm	100%	0	1.00	&
65 mm	100%	0	1.00	&
50 mm	100%	0	1.00	&
80 mm	100%	0	1.00	&
100 mm	100%	0	1.00	&

5.4.2 Scatter diagrams

Some area ratios were close, so the data of such area ratios were plotted together as shown in Figures (5.10, 5.11, 5.12 and 5.13). Indeed, data with the same area ratio are expected to overlaps if the throat area ratio controls solely the valve resistance.

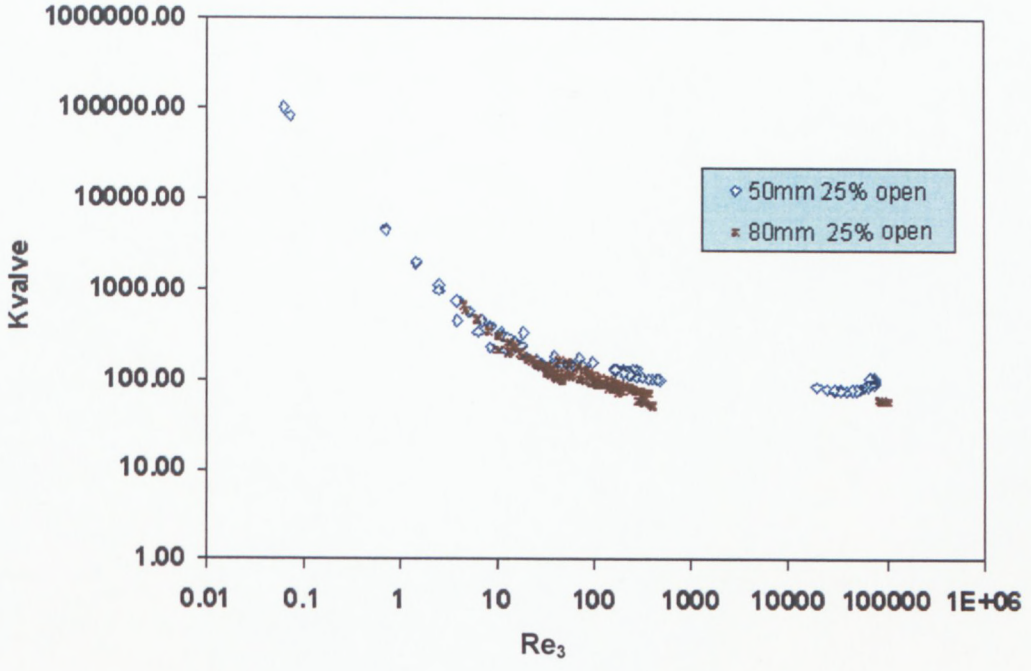

Figure 5.10: k_v vs Re_3 area ratio 0.30

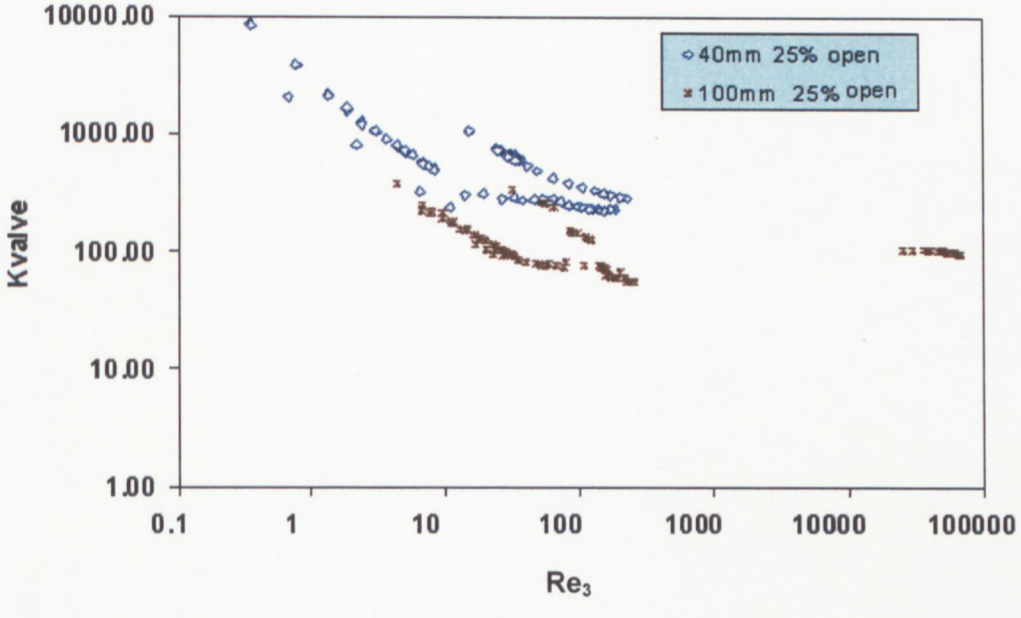

Figure 5.11: k_v vs Re_3 area ratio 0.33

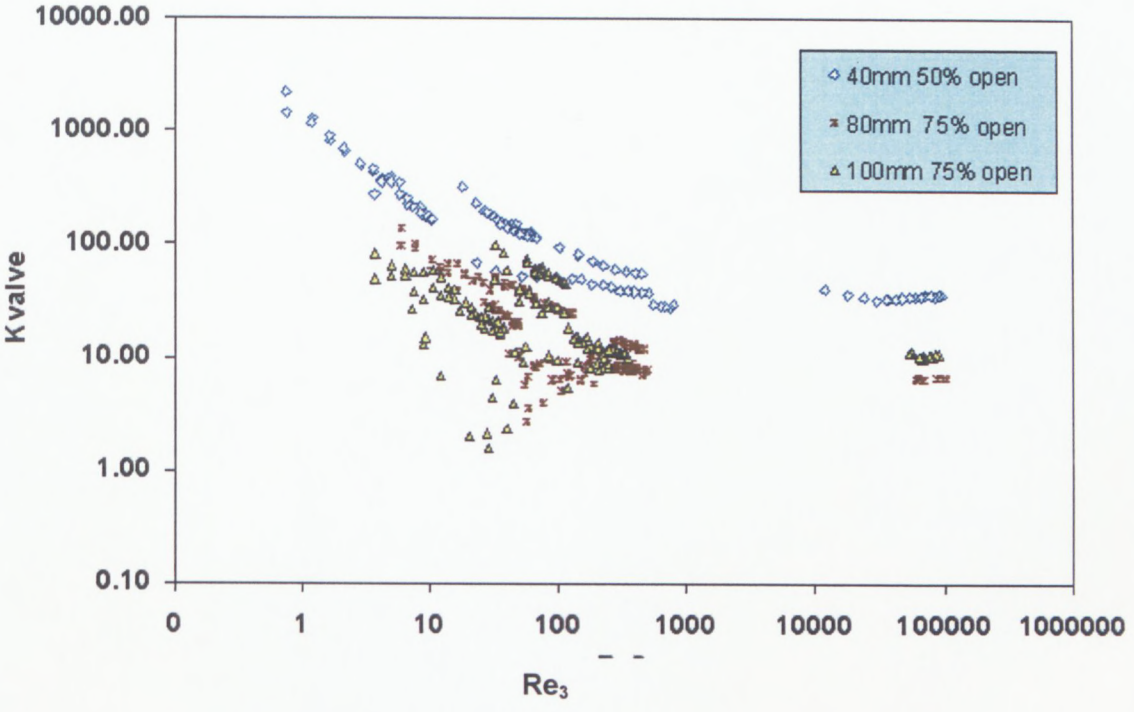

Figure 5.12: k_v vs Re_3 area ratio 0.51

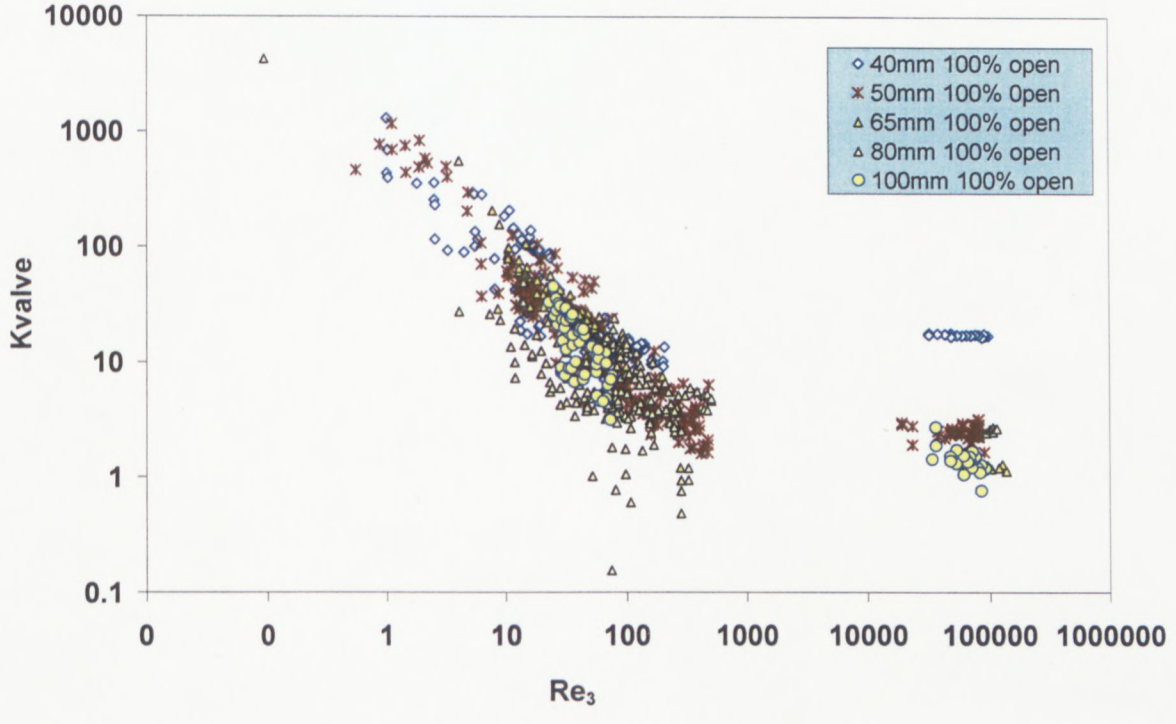

Figure 5.13: k_v vs Re_3 area ratio 1

From Figure 5.13, it is apparent that the overlapping of data is better at lower Reynolds numbers; separation of data begins in the transitional region, while a complete separation is observed in the turbulent zone.

5.4.3 Generalised valve area ratio characteristic

Further analysis of the area ratio valve characteristics, revealed normalising both the valve rounds openings and area openings fallout into a single curve as shown in Figure 5.14 . This finding is crucial as it could serve as the basis for a dynamic similarity on which to build up a generalised approach.

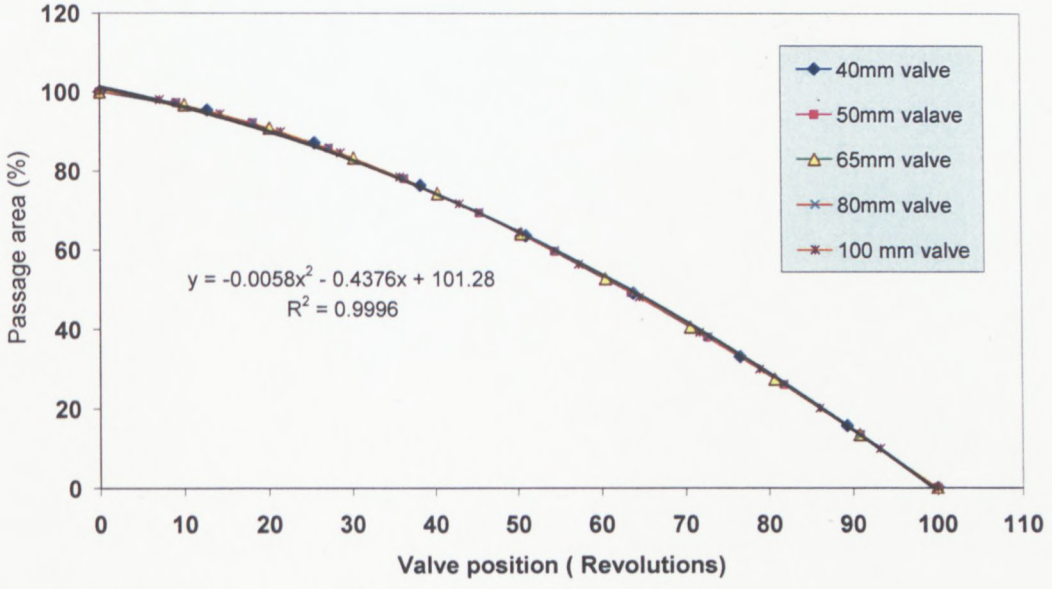

Figure 5.14: Generalised valve area characteristic

5.4.4 Conclusions to approach three

This approach has some merits, and could have been fully investigated if the experimental design had been conducted in terms of area ratios from the onset so that exactly identical area ratios were tested. With the current data base, obtained on the flow ratio basis, it is indecisive to say whether some scatter was because of the slight difference in area ratios, or the result of a true phenomenon. Therefore, it would be hazardous to produce, with confidence, a quantitative model. This approach is strongly recommended for future research.

5.5 *Approach four*: ANALYSIS OF DATA IN TERMS OF VALVE OPENING (FLOW RATIO)

A point of uncertainty related to the previous approach is that it was not known if the flow was controlled solely by the transversal most restricted area inside the diaphragm valve. Compared to one-dimensional pipe flow, the flow pattern inside the valve is quite complex. The closing member (diaphragm) has a paraboloidal shape, the flow inside the valve is three-dimensional with centrifugal forces involved as the fluid flows around the diaphragm. All these complexities led the author to introduce the so-called "gravity test" (Sections 3.5.2 and 3.5.3) to determine the valve opening in terms of flow ratio.

5.5.1 Valve flow ratio (θ)

As was explained earlier, the valve opening was determined in accordance with the flow ratio, which is the flow through the valve under a constant head of water flowing by gravity. It is probably debatable whether other materials would yield the same results as

with water. In fact, the rationale behind this procedure was to find a consistent and easily reproducible way of determining the valve opening positions.

5.5.2 Three regions

The approach here consists of grouping the data in terms of flow ratio regardless of the valve size. This approach has been broken up into three regions i.e. laminar, transition and turbulent.

- The laminar region comprised all data with a Reynolds number less than 10. It was found that in this region a single curve predicted all the data well regardless of the size and the opening, so that a single loss coefficient constant C_v was sufficient to predict the valves loss coefficients in this region. The analysis of all the data with Reynolds numbers less than 10, by an iterative procedure reduced to a loss coefficient constant of 1006, as shown if Figure 5.16.

- The transitional region was limited to the interval $10 < Re < 1000$. In this region, a regression analysis was performed to predict the valve loss coefficient for all the four flow ratios tested. In this instance, the diameter became a variable. To avoid the appearance of the diameter unit, all diameters were normalised with D100 which is the port diameter of the 100 mm valve. See Figures 5.17- 5.20.

- The turbulent region went beyond Reynolds number of 1000. Although the bulk experiments were conducted in laminar flow, an appreciable amount of turbulent data was obtained with water. The loss coefficient in this region was constant but dependent

on the valve size and opening. The analysis of the data showed that the scaling factor is $1/\theta^2$, meaning that the loss coefficients at any opening position can be predicted from the fully opened position loss coefficient. However, at lower openings (less than 40%) there was a noticeable divergence between the observed and the predicted data. (see Figure 5.15). A better correlation (Equation 5.18) was derived and which addresses the problem.

$$k_{v\theta} = \frac{k_{v100\%}}{\theta^2}(1.7 - 0.7\theta) \qquad \text{Eq 5.18}$$

It was also noticed that in Equation 5.18, for bigger valve sizes, the fully opened position loss coefficient ($k_{v100\%}$) was not a good predictor. But other constants did, such as the fraction of $k_{v25\%}$ or $k_{v75\%}$, this is probably due to higher experimental uncertainty in the fully opened position.

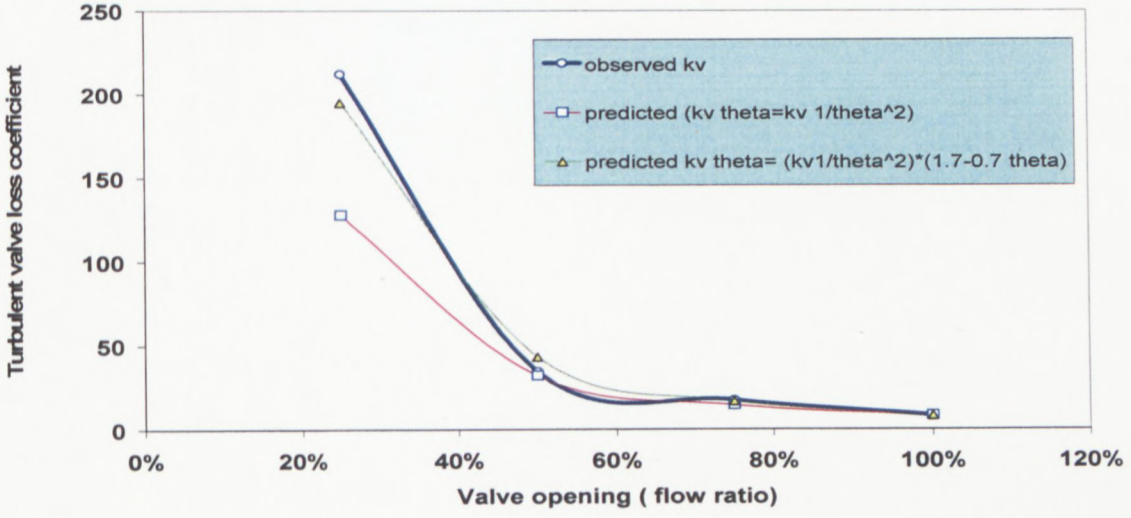

Figure 5.15: Comparison between turbulent observed k_v and predicted k_v

5.5.3 Scatter diagrams

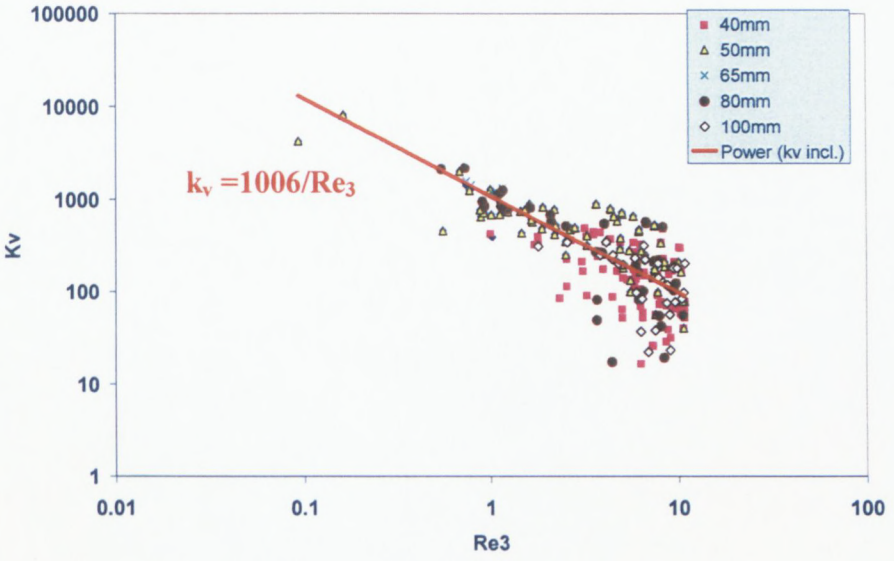

Figure 5.16: Laminar zone single line approximation for all data with $Re_3 < 10$.

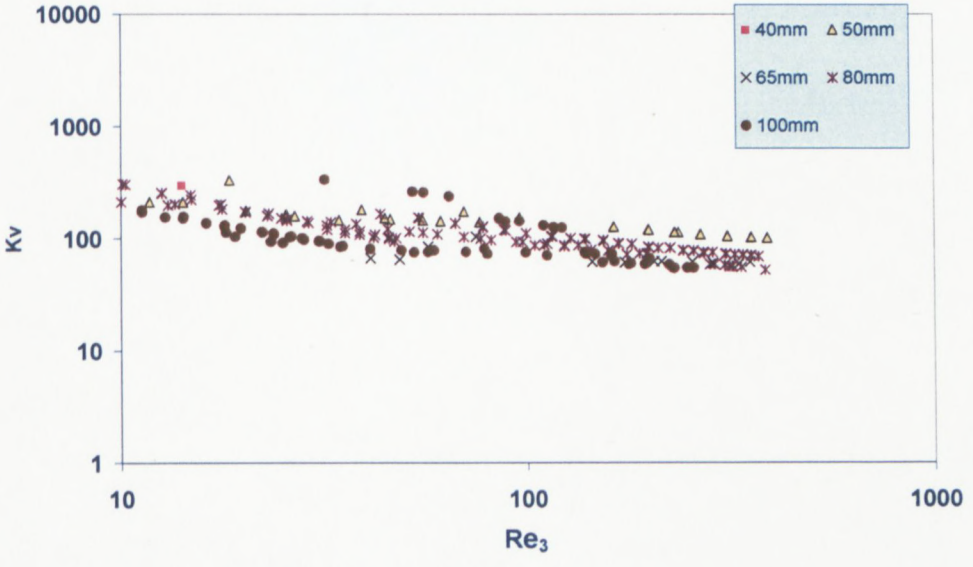

Figure 5.17: Diaphragm valve at 25% opening (flow ratio) Transitional region

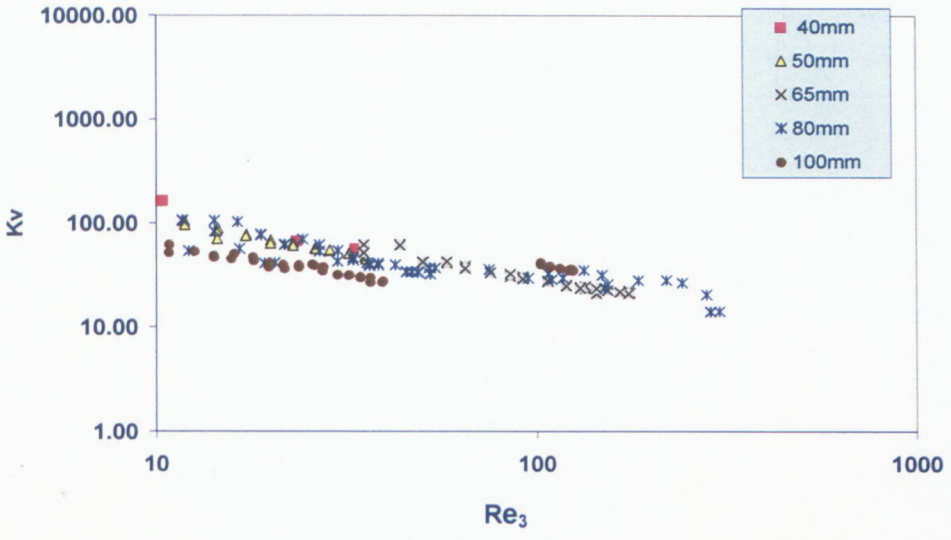

Figure 5.18: Diaphragm valve at 50% opening (flow ratio) Transitional region

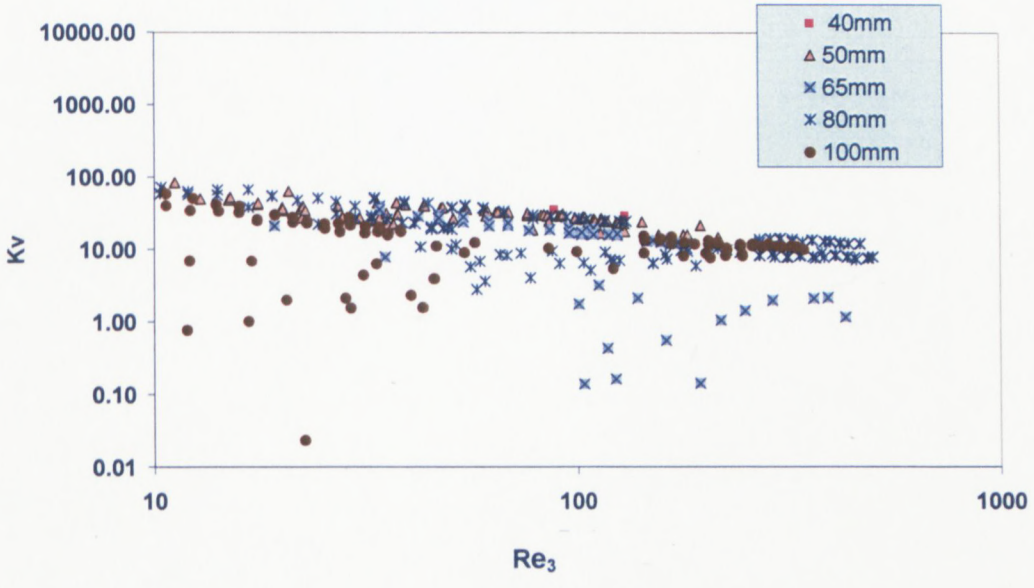

Figure 5.19: Diaphragm valve at 75 % opening (flow ratio) Transitional region

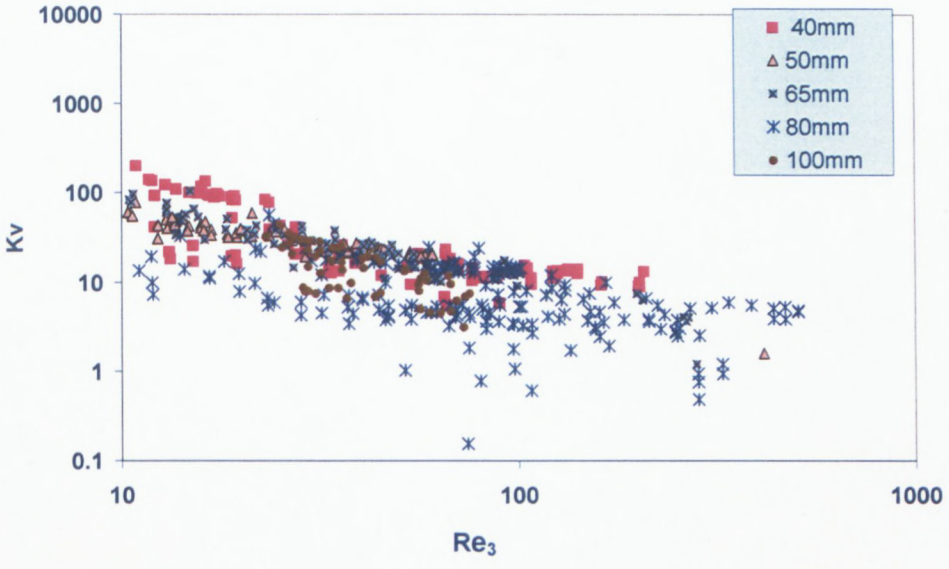

Figure 5. 20: Diaphragm valve at 100% opening (flow ratio) Transitional region

5.5.4 Regression analysis

The regression analysis of the transitional data was performed similarly to the one performed in section 5.2, the difference being the introduction of the factor D/D_{100} instead of Θ, giving Equation 5.19 whose constants are given in Table 5.8.

$$kv_{\theta} = C\,\mathrm{Re}^{a}\left(D/D_{100}\right)^{b} \qquad \text{Eq 5.19}$$

Table 5.8: Constants in correlation Equation 5.19

	θ	a	b	C
Valve opening	25%	0.44	0.99	584
	50%	0.60	0.88	326
	75%	0.59	1.27	144
	100%	0.87	0.95	261

5.5.5 Conclusion to approach 4

There was a noticeable overlapping of loss coefficient data of the different valve sizes, when grouped according to a same flow ratio, as shown in the scatter diagrams (Figures 5.17 to 5.20). Three regions were identified and appeared to exhibit different behaviours:

i. A laminar regions (Re < 10), essentially a viscous driven region where all the data converge. The effect of the size or opening was insignificant. A loss coefficient constant of 1006 was derived from the available data.

ii. A transitional region ($10 \leq Re < 1000$), a mixture of inertial and viscous forces started to appear. The diameter or valve size started to have an effect on the loss coefficient.

Equation 5.19 was derived to predict k_v in this region, this equation is diameter dependent. An interesting feature since there is no geometric similarity.

iii. A turbulent region ($Re \geq 1000$) where inertial forces predominate, showed constants k_v over a wide range of Reynolds number. But at same time, k_v was sensitive to change of valve opening (θ). It was found that the k_v at any opening could be predicted by dividing the fully opened position k_v by θ^2, this scaling factor is valid in wide opening positions. For valve openings ($\theta < 0.3$), Equation 5.18 is used to better predict k_v.

The limitation of this approach was, in the transitional region, the model provided k_v only for specific θ i.e. (0.25, 0.5, 0.75 or 1) for other intermediate θ, interpolation might be used. This process might be lengthy and inaccurate.

5.6 EVALUATION OF THE CORRELATIONS DEVELOPED IN THIS STUDY

It is time to assess the accuracy of the correlations developed thus far. The correlations were tested with the 40 mm valve data. The experimental data for the 40 mm valve was chosen, because of the higher magnitude of differential pressure drop in this test section, hence providing less experimental uncertainty. Each approach was applied to this sample data in order to predict the valve loss coefficient k_v. Errors of estimate were calculated between the predicted values and the measured values of k_v.

It should be noted that all the approaches were pipe Reynolds number based. Approaches using the throat Reynolds number were omitted from this evaluation, as it was shown in the scatter diagrams that there was not a substantial advantage in using the

throat as a characteristic length. Besides, from a practical stand point, this length is not easily accessible for measurement. The analysis of data in terms of area ratios was also omitted as the experiments were not conducted on same area ratios, but rather on the flow ratios, as presented in Sections 3.5.2 and 3.5.3.

5.6.1 Correlation 1

This method considered each valve and each opening separately. It used a valve loss coefficient constant in conjunction with a turbulent loss coefficient to predict k_v. This method was based on Table 4.4. The relationships for the four openings of the 40 mm valve are given in Equations (5.20 to 5.23).

$$kv_{100\%} = 1200Re^{-1}+8.1 \qquad \text{Eq 5.20}$$

$$kv_{75\%} = 1076Re^{-1}+18 \qquad \text{Eq 5.21}$$

$$kv_{50\%} = 1834Re^{-1}+35 \qquad \text{Eq 5.22}$$

$$kv_{25\%} = 2020Re^{-1}+211 \qquad \text{Eq 5.23}$$

5.6.2 Correlation 2

A) Instead of having many equations for each valve opening, this approach offered one equation which predicted the loss coefficient for any opening. The correlation of the 40 mm valve was presented at the Hydrotransport 17 conference (Mbiya *et al.*, 2007). Equation 5.24 was developed for the 40 mm valve. This equation applies to the laminar and transitional regions.

$$k_v = 224.6\,\mathrm{Re}^{-0.503}\ \theta^{-1.836} \qquad \text{Eq 5.24}$$

B) It was noticed that with correlations 2A (Equation 5.24 and those similar for other valve sizes) at very low Reynolds numbers these correlations did not fit, the experimental values well. Thus, two zones were introduced - laminar and transitional. They are markedly different in behaviour and were treated differently. The first zone was the strongly viscous driven region and this zone was found to cease at about Re =10 for all the valve sizes. After this zone, a transitional zone began and was correlated with similar equations as in 2A. The equations for the 40 mm valve were:

$$\text{For } Re < 10, \quad k_v = 1006/Re \qquad \text{Eq 5.25}$$

$$\text{For } 10 \leq Re < 1000, \quad k_v = 258 Re^{-0.56} \theta^{-2.02} \qquad \text{Eq 5.26}$$

5.6.3 Correlation 3

A generalised correlation was established from the relations of correlations 2A. The advantage of this method was that only one constant was needed per valve to predict the loss coefficient for each opening.

$$k_v = \frac{C_\Omega}{\sqrt{Re}\,\theta^2} \qquad \text{Eq 5.14}$$

For the 40 mm valve the constant C_Ω had the value of 200.

5.6.4 Correlation 4

A) This method was based on the analysis of data in terms of flow ratio, regardless of valve size. In this approach the loss coefficient was calculated only for specific valve

openings, namely those giving (25, 50, 75 or 100%) of the flow. For other valve opening positions, interpolation could be used, there was no guarantee the interpolated values worked.

$$kv_\theta = C\,\mathrm{Re}^a \left(D/D_{100} \right)^b \qquad \text{Eq 5.19}$$

The constants shown in

Table 5.8 apply to the range of valves tested.

Table 5.9: Constants in correlation Equation 5.19

	θ	a	b	C
Valve opening	25%	-0.44	-0.99	584
	50%	-0.60	-0.88	326
	75%	-0.59	-1.27	144
	100%	-0.87	-0.95	261

B) Similarly to correlations 2B, two zones were identified, the viscous driven zone communal to all the valves sizes and a transitional zone treated separately as follows:

$$\text{for } \mathrm{Re} < 10, \quad k_v = 1006 / R_e \qquad \text{Eq 5.25}$$

$$\text{for } \quad 10 \le \mathrm{Re} < 1000, \quad kv_\theta = C\,\mathrm{Re}^a \left(D/D_{100} \right)^b \qquad \text{Eq 5.27}$$

The constants *a, b* and C are given in Table 5.10, for the range of valves tested.

Table 5.10: Constants in Equation 5.27

Θ	a	b	C
25%	-0.29	-0.63	332
50%	-0.40	-0.41	166
75%	-1.01	-1.36	344
100%	-0.88	-0.98	282

5.6.5 Comparison of different methods

The uncertainty of each method described above was evaluated as, respectively, the minimum, maximum, mean and standard deviation of the absolute deviations between the experimental data of the 40mm valve and the predicted k_v. The root mean square (RMS) of the relative deviations between the experimental data of the 40mm valve and the predicted k_v were also evaluated. The results are shown in Table 5.11

Table 5.11: Uncertainties of different methods considered

		Absolute deviation [%]				Deviation [%]	N
		Min	Max	Mean	Stdev	RMS	
Correlation 1	Method 1	0.12	429	60	61	85	390
Correlation 2	Method 2A	0.05	390	45	48	66	390
	Method 2B	0.31	377	44	50	66	390
Correlation 3	Method 3	0.30	342	44	46	64	390
Correlation 4	Method 4A	0.11	227	42	29	51	390
	Method 4B	0.02	253	53	38	65	390

Table 5.11 shows that method 4B presents the least minimum deviation and method 4A, the least maximum deviation. Looking at the standard deviations, it can be concluded that there is no significant difference between these methods. However method 4A seems to presents the least uncertainties, this is due the presence of the factor (D/D_{100}) which account for the valve size.

Figure 5.21 to Figure 5.24 show the plots of the aforementioned methods and the data of the 40 mm valve.

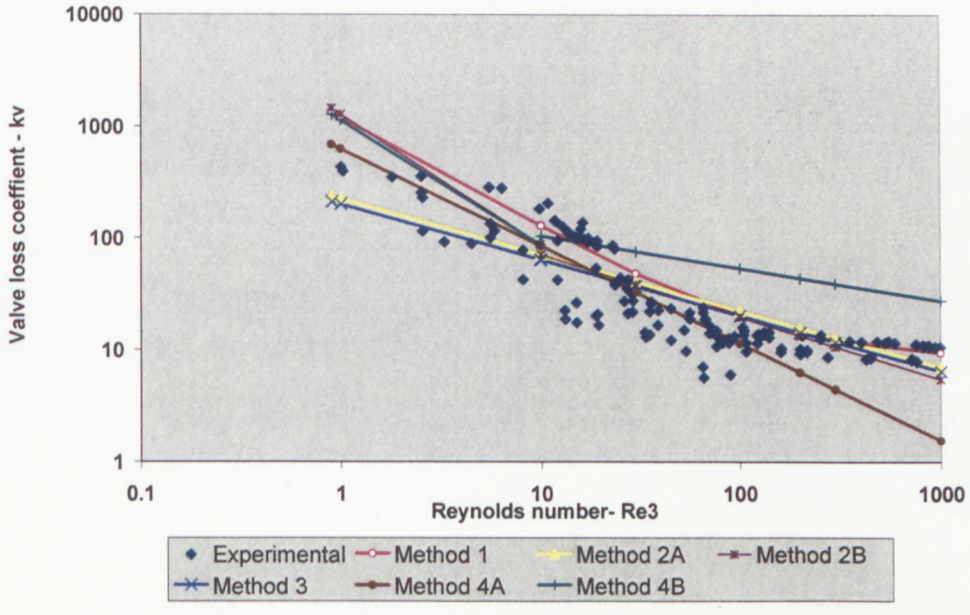

Figure 5.21: Comparison between experimental and predicted kv for 40 mm valve at 100% opening

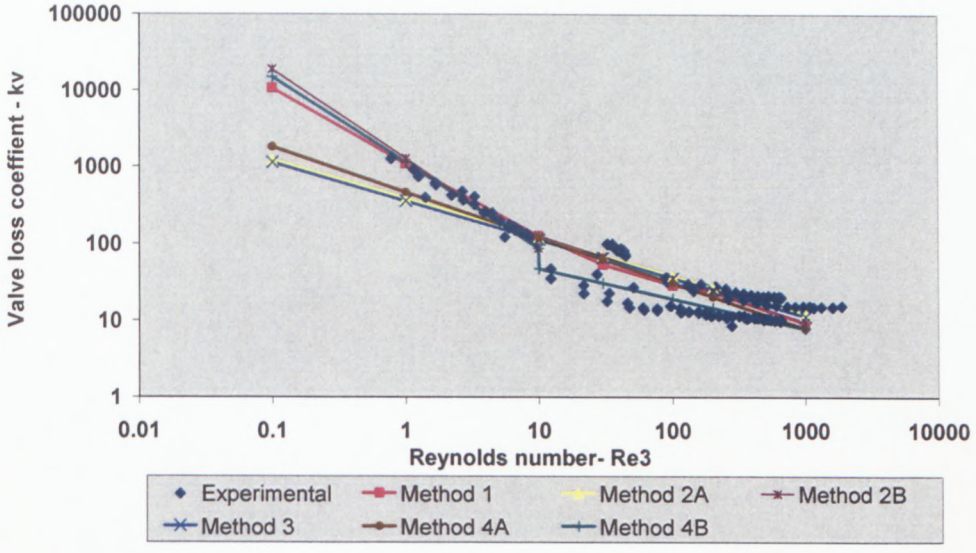

Figure 5.22: Comparison between experimental and predicted kv for 40 mm valve at 75% opening

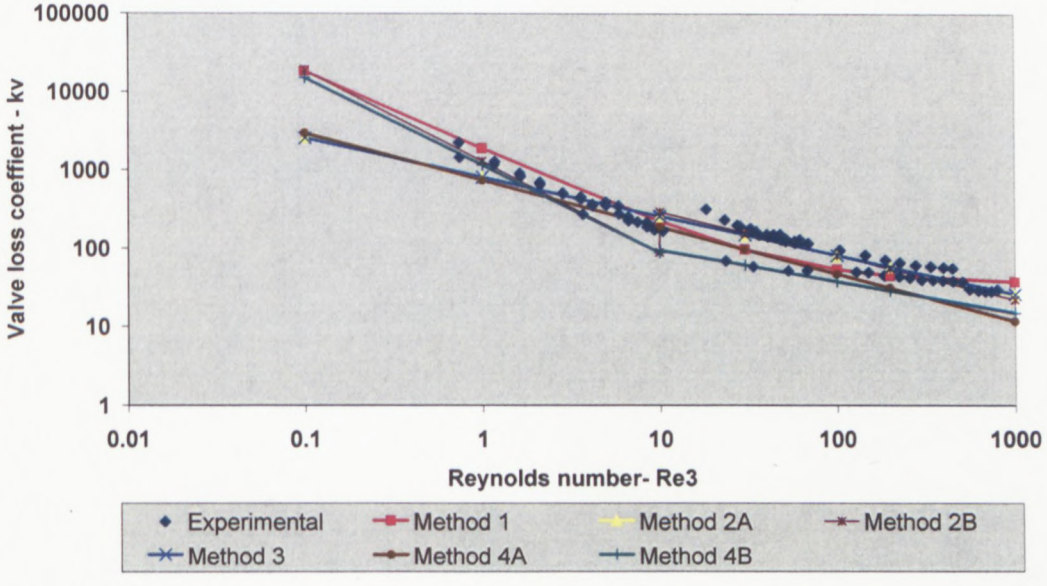

Figure 5.23: Comparison between experimental and predicted kv for 40 mm valve at 50% opening

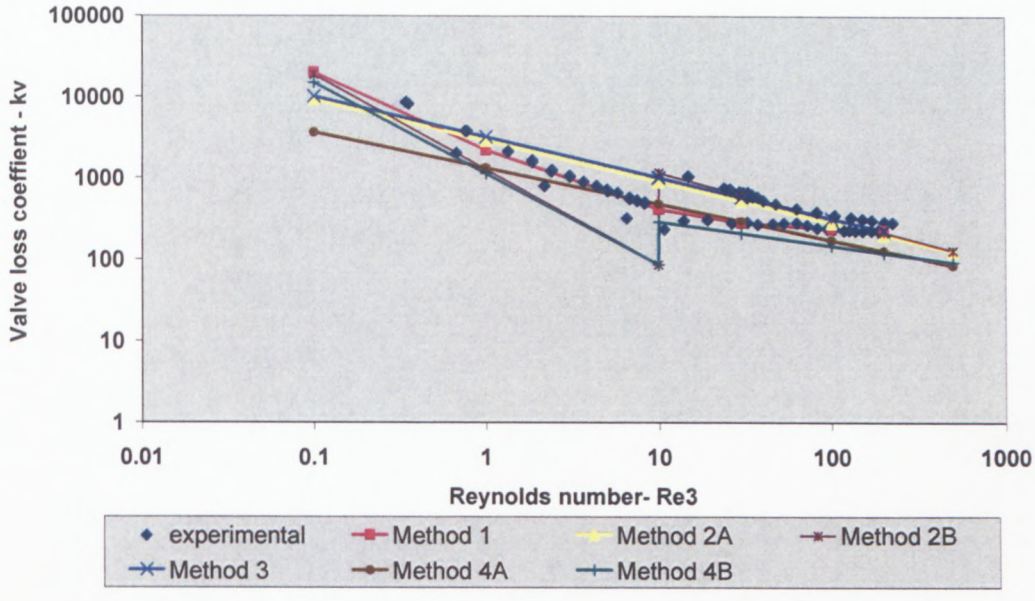

Figure 5.24: Comparison between experimental and predicted kv for 40 mm valve at 25% opening

From Figure 5.21 to Figure 5.24 it is evident that at lower Reynolds numbers, methods 2B and 4B better fit the experimental data. This implies fitting two sets of equations for the laminar region and the transitional region would be a better option.

5.7 PRESENTATION OF THE NEW MODEL: The two-constant model

This model was inspired by the methods explained earlier in Section 5.6. It combined the advantages of these methods such as separation in two zones and inclusion of a turbulent component. As its name implies, this model requires two constants only to fully evaluate the loss coefficients of a diaphragm valve, in different opening positions and for the full range from viscous flow to turbulent flow.

The model contains two correlations:

5.7.1 First correlation

The first correlation (Equation 5.25) applies to all valve sizes. By all it is meant the range of valves tested in this study i.e. 40 mm to100 mm.

$$k_v = \frac{1006}{Re} \qquad \text{Eq 5.25}$$

This correlation is valid up to a Reynolds number of 10; beyond a second correlation will apply.

5.7.2 Second correlation

The second correlation, Equation 5.28, evaluates the valve loss coefficient per size, for different valves opening and from transition to turbulence. Although the transitional zone was unstable, that was why the large scatter of experimental data was noticed in this region, this model attempted to provide indicatives values of k_v which were most of the time conservative.

$$k_v = \frac{C_\Omega}{\sqrt{Re}\,\theta^2} + \frac{\lambda_\Omega}{\theta^2} \qquad \text{Eq 5.28}$$

This correlation is valid for Reynolds number greater than 10. As it was found that turbulent loss coefficients changed drastically with the valve opening, an adjusting function ($1/\theta^2$) was applied to the turbulent component (λ_Ω) which normally was the

turbulent loss coefficient for the full opening position. This adjusting function is valid for valves opening positions ($0.4 \leq \theta \leq 1$), for valve opening positions ($0 < \theta < 0.4$), an adjusting function should be used as given in Equation 5.29

$$k_v = \frac{C_\Omega}{\sqrt{Re}\,\theta^2} + \frac{\lambda_\Omega(1.77 - 0.7\theta)}{\theta^2} \qquad \text{Eq 5. 29}$$

The two parameters (C_Ω and λ_Ω) were found by iterations of the experimental values of k_v. In the iteration, the initial value of λ_Ω was taken as the turbulent k_v at full opening position for valve size smaller than 65 mm. For bigger sizes, the 25% opening turbulent k_v values were used.

Table 5.12 gives the values of the two parameters for the range of valves tested in this study, the last column N is the number of data used in the iteration.

Table 5.12: Parameters C_Ω and λ_Ω for the range of valve tested

Valve size	C_Ω	λ_Ω	N
40 mm	128	8.0	528
50 mm	90	3.4	813
65 mm	60	1.5	313
80 mm	47	2.9	642
100mm	43	4.1	459

5.7.3 Valves size effect on the parameters of the model

Considering Figure 5.25, which shows the variation of both C_Ω and λ_Ω with the valve size, it is apparent that there is definitively a size effect on both C_Ω and λ_Ω, which once again confirmed the lack of dynamic similarity between diaphragm valves of different sizes.

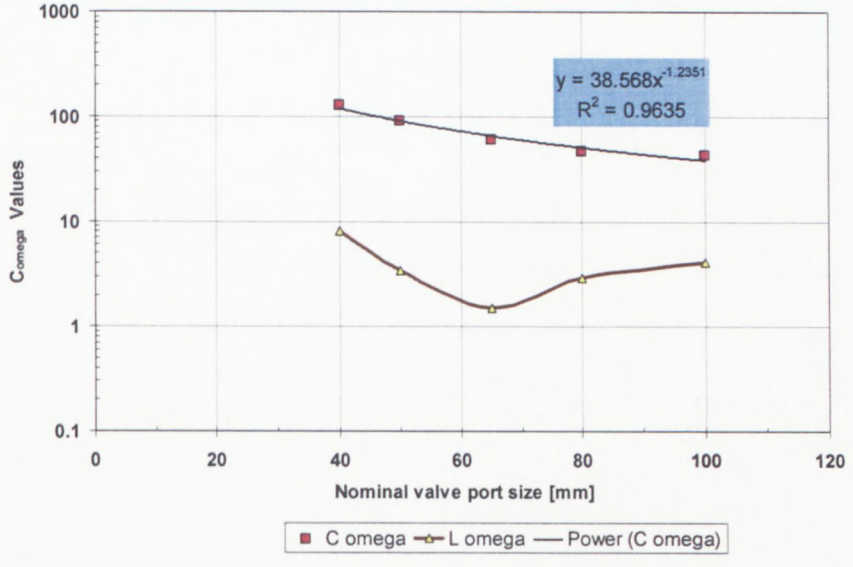

Figure 5.25: Valve size effect on C_Ω (C_{omega}) and λ_Ω (λ_{omega})

However, the variation of C_Ω was uniform and could be predicted reasonably well with a power law model (Equation 5.30). In this equation D stands for the nominal valve port diameter in [mm].

$$C_\Omega = \frac{38.6}{D^{1.24}} \qquad \text{Eq 5.30}$$

Replacing Equation 5.30 in Equation 5.28 gives Equation 5.31, the final form and highlights valve size effect on the diaphragm valve loss coefficient as well as valve opening position.

$$k_v = \frac{38.6}{D^{1.24}\sqrt{Re}\,\theta^2} + \frac{\lambda_\Omega}{\theta^2} \qquad \text{Eq 5.31}$$

5.7.4 Comparison of the two-constant model with different methods

The two-constant was analysed similarly to the different methods considered earlier (Section 5.6.5). The results are shown in Table 13. Looking at RMS deviations, Standard deviations, and maximum deviations, the two constant-model is the second best after Method 4A. It should be noted that these methods are valid for laminar flow only, whereas the two-constant model is valid also for turbulent flow. This comparison was, however, limited to the laminar data only of the 40 mm valve.

Table 5.13: Uncertainties of two-constant model and different methods

Model	Absolute deviation [%]				Deviation [%]	N
	Min	Max	Mean	Stdv	RMS	
Two-const model	0.31	242	54	32	63	390
Method 1	0.12	429	60	61	85	390
Method 2A	0.05	390	45	48	66	390
Method 2B	0.31	377	44	50	66	390
Method 3	0.30	342	44	46	64	390
Method 4A	0.11	227	42	29	51	390
Method 4B	0.02	253	53	38	65	390

5.8 CONCLUSION

This chapter gives an overview of the approaches and methods explored in the quest for correlations predicting diaphragm valve loss coefficients.

It was demonstrated that approaches using the throat Reynolds numbers were not advantageous over those utilising the traditional pipe Reynolds numbers.

Approaches analysing the valve data in terms of identical area ratios presented some merits, as it was found a single curve fitted different valve size data, by normalizing both the area ratio and the number of valve handwheel revolutions. This approach is recommended for future research. Quantitative correlations were not sought as the valves positions tested were not of same area ratios.

The approach analysing the data in terms of same flow ratio (regardless of valve sizes) performed well in terms of uncertainties. Nevertheless this approach is not practical, because it requires interpolation for intermediate valve opening positions. It revealed, however, some interesting features, such as the separation of zones and the size effect in the transitional and turbulent flow.

A correlation was also found for turbulent flow of water, with an adjusting function for valve closure positions.

A careful combination of the different methods explored led the author to introduce the two-constant model, which combined with a loss coefficient constant eventually produced a correlation that predicted the diaphragm valve loss coefficient data for the entire range of Reynolds numbers and for different opening positions and valve sizes.

The next chapter compares this model to the models available in the literature.

CHAPTER 6

CHAPTER 6

EVALUATION AND DISCUSSIONS OF THE NEW MODEL

6.1 INTRODUCTION

In this chapter the two-constant model developed in this study is evaluated in terms of uncertainty and valve size effects. Possible problem areas associated with the models are also discussed. Furthermore, a comparison with existing models is made. The literature and correlations available to determine loss coefficients for straight-through diaphragm valves is scant, only two models were found for comparison in laminar and three for turbulent flow. Hooper (1981) and ESDU (2004) were compared in the laminar and transitional zones, while three others [Hooper (1981), Miller (1990) and Perry (1997)] were compared in the turbulent zone.

6.2 THE TWO-CONSTANT MODEL

6.2.1 Equations

The two-constant model can be summarised by the following equations:

$$k_v = \frac{1006}{Re} \qquad \text{Eq 5. 25}$$

$$k_v = \frac{38.6}{D^{1.24}\sqrt{Re}\,\theta^2} + \frac{\lambda_\Omega}{\theta^2} \qquad \text{Eq 5. 31}$$

Equation 5.25 applies for Reynolds numbers less than 10 for all valve sizes. Equation 5.31 applies for Re ≥ 10 and ($\theta \geq 0.3$), values of λ_Ω for the range of valve tested are shown in Table 5.12. The details of the development of this model were given in chapter 5.

6.2.2 Uncertainty of the two-constant model

Table 6.1 gives the uncertainties between the predicted and the experimental k_v values of the new model per valve size, with turbulent data included. Moderate deviations were noticed in the smaller valve sizes (40 mm and 50 mm), whereas in the larger sizes (80 mm and 100 mm) the deviations were high, with a maximum of 775% observed in the 100 mm valve. This was due, on one hand, to the lower pressure drops in this pipe, and on the other hand, to the transitional regime. Overall, the two constant-model presents a mean deviation of ± 59%, with a RMS deviation of 70%. A total of 2775 data points were considered in the analysis.

Table 6.1: Two-constant model uncertainties

Valve size	Absolute deviation [%]				Deviation [%]	N
	Min	Max	Mean	Stdev	RMS	
40 mm	0.07	242	42	33	54	528
50 mm	0.22	191	60	27	66	813
65 mm	0.55	536	65	53	72	313
80 mm	1.08	283	56	31	72	642
100 mm	1.83	775	73	73	85	459
ALL	0.07	775	59	47	70	2755

6.2.3 Comparison between predicted and observed values of kv

A plot of the observed k_v values versus the calculated k_v values using the two constants model is shown in Figure 6.1. It is evident that there is a strong positive correlation between the predicted and the observed values of k_v (R = 84%). The slope of the predictive line was 0.99, close to the ideal situation of slope 1. This means that overall there is a reasonable correlation between the predicted and the measured k_v values. The overall ratio between the predicted k_v over the measured k_v was 1.11 implying the predicted values in most cases overestimated the measured values. This means the model in general is on the conservative side for design purposes.

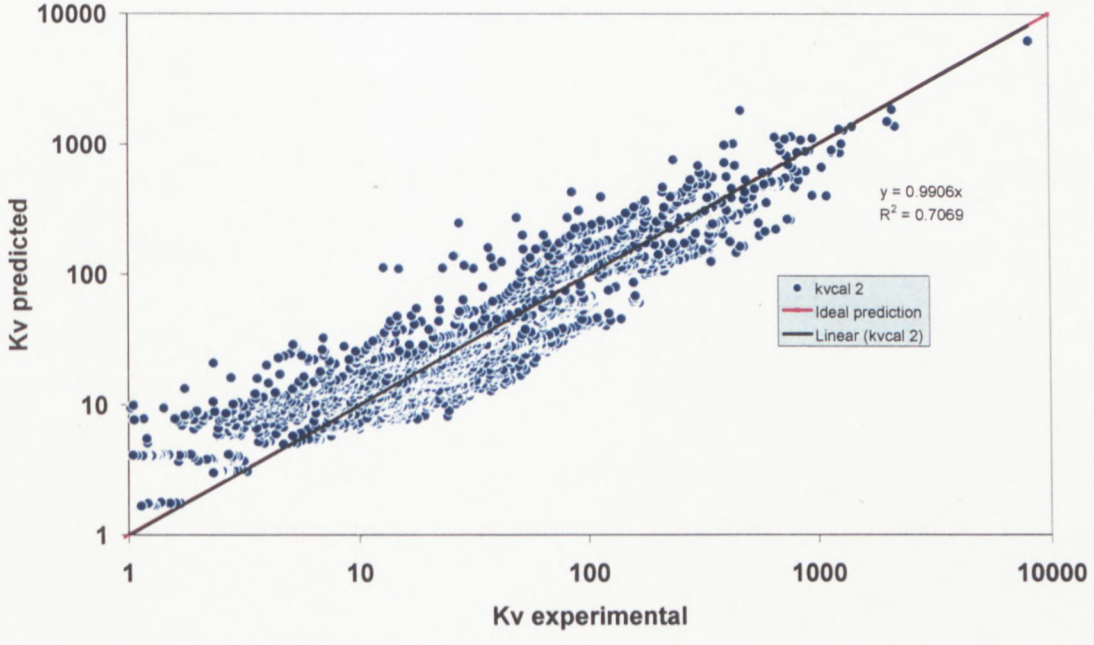

Figure 6.1: Comparison between predicted and calculated k_v values

There are some cases, however, where this ratio was far from 1 on both sides. These problematic cases were found in the transitional region, where fluids are generally unstable, and at very low opening positions.

At lower valve opening positions ($\theta \leq 0.3$) the results seem not to fit the model. This could be because of practical difficulty in testing at this position. This fact was corroborated by Netto and Weaver (1987) who mentioned that at small valve opening positions, valves lose stability through static divergence and static instability occurs. This induces a variation of the valve loss coefficients.

6.2.4 Residuals

It was worth looking at the residuals between the predicted and the measured k_v values. As the magnitude of the k_v values vary significantly from laminar to turbulent flow, with some decades of magnitudes in difference, it was decided to calculate residuals as the difference of the logarithm of the k_v values. These residuals were plotted against Reynolds number in Figure 6.2. There is a good balance between the positive and negative residuals, the absence of any particular pattern or structure meant the correlation was well formulated.

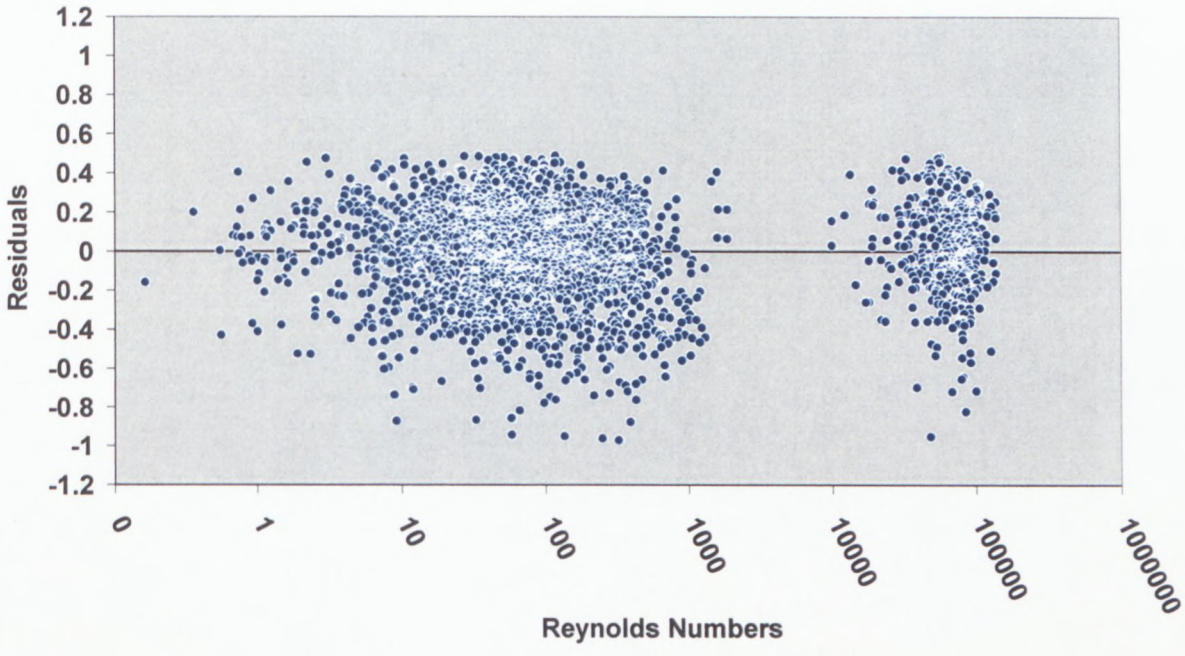

Figure 6.2: Residuals versus Reynolds number

There is, however, a gap between the laminar and transitional flow and turbulent flow data. The reader is reminded of the fact that this work focused on laminar pipe flow. The turbulent data was obtained with water. This is not an issue as it is known that in high turbulent flow the inertial forces dominate e.g. (Murdock, 1976) and, therefore, the rheology of the fluids has little impact on the loss coefficient. This fact is also highlighted by Turian *et al.*, (1987) who stressed that in turbulent flow, loss coefficients of non-Newtonian fluids approach constant asymptotic values, the latter were the same as the limiting values for flow of water.

6.3 COMPARISON OF THE NEW MODEL WITH EXISTING MODELS

6.3.1 Comparison in turbulent flow

It is known that in turbulent flow, the loss coefficients become constant and independent of the Reynolds number e.g. (Turian *et al.*, 1998). gives the comparison between turbulent loss coefficient of this work and those of the works of Miller (1990), Perry *et al.* (1997) and Hooper (1981).

Table 6.2: Comparison of turbulent loss coefficients

Valve Opening [%]	Turbulent loss coefficient							
	Miller (1990)	Perry *et al.* (1997)	Hooper (1981)	This work (2007)				
				Valve size [mm]				
				40	50	65	80	100
25	4	21		211	85	63	67	100
50	1.2	4.3		35	25	16	18	29
75	0.8	2.6		18	8.1	2.8	6.8	10
100	0.8	2.3	2	8.1	2.5	1.2	2.5	1.4

The effect of valve size on loss coefficient is ignored by other authors. Here, however, it is shown that the turbulent loss coefficient is not independent of the valve size.

Excluding the 40 mm valve of this work and Miller (1990), an average $k_v = 2$ can be put forward for all valve sizes in the fully opened position. There is no agreement of the k_v values at other valve openings (see Table 6.2). This may be attributed to the way each author approached the valve opening benchmarking. The inconsistency in loss coefficient data was already mentioned by Brooks (1993) who said: "An additional problem is the lack of a standard for testing duct and fitting performance. Even if everything else was equal (construction, flow condition, etc) two researchers may not have used the same methods to develop the loss coefficient data."

6.3.2 Comparison in laminar flow

A comparison of the new model with Hooper (1981) and ESDU (2004) is given in Figures 6.3 and 6.4 for the fully opened position. A comparison in the half opened position is also shown in Figures 6.5 and Figures 6.6. For other opening positions, see Appendix H. The Hooper (1981) model fits the data reasonably well at lower Reynolds numbers; ESDU (2004) fits well the 40 mm data, but not the other valves. However, the trend toward lower Reynolds number goes through the data, it is not explained why this correlation was not done for Reynolds numbers less than 30.

Error bars indicating the uncertainty per valve size, in terms of mean deviations (Table 6.1) have been included for the two-constant model to enable realistic comparison with the existing models.

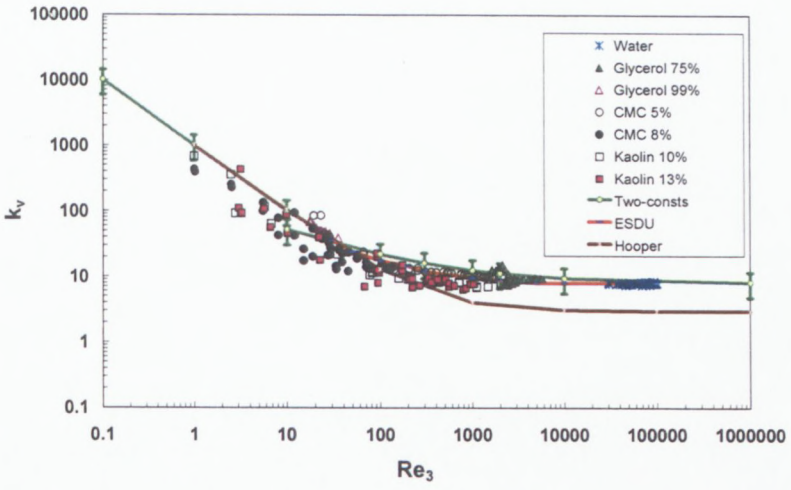

Figure 6.3: Comparison with Hooper (1981) and ESDU (2004) for the 40 mm valve in fully opened position

Looking at Figure 6.3, it is apparent that there is a good agreement between the two-constant model and the two other models i.e. ESDU (2004) and Hooper (1981) in the laminar flow region, but the Hooper's model under predicted the turbulent loss coefficient for the 40 mm valve in the fully opened position.

For other valve sizes in the fully opened position, the two-constant and the Hooper models performed well, except in 100 mm valve where the two-constant model over predicted the turbulent loss coefficient. The ESDU model, however over predicted the turbulent loss coefficient in the fully opened position for all the valve sizes but the 40 mm valve size (see Figure 6.4).

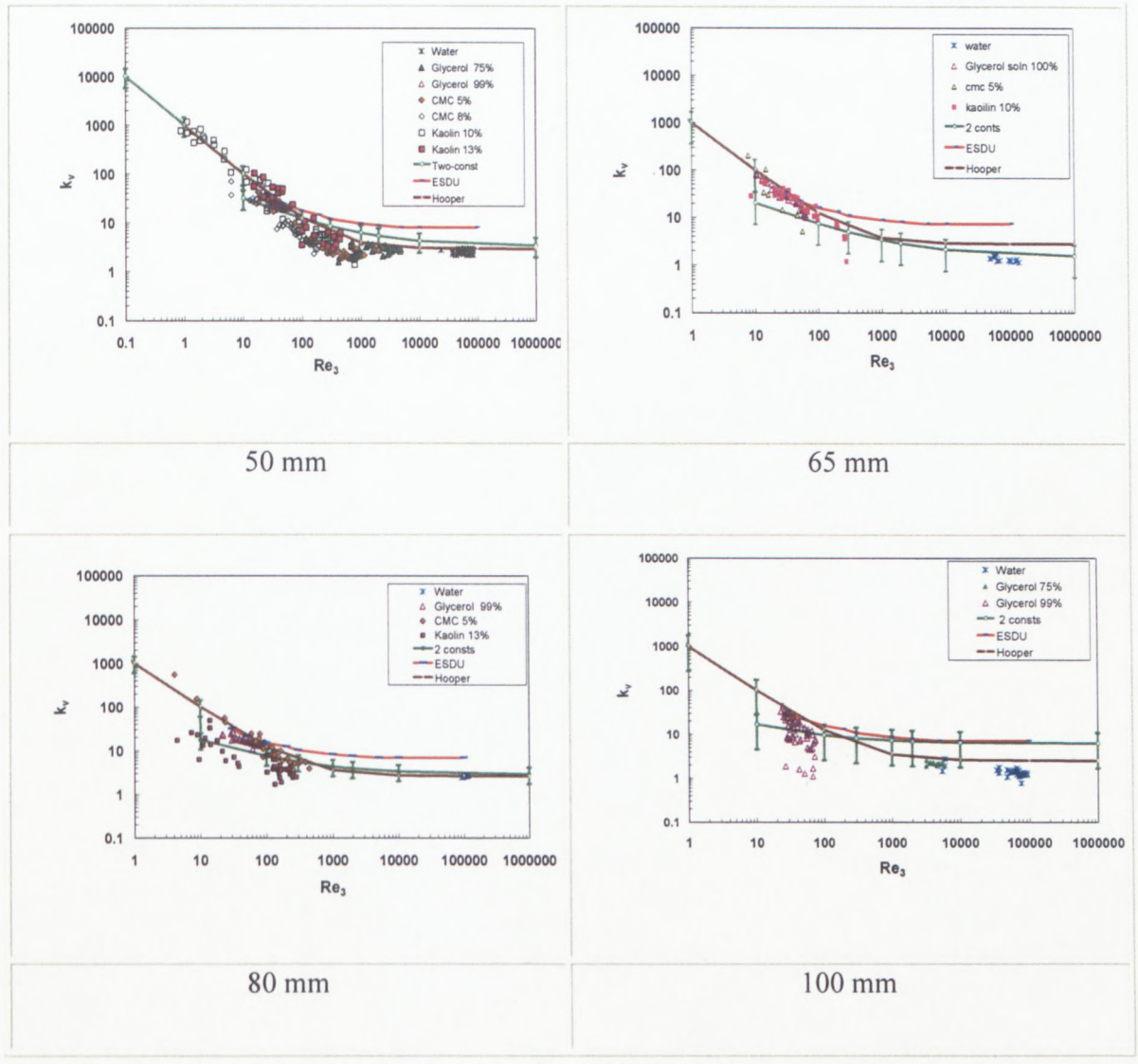

Figure 6.4: Comparison with Hooper (1981) and ESDU (2004) for other valve sizes in **fully opened position**

In the closure positions, however ESDU and the two-constant model continued to perform well, while the prediction of the Hooper model deteriorated (see Figure 6.5, Figure 6.6 and Appendix H).

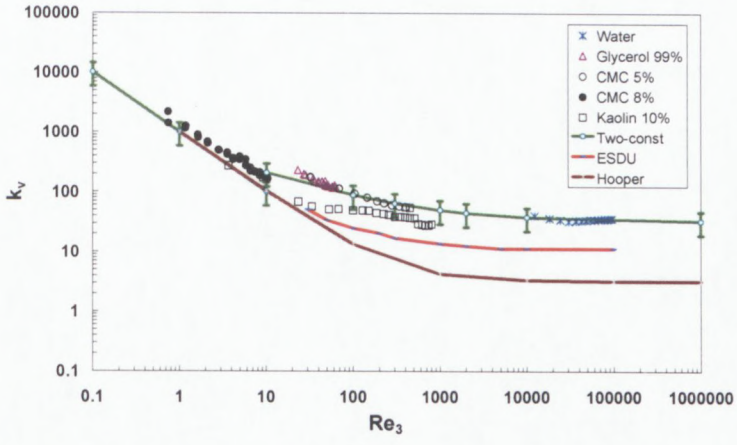

Figure 6.5: Comparison with Hooper (1981) and ESDU (2004) for the 40 mm valve in half opened position

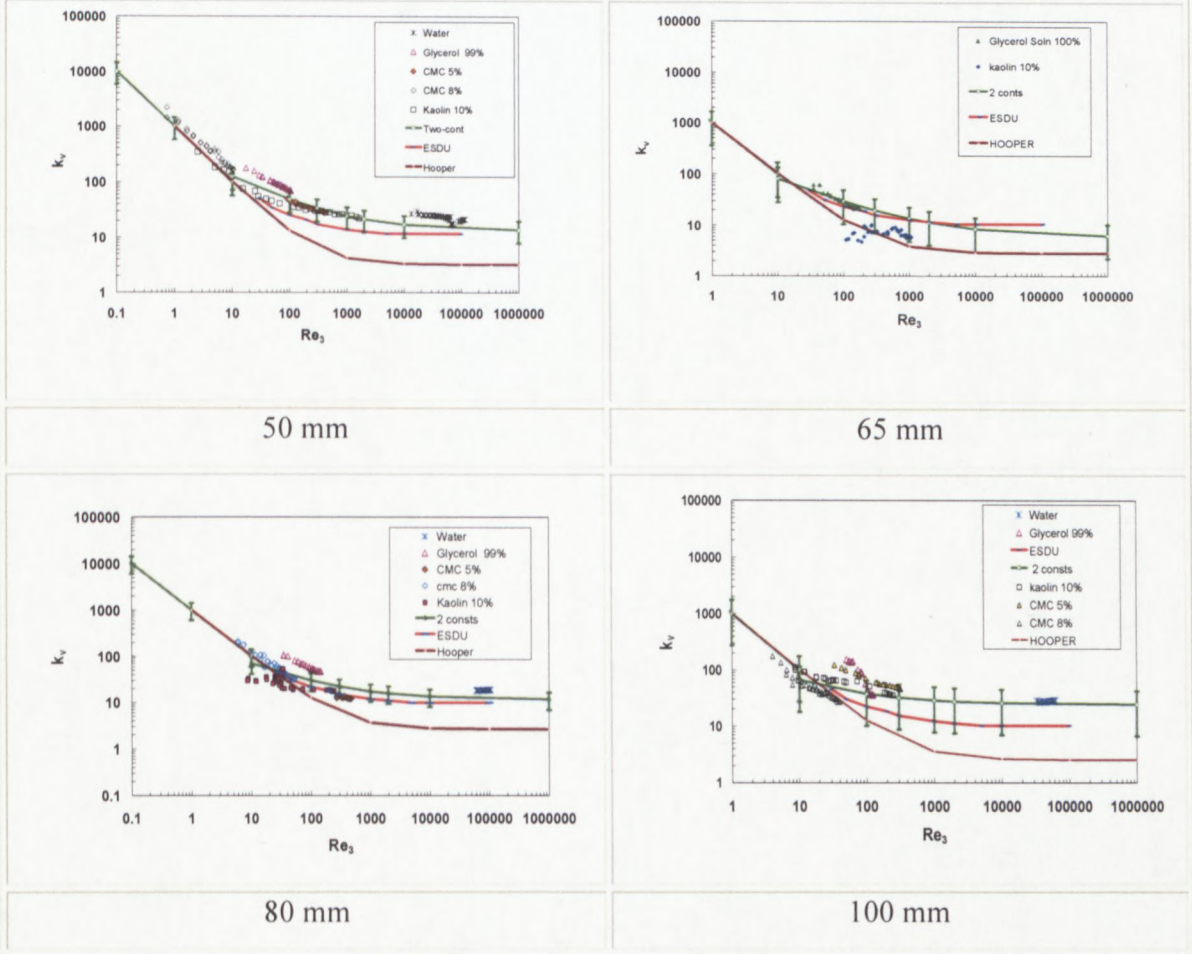

Figure 6. 6: Comparison with Hooper (1981) and ESDU (2004) for other valve sizes in half opened position

6.4 CONCLUSION

The two-constant model was evaluated and found to adequately predict the experimental data produced in the experimental programme of this study. Comparison with available data and models was made. It was found the work of Hooper (1981) agrees well with this work at lower Reynolds numbers and the fully opened position. The ESDU model worked well with the 40 mm valve in the fully opened position, and in the closure positions with other valve sizes. In turbulent flow a value of $k_v = 2$ was found by most researchers for valve sizes ranging from 40 mm up to 100 mm nominal bore. No agreement was found in other opening positions, probably due to the difference in the methods of setting the valve opening positions.

The new model performed well over the wide range of testing conditions: from laminar, transitional and turbulent flows. Furthermore it worked in the valve fully opened position and the valve closure positions, with the exception of the 100mm valve in the fully opened position.

This work demonstrates the importance of a large database of experimental results over a wide range of valves and flow conditions to develop predictive models for pressure losses in diaphragm valves

CHAPTER 7

CHAPTER 7

SUMMARY, CONCLUSIONS AND RECOMMENDATIONS

7.1 INTRODUCTION

A diaphragm valve is commonly used for flow service of slurry, because of features which isolate a fluid controlled by the valve from its operating mechanism, thus minimising contamination, tear and erosion. This type of valve is found in many industrial applications, such as pharmaceutical, chemical, breweries, dairy, food, petroleum, mining, etc. (Warring, 1982). The straight-through diaphragm valve, which was investigated here, has an ability to handle solids. Moreover it presents many advantages such as: low resistance coefficient, has no dead areas where particles may collect, easy maintenance (not requiring to be removed from a pipeline), can be used for throttling and is adaptive to automation (Miles, 2000). Although there is widespread use of this type of valve throughout industry, there is insufficient loss coefficient data available for predicting pressure losses (Kittredge and Rowley, 1957; Miller, 1990 and Jacobs, 1993). This fact is also stressed by Spence and Nash (2004), who said: 'A large number of standards and specifications for valves are issued by international and

national standard organisations and industrial companies; such standards usually refer to materials and constructions of valves and do not give pressure loss data.'

This work is an addition to a relatively small body of information on straight-through diaphragm valves related to loss coefficients. The objective was to provide experimental data and correlations for the prediction of pressure losses across diaphragm valves mainly in pipe laminar flow. As these valves are commonly used for flow control purposes, the correlations developed in this study had to take into account the degree of valve opening.

7.2 SUMMARY

An experimental rig was built and commissioned for measuring pressure losses through valves. Five (nominal bore: 40, 50, 65, 80 and 100 mm) straight-through valves obtained from a South African distributor (Natco) were mounted horizontally and tested in the fully opened position, ¾, ½, and ¼ opening positions respectively. These positions were determined using a gravity test. An inspection of the internal sizes revealed the lack of geometrical similarity between valves. Newtonian fluids: water, glycerol solutions at 99% and 75 % (volume / volume) and non-Newtonian fluids: Carboxymethylcellulose (CMC) at 5 % and 8 % (weight / weight) and kaolin slurries of 10% and 13% (volume / volume) were tested. The experimental errors were investigated and found to be acceptable. The subsequent data base was analysed and only the test runs with friction

factors conforming to 16/Re within 10%, in laminar flow or conforming to the Blasius' equation in turbulent flow were considered.

Using dimensional analysis, a functional relationship was established. The constants of the functional relationship were computed for the laminar data of the database.

In the analysis stage, several approaches and methods were explored before an empirical model the so-called " two-constant model "was adopted.

A three-constant model was first developed with a multiple linear regression analysis performed with primarily pipe laminar data from the experimental database of this study. With relatively less variability in two of the three constants prompted the author to suggest a generalised correlation for laminar flow and transition with one constant (C_Ω) per valve size, but with that generalised correlation for laminar flow the difference between the calculated and observed values rose at both lower and higher Reynolds numbers. These problems were resolved by the introduction, on one hand, of a loss coefficient constant of 1006 for Reynolds number less than 10 and on the other hand, by extending the correlation to turbulent flow of water and the introduction of a second constant. As in turbulent flow, loss coefficients change notably with valve openings, a scaling factor ($1/\theta^2$) was introduced, but for valve closing positions an adjusting function must be used to better predict turbulent loss coefficients. The final form of this study's model is constituted of two sets of equation as:

$$\text{For } Re < 10, \quad k_v = \frac{1006}{Re} \qquad \text{Eq 5.25}$$

$$\text{For } Re \geq 10, \quad k_v = \frac{38.6}{D^{1.24}\sqrt{Re}\,\theta^2} + \frac{\lambda_\Omega}{\theta^2} \qquad \text{Eq 5.31}$$

Where D is the nominal valve port diameter in [mm] and λ_Ω, the nominal turbulent coefficient, is the only parameter to be found per valve size (See Table 5.12), its best estimate being the loss coefficient in the fully opened position for smaller valve sizes and the loss coefficients in the closure positions for larger valve sizes.

7.3 CONCLUSIONS

The following conclusions can be made from this study:

- A test rig was designed, constructed and commissioned to conduct pressure drop experiments in five diaphragm valves;
- a range of Newtonian and non-Newtonian fluids were tested in laminar and transitional flow and water was tested in turbulent flow;
- a two-constant model was developed to predict laminar, transitional and turbulent flow losses, in various valve opening positions.
- Comparison of the two-constant model with existing models was made; it was found that, the work of Hooper (1981) agrees well with this work at lower

Reynolds numbers (Re < 100) and the fully opened position. The ESDU model worked well with the 40 mm valve in the fully opened position, and in the closure positions with other valve sizes.

- Hooper's (1981) loss coefficient constant (C_v = 1000) was confirmed and is valid at lower Reynolds number only, (Re < 100). His turbulent loss coefficient (k_v = 2) is surprisingly close to most k_v values in the fully opened positions of medium sized valves (40 mm ≤ D ≤ 100 mm);
- the valve port diameter or precisely the valve size, affects the loss coefficient. The same trend with ESDU (2004) data was obtained. Therefore a valve loss coefficient must be specified with its size, as a consequence of lack of geometric similarity;
- in turbulent flow, the valve loss coefficient is sensitive to the valve opening, for wide opening positions $\theta > 0.3$ the scaling factor is proportional to the inverse squared of the valve opening; $(1/\theta^2)$;
- the lack of consistency in valve loss coefficients, even in turbulent flow, implies that a valve should be tested at least in the fully opened position to evaluate its nominal turbulent loss coefficient, (λ_Ω);
- it was found, also, the throat Reynolds number does not necessarily improve the loss coefficients results with regard to data scatter and,
- the database produced in this study and the correlations developed herein constituted an addition to the existing literature on diaphragm valves.

7.4 RECOMMENDATIONS FOR FUTURE RESEARCH

For future research on straight-through diaphragm valves the following aspects are recommended:

- The gravity test introduced in this study was conducted in turbulent flow with water. It is not known whether utilising other fluids would yield the same valve settings. This procedure merits some in-depth investigations;
- this study was conducted with medium size valves (40 mm $\leq$ D $\leq$ 100 mm), it is not known whether the finding of this study will apply out of this range, and more test work with smaller and larger valves than those tested here would be interesting;
- the analysis of data in terms of same area ratio yielded a single curve for all the valve sizes tested. It is recommended an experimental investigation on diaphragm valves be conducted, and valves be positioned from onset on the same area ratios and,
- a colloquium of researchers working on diaphragm valves would be necessary to standardise the test procedures of this type of valves.

REFERENCES

REFERENCES

Banerjee, T.K., Manas, D. & Das, S.K. 1994. Non-Newtonian liquid flow through globe and gate valve. *Canadian Journal of Chemical Engineering*, 72:207-211.

Baudouin, M.M. 2003. Contraction and expansion losses for non-Newtonian fluids. Unpublished MTech (Civil Engineering) thesis, Cape Technikon, Cape Town.

Baudouin, M.M., Pienaar, V.G. & Slatter, P.T. 2004. A kinetic energy correction factor for the laminar pipe flow of viscoplastic fluids. In Celata, G.P., Di Marco, P., Mariani, A. & Shah, R.K. (eds). *Proceedings of the 3rd International Symposium on Two-Phase Flow Modelling and Experimentation, Pisa, 22-24 September 2004.* Pisa: Edizioni ETS. [CD-Rom].

Beck, C. 1944. Laminar flow friction losses through fittings, bends and valves. *American Society of Naval Engineering*, 56:235-271.

Brinkworth, B.J. 1968. Introduction to experimentation. London: English Universities Press.

Brooks, P.J. 1993. New ASHRAE local loss coefficients for HVAC fittings. *ASHRAE Transactions*, 99(2):169-193, June.

Buckingham, E. 1914. On physically similar systems: illustrations of the use of dimensional equations. *Physical Review*, 4:345-376.

Centuryinstrument. 2004. The history of the diaphragm valve. http://www.centuryinstrument.com/history.html [5 October 2004].

Chhabra, R.P. & Richardson, J.F. 1999. *Non-Newtonian flow in the process industries: fundamentals and engineering applications.* Oxford: Butterworth-Heinemann.

Colebrook, C.F. 1939. Turbulent flow in pipes, with particular reference to the transition region between the smooth and the rough pipes laws. *J. Inst Civil Eng* ,no 4, paper 5204

Crane Co. 1999. *Flow of fluids through valves, fittings and pipes: metric edition – SI units.* Technical paper no. 410M. London: Crane Co.

Cross, M.M. 1964. Rheology of non-Newtonian fluids: a new flow equation for pseudoplastic systems. *Journal of Colloid Science*, 20:417-437.

Darby, R. 1999. Correlate pressure drop through fittings. *Chemical Engineering*, July: 101-104.

Donald, E.S. 1996. Error Analysis (Non–Calculus). Http://www.lhup.edu/~dsimanek/error.htm [10march 2006]

Douglas, J.F., Gasiorek, J.M. & Swaffield, J.A. 2000. *Fluid mechanics.* 4th ed. Harlow: Longman Scientific & Technica3-63-6l.

Douglas, J.F. & Matthews, R.D. 1996. *Solving problems in fluid mechanics.* 3rd ed. Harlow: Longman.

Edwards, M.F., Jadallah, M.S.M. & Smith, R. 1985. Head losses in pipe fittings at low Reynolds numbers. *Chemical Engineering Research & Design*, 63(1):43-50.

Engineering Sciences Data Unit. 2004. *Pressure losses in valves*. Data item 69022.

ESDU *see* Engineering Sciences Data Unit.

Fester, V.G., Kazadi, D.M., Mbiya, B.M. & Slatter, P.T. 2007. Loss coefficients for flow of Newtonian and non-Newtonian fluids through diaphragm valves. *Chemical Engineering Research and Design: Transactions IChemE, Part A*, 85(A9):1314-1324, September.

Finnemore, E.J. & Franzini, J.B. 2002. *Fluid mechanics with engineering applications.* 10th ed. Boston, MA: McGraw-Hill.

Globalspec. 2004. About diaphragm valves. http://flow.control.globalspec.com/LearnMore/Flow_Control_Transfer/Valves/Diaphragm_Valves [12 December 2004].

Govier, G.W. & Aziz, K. 1972. *The flow of complex mixtures in pipes.* New York: Van Nostrand Reinhold.

Haldenwang, R. 2003. Flow of non-Newtonian fluids in open channels. Unpublished DTech (Civil Engineering) thesis, Cape Technikon, Cape Town.

Hooper, W.B. 1981. The two-k method predicts head losses in pipe fittings. *Chemical Engineering*, 24:96-100, August.

Jacobs, B.E.A. 1993. Laminar/turbulent flow through an annulus with sudden constriction; as found in the gannet project flow line bundles. In Shook, C.A. (ed.). *Proceedings of the 12th International Conference on Slurry Handling and Pipeline Transport, Bruges, Belgium, 28-30 September 1993.* London: Mechanical Engineering Publications. [supplement to the proceedings]

Jadallah, M.S.M. 1980. Flow in pipe fittings at low Reynolds numbers. Unpublished PhD (Chemical Engineering) thesis, University of Bradford.

Kittredge, C.P. & Rowley, D.S. 1957. Resistance coefficients for laminar and turbulent flow through one-half-inch valves and fittings. *Transactions of the American Society of Mechanical Engineering*, 79:1759-1765, November.

Lazarus, J.H. & Slatter, P.T. 1988. A method for the rheological characterisation of tube viscometer data. *Journal of Pipelines*, 7:165-176

Mathews, J.H. & Fink, K.D. 1999. *Numerical methods using MATLAB.* 3rd ed. Upper Saddle River, NJ: Prentice Hall.

Massey, B.S. 1975. *Mechanics of fluids.* 3rd ed. New York: Van Nostrand Reinhold.

Mbiya, B.M., Pienaar, V.G. & Slatter, P.T. 2007. In *Hydrotransport 17: Proceedings of the 17th International Conerence on Hydraulic Transport of Solids, Cape Town, South Africa, 7-11 May 2007.* Cranfield, Bedfordshire: BHR: 121-134.

Metzner, A.B. & Reed, J.C. 1955. Flow of non-Newtonian fluids – correction of the laminar, transition and turbulent-flow regions. *AIChE Journal*, 1(4):434-440.

Miles, K. & Associates. 1985. *Valves: principles and practices.* Northcliff: K. Miles & Associates cc.

Miles, K. & Associates. 2000. *Knowing more about valves.* Northcliff: K. Miles & Associates cc.

Miller, D.S. 1990. *Internal flow systems.* 2nd ed. Cranfield, Befordshire: BHR Information Services.

Murdock, J.W. 1976. *Fluid mechanics and its applications.* Boston, MA: Houghton Mifflin.

Neill, R.I.G. 1988. The rheology and flow behaviour of high concentration mineral slurries. Unpublished MSc (Civil Engineering) thesis, University of Cape Town.

Netto, W.D. & Weaver, D.S. 1987. Divergence and limit cycle oscillations in valves operating at small openings. *Journal of Fluids and Structures*, 1:3-18.

Paterson, A. & Cooke, R. 1999. The design of slurry pipeline systems. Short course presented at the Cape Technikon, Cape Town, 24-26 March, 1999.

Perry, R.H., Green, D.W. & Maloney, J.O. 1997. *Perry's chemical engineers' handbook.* 7th ed. New York: McGraw-Hill.

Pienaar, V.G. 1998. Non-Newtonian fitting losses. Unpublished MTech (Chemical Engineering) thesis, Cape Technikon, Cape Town.

Pienaar, V.G., Alderman, N.J. & Heywood, N.I. 2001. A review of frictional pressure losses for flow of non-Newtonian fluids through pipe fittings. *Aspen Technology's Internet Process Manual: Slurry Handling,* vol. 2, part 6.

Pienaar, V.G. 2004. Viscous flow through sudden contractions. Unpublished DTech (Chemical Engineering) thesis, Cape Technikon, Cape Town.

Pienaar, V.G., Slatter, P.T., Alderman, N.J. & Heywood, N.I. 2004. A review of frictional pressure losses for flow of Newtonian and non-Newtonian slurries through valves. In Heywood, N. (ed.). *Hydrotransport 16: Proceedings of the 16th International Conference on Hydrotransport, Santiago, Chile, 26-28 April, 2004.* Vol. 1. Cranfield, Bedfordshire: BHR:189-204.

Pienaar, V. G., Slatter P. T., Ramohlola N. S., Kazadi D. 2006. Resistance coefficients of mineral tailings flowing in diaphragm control valves. *IMPC Conference on Mineral Processing, Istanbul, Turkey 3 - 7 Sept, 2006.* Istanbul, Turkey.

Prasuhn, A.L. 1980. *Fundamentals of fluid mechanics.* Englewood Cliffs, NJ: Prentice Hall.

Saundersvalves. 2004. Product overview: industrial diaphragm valves. http://www.saundersvalves.com/site/index [12 December 2004].

Shook, C.A. & Roco, M.C. 1991. *Slurry flow: principles and practice.* Boston, MA: Butterworth-Heinemann.

Skelland, A.H.P. 1967. *Non-Newtonian flow and heat transfer.* NewYork: John Wiley and Sons Inc

Slatter, P.T. 1994. Transitional and turbulent flow of non-Newtonian slurries in pipes. Unpublished PhD (Civil Engineering) Thesis, University of Cape Town.

Slatter, P.T. 1996. Turbulent flow of non-Newtonian slurries in pipes, *J. Hydrol. Hydromech* 44: 24-3

Slatter, P.T. 1999. A new friction factor for yield stress fluids. In *Hydrotransport 14: Proceedings of the 14th International Conference on Slurry Handling and Pipeline Transport, Maastricht, The Netherlands, 8-10 September 1999.* Cranfield, Bedfordshire: BHR: 255-265.

Slatter, P.T. 2002. Non-Newtonian pipe flow – A place in the sun at last! *11th International conference on Transport and sedimentation of solid particles, September 2002.* Ghent. Vol 2:33-40

Slatter, P.T. 2006. Modelling the hydrodynamics of minerals processing suspensions. In Onal, G. *et al.* (eds). *Proceedings of the XIII International Mineral Processing Congress, Istanbul, Turkey, 3-8 September 2006.* Istanbul: Promed. Vol 3: 1753-1758.

South Africa. 1998. *National Water Act, 1998 (Act No. 36 of 1997) and Regulations: incorporating Water Services Act, 1997 (Act No. 108, 1997).* Pretoria: Government Printer.

Spence, J. & Nash, D.H. 2004. Milestones in pressure valve technology. *International Journal of Pressure Vessels and Piping*, 81(2):89-118, February.

Streeter, V.L. & Wylie, E.B. 1975. *Fluid mechanics.* 6th ed. New York: McGraw-Hill.

Tietjens, O.G., Prandtl, L. & Den Hartog, J.P. 1934. *Applied hydro- and aeromechanics: based on lectures of L. Prandtl. Translated by J.P. den Hartog.* London: McGraw-Hill.

Turian, R.M., Ma, T.-W., Hsu, F.-L.G., Sung, M.D.-J. & Plackmann, G.W. 1998. Flow of concentrated non-Newtonian slurries: 2. Friction losses in bends, fittings, valves and Venturi meters. *International Journal of Multiphase Flow*, 24(2):243-269, March.

Warring, R.H. 1982. *Handbook of valves, piping, and pipelines.* Houston, TX: Gulf.

Waterfield, T.O.W. 1982. Designing the "VeeValv" diaphragm valve. *Materials & Design*, 3:575-580.

Yang, F. & Kao, I. 2000. Analysis of fluid flow and deflection for pressure-balanced MEMS diaphragm valves. *Sensors and Actuators A: Physical*, 79(1):13-21.

Young, D.F., Munson, B.R. & Okiishi, T.H. 1997. *A brief introduction to fluid mechanics.* New York: Wiley.

APPENDICES

APPENDICES

Appendix A

Typical Example of Relative Density Test

Relative density test work for Kaolin

Description	Unit	Value		No.	M1	M4	M2	M3	DM	Rd
Date		22/06/2006		1	90.742	339.446	122.276	342.171	1.0946	1.0980
Time		11:36:00 AM		2	67.870	316.920	109.133	320.535	1.0960	1.0994
Test Rig		valves test rig		3	97.090	345.879	167.809	351.680	1.0894	1.0927
Tested by		Mume			B	B + W	B + S	B + S + W		
Test Material		Kaolin	Notes :						Ave Rd	1.0967
Sampling point		Tapping	1)	Calculation Corrects for temperature						
Water temperature	°C	25	2)	Holds only for Rd's up to			1.6	5.86	%Cv	Kaolin
Sample temperature	°C	26	3)	Temperature of water & mixtures must be within 2°C						

Appendix B

Gravity Test for 65 mm Bore Diaphragm Valve

TIME (sec)	Mass of water [Kg]										
Position →	Fully Opened	1 Rev	2 Rev	3 Rev	4 Rev	5 Rev	6 Rev	7 Rev	8 Rev	9 Rev	10 Rev
0	606.5	611.5	608.5	602	610	603.5	603	607	605	607	602
1	592	597	593.5	588	596	592	591.5	597.5	597.5	605	601.5
2	578.5	583.5	580	575.5	583	579.5	579.5	589	591	603	600.5
3	565	568.5	565.5	559.5	568.5	568	568.5	577	584.5	601	599.5
4	550	555	552	546	555.5	555.5	556.5	567.5	577	599	599
5	536.5	541.5	538	531.5	544	545	545.5	557.5	571	597	598
6	522	526.5	523.5	518	527.5	532	534	548	565.5	595.5	597.5
7	508.5	513	510	503.5	514.5	519.5	521.5	537.5	558	593.5	596.5
8	494.5	498.5	495.5	491	500.5	508	510.5	529	552	591.5	596
9	481.5	485.5	482	476.5	487	496	498	518.5	545	590	595
10	467.5	471	469	462	473	484.5	486.5	508	539	588	594
11	449.5	457.5	454	448.5	462	475	475	499	532.5	586	593.5
12	436	444	440.5	434.5	446.5	460.5	463	488.5	526.5	584.5	592.5
13	422	429.5	426	421	432.5	449.5	452.5	479	519.5	582.5	592
14	409	414	411.5	409	420	437.5	441.5	471.5	513	580.5	591.5

TIME (sec)	Mass of water [Kg]										
Position →	Fully Opened	1 Rev	2 Rev	3 Rev	4 Rev	5 Rev	6 Rev	7 Rev	8 Rev	9 Rev	10 Rev
15	396.5	399.5	399.5	393	406	426.5	431	459.5	507	578.5	590.5
16	382	387	385.5	380	392	414	419	450	500.5	577	589.5
17	369	374	371.5	365.5	379	403	407.5	440	494.5	575	589
18	355.5	359.5	358	352.5	363	389	393.5	431	489	573.5	588
19	342.5	347	345	338.5	350.5	375.5	378.5	420.5	481.5	572	587.5
20	329	333.5	331.5	326.5	337.5	363	368	412.5	475.5	570	586.5
21	316	320.5	318.5	313	325	353	357	402	469	568	585.5
22	303	307	306.5	299	311.5	342.5	347	392	463	566.5	585
23	289	294	292	286.5	301	334	336.5	382.5	456	564.5	584
24	276.5	281.5	279.5	273	286.5	322	325	372.5	451	563	583.5
25	263	267	266	260.5	273	311	314.5	363.5	444	561	582.5
26	250.5	255	253.5	249	261	299.5	303.5	356	437.5	559.5	582
27	238	241.5	240.5	234.5	248	288.5	292.5	344.5	431.5	557.5	581
28	224	229.5	228.5	222	236	277.5	280.5	335.5	424.5	556	580.5
29	210	217	215.5	209	225.5	268	269.5	326	418	554	579.5
30	197.5	204	201.5	197	210.5	256	258.5	317	410.5	552	578.5
31	185.5	192	188.5	184	199	245	247.5	307.5	403.5	550.5	578
32	172.5	179	176.5	173	186	235	237.5	299.5	398	548.5	577.5
33	160	166.5	164	159.5	175	224	226	289.5	392	547	576.5

TIME (sec)	Mass of water [Kg]										
Position →	Fully Opened	1 Rev	2 Rev	3 Rev	4 Rev	5 Rev	6 Rev	7 Rev	8 Rev	9 Rev	10 Rev
34	147.5	155.5	152	146	162.5	213.5	215.5	279.5	386	545	575.5
35	135	142	141.5	133.5	152.5	205	205	271	379.5	543.5	575
36	123	130.5	130.5	120.5	138.5	192.5	193.5	261.5	374	542	574
37	110.5	118.5	117.5	109	127	182	183.5	252.5	367.5	540	573.5
38	99	108	105.5	98.5	116.5	171.5	175	245.5	361	538	572.5
39		96	94.5		104.5	162.5	165	234.5	355.5	536.5	571.5
40					94	151.5	153.5	225.5	349	534.5	571
41						143	142.5	216.5	343	533	570
42						131.5	137	208	338	531	569.5
43						121.5	127.5	198.5	330.5	529.5	568.5
44						112.5	117.5	191.5	325	527.5	568
45						102.5	106.5	181.5	318.5	526	567
46							97	172	313	524	566.5
47								163.5	306.5	522.5	565.5
48								154.5	301.5	521	565
49								146	295	519	564
50								139	289	517.5	563
51								128.5	283	515.5	562.5

Appendix C

Dry kaolin Composition

Composition	Proportion (%)
SiO_2	46
Al_2O_3	38
Fe_2O_3	0.85
TiO_2	0.58
CaO	0.10
MgO	0.18
K_2O	1.00
Na_2O	0.20
LOI	13.10

These proportions are reflected in the pie chart below:

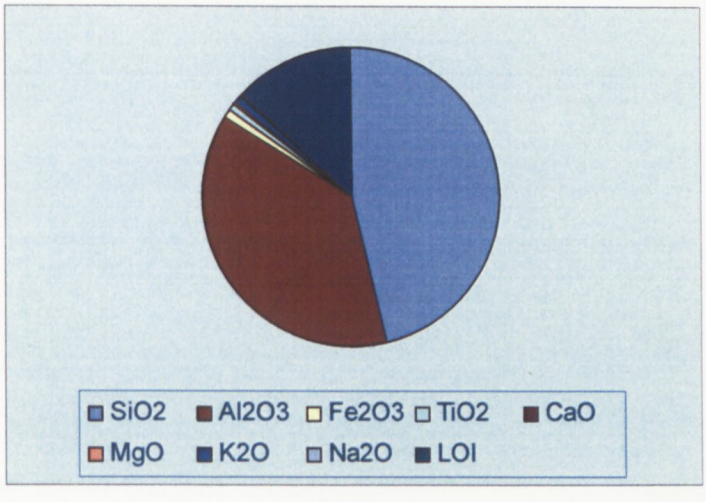

Appendix C

Physical properties of dry Kaolin

	Physical properties		Typical
1	Abrasiveness (Einlehner tester)		35 g/m^2
2	Particle size distribution		
		Below 20 micron	100%
		12 micron	94%
		10 micron	90%
		6 micron	80%
		4 micron	70%
		3 micron	60%
		2 micron	48%
3	Reflectance minimum (Elrepho)		83%
4	pH value		5
5	Moisture		
		Powder	0 – 1%
		Pellets	8 – 12%
6	Oil absorption of powder		45 – 50%
7	Bulk density of powder in bags		0.7 g/cc

Appendix D

Viscosity of glycerine solutions (Perry, 1997)

Aqueous Glycerol solutions					
% Weight Glycerol	Grams per litre	Relative density 20 °C/25 °C	Viscosity (mPa.s)		
			20 °C	25 °C	30 °C
100	1261	1.26201	1495	942	622
99	1246	1.25945	1194	772	509
98	1231	1.25685	971	627	423
97	1216	1.25425	802	521	353
96	1201	1.25165	659	434	296
95	1186	1.24910	543.5	365	248
80	996.8	1.20925	61.8	45.72	34.81
25	265.0	1.06115	2.089	1.085	1.586
10	102.2	1.02370	1.307	1.149	1.021

Appendix E

Pipe Internal diameters

	Internal Diameters [mm]				
Pipe Position	F-LHS Pipe	LHS Pipe	RHS Pipe	F-RHS Pipe	average
Top	42.17	42.09	42.05	42.07	42.12
2nd Top	52.99	52.98	53.17	52.15	52.80
3rd Top	62.95	63.24	62.99	63.09	63.08
4th Top	80.40	80.47	80.45	80.41	80.43
2nd Bottom*	95.77	99.19	99.24	98.88	98.58
Bottom	96.21	99.25	96.68	96.21	97.17

Standard deviations of pipe internal diameters

	Standard Deviation [mm]				
Pipe Position	F-LHS Pipe	LHS Pipe	RHS Pipe	F-RHS Pipe	average
Top	0.15	0.12	0.19	0.10	0.13
2nd Top	0.02	0.15	0.06	0.09	0.08
3rd Top	0.09	0.11	0.22	0.43	0.19
4th Top	0.08	0.12	0.07	0.09	0.09
2nd Bottom	0.42	0.13	0.14	0.27	0.22
Bottom	0.03	0.25	0.26	0.03	0.18

* 2nd Bottom pipe was not part of this study

Relative Error of pipe diameter measurements at 95% confidence level

	Relative Error [± %]				
Pipe Position	F-LHS Pipe	LHS Pipe	RHS Pipe	F-RHS Pipe	average
Top	0.70	0.58	0.88	0.49	0.63
2nd Top	0.08	0.58	0.22	0.33	0.32
3rd Top	0.29	0.35	0.71	0.14	0.60
4th Top	0.20	0.29	0.17	0.23	0.22
2nd Bottom	0.09	0.27	0.28	0.55	0.44
Bottom	0.05	0.51	0.55	0.05	0.37

Number of pipe diameter measurements

	Number of measurements per pipe			
Pipe Position	F-LHS Valve	LHS Valve	RHS Valve	F-RHS Valve
Top	25	20	4	14
2nd Top	15	17	10	15
3rd Top	15	21	17	10
4th Top	16	13	22	22
2nd Bottom	9	14	19	15
Bottom	10	15	24	10

Locations of pressure tappings on test sections

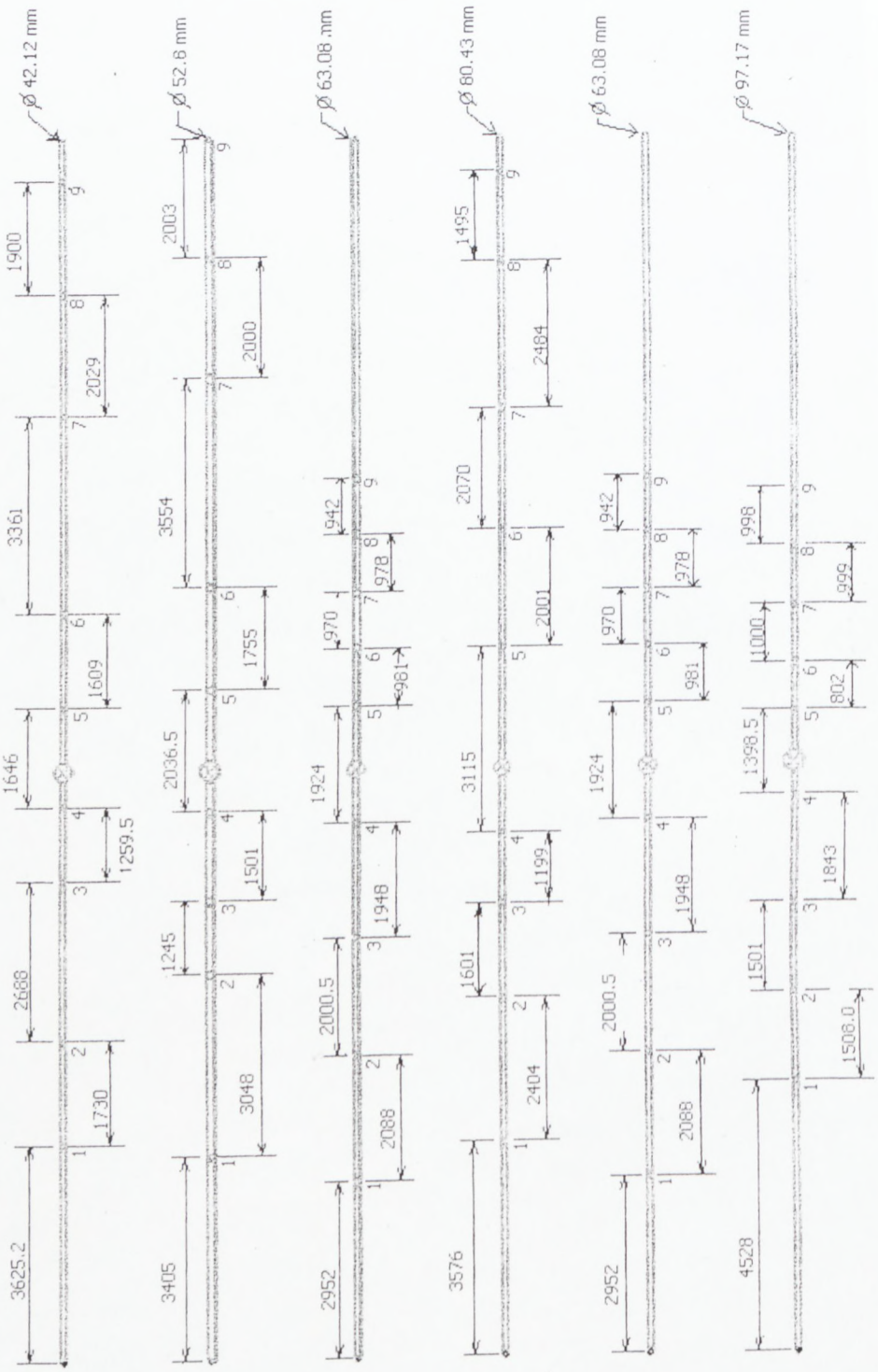

Appendix F

Relative errors of major parameters in 50 mm ID pipe

	Average	Standard	Error	95% Confidence
Re_3	73433.7	72.150	0.20	144.30
k_v	1.91837	0.097	10.13	0.19
PTT 1 [Pa]	25250.3	55.006	0.44	110.01
PTT 2 [Pa]	24243.8	38.158	0.31	76.32
PTT 3 [Pa]	23759.5	34.265	0.29	68.53
PTT 4 [Pa]	23300.3	31.868	0.27	63.74
PTT 5 [Pa]	20725.9	43.119	0.42	86.24
PTT 6 [Pa]	19794.2	21.613	0.22	43.23
PTT 7 [Pa]	19099.6	21.356	0.22	42.71
PTT 8 [Pa]	18405.2	21.273	0.23	42.55
PTT 9 [Pa]	17693.5	19.987	0.23	39.97
Q [l/sec]	3.05019	0.003	0.20	0.006
V [m/s]	1.39306	0.001	0.20	0.002
τ_o (US)	4.58416	0.186	8.14	0.37
τ_o (DS)	4.63651	0.077	3.30	0.15
f (US)	0.00473	0.0002	8.03	0.0004
f (DS)	0.00479	0.0001	3.34	0.0002

Relative errors in 63 mm ID pipe

	Average	Standard	Error	95% Confidence
Re_3	77810	385.052	0.99	770.10
k_v	1.59423	0.18385	23.06	0.37
PTT 1 [Pa]	30184.3	35.8725	0.24	71.75
PTT 2 [Pa]	29341.1	31.8051	0.22	63.61
PTT 3 [Pa]	29142.1	31.5885	0.22	63.18
PTT 4 [Pa]	28617.4	29.8224	0.21	59.64
PTT 5 [Pa]	27298.5	28.2596	0.21	56.52
PTT 6 [Pa]	26802	24.6604	0.18	49.32
PTT 7 [Pa]	26288.6	25.8181	0.20	51.64
PTT 8 [Pa]	25592.7	26.6816	0.21	53.36
PTT 9 [Pa]	25019.4	60.1792	0.48	120.36
Q [l/sec]	3.85544	0.01908	0.99	0.04
V [m/s]	1.23367	0.0061	0.99	0.01
τ_o (US)	4.02001	0.18168	9.04	0.36
τ_o (DS)	3.59023	0.17583	9.79	0.35
f (US)	0.00528	0.00025	9.47	0.0005
f (DS)	0.00472	2.40E-03	101.69	0.0048

Relative errors in 80mm ID pipe

	Average	Standard	Error	95% Confidence
Re_3	70579.1	432.098	1.22	864.20
k_v	2.50661	0.25013	19.96	0.50
PTT 1 [Pa]	27966	40.5213	0.29	81.04
PTT 2 [Pa]	27796.1	45.455	0.33	90.91
PTT 3 [Pa]	27671.4	34.322	0.25	68.64
PTT 4 [Pa]	27462.8	36.5886	0.27	73.18
PTT 5 [Pa]	26261.8	33.2696	0.25	66.54
PTT 6 [Pa]	25881.1	25.1512	0.19	50.30
PTT 7 [Pa]	25762.6	22.8159	0.18	45.63
PTT 8 [Pa]	25440	20.9992	0.17	42.00
PTT 9 [Pa]	25264	19.7212	0.16	39.44
Q [l/sec]	4.45903	0.0273	1.22	0.05
V [m/s]	0.87764	0.00537	1.22	0.01
τ_o (US)	2.11362	0.38919	36.83	0.78
τ_o (DS)	2.14098	0.12323	11.51	0.25
f (US)	0.00549	0.00103	37.52	0.0021
f (DS)	0.00556	3.30E-04	11.87	0.0007

Relative errors in 100mm ID pipe

	Average	Standard	Error	95% Confidence
Re_3	82923.89	314.01	0.76	628.02
k_v	1.28	0.1	15.63	0.20
PTT 2 [Pa]	85.9	7.44	17.32	14.88
PTT 3 [Pa]	195.33	7.31	7.48	14.62
PTT 4 [Pa]	262.52	5.87	4.47	11.74
PTT 5 [Pa]	865.58	26.41	6.10	52.82
PTT 6 [Pa]	998.78	25.54	5.11	51.08
PTT 7 [Pa]	1083.36	24.85	4.59	49.70
PTT 8 [Pa]	1283.87	28.17	4.39	56.34
PTT 9 [Pa]	1651.48	24.73	2.99	49.46
Q [l/sec]	6.33	0.02	0.63	0.04
V [m/s]	0.85	0.001	0.24	0.00
τ_o (US)	1.58	0.06	7.59	0.12
τ_o (DS)	2.3	0.14	12.17	0.28
f (US)	4.66E-03	4.40E-06	0.19	0.00
f (DS)	4.33E-03	1.89E-04	8.73	0.0004

Appendix G

Water in 40 mm valve, 100% open

Date:	13/10/2004	Test done by Daniel	
Valve Type:	Diaphragm		
Valve dimension[m]:	0.04		
Valve position:	1	Area[m^2]	
Pipe Diameter [m]:	0.04212	0.00139337	

Material Type:	Water
Density[kg/m^3]:	999.87
Concentration:	
τ_y:	0
K:	0.001
n:	1
PPT used:	101
Range selected:	0-130

			Axial distances [m]	-6.298	-4.568	-1.88	-0.6205	1.0755	3.8045	6.0455	8.0745	9.9745
			Valve plane									
			Non-dim distances [L/D]:	-149.5251662	-108.452042	-44.634378	-14.7317189	25.53418803	90.32526116	143.5303894	191.7022792	236.811491
			Distances[m]:	0	1.73	4.418	5.6775	7.3735	10.1025	12.3435	14.3725	16.2725
Run #	Re_3		k_v	Pod 1	Pod 2	Pod 3	Pod 4	Pod 5	Pod 6	Pod 7	Pod 8	Pod 9	Average Q
													[l/s]
Run 3	86986		8.89	56112	54430	52225	49596	28504	25690	23407	21050	19044	2.88
Run 4	87522		9.69	56153	54156	51297	49692	28283	25937	23172	21131	19342	2.90
Run 6	36757		7.65	30516	30054	29463	29335	26128	25586	25135	24736	24355	1.22
Run 7	45279		7.77	33177	32798	32077	31859	26829	25934	25295	24750	24211	1.50
Run 9	52058		8.13	36043	35376	33977	33803	27370	26391	25500	24772	24102	1.72
Run 10	52099		7.59	35953	35471	34487	33909	27288	26402	25543	24753	24065	1.72
Run 11	59107		7.56	38891	38044	37209	36665	27992	26776	25746	24801	23954	1.96
Run 12	59182		7.54	39065	38214	37060	36159	28120	26787	25771	24831	23919	1.96
Run 13	63715		7.83	41172	40279	38562	38439	28721	27028	25819	24826	23773	2.11
Run 14	63777		7.87	41115	40566	39150	38336	28616	27056	25783	24719	23744	2.11
Run 15	75397		7.55	47361	46278	44150	43284	30044	27757	26319	24797	23446	2.49
Run 16	75422		8.29	47656	46144	44192	43763	29539	27740	26105	24782	23499	2.50
Run 17	83856		7.39	51229	49810	47901	46145	29347	26897	25287	23178	21687	2.77
Run 18	83922		7.60	51001	49460	47449	46538	29671	27033	25190	23336	21789	2.78
Run 25	97392		7.76	56404	54687	51225	50437	27312	24209	21641	19294	17135	3.22
Run 26	97470		7.86	56617	54857	51671	50124	27211	24305	21651	19328	17197	3.22
Run 27	100430		8.06	53602	52133	48203	46671	22653	19375	16515	14084	11916	3.32
Run 28	100455		7.71	53578	51594	48773	47083	22417	19344	16598	14160	11819	3.32
Run 29	92986		7.84	48037	46385	43769	41890	21241	18445	16010	13935	11896	3.08
Run 30	92986		7.69	47609	46573	42908	41836	21143	18539	16103	13892	11934	3.08
Run 32	70305		8.02	33330	32238	30619	29890	17721	16142	14539	13352	12122	2.33
Run 33	95250		8.08	49811	47785	44956	44118	20908	18662	16147	13902	12012	3.15
Run 34	95498		7.72	49870	48240	44665	43901	21052	18678	16264	13967	11832	3.16
Run 35	30734		7.65	28615	28422	27999	27831	25654	25296	24932	24638	24400	1.02

Water in 40 mm valve, 75% open

Date:	03/03/2005
Valve Type:	Diaphragm
Valve dimension[m]:	.04
Valve position:	3/4Open
Pipe Diameter [m]:	0.04212

Area[m^2]	0.00139337

Material Type:	Water
Density[kg/m^3]:	999.87
Concentration:	0
τ_y:	0
K:	0.001
n:	1
PPT used:	101
Range selected:	0-130

Axial distances [m]	-6.298	-4.568	-2.932	-0.6205		1.0755	6.0455	8.0745	9.9745			
Valve plane												
Non-dim distances [L/D]:	-149.5251662	-108.45204	-69.610636	-14.7317189	0	25.534188	143.530389	191.702279	236.811491			
Distances[m]:	0	1.73	3.366	5.6775	7.3735	8.9825	12.3435	14.3725	16.2725			

Run #	Re_3	$k_{v\ excl.}$	k_v	Pod 1	Pod 2	Pod 3	Pod 4	Pod 5	Pod 6	Pod 7	Pod 8	Pod 9	Average Q [l/s]
Run 2	97378		16.7	89249	86886	85098	81828	35421	33232	28728	26136	23684	3.22
Run 4	91721		16.7	82729	80965	78900	75887	34320	32474	28386	26143	23711	3.03
Run 5	90045		17.3	82744	80418	79040	76088	34505	32304	28476	26034	23826	2.98
Run 7	86788		16.1	75891	74578	72871	70089	33839	31934	28471	26242	24232	2.87
Run 9	81638		17.0	72260	70558	69132	66679	32636	31067	27857	25832	23900	2.70
Run 11	76514		17.2	66352	65417	64117	61820	31781	30433	27450	25705	24071	2.53
Run 12	70623		17.0	60495	59764	58165	56540	31190	29719	27179	25560	24127	2.34
Run 13	70682		16.9	60591	59221	58427	56474	31257	29665	27183	25546	24135	2.34
Run 14	64692		17.0	55113	53830	53066	51480	29974	29024	26834	25423	24241	2.14
Run 17	59542		16.8	50394	49725	48599	47468	29223	28252	26509	25378	24236	1.97
Run 19	54084		17.0	46172	45327	44733	43435	28462	27728	26216	25241	24333	1.79
Run 20	48439		17.6	42013	41412	40659	39948	27767	27262	25850	25083	24403	1.60
Run 21	48480		16.5	41920	41210	40853	39878	27964	27194	25951	25105	24360	1.60
Run 22	43251		17.2	38663	38202	37583	36812	27234	26707	25645	24988	24381	1.43
Run 24	37693		17.5	35383	35112	34514	34051	26850	26271	25405	24895	24435	1.25
Run 26	31981		17.7	32573	32265	31975	31559	26227	25809	25169	24798	24438	1.06
Run 27	31985		17.1	32555	32224	31961	31477	26192	25790	25190	24787	24419	1.06

Water in 40 mm valve, 50% open

Date:	03/03/2005
Valve Type:	Diaphragm
Valve dimension[m]:	0.04
Valve position:	Open
Pipe Diameter [m]:	0.04212

Area[m^2]
0.00139337

Material Type:	Water
Density[kg/m^3]:	999.87
Concentration:	0
τ_y:	0
K:	0.001
n:	1
PPT used:	101
Range selected:	0-130

Axial distances [m]	-6.298	-4.568	-2.932	-0.6205		1.0755	6.0455	8.0745	9.9745		
Valve plane											
Non-dim distances [L/D]:	-119.280303	-86.515152	-55.530303	-11.75189394	0	20.369318	114.49811	152.92614	188.91098		
Distances[m]:	0	1.73	3.366	5.6775	7.3735	8.9825	12.3435	14.3725	16.2725		

Run #	Re_3		k_v	Pod 1	Pod 2	Pod 3	Pod 4	Pod 5	Pod 6	Pod 7	Pod 8	Pod 9
Run 1	95152		35.5	131763	129978	128447	125930	33364	31766	28047	25832	23861
Run 2	95135		35.7	132299	130676	128675	126125	33418	31632	28055	25839	23839
Run 3	91050		35.3	122238	120906	119174	117101	32873	31219	27759	25772	23922
Run 4	91079		35.4	122626	121105	119089	117142	32951	31088	27823	25829	23939
Run 5	84294		34.9	107957	105913	104889	103544	30307	30309	27433	25651	24075
Run 6	84390		34.7	108223	106977	105582	103851	32046	30240	27504	25539	23982
Run 7	78337		35.2	96933	95704	94259	92896	30684	29458	26958	25616	24041
Run 9	72168		35.1	86048	84493	83612	81627	30113	28794	26730	25438	24265
Run 10	72245		34.9	85943	84414	83726	82144	44608	28910	26695	25402	24224
Run 11	66139		34.8	75694	74972	74108	72348	29203	28283	26312	25240	24260
Run 13	78434		35.0	97176	95759	94953	92414	30905	29543	27097	25537	24111
Run 14	78442		35.1	96862	95933	94747	92951	30905	29608	27012	25507	24135
Run 16	66573		34.6	76519	75541	74483	73299	29389	28252	26432	25304	24238
Run 18	60318		34.2	67046	66226	65645	64278	28830	27685	26172	25192	24344
Run 19	54445		34.1	59166	58555	57620	56321	28265	27204	25896	25090	24364
Run 22	48234		33.5	51473	50793	50288	49615	27145	26664	25612	24983	24385
Run 24	42292		32.9	45082	44520	44315	43553	26839	26194	25393	24902	24426
Run 25	36676		32.8	40006	39647	39237	38894	26097	25841	25184	24796	24426
Run 26	36629		32.6	39911	39432	39224	38833	26031	25819	25186	24795	24434
Run 27	30345		32.0	35037	34882	34619	34163	25591	25403	24990	24667	24426
Run 29	24191		33.9	31531	31269	31128	30854	25278	25087	24771	24578	24407
Run 32	18199		35.9	28589	28430	28357	28215	24807	24762	24582	24467	24375
Run 34	12271		39.8	26458	26410	26369	26348	24603	24532	24431	24380	24324

Water in 50 mm valve, 100% open

Date:	26/07/2004
Valve Type:	Diaphragm
Valve dimension[m]:	50
Valve position:	1
Pipe Diameter [m]:	0.0528

Area[m^2]
0.002189564

Material Type:	Water
Density[kg/m^3]:	1000
Concentration:	
τ_y:	0
K:	0.001
n:	1
PPT used:	101
Range selected:	0-40

			Axial distances [m]	-6.574	-5.47	-3.526	-1.531	0.5095	2.5085	4.1075	7.6655	9.6685
			Valve plane									
			Non-dim distances [L/D]:	-124.5075758	-103.59848	-66.780303	-28.99621212	9.64962121	47.5094697	77.7935606	145.179924	183.11553
			Distances[m]:	0	1.104	3.048	5.043	7.0835	9.0825	10.6815	14.2395	16.2425
Run #	Re_3		k_v	Pod 1	Pod 2	Pod 3	Pod 4	Pod 5	Pod 6	Pod 7	Pod 8	Pod 9
Run 1	19218		3.0	25288	25207	25196	25117	24906	24833	24759	24667	24583
Run 3	19229		2.9	25304	25260	25197	25161	24891	24839	24757	24650	24588
Run 5	23463		2.8	25591	25510	25453	25353	25063	24976	24844	24688	24608
Run 6	23456		1.9	25562	25540	25401	25329	25067	24915	24848	24702	24604
Run 11	37782		2.3	26780	26644	26421	26206	25502	25292	25024	24707	24482
Run 12	37800		2.5	26783	26639	26454	26237	25495	25314	25028	24695	24487
Run 14	49434		2.6	27988	27845	27505	27163	25945	25568	25150	24637	24244
Run 15	49664		2.6	28044	27806	27555	27134	25910	25574	25164	24604	24275
Run 16	49620		2.5	28010	27849	27484	27154	25941	25589	25132	24626	24252
Run 17	49632		2.5	28032	27868	27509	27111	25930	25576	25136	24612	24261
Run 18	58740		2.5	29143	28927	28466	27944	26337	25871	25283	24560	24124
Run 19	58357		2.4	29170	28880	28452	28005	26330	25786	25251	24569	24045
Run 20	58734		2.3	29159	28857	28474	28025	26323	25858	25290	24469	24010
Run 30	79108		2.2	26636	26133	25444	24648	21746	20950	19990	18743	17892
Run 31	79185		2.4	26697	26246	25544	24688	21742	20961	19975	18705	17909
Run 32	79125		2.4	26747	26219	25523	24722	21714	20936	19967	18732	17947
Run 33	80853		2.6	27317	26773	26069	25199	21885	21052	19992	18695	17863
Run 35	80800		2.7	27315	26827	26135	25165	21860	21003	20006	18723	17840
Run 36	80801		2.7	27241	26798	26068	25169	21843	21022	19989	18738	17879
Run 37	79006		2.8	26877	26399	25785	24882	21699	20898	19903	18713	17901
Run 38	78998		2.6	26916	26432	25734	24940	21703	20896	19954	18699	17867
Run 40	81094		2.3	27027	26554	25817	24955	21960	21105	20096	18824	17947
Run 41	81151		2.2	27021	26555	25765	24935	21952	21100	20108	18775	17983
Run 42	81054		2.4	26981	26558	25790	24924	21916	21086	20063	18807	17950
Run 43	78629		2.3	26506	26118	25335	24572	21735	20915	19923	18761	17957
Run 44	78666		2.3	26522	26101	25341	24557	21765	20926	19951	18734	17951
Run 45	78653		2.3	26567	26083	25366	24535	21742	20958	19942	18751	17922
Run 46	72341		2.4	25305	24888	24334	23601	21218	20501	19703	18659	17959
Run 47	72285		2.3	25317	24970	24357	23609	21179	20540	19742	18637	17958
Run 48	72227		2.3	25316	24899	24352	23648	21240	20518	19728	18716	17938
Run 49	67064		2.4	24404	24065	23574	22994	20833	20232	19515	18592	18001
Run 50	67022		2.2	24439	24114	23507	22973	20846	20240	19537	18627	18009
Run 51	47470		2.3	27846	27596	27312	26992	25904	25566	25160	24676	24357
Run 52	47463		2.4	27830	27612	27325	26986	25879	25550	25154	24645	24346
Run 53	42941		2.2	27346	27109	26883	26586	25719	25451	25111	24730	24422
Run 54	90286		1.6	22972	22398	21401	20673	17236	16439	15335	13990	12870

Water in 50 mm valve, 75% open

Date:	22/03/2005	
Valve Type:	Diaphragm	
Valve dimension[m]:	50	
Valve position:	3/4	Area[m^2]
Pipe Diameter [m]:	0.0528	0.002189564

Material Type:	Water
Density[kg/m^3]:	1000
Concentration:	
τ_y:	0
K:	0.001
n:	1
PPT used:	101
Range selected:	0-40

Axial distances [m]	-6.574	-5.47	-3.526	-1.531	0.5095	2.5085	4.1075	7.6655	9.6685		
Valve plane											
Non-dim distances [L/D]:	-124.5075758	-103.59848	-66.780303	-28.99621212	9.64962121	47.5094697	77.7935606	145.179924	183.11553		
Distances[m]:	0	1.104	3.048	5.043	7.0835	9.0825	10.6815	14.2395	16.2425		
Run #	Re_3		k_v	Pod 1	Pod 2	Pod 3	Pod 4	Pod 5	Pod 6	Pod 7	Pod 8	Pod 9	Average Q
													[l/s]
Run 1	138698		8.0	72044	68171	66623	64918	34589	32410	28597	26053	23446	5.75
Run 3	127425		7.8	64011	60697	59325	58345	32974	31108	27985	25835	23624	5.28
Run 5	122931		7.7	60571	57718	56318	55308	31852	30725	27746	25767	23840	5.10
Run 6	117577		7.4	56739	54319	53007	51857	31223	30151	27480	25735	23923	4.88
Run 11	109620		7.8	53982	51519	50313	49257	30807	29862	27313	25727	24069	4.55
Run 12	103341		7.2	50147	48147	47268	46003	30867	29325	27223	25633	24239	4.29
Run 14	97975		7.0	47144	45153	44231	43459	30087	28959	26978	25632	24319	4.06
Run 15	98217		6.8	47122	45006	44255	43383	30215	28891	26972	25655	24238	4.07
Run 16	91448		6.9	44154	42224	41609	40884	29654	28394	26707	25538	24370	3.79
Run 17	90824		7.1	44191	42432	41868	40964	29690	28421	26658	25592	24387	3.77
Run 18	79536		8.0	41031	39764	39157	38523	28184	27765	26331	25408	24478	3.30
Run 19	77675		7.1	38270	37172	36588	36134	28307	27173	26028	25319	24553	2.94
Run 20	77677		6.9	38313	37244	36718	36174	27714	27204	26084	25279	24507	2.94
Run 30	72740		7.2	36928	35983	35626	34968	27307	26959	25932	25243	24559	2.76
Run 31	68200		7.6	35689	34777	34505	34064	27032	26688	25751	25184	24588	2.58
Run 32	68174		7.7	35905	34821	34508	34214	27211	26609	25784	25159	24564	2.58
Run 33	63010		7.6	34408	33743	33296	32932	26736	26432	25678	25125	24589	2.39
Run 35	62983		8.0	34441	33686	33332	32847	26845	26499	25635	25124	24607	2.38
Run 36	57699		8.1	33116	32544	32224	31920	26585	26224	25515	25084	24616	2.18
Run 37	52821		8.6	31979	31377	31116	30813	26150	25949	25400	25008	24646	2.00
Run 38	47867		8.7	30781	30319	30059	29823	26063	25725	25271	24946	24631	1.81
Run 40	43555		8.8	29904	29468	29316	29133	25908	25625	25193	24902	24628	1.64
Run 41	43544		9.1	29780	29558	29290	29090	25876	25572	25153	24915	24646	1.64
Run 42	38079		9.7	28841	28406	28280	28104	25534	25379	25045	24838	24630	1.43
Run 43	33332		9.8	27872	27570	27446	27371	25285	25205	24947	24786	24627	1.25
Run 44	28795		9.7	27111	26884	26853	26650	25201	25035	24858	24743	24596	1.08

Water in 50 mm valve, 50% open

Date:	07/03/2005
Valve Type:	Diaphragm
Valve dimension[m]:	50
Valve position:	1/2
Pipe Diameter [m]:	0.0528

Area[m^2]
0.002189564

Material Type:	Water
Density[kg/m^3]:	1000
Concentration:	
τ_y:	0
K:	0.001
n:	1
PPT used:	101
Range selected:	0-40

			Axial distances [m]	-6.574	-5.47	-3.526	-1.531	0.5095	2.5085	4.1075	7.6655	9.6685
			Valve plane									
			Non-dim distances [L/D]:	-124.5075758	-103.59848	-66.780303	-28.99621212	9.64962121	47.5094697	77.7935606	145.179924	183.11553
			Distances[m]:	0	1.104	3.048	5.043	7.0835	9.0825	10.6815	14.2395	16.2425
Run #	Re_3		k_v	Pod 1	Pod 2	Pod 3	Pod 4	Pod 5	Pod 6	Pod 7	Pod 8	Pod 9	Average Q
													[l/s]
Run 1	65590		23.9	48263	47154	46785	46458	27206	26772	25787	25140	24465	2.72
Run 3	65661		23.8	48180	47165	46919	46377	27671	26703	25742	25114	24440	2.72
Run 5	61163		23.7	45147	44353	43944	43570	27312	26497	25652	25071	24470	2.54
Run 6	61076		23.8	45143	44473	43852	43512	27056	26492	25633	25049	24437	2.53
Run 11	56862		23.8	42493	41750	41388	40953	26716	26270	25513	25004	24479	2.36
Run 12	52478		23.8	39823	39292	38922	38510	26531	26013	25372	24952	24489	2.18
Run 14	52436		23.9	39911	39300	39039	38730	26415	26008	25391	24942	24494	2.17
Run 15	48710		23.7	37810	37260	36837	36698	26200	25827	25294	24887	24490	2.02
Run 16	43852		24.9	35572	35088	34854	34654	25856	25647	25108	24837	24498	1.82
Run 17	43901		24.3	35572	35021	34838	34644	25906	25623	25153	24835	24495	1.82
Run 18	43930		24.3	35579	35127	34895	34676	25871	25619	25155	24844	24497	1.82
Run 19	39620		23.9	33575	33187	33026	32872	25812	25447	25070	24794	24492	1.64
Run 20	39679		24.1	33555	33184	33039	32874	25673	25435	25054	24791	24502	1.65
Run 30	35180		24.9	31700	31485	31264	31165	25383	25250	24905	24745	24489	1.46
Run 31	35214		24.6	31738	31433	31268	31158	25443	25286	24937	24722	24503	1.46
Run 32	30859		24.4	30124	29999	29804	29686	25224	25090	24848	24660	24479	1.28
Run 33	26671		25.5	28805	28575	28517	28444	25077	24943	24742	24599	24477	1.11
Run 35	21963		26.4	27460	27292	27252	27149	24874	24789	24611	24533	24430	0.91
Run 36	21983		25.3	27407	27275	27247	27179	24833	24770	24625	24538	24435	0.91
Run 37	18031		26.1	26489	26405	26355	26313	24701	24623	24544	24470	24405	0.75
Run 38	18028		26.9	26461	26369	26329	26331	24682	24623	24530	24476	24412	0.75
Run 40	13442		26.9	25578	25542	25489	25460	24541	24509	24446	24406	24360	0.56

Water in 50 mm valve, 25% open

Date:	23/03/2005
Valve Type:	Diaphragm
Valve dimension[m]:	50
Valve position:	1/4
Pipe Diameter [m]:	0.0528

Area[m^2]	0.002189564

Material Type:	Water
Density[kg/m^3]:	1000
Concentration:	
τ_y:	0
K:	0.001
n:	1
PPT used:	101
Range selected:	0-40

Axial distances [m]			-6.574	-5.47	-3.526	-1.531	0.5095	2.5085	4.1075	7.6655	9.6685	
Valve plane												
Non-dim distances [L/D]:			-124.5075758	-103.59848	-66.780303	-28.99621212	9.64962121	47.5094697	77.7935606	145.179924	183.11553	
Distances[m]:			0	1.104	3.048	5.043	7.0835	9.0825	10.6815	14.2395	16.2425	
Run #	Re_3		k_v	Pod 1	Pod 2	Pod 3	Pod 4	Pod 5	Pod 6	Pod 7	Pod 8	Pod 9	Average Q
													[l/s]
Run 1	73202		106.7	133938	132748	132200	131522	27665	27541	26178	25376	24465	3.04
Run 3	75991		98.8	133970	132688	131992	131451	27082	27486	26194	25345	24426	3.15
Run 5	76067		95.9	130640	129180	128589	127887	28363	27453	26144	25360	24525	3.15
Run 6	73502		102.0	130476	129158	128584	127940	27126	27425	26209	25396	24447	3.05
Run 11	74862		95.0	126800	125903	125307	124751	27315	27344	26125	25334	24427	3.10
Run 12	74423		96.8	127108	125665	125114	124511	27595	27325	26097	25300	24506	3.09
Run 14	71634		99.5	122769	121575	121316	120788	27201	27293	26112	25360	24462	2.97
Run 15	75097		90.1	122999	121987	121350	120907	27650	27680	26627	25718	24903	3.11
Run 16	73146		90.7	118159	116839	116428	116143	27424	27534	26437	25722	24923	3.03
Run 17	70633		97.4	118177	117146	116721	116299	26958	27569	26413	25690	24904	2.93
Run 18	69663		96.7	115285	114576	113803	113144	27944	27447	26395	25663	24838	2.89
Run 19	66619		105.8	115216	113882	113553	113062	27475	27493	26418	25646	24917	2.76
Run 20	72720		87.9	113602	111970	111703	111106	26197	26867	25898	25208	24502	3.02
Run 30	68238		86.9	101498	100628	100175	99712	25817	26669	25648	25111	24585	2.83
Run 31	63030		84.2	88959	88337	87937	87812	25799	26393	25625	25099	24542	2.61
Run 32	63041		84.9	89557	88409	88138	87745	25668	26372	25614	25082	24511	2.61
Run 33	57850		83.5	78027	77308	77024	76769	25708	26134	25431	25002	24612	2.40
Run 35	53606		79.3	68890	68347	67731	67738	25984	25954	25380	24975	24505	2.22
Run 36	49255		79.4	61537	61299	61023	60399	26222	25831	25190	24944	24598	2.04
Run 37	49261		76.5	60668	60814	60610	60500	26177	25833	25278	24961	24589	2.04
Run 38	43550		76.4	53078	52527	52590	52299	25229	25592	25110	24919	24485	1.81
Run 40	38155		74.6	46115	46001	45784	45598	24882	25340	25008	24731	24472	1.58
Run 41	38145		75.1	46167	45976	45781	45678	24821	25271	25052	24837	24556	1.58
Run 42	33952		77.7	41624	41449	41216	41050	24848	25099	24838	24751	24599	1.41
Run 43	33898		75.2	41568	41162	41211	40894	24910	25235	24834	24738	24450	1.41
Run 44	29253		77.1	37553	37004	37071	37074	24678	25019	24820	24606	24530	1.21
Run 45	29225		77.4	37622	37318	37117	37159	24641	24991	24877	24679	24581	1.21
Run 46	24199		79.2	33435	33335	33301	33133	24649	24841	24682	24599	24540	1.00
Run 47	19532		83.9	30548	30482	30432	30370	24565	24717	24535	24582	24455	0.81

Water in 65 mm valve, 75% open

Date:	12/04/2005	
Valve Type:	Diaphragm	
Valve dimension[m]:	0.065	
Valve position:	¾ Open	Area[m^2]
Pipe Diameter [m]:	0.06308	0.003125167

Material Type:	Water
Density[kg/m^3]:	999.87
Concentration:	0
τ_y:	0
K:	0.001
n:	1
PPT used:	101 to 109
Range selected:	0-40

		Axial distances [m]	-5.7395	-3.865	-2.885	-0.937	0.987	2.938	6.427	8.432	10.433	
		Valve plane										
		Non-dim distances [L/D]:	-90.98763475	-61.2714014	-45.73557387	-14.85415346	15.64679772	46.57577679	101.8864933	133.6715282	165.3931516	
		Distances[m]:	0	1.8745	2.8545	4.8025	6.7265	8.6775	12.1665	14.1715	16.1725	
Run #	Re_3	k_v	PTT 1	PTT 2	PTT 3	PTT 4	PTT 5	PTT 6	PTT 7	PTT 8	PTT 9	Average Q
			[Pa]	[Pa]	[Pa]	[Pa]	[Pa]	[Pa]	[Pa]	[Pa]	[Pa]	[l/s]
Run 1	139033.4081	2.51	34278	32886	32365	30835	23381	21513	19248	18009	16344	6.89
Run 2	138812.3245	2.48	34056	32581	32135	30628	22909	21348	19291	18013	16439	6.88
Run 3	138812.3245	2.70	42904	41281	40814	39202	30883	29171	26946	25563	23877	6.88
Run 4	133418.8051	2.34	32842	31516	31072	29581	22501	21026	19102	17936	16337	6.61
Run 5	133418.8051	2.51	41565	40112	39656	38070	30406	28821	26744	25479	23751	6.61
Run 6	129442.2127	2.46	32054	30722	30315	28948	22324	20892	18973	17917	16412	6.41
Run 7	125572.5308	2.43	31148	29910	29400	28334	21890	20697	18868	17816	16436	6.22
Run 8	120968.2328	2.40	30220	29044	28644	27430	21628	20444	18766	17742	16471	5.99
Run 9	120968.2328	2.59	38743	37483	37053	35750	29472	28197	26382	25274	23903	5.99
Run 10	116264.0258	2.31	29207	28103	27733	26702	21333	20124	18628	17705	16465	5.76
Run 11	111270.5219	2.35	28308	27350	27068	25951	20980	19975	18522	17701	16534	5.51
Run 12	107091.4904	2.32	27503	26604	26320	25340	20741	19768	18384	17691	16517	5.31
Run 13	101458.6772	2.39	26551	25654	25405	24577	20365	19496	18270	17509	16581	5.03
Run 14	101458.6772	2.58	34780	33836	33556	32654	28093	27161	25834	25013	24007	5.03
Run 15	97557.93754	2.50	25885	25120	24825	24064	20193	19336	18167	17493	16627	4.83
Run 16	92976.05274	2.41	25116	24448	24161	23475	19871	19162	18068	17458	16625	4.61
Run 17	88328.92753	2.42	24493	23869	23594	22925	19598	18913	17980	17447	16636	4.38
Run 18	88567.08023	2.44	24454	23831	23601	22928	19682	18947	18012	17408	16695	4.39
Run 19	85676.70846	2.54	24021	23409	23230	22573	19508	18873	17901	17412	16677	4.25
Run 20	85676.70846	2.76	32062	31394	31197	30477	27180	26493	25440	24924	24121	4.25
Run 21	82215.45892	2.65	23563	23015	22773	22231	19289	18711	17845	17339	16712	4.07
Run 22	78561.46545	2.58	23060	22503	22317	21801	20203	18551	17767	17272	16693	3.89
Run 23	75629.18816	2.60	22633	22117	21939	21469	18951	18404	17664	17254	16657	3.75
Run 24	71966.72482	3.01	22148	21704	21521	21086	18774	18262	17575	17173	16721	3.57
Run 25	71966.72482	3.24	30031	29547	29355	28881	26393	25830	25088	24655	24162	3.57
Run 26	66763.91092	2.53	21508	21067	20955	20569	18519	18058	17489	17106	16642	3.31
Run 27	55584.03827	2.95	20137	19835	19746	19457	17994	17653	17215	16956	16637	2.75
Run 28	49320.33813	2.84	19459	19229	19131	18918	17655	17444	17095	16900	16609	2.44
Run 29	45280.86804	3.09	19082	18873	18799	18603	17534	17320	17010	16815	16593	2.24

Water in 65 mm valve, 25% open

Date:	13/04/2005	
Valve Type:	Diaphragm	
Valve dimension[m]:	0.065	
Valve position:	¼ Open	Area[m^2]
Pipe Diameter [m]:	0.06308	0.003125167

Material Type:	Water
Density[kg/m^3]:	999.87
Concentration:	0
τ_y:	0
K:	0.0018
n:	1
PPT used:	101 to 109
Range selected:	0-130

		Axial distances [m]	-5.7395	-3.865	-2.885	-0.937	0.987	2.938	6.427	8.432	10.433	
		Valve plane										
		Non-dim distances [L/D]:	-90.98763475	-61.2714014	-45.73557387	-14.85415346	15.64679772	46.57577679	101.8864933	133.6715282	165.3931516	
		Distances[m]:	0	1.8745	2.8545	4.8025	6.7265	8.6775	**12.1665**	14.1715	16.1725	
Run #	Re_3	k_y	PTT 1	PTT 2	PTT 3	PTT 4	PTT 5	PTT 6	PTT 7	PTT 8	PTT 9	Average Q
			[Pa]	[Pa]	[Pa]	[Pa]	[Pa]	[Pa]	[Pa]	[Pa]	[Pa]	[l/s]
Run 1	57163	71.69	126926	126073	125785	124872	29442	27335	25702	24796	23790	5.10
Run 2	54888	70.81	117759	116749	116486	115646	28412	27109	25525	24697	23776	4.90
Run 3	52816	69.02	109236	108363	108155	107391	28207	26912	25531	24701	23801	4.71
Run 4	50346	67.76	100096	99354	99036	98317	27966	26745	25342	24627	23767	4.49
Run 5	48838	65.69	94090	93458	93180	92453	28445	26663	25414	24652	23814	4.36
Run 6	46622	64.67	86784	86263	85991	85275	27488	26447	25260	24636	23858	4.16
Run 7	44503	63.33	80430	79786	79626	78958	28635	26257	25168	24549	23803	3.97
Run 8	42193	62.70	74247	73679	73497	72907	28220	26008	25059	24431	23832	3.76
Run 11	40173	60.75	68185	67661	67520	67023	26776	25819	24920	24368	23825	3.58
Run 12	37516	60.59	62402	62042	61882	61472	26365	25602	24762	24318	23806	3.35
Run 13	35803	61.11	59144	58685	58520	58158	26251	25465	24669	24257	23825	3.19
Run 14	33814	61.81	55270	54793	54746	54398	26139	25308	24605	24197	23983	3.02
Run 15	31521	59.80	50814	50449	50363	50029	26134	25102	24478	24133	23779	2.81
Run 16	29536	58.87	47204	46864	46873	46502	26698	24977	24386	24101	23770	2.63
Run 17	27913	58.22	44490	44193	44122	43943	25790	24794	24314	24024	23756	2.49
Run 18	25772	58.80	41523	41305	41174	40973	25879	24660	24198	23987	23731	2.30

Water in 65 mm valve, 50% open

Date:	16/03/2005	
Valve Type:	Diaphragm	
Valve dimension[m]:	0.08	
Valve position:	1/2	Area[m^2]
Pipe Diameter [m]:	0.08043	0.005080729

Material Type:	Water
Density[kg/m^3]:	999.87
Concentration:	0
τ_y:	0
K:	0.001
n:	1
PPT used:	101
Range selected:	0-130

		Axial distances [m]	-5.7395	-3.865	-2.885	-0.937	0.987	2.938	6.427	8.432	10.433	
		Valve plane										
		Non-dim distances [L/D]:	-71.36018898	-48.05420863	-35.86970036	-11.64988188	12.27154047	36.52865846	79.90799453	104.8365038	129.7152804	
		Distances[m]:	0	1.8745	2.8545	4.8025	6.7265	8.6775	**12.1665**	14.1715	16.1725	
Run #	Re_3	k_v	PTT 1	PTT 2	PTT 3	PTT 4	PTT 5	PTT 6	PTT 7	PTT 8	PTT 9	Average Q
			[Pa]	[Pa]	[Pa]	[Pa]	[Pa]	[Pa]	[Pa]	[Pa]	[Pa]	[l/s]
Run 1	105304	18.64	44807	44255	44257	43646	27624	27023	26584	25967	25605	6.65
Run 2	102937	18.40	43936	43857	43225	42935	27488	26959	26469	26001	25517	6.50
Run 3	100147	18.55	42882	42845	42340	42095	27651	26937	26456	25958	25582	6.33
Run 4	96859	18.77	42055	41894	41426	41034	27301	26740	26338	25978	25506	6.12
Run 5	94666	18.66	41078	40908	40607	40171	27271	26696	26298	25861	25492	5.98
Run 6	91131	18.47	39917	39993	39422	39051	27004	26568	26234	25826	25460	5.76
Run 7	91542	18.51	40178	39795	39562	39049	27040	26575	26222	25793	25481	5.78
Run 8	89380	18.23	39421	39358	38728	38526	26988	26569	26167	25722	25464	5.65
Run 11	86874	18.28	38403	38395	37944	37605	26927	26438	26077	25690	25383	5.49
Run 12	83118	18.26	37541	37427	37031	36712	26729	26342	26081	25715	25407	5.25
Run 13	83203	18.24	37502	37276	36929	36704	26693	26326	26056	25612	25457	5.26
Run 14	79858	18.17	36442	36312	35980	35774	26663	26257	25971	25641	25383	5.05
Run 15	77541	18.04	35799	35559	35365	35151	26550	26155	25903	25603	25299	4.90
Run 16	77554	18.04	35895	35722	35366	35211	26510	26206	25896	25612	25306	4.90
Run 17	75173	18.24	35259	35191	34808	34636	26597	26155	25880	25527	25349	4.75
Run 18	74745	18.18	35171	34895	34703	34503	26495	26103	25859	25526	25318	4.72
Run 19	74746	18.35	34493	34364	34034	33840	26129	26035	25769	25535	25258	4.54
Run 20	74747	18.49	32909	32688	32579	32307	26289	25855	25691	25489	25272	4.14
Run 21	74748	18.65	32718	32778	32500	32330	26278	25901	25645	25510	25255	4.14
Run 22	74749	18.18	32314	32147	31964	31840	25970	25831	25630	25415	25214	3.98
Run 23	74750	18.48	32186	32192	31948	31747	26173	25770	25606	25401	25223	3.99
Run 24	74751	17.94	31735	31634	31414	31231	26064	25779	25613	25396	25230	3.83

Water in 80 mm valve, 100% open

Date:	02/09/2004	
Valve Type:	Diaphragm	
Valve dimension[m]:	0.09	
Valve position:	Open	Area[m^2]
Pipe Diameter [m]:	0.08043	0.005080729

Material Type:	Water
Density[kg/m^3]:	1000
Concentration:	
τ_y:	0
K:	0.001
n:	1
PPT used:	101
Range selected:	0-40

		Axial distances [m]	-5.7395	-3.865	-2.885	-0.937	0.987	2.938	6.427	8.432	10.433	
		Valve plane										
		Non-dim distances [L/D]:	-71.36018898	-48.05420863	-35.86970036	-11.64988188	12.27154047	36.52865846	79.90799453	104.8365038	129.7152804	
		Distances[m]:	0	1.8745	2.8545	4.8025	6.7265	8.6775	12.1665	14.1715	16.1725	
Run #	Re_3		k_v	PTT 1	PTT 2	PTT 3	PTT 4	PTT 5	PTT 6	PTT 7	PTT 8	PTT 9	Average Q
				[Pa]	[Pa]	[Pa]	[Pa]	[Pa]	[Pa]	[Pa]	[Pa]	[Pa]	[l/s]
Run 1	93477.83059		2.44	30067	29782	29575	29302	27260	26637	26427	25912	25661	5.90
Run 2	100489.4565		2.61	30866	30597	30366	29932	27679	26911	26639	26025	25704	6.35
Run 3	106225.153		2.72	31424	31118	30855	30407	27820	27048	26718	26119	25793	6.71
Run 4	107282.0411		2.50	31478	31157	30946	30437	27822	27044	26794	26091	25691	6.78
Run 5	112488.4305		2.65	32218	31813	31623	31023	28157	27321	26964	26246	25832	7.11
Run 6	115362.6161		2.66	32475	32069	31815	31313	28297	27425	26977	26233	25880	7.29

Water in 80 mm valve, 75% open

Date:	16/03/2005	
Valve Type:	Diaphragm	
Valve dimension[m]:	0.08	
Valve position:	¾ Open	Area[m^2]
Pipe Diameter [m]:	0.08043	0.005080729

Material Type:	Water
Density[kg/m^3]:	999.87
Concentration:	0
τ_y:	0
K:	0.001
n:	1
PPT used:	101
Range selected:	0-40

Axial distances [m]	-5.7395	-3.865	-2.885	-0.937	0.987	2.938	6.427	8.432	10.433		
Valve plane											
Non-dim distances [L/D]:	-71.36018898	-48.05420863	-35.86970036	-11.64988188	12.27154047	36.52865846	79.90799453	104.8365038	129.7152804		
Distances[m]:	0	1.8745	2.8545	4.8025	6.7265	8.6775	12.1665	14.1715	16.1725		

Run #	Re_3		k_v	PTT 1	PTT 2	PTT 3	PTT 4	PTT 5	PTT 6	PTT 7	PTT 8	PTT 9	Average Q
				[Pa]	[Pa]	[Pa]	[Pa]	[Pa]	[Pa]	[Pa]	[Pa]	[Pa]	[l/s]
Run 1	103144.9782		6.67	34551	34398	33935	33246	27075	26861	26506	26077	25640	6.52
Run 2	98707.04744		6.67	33765	33411	33052	32609	27057	26704	26325	25862	25537	6.24
Run 3	87018.0008		6.70	31804	31536	31265	30777	26679	26341	26062	25794	25462	5.50
Run 4	69844.13377		6.41	29435	29332	29125	28907	26064	25928	25757	25562	25333	4.41
Run 5	67341.53912		6.49	29169	29038	28877	28595	25988	25890	25696	25482	25300	4.25
Run 6	63813.70495		6.77	28804	28675	28506	28307	25901	25764	25619	25410	25273	4.03
Run 7	61422.3898		6.51	28459	28416	28197	28059	25879	25733	25574	25365	25240	3.88

Water in 80 mm valve, 50% open

Date:	16/03/2005	
Valve Type:	Diaphragm	
Valve dimension[m]:	0.08	
Valve position:	1/2	Area[m^2]
Pipe Diameter [m]:	0.08043	0.005080729

Material Type:	Water
Density[kg/m^3]:	999.87
Concentration:	0
τ_y:	0
K:	0.001
n:	1
PPT used:	101
Range selected:	0-130

			Axial distances [m]	-5.7395	-3.865	-2.885	-0.937	0.987	2.938	6.427	8.432	10.433
			Valve plane									
			Non-dim distances [L/D]:	-71.36018898	-48.05420863	-35.86970036	-11.64988188	12.27154047	36.52865846	79.90799453	104.8365038	129.7152804
			Distances[m]:	0	1.8745	2.8545	4.8025	6.7265	8.6775	12.1665	14.1715	16.1725
Run #	Re_3		k_v	PTT 1	PTT 2	PTT 3	PTT 4	PTT 5	PTT 6	PTT 7	PTT 8	PTT 9	Average Q
				[Pa]	[Pa]	[Pa]	[Pa]	[Pa]	[Pa]	[Pa]	[Pa]	[Pa]	[l/s]
Run 1	105304		18.64	44807	44255	44257	43646	27624	27023	26584	25967	25605	6.65
Run 2	102937		18.40	43936	43857	43225	42935	27488	26959	26469	26001	25517	6.50
Run 3	100147		18.55	42882	42845	42340	42095	27651	26937	26456	25958	25582	6.33
Run 4	96859		18.77	42055	41894	41426	41034	27301	26740	26338	25978	25506	6.12
Run 5	94666		18.66	41078	40908	40607	40171	27271	26696	26298	25861	25492	5.98
Run 6	91131		18.47	39917	39993	39422	39051	27004	26568	26234	25826	25460	5.76
Run 7	91542		18.51	40178	39795	39562	39049	27040	26575	26222	25793	25481	5.78
Run 8	89380		18.23	39421	39358	38728	38526	26988	26569	26167	25722	25464	5.65
Run 11	86874		18.28	38403	38395	37944	37605	26927	26438	26077	25690	25383	5.49
Run 12	83118		18.26	37541	37427	37031	36712	26729	26342	26081	25715	25407	5.25
Run 13	83203		18.24	37502	37276	36929	36704	26693	26326	26056	25612	25457	5.26
Run 14	79858		18.17	36442	36312	35980	35774	26663	26257	25971	25641	25383	5.05
Run 15	77541		18.04	35799	35559	35365	35151	26550	26155	25903	25603	25299	4.90
Run 16	77554		18.04	35895	35722	35366	35211	26510	26206	25896	25612	25306	4.90
Run 17	75173		18.24	35259	35191	34808	34636	26597	26155	25880	25527	25349	4.75
Run 18	74745		18.18	35171	34895	34703	34503	26495	26103	25859	25526	25318	4.72
Run 19	71875		18.35	34493	34364	34034	33840	26129	26035	25769	25535	25258	4.54
Run 20	65482		18.49	32909	32688	32579	32307	26289	25855	25691	25489	25272	4.14
Run 21	65567		18.65	32718	32778	32500	32330	26278	25901	25645	25510	25255	4.14
Run 22	63004		18.18	32314	32147	31964	31840	25970	25831	25630	25415	25214	3.98
Run 23	63086		18.48	32186	32192	31948	31747	26173	25770	25606	25401	25223	3.99
Run 24	60682		17.94	31735	31634	31414	31231	26064	25779	25613	25396	25230	3.83

Water in 80 mm valve, 25% open

Date:	15/03/2005	
Valve Type:	Diaphragm	
Valve dimension[m]:	0.08	
Valve position:	¼ Open	Area[m^2]
Pipe Diameter [m]:	0.08043	0.005080729

Material Type:	Water
Density[kg/m^3]:	999.87
Concentration:	0
τ_y:	0
K:	0.001
n:	1
PPT used:	101
Range selected:	0-130

			Axial distances [m]	-5.7395	-3.865	-2.885	-0.937	0.987	2.938	6.427	8.432	10.433	
			Valve plane										
			Non-dim distances [L/D]:	-71.36018898	-48.05420863	-35.86970036	-11.64988188	12.27154047	36.52865846	79.90799453	104.8365038	129.7152804	
			Distances[m]:	0	1.8745	2.8545	4.8025	6.7265	8.6775	12.1665	14.1715	16.1725	
Run #	Re_3		k_v	PTT 1	PTT 2	PTT 3	PTT 4	PTT 5	PTT 6	PTT 7	PTT 8	PTT 9	Average Q
				[Pa]	[Pa]	[Pa]	[Pa]	[Pa]	[Pa]	[Pa]	[Pa]	[Pa]	[l/s]
Run 1	105709		57.34	78920	78629	78238	77958	27794	26879	26489	25916	25533	6.68
Run 2	105293		57.22	78570	78282	77679	77149	26081	26810	26514	25878	25512	6.65
Run 3	102471		57.87	75872	75399	75094	74495	27750	26826	26366	25835	25559	6.47
Run 4	99291		57.70	72710	72582	72176	71810	25925	26671	26324	25803	25518	6.27
Run 5	99501		58.00	73221	72397	72141	71534	27426	26665	26311	25821	25542	6.29
Run 6	97035		57.26	70412	70286	69796	69390	26086	26677	26303	25824	25481	6.13
Run 7	93980		57.58	67602	67564	67127	66898	26705	26531	26175	25732	25456	5.94
Run 8	93785		57.82	67593	67558	67279	66845	27184	26565	26171	25712	25461	5.93
Run 11	90525		58.43	65192	65060	64638	64308	27304	26455	26121	25681	25432	5.72
Run 12	90298		58.77	65241	65131	64649	64315	27229	26403	26135	25717	25436	5.70
Run 13	88700		59.52	64068	63925	63685	63218	25864	26347	26060	25646	25465	5.60
Run 14	88803		59.86	64421	64048	63492	63230	26441	26364	26032	25677	25409	5.61
Run 15	85215		58.90	61121	61079	60592	60449	25817	26336	26025	25580	25333	5.38
Run 16	82281		60.88	59270	59183	58757	58539	26710	26219	25917	25582	25411	5.20

Water in 100 mm valve, 100% open

Date:	08/09/2004	
Valve Type:	Diaphragm	
Valve dimension[m]:	0.09	
Valve position:	Open	Area[m^2]
Pipe Diameter [m]:	0.09717	0.007415736

	Water
Material Type:	0
Density[kg/m^3]:	999.98
Concentration:	0
τ_y:	0
K:	0.0014
n:	1
PPT used:	101
Range selected:	0-130

			Axial distances [m]	-5.7395	-3.865	-2.885	-0.937	0.987	2.938	6.427	8.432	10.433	
			Valve plane										
			Non-dim distances [L/D]:	-59.06658434	-39.77565092	-29.69023361	-9.642893897	10.157456	30.23566945	66.14181332	86.77575383	107.3685294	
			Distances[m]:	0	1.8745	2.8545	4.8025	6.7265	8.6775	12.1665	14.1715	16.1725	
Run #	Re_3		k_v	PTT 1	PTT 2	PTT 3	PTT 4	PTT 5	PTT 6	PTT 7	PTT 8	PTT 9	Average Q
				[Pa]	[Pa]	[Pa]	[Pa]	[Pa]	[Pa]	[Pa]	[Pa]	[Pa]	[l/s]
Run 1	56613		1.28	2500	2344	2307	2190	1615	1457	1366	1201	797	6.05
Run 2	58314		1.17	2500	2345	2310	2185	1628	1472	1391	1228	833	6.23
Run 3	70603		1.32	2500	2309	2255	2061	1308	1040	958	705	243	7.54
Run 4	70413		1.20	2500	2300	2244	2084	1345	1081	939	739	188	7.52
Run 5	65024		1.15	2500	2336	2277	2137	1456	1273	1156	941	429	6.95
Run 6	65821		1.18	2500	2341	2284	2138	1471	1238	1178	965	501	7.03
Run 7	60643		1.26	2500	2339	2271	2164	1482	1339	1250	1094	676	6.48
Run 8	60703		0.76	2500	2332	2261	2165	1493	1334	1325	1244	683	6.49
Run 11	57164		1.18	2500	2355	2316	2194	1644	1504	1418	1207	813	6.11
Run 12	59428		1.08	2500	2359	2319	2192	1600	1478	1401	1244	807	6.35
Run 13	53838		1.43	2500	2367	2332	2221	1728	1511	1457	1315	962	5.75
Run 14	54451		1.51	2500	2370	2334	2216	1690	1534	1472	1271	987	5.82
Run 15	51353		1.66	2500	2387	2362	2252	1804	1669	1543	1393	1115	5.49
Run 16	50981		1.20	2500	2394	2342	2251	1793	1641	1584	1470	1094	5.45
Run 17	49216		1.38	2500	2384	2375	2276	1846	1681	1656	1504	1210	5.26
Run 18	48995		1.49	2500	2396	2361	2271	1832	1711	1620	1546	1242	5.23
Run 19	46331		1.39	2500	2392	2384	2294	1888	1773	1743	1637	1382	4.95
Run 20	47114		1.34	2500	2414	2367	2314	1866	1836	1700	1608	1296	5.03
Run 21	43557		1.04	2500	2401	2377	2340	1959	1792	1835	1724	1455	4.65
Run 22	43644		1.52	2500	2417	2394	2321	1981	1906	1813	1653	1442	4.66
Run 23	38271		1.71	2500	2421	2415	2346	2075	1931	1919	1854	1675	4.09
Run 24	37924		1.30	2500	2432	2409	2347	2048	1981	1995	1876	1715	4.05
Run 25	37924		1.49	2500	2439	2423	2366	2110	2087	2040	1973	1811	3.63
Run 26	37924		1.37	2500	2450	2425	2391	2144	2114	2046	1961	1777	3.65
Run 27	37924		1.86	2500	2443	2447	2421	2263	2265	2160	2192	2063	2.77
Run 28	37924		2.70	2500	2461	2453	2430	2270	2204	2156	2125	2048	2.76
Run 29	37924		1.42	2500	2479	2468	2417	2285	2204	2265	2243	2126	2.58

Water in 100 mm valve, 75% open

Date:	17/03/2005	
Valve Type:	Diaphragm	
Valve dimension[m]:	0.1	
Valve position:	¾ Open	Area[m^2]
Pipe Diameter [m]:	0.09717	0.007415736

Water

Material Type:	0
Density[kg/m^3]:	999.98
Concentration:	0
τ_y:	0
K:	0.001
n:	1
PPT used:	101
Range selected:	0-130

			Axial distances [m]	-5.7395	-3.865	-2.885	-0.937	0.987	2.938	6.427	8.432	10.433	
			Valve plane										
			Non-dim distances [L/D]:	-59.06658434	-39.77565092	-29.69023361	-9.642893897	10.157456	30.23566945	66.14181332	86.77575383	107.3685294	
			Distances[m]:	0	1.8745	2.8545	4.8025	6.7265	8.6775	**12.1665**	14.1715	16.1725	
Run #	Re_3		k_v	PTT 1	PTT 2	PTT 3	PTT 4	PTT 5	PTT 6	PTT 7	PTT 8	PTT 9	Average Q
				[Pa]	[Pa]	[Pa]	[Pa]	[Pa]	[Pa]	[Pa]	[Pa]	[Pa]	[l/s]
Run 1	91022		10.84	0	178	292	315	5369	5480	5633	5814	6242	6.95
Run 2	86666		10.83	0	65	201	325	4805	4895	4999	5188	5591	6.61
Run 3	81916		10.36	0	110	227	319	4204	4170	4368	4569	4901	6.25
Run 4	79414		10.55	0	35	171	286	3959	3990	4095	4327	4643	6.06
Run 5	77235		10.48	0	38	184	215	3748	3784	3892	4050	4352	5.89
Run 6	73020		10.32	0	92	184	256	3315	3315	3454	3661	3903	5.57
Run 7	68488		10.60	0	42	112	253	2901	2884	3013	3170	3382	5.23
Run 8	68515		9.96	0	2	161	246	2907	2903	2973	3138	3385	5.23
Run 11	65426		10.17	0	60	80	179	2590	2701	2692	2771	3081	4.99
Run 12	58421		11.24	0	85	118	193	2170	2441	2381	2482	2644	4.46
Run 13	56108		11.54	0	145	125	118	2144	2221	2271	2248	2404	4.28
Run 14	54657		11.25	0	182	126	160	2070	2025	2172	2177	2383	4.17

Water in 100 mm valve, 50% open

Date:	17/03/2005	
Valve Type:	Diaphragm	
Valve dimension[m]:	0.1	
Valve position:	½ Open	Area[m^2]
Pipe Diameter [m]:	0.09717	0.007415736

Water

Material Type:	0
Density[kg/m^3]:	999.98
Concentration:	0
τ_y:	0
K:	0.001
n:	1
PPT used:	101
Range selected:	0-130

			Axial distances [m]	-5.7395	-3.865	-2.885	-0.937	0.987	2.938	6.427	8.432	10.433	
			Valve plane										
			Non-dim distances [L/D]:	-59.06658434	-39.77565092	-29.69023361	-9.642893897	10.157456	30.23566945	66.14181332	86.77575383	107.3685294	
			Distances[m]:	0	1.8745	2.8545	4.8025	6.7265	8.6775	12.1665	14.1715	16.1725	
Run #	Re_3		k_v	PTT 1	PTT 2	PTT 3	PTT 4	PTT 5	PTT 6	PTT 7	PTT 8	PTT 9	Average Q
				[Pa]	[Pa]	[Pa]	[Pa]	[Pa]	[Pa]	[Pa]	[Pa]	[Pa]	[l/s]
Run 1	62493		28.82	0	23	108	157	6065	6135	6233	6335	6420	4.77
Run 2	62500		28.78	0	40	85	176	5960	6093	6194	6328	6420	4.77
Run 3	59636		28.57	0	18	86	148	5638	5668	5702	5857	6054	4.55
Run 4	59649		28.69	0	39	97	153	5667	5718	5768	5839	6076	4.55
Run 5	56889		28.16	0	38	79	136	5138	5190	5143	5261	5476	4.34
Run 6	56751		28.52	0	32	78	132	5118	5124	5162	5309	5494	4.33
Run 7	54969		27.74	0	3	75	117	4568	4723	4754	4870	5094	4.20
Run 8	54975		27.90	0	64	73	127	4369	4671	4761	4898	5092	4.20
Run 11	52262		27.94	0	3	60	127	4064	4268	4301	4418	4602	3.99
Run 12	49705		27.81	0	-3	66	105	3857	3862	3911	3977	4170	3.79
Run 13	49771		27.84	0	37	66	110	3501	3827	3908	3953	4128	3.80
Run 14	46695		27.40	0	-5	55	91	3158	3376	3387	3502	3649	3.56
	46754		27.21	0	0	66	99	3316	3342	3398	3490	3648	3.57
	44366		27.25	0	69	77	135	3074	3053	3077	3179	3291	3.39
	42887		27.01	0	18	63	84	2793	2779	2833	2884	2994	3.27
	40570		27.43	0	30	54	79	2501	2493	2540	2601	2657	3.10
	40541		27.44	0	36	50	65	2532	2514	2531	2582	2644	3.09
	37904		27.40	0	18	33	66	2154	2181	2238	2272	2393	2.89
	35491		26.47	0	4	49	63	1893	1969	1946	2010	2124	2.71
	33026		28.57	0	53	43	54	1755	1729	1771	1878	1917	2.52

Water in 100 mm valve, 25% open

Date:	18/03/2005	
Valve Type:	Diaphragm	
Valve dimension[m]:	0.1	
Valve position:	¼ Open	Area[m^2]
Pipe Diameter [m]:	0.09717	0.007415736

Material Type:	Water
Density[kg/m^3]:	999.87
Concentration:	0
τ_y:	0
K:	0.001
n:	1
PPT used:	101
Range selected:	0-130

			Axial distances [m]	-5.7395	-3.865	-2.885	-0.937	0.987	2.938	6.427	8.432	10.433	
			Valve plane										
			Non-dim distances [L/D]:	-59.06658434	-39.77565092	-29.69023361	-9.642893897	10.157456	30.23566945	66.14181332	86.77575383	107.3685294	
			Distances[m]:	0	1.8745	2.8545	4.8025	6.7265	8.6775	12.1665	14.1715	16.1725	
Run #	Re_3		k_v	PTT 1	PTT 2	PTT 3	PTT 4	PTT 5	PTT 6	PTT 7	PTT 8	PTT 9	Average Q
				[Pa]	[Pa]	[Pa]	[Pa]	[Pa]	[Pa]	[Pa]	[Pa]	[Pa]	[l/s]
Run 1	68459		95.72	51042	51034	50987	50910	26626	26432	26379	26367	25851	5.23
Run 2	66565		96.67	49724	49701	49632	49505	26726	26376	26279	26216	25806	5.08
Run 3	64240		96.95	48254	48221	48149	48064	25902	26278	26224	26170	25710	4.90
Run 4	64195		97.12	48210	48234	48161	48093	26442	26328	26239	26146	25735	4.90
Run 5	61710		97.94	46611	46598	46540	46411	26694	26254	26127	26018	25645	4.71
Run 6	59705		99.69	45355	45293	45221	45175	26253	26126	25960	25971	25639	4.56
Run 7	57573		97.98	44055	44007	43898	43880	26405	26071	26049	25965	25541	4.39
Run 8	55312		97.61	42555	42553	42495	42410	26373	26013	26011	25916	25537	4.22
Run 11	55313		98.35	42538	42555	42427	42400	25765	25868	25970	25883	25547	4.22
Run 12	53312		100.52	41488	41467	41435	41472	25374	25915	25846	25783	25519	4.07
Run 13	50754		103.10	40316	40316	40189	40157	26140	25824	25779	25753	25483	3.87
Run 14	48202		101.87	38727	38716	38666	38636	26080	25722	25672	25691	25381	3.68
Run 15	46035		102.02	37550	37491	37503	37428	25540	25664	25548	25610	25275	3.51
Run 16	46042		102.16	37530	37559	37483	37477	25262	25710	25660	25564	25368	3.51
Run 17	41032		104.03	34912	34923	34805	34776	25331	25448	25396	25390	25243	3.13
Run 18	38680		102.55	33787	33720	33756	33738	25270	25367	25342	25314	25158	2.95
Run 19	36600		104.95	32863	32862	32769	32851	25343	25282	25260	25192	25125	2.79
Run 20	29611		104.03	30073	30067	30040	30066	25035	25116	25093	25016	24965	2.26
Run 21	24892		102.79	28400	28414	28380	28357	25064	25021	24956	24936	24900	1.90

Glycerine 75%

Glycerine 75% in 40 mm valve, 100% open

Date:	30/11/2004	
Valve Type:	Diaphragm	
Valve dimension[m]:	0.04	
Valve position:	1	Area[m^2]
Pipe Diameter [m]:	0.04212	0.00139337

Material Type:	GLYCERINE 75%
Density[kg/m^3]:	1197.2
Concentration:	0.7353
τ_y:	0
K:	0.02
n:	1
PPT used:	101
Range selected:	0-130

			Axial distances [m]	-6.298	-4.568	-2.932	-0.8315	1.0755	2.6845	6.0455	8.0745	9.9745
			Valve plane									
			Non-dim distances [L/D]:	-149.5251662	-108.4520418	-69.61063628	-19.74121557	25.53418803	63.7345679	143.5303894	191.7022792	236.811491
			Distances[m]:	0	1.73	3.366	5.4665	7.3735	8.9825	12.3435	14.3725	16.2725
Run #	Re_3		k_v	PPT1	PPT2	PPT3	PPT4	PPT5	PPT6	PPT7	PPT8	PPT9	Average Q
				[Pa]	[Pa]	[Pa]	[Pa]	[Pa]	[Pa]	[Pa]	[Pa]	[Pa]	[l/s]
Run 1	1633		12.39	33226	32820	32466	31781	28521	27939	27100	26583	26140	0.90
Run 2	1631		12.89	33238	32800	32462	31774	28538	27926	27120	26589	26200	0.90
Run 3	1787		12.55	34150	33760	33366	32537	28794	28176	27400	26900	26450	0.99
Run 4	1788		12.58	34094	33710	33318	32525	28796	28140	27380	26930	26450	0.99
Run 5	1928		13.75	35109	34630	34182	33276	29025	28370	27602	27090	26740	1.07
Run 6	1924		12.86	35012	34510	34124	33294	29004	28299	27593	27090	26660	1.06
Run 7	2135		14.76	36422	35860	35378	34499	29387	28576	27703	27230	26940	1.18
Run 8	2123		15.24	36380	35830	35518	34415	29412	28543	27700	27260	27000	1.17
Run 9	2280		13.18	37515	36930	36447	35427	29587	28765	27803	27270	26770	1.26
Run 10	2283		8.64	37480	36728	36533	35450	29637	28767	27820	26865	26116	1.26
Run 11	2282		8.19	37236	36835	36346	35477	29767	28776	27833	26850	26104	1.26
Run 12	2472		7.35	39564	38770	37930	37182	29970	29155	28344	26928	26094	1.37
Run 13	2478		11.12	39722	38678	38200	37021	30377	29023	27845	26938	26137	1.37
Run 14	2605		9.39	41567	40517	39706	37802	30797	29305	28253	27034	25933	1.44
Run 15	2600		9.51	41231	40274	39894	38011	30597	29339	28138	26954	25924	1.44
Run 16	2728		7.72	43368	42648	41441	39897	31703	30483	28837	27187	25895	1.51
Run 17	2721		8.02	43641	42342	41804	40048	31620	30467	28811	27114	25891	1.50
Run 18	2852		9.45	45842	44343	43583	41701	32219	31106	28952	27314	25909	1.58
Run 19	2852		9.18	45790	44456	43495	41558	32436	31113	28946	27359	25840	1.58
Run 20	2954		8.56	47431	45809	44807	42962	32885	31585	29325	27445	25823	1.63
Run 21	2953		8.77	47379	45973	44905	43075	32945	31598	29280	27459	25823	1.63
Run 22	3121		8.80	49821	48121	47021	44884	33770	32312	29633	27596	25799	1.72
Run 23	3118		8.90	49798	48042	46970	44952	33746	32280	29597	27633	25792	1.72
Run 24	3378		8.85	53519	51519	50212	47690	34914	33241	30156	27682	25760	1.87
Run 25	3372		8.89	53455	51536	50141	47832	34923	33275	30166	27761	25793	1.86
Run 26	3626		8.87	57214	55037	53493	50833	36093	34239	30646	28039	25708	2.00
Run 27	3622		9.18	57251	55045	53511	50901	36150	34185	30577	28040	25724	2.00
Run 28	4086		9.10	64848	62259	60125	56807	38459	36155	31558	28414	25532	2.26
Run 29	4083		9.29	64879	62163	60095	56856	38381	36170	31518	28444	25566	2.26
Run 30	4455		8.95	71623	68605	65967	62225	40541	37875	32519	28741	25399	2.46
Run 31	4464		9.19	71489	68602	65961	62318	40592	37850	32389	28656	25424	2.47
Run 32	4663		9.12	75529	72355	69455	65505	41702	38950	32965	29070	25365	2.58
Run 33	4670		9.16	75612	72303	69468	65574	41868	38876	32934	28897	25347	2.58
Run 34	4822		9.62	78401	74822	71932	67677	42588	39547	33040	29112	25332	2.66
Run 35	4814		9.39	78376	74788	71905	67673	42721	39550	33207	29094	25374	2.66
Run 36	5022		9.26	82313	78807	75480	70775	43810	40489	33679	29334	25201	2.78
Run 37	5544		9.48	81107	77001	72603	67470	34954	30961	22604	17468	12682	3.06
Run 38	5560		9.31	81098	76893	72700	67254	34819	30858	22596	17397	12588	3.07
Run 39	5814		9.21	86979	82184	77568	72013	36695	32566	23531	17948	12666	3.21
Run 40	5721		9.16	98023	93347	89230	83508	49362	45093	36470	31144	25894	3.16

Glycerine 75% in 50 mm valve, 100% open

Date:	01/12/2004	
Valve Type:	Diaphragm	
Valve dimension[m]:	0.05	
Valve position:	1	Area[m^2]
Pipe Diameter [m]:	0.0528	0.002189564

Material Type:	Glycerine 75%
Density[kg/m^3]:	1197.2
Concentration:	0.7353
τ_y:	0
K:	0.02
n:	1
PPT used:	101
Range selected:	0-130

		Axial distances [m]	-5.824	-4.72	-3.526	-1.031	1.2565	3.0115	5.6655	7.6655	9.6685	
		Valve plane										
		Non-dim distances [L/D]:	-110.3030303	-89.39393939	-66.78030303	-19.52651515	23.79734848	57.03598485	107.3011364	145.1799242	183.1155303	
		Distances[m]:	0	1.104	2.298	4.793	7.0805	8.8355	**11.4895**	13.4895	15.4925	
Run #	Re_3		k_v	PPT1	PPT2	PPT3	PPT4	PPT5	PPT6	PPT7	PPT8	PPT9	Average Q
				[Pa]	[Pa]	[Pa]	[Pa]	[Pa]	[Pa]	[Pa]	[Pa]	[Pa]	[l/s]
Run 1	4298		2.90	42027	41132	39631	37615	33444	32130	29640	28224	26432	2.98
Run 2	4787		2.86	45489	44239	42504	40029	34948	33319	30299	28617	26386	3.32
Run 3	4799		2.85	45536	44366	42494	40034	34937	33292	30317	28624	26382	3.32
Run 4	4651		2.92	44580	43368	41691	39333	34537	32978	30140	28549	26434	3.22
Run 5	4660		2.61	44279	43437	41699	39387	34550	33027	30142	28532	26383	3.23
Run 6	4238		2.95	41840	40785	39416	37363	33341	32074	29572	28315	26426	2.94
Run 7	4266		2.91	41910	40735	39409	37362	33320	32062	29596	28298	26440	2.96
Run 8	3893		2.91	39703	38723	37498	35772	32315	31300	29180	28123	26459	2.70
Run 9	3906		2.81	39678	38743	37501	35823	32334	31268	29194	28108	26456	2.71
Run 10	3726		3.11	38682	37691	36579	35040	31913	30928	28942	28010	26481	2.58
Run 11	3729		2.90	38618	37714	36602	35034	31877	30916	28954	28024	26458	2.58
Run 12	3383		2.95	36664	35863	34927	33583	31038	30230	28564	27829	26479	2.34
Run 13	3386		2.92	36615	35800	34911	33596	31026	30223	28551	27830	26476	2.35
Run 14	3376		2.61	36472	35855	34936	33567	30971	30146	28579	27844	26473	2.34
Run 15	3188		2.80	35504	34789	34100	32829	30484	29845	28342	27732	26484	2.21
Run 16	3193		2.74	35505	34825	34036	32792	30483	29843	28341	27726	26463	2.21
Run 17	3071		2.42	34730	34015	33407	32297	30093	29675	28216	27661	26469	2.13
Run 18	3104		3.01	35138	34369	33614	32513	30341	29616	28245	27673	26489	2.15
Run 19	2851		2.24	33014	32801	32419	31283	29322	28742	27843	27537	26457	1.98
Run 20	2850		2.26	33513	32673	32123	31371	29416	28979	27967	27520	26474	1.97
Run 21	2611		3.47	31897	31284	30887	29939	28783	28212	27601	27368	26643	1.81
Run 22	2616		3.00	31686	31327	30778	30186	28932	28630	27610	27310	26631	1.81
Run 23	2374		2.09	30830	30287	30063	29474	28573	28046	27431	27242	26543	1.64
Run 24	2383		3.16	30768	30362	30042	29493	28422	28079	27343	27230	26564	1.65
Run 25	2034		2.79	29856	29493	29305	28877	28073	27745	27168	27122	26517	1.41
Run 26	2037		3.13	29849	29507	29309	28890	28058	27759	27141	27130	26514	1.41
Run 27	1566		3.61	28868	28560	28432	28108	27554	27377	26872	26957	26410	1.09
Run 28	1563		2.64	28851	28525	28442	28070	27570	27367	26893	26947	26397	1.08
Run 29	1332		3.47	28421	28150	28032	27738	27342	27202	26769	26876	26368	0.92
Run 30	1333		3.73	28427	28128	28051	27759	27355	27194	26755	26867	26361	0.92

Glycerine 75% in 65 mm valve, 100% open

Date:	02/12/2004	
Valve Type:	Diaphragm	
Valve dimension[m]:	0.06	
Valve position:	1	Area[m^2]
Pipe Diameter [m]:	0.06308	0.003125167

Material Type:	Glycerine 75%
Density[kg/m^3]:	1192.5
Concentration:	0.75
τ_y:	0
K:	0.02
n:	1
PPT used:	101
Range selected:	0-130

			Axial distances [m]	-6.9735	-4.8855	-2.885	-1.2665	0.987	2.938	5.449	7.454	9.455	
			Valve plane										
			Non-dim distances [L/D]:	-110.5500951	-77.44927077	-45.73557387	-20.07767914	15.64679772	46.57577679	86.38237159	118.1674065	149.8890298	
			Distances[m]:	0	2.088	4.0885	5.707	7.9605	9.9115	12.4225	14.4275	16.4285	
Run #	Re_3		k_v	PPT1	PPT2	PPT3	PPT4	PPT5	PPT6	PPT7	PPT8	PPT9	Average Q
				[Pa]	[Pa]	[Pa]	[Pa]	[Pa]	[Pa]	[Pa]	[Pa]	[Pa]	[l/s]
Run 1	8140		1.52	59768	56265	52784	50042	42859	39454	34596	31263	27846	6.76
Run 2	8093		1.60	59527	56341	52799	49954	42825	39495	34525	31251	27867	6.72
Run 3	7725		1.56	56382	53201	50202	47692	41241	38236	33838	30849	27840	6.42
Run 4	7888		1.41	56236	53191	50158	47681	41298	38222	33853	30913	27828	6.55
Run 5	6984		1.75	52702	50021	47346	45136	39565	36933	33055	30404	27865	5.80
Run 6	7247		1.55	52808	50065	47214	45189	39617	36924	33074	30429	27801	6.02
Run 7	6533		1.72	48526	46269	43976	42163	37528	35309	32115	29956	27814	5.43
Run 8	6535		2.70	48511	46329	44046	42473	37839	35611	32383	30271	28708	5.43
Run 9	5836		2.03	44805	42898	40972	39487	35706	33809	31090	29333	27598	4.85
Run 10	5641		1.95	44993	43283	41389	39867	36108	34249	31532	29708	28013	4.69
Run 11	5077		2.10	40412	39041	37605	36456	33647	32253	30220	28890	27658	4.22
Run 12	5069		2.76	40219	38939	37555	36442	33603	32278	30251	29140	27993	4.21
Run 13	4561		2.00	38313	37209	36010	35125	32746	31513	29789	28615	27590	3.79
Run 14	4497		2.24	38292	37183	35949	35050	32619	31438	29729	28608	27569	3.74
Run 15	3663		2.28	35320	34422	33515	32897	31282	30424	29203	28369	27638	3.04
Run 16	3692		2.68	35336	34472	33545	32942	31166	30329	29025	28185	27474	3.07

Glycerine 75% in 80 mm valve, 100% open

Date:	02/12/2004	
Valve Type:	Diaphragm	
Valve dimension[m]:	0.08	
Valve position:	1	Area[m^2]
Pipe Diameter [m]:	0.08043	0.005080729

Material Type:	GLYCERINE 75%
Density[kg/m^3]:	1192.5
Concentration:	0.75
τ_y:	0
K:	0.02
n:	1
PPT used:	101
Range selected:	0-40

			Axial distances [m]	-6.413	-4.809	-2.408	-1.209	0.707	3.907	5.977	8.461	9.956	
			Valve plane										
			Non-dim distances [L/D]:	-79.73393013	-59.79112272	-29.93907746	-15.03170459	8.790252393	48.57640184	74.31306726	105.1970658	123.7846575	
			Distances[m]:	0	1.604	4.005	5.204	7.12	10.32	12.39	14.874	16.369	
Run #	Re_3		k_v	PPT1	PPT2	PPT3	PPT4	PPT5	PPT6	PPT7	PPT8	PPT9	Average Q
				[Pa]	[Pa]	[Pa]	[Pa]	[Pa]	[Pa]	[Pa]	[Pa]	[Pa]	[l/s]
Run 1	6817		3.51	41904	41273	39657	39061	34254	32368	31229	29887	29126	7.22
Run 2	7042		3.00	41679	41155	39781	39079	34414	32446	31306	29890	29189	7.46
Run 3	6246		3.65	40090	39389	38066	37454	33366	31658	30658	29468	28804	6.62
Run 4	6097		4.05	40197	39505	38252	37677	33518	31820	30754	29616	28964	6.46
Run 5	5813		3.62	38714	38025	36991	36448	32714	31295	30454	29388	28823	6.16
Run 6	5618		4.01	38684	38090	37025	36492	32861	31308	30427	29402	28823	5.95
Run 7	5652		3.56	38643	38040	37031	36574	32825	31344	30474	29400	28795	5.99
Run 8	4596		4.28	35390	34927	34096	33818	31264	30196	29584	28853	28468	4.87
Run 9	4677		4.08	35338	34913	34117	33762	31267	30194	29590	28855	28482	4.96
Run 10	3727		4.59	32557	32316	31745	31587	29959	29261	28840	28377	28170	3.95
Run 11	3584		4.83	32577	32324	31801	31532	29951	29219	28848	28373	28164	3.80
Run 12	2935		5.94	30871	30881	30372	30201	29159	28647	28388	28144	27989	3.11

Glycerine 75% in 100 mm valve, 100% open

Date:	03/12/2004	
Valve Type:	Diaphragm	
Valve dimension[m]:	0.1	
Valve position:	1	Area[m^2]
Pipe Diameter [m]:	0.09717	0.007415736

Material Type:	GLYCERINE 75%
Density[kg/m^3]:	0.75
Concentration:	1192.5
τ_y:	0
K:	0.02
n:	1
PPT used:	101
Range selected:	0-130

			Axial distances [m]	-4.55181	-3.04175	-2.54175	-1.03975	0.69975	2.50175	3.50075	5.00975	9.51075	
			Valve plane										
			Non-dim distances [L/D]:	-46.84377894	-31.30338582	-26.15776474	-10.70031903	7.201296697	25.74611506	36.02706597	51.55655038	97.87743131	
			Distances[m]:	0	1.51006	2.01006	3.51206	5.25156	7.05356	8.05256	9.56156	14.06256	
Run #	Re_3		k_v	DP1	DP2	DP3	DP4	DP5	DP6	DP7	DP8	DP9	Average Q
				[Pa]	[Pa]	[Pa]	[Pa]	[Pa]	[Pa]	[Pa]	[Pa]	[Pa]	[l/s]
Run 1	5891		1.98	0	276	432	771	2498	2897	3131	3609	4854	7.54
Run 2	5891		1.96	0	255	409	754	2438	2874	3086	3613	4881	7.54
Run 3	5420		2.22	0	234	390	697	2247	2653	2873	3298	4428	6.94
Run 4	5358		2.11	0	237	409	693	2281	2696	2868	3310	4495	6.86
Run 5	5334		2.06	0	221	375	659	2082	2505	2678	3085	4162	6.83
Run 6	5366		2.11	0	209	370	651	2127	2530	2698	3103	4178	6.87
Run 7	4838		2.16	0	191	337	581	1886	2224	2392	2723	3733	6.19
Run 8	4926		2.11	0	183	350	597	1917	2253	2409	2751	3749	6.31
Run 9	4564		1.89	0	141	281	486	1565	1857	1968	2250	3140	5.84
Run 10	4557		2.07	0	125	291	486	1565	1865	1988	2268	3098	5.83
Run 11	4153		2.10	0	96	244	407	1315	1578	1707	1885	2648	5.32
Run 12	4007		2.28	0	69	239	404	1327	1551	1670	1891	2632	5.13
Run 13	3637		2.33	0	59	206	318	1053	1248	1354	1451	2007	4.66
Run 14	3608		2.14	0	47	181	320	1064	1273	1299	1497	2102	4.62
Run 15	3194		2.53	0	-2	165	249	835	1002	1051	1174	1598	4.09
Run 16	3178		1.85	0	34	137	244	817	987	1019	1093	1670	4.07

Glycerine 100%

Glycerine 100% in 40 mm valve, 100% open

Date:	22/11/2004	
Valve Type:	Diaphragm	
Valve dimension[m]:	0.04	
Valve position:	1	Area[m^2]
Pipe Diameter [m]:	0.04212	0.00139337

Material Type:	Glycerine 100%
Density[kg/m^3]:	1270
Concentration:	0.75
τ_y:	0
K:	0.842238
n:	1
PPT used:	101
Range selected:	0-40

			Axial distances [m]	-5.7395	-3.865	-2.885	-0.937	0.987	2.938	6.427	8.432	10.433	
			Valve plane										
			Non-dim distances [L/D]:	-136.2654321	-91.76163343	-68.49477683	-22.24596391	23.43304843	69.75308642	152.5878443	200.1899335	247.697056	
			Distances[m]:	0	1.8745	2.8545	4.8025	6.7265	8.6775	12.1665	14.1715	16.1725	
Run #	Re_3		k_v	PTT 1	PTT 2	PTT 3	PTT 4	PTT 5	PTT 6	PTT 7	PTT 8	PTT 9	Average Q
				[Pa]	[Pa]	[Pa]	[Pa]	[Pa]	[Pa]	[Pa]	[Pa]	[Pa]	[l/s]
Run 1	12		139.06	0	5067	9585	15691	23742	28501	38160	43800	49240	0.26
Run 2	12		142.87	0	4983	9420	15602	23642	28448	37999	43590	49173	0.26
Run 3	13		124.86	0	5515	10347	16923	25809	30952	41369	47605	53511	0.28
Run 4	13		125.19	0	5492	10345	17047	25820	30912	41304	47422	53390	0.28
Run 5	14		110.54	0	5828	11001	18036	27402	32864	43818	50258	56724	0.30
Run 6	14		112.61	0	5982	11007	18059	27399	32822	43786	50249	56600	0.30
Run 7	15		101.34	0	6674	11967	19470	29645	35474	47422	54393	61247	0.33
Run 8	15		101.72	0	6711	11864	19427	29640	35407	47224	54220	61057	0.32
Run 9	16		100.74	0	6775	12571	20450	31294	37350	49796	57142	64262	0.34
Run 10	15		100.32	0	7099	12463	20440	31209	37175	49528	56778	63907	0.34
Run 11	17		94.46	0	7191	13307	21632	33157	39615	52640	60379	67919	0.36
Run 12	16		97.10	0	7595	13205	21576	33001	39499	52569	60215	67777	0.36
Run 13	17		93.16	0	7651	13770	22444	34504	41249	54812	62866	70736	0.38
Run 14	17		90.77	0	8019	13725	22407	34396	41153	54556	62641	70382	0.37
Run 15	18		93.03	0	7698	14127	22957	35632	42415	56301	64577	72649	0.38
Run 16	17		96.47	0	8454	13998	23001	35448	42256	56222	64290	72408	0.38
Run 17	17		98.88	0	8219	13902	22749	35299	42071	55768	63860	71806	0.38
Run 18	19		91.58	0	8996	15164	24796	38607	46018	61144	70039	78797	0.41
Run 19	19		84.67	0	9473	15233	24857	38624	46034	61249	70217	79009	0.42
Run 20	19		93.34	0	8234	15423	25197	39055	46567	61929	70951	79808	0.42
Run 21	23		79.23	0	10634	18879	30748	48319	57481	76186	87239	98026	0.51

Glycerine 100% in 50 mm valve, 100% open

Date:	23/11/2004	
Valve Type:	Diaphragm	
Valve dimension[m]:	0.050	
Valve position:	Open	Area[m^2]
Pipe Diameter [m]:	0.0528	0.002189564

Material Type:	Glycerine 100%
Density[kg/m^3]:	1256
Concentration:	0
τ_y:	0
K:	0.8436
n:	1
PPT used:	101
Range selected:	0-130

		Axial distances [m]	-6.574	-3.526	-2.281	-1.031	1.2565	3.0115	5.6655	7.6655	9.6685
		Valve plane									
		Non-dim distances [L/D]:	-124.5075758	-66.78030303	-43.20075758	-19.52651515	23.79734848	57.03598485	107.3011364	145.1799242	183.1155303
		Distances[m]:	0	3.048	4.293	5.543	7.8305	9.5855	12.2395	14.2395	16.2425
Run #	Re_3		k_v	DP1	DP2	DP3	DP4	DP5	DP6	DP7	DP8	DP9	Average Q
				[Pa]	[Pa]	[Pa]	[Pa]	[Pa]	[Pa]	[Pa]	[Pa]	[Pa]	[l/s]
Run 1	11		59.27	0	4009	5566	7064	10374	12671	16324	18870	21348	0.29
Run 2	10		60.55	0	3964	5475	7018	10248	12425	16113	18566	21070	0.29
Run 3	11		77.91	0	4154	5727	7288	10828	13114	16923	19344	21965	0.30
Run 4	11		55.05	0	4183	5624	7290	10754	12960	16692	19226	21862	0.30
Run 5	12		43.28	0	4800	6519	8467	12427	14975	19428	22330	25524	0.34
Run 6	12		31.02	0	4825	6504	8347	12356	14904	19289	22366	25456	0.34
Run 7	13		50.21	0	5141	6821	8880	13054	15758	20392	23529	26692	0.36
Run 8	13		40.24	0	5005	6877	8809	13024	15845	20373	23475	26764	0.36
Run 9	14		50.83	0	5419	7243	9423	13876	16741	21676	24977	28346	0.38
Run 10	14		48.24	0	5475	7223	9394	13802	16681	21588	24876	28226	0.38
Run 11	14		48.67	0	5411	7172	9263	13669	16463	21429	24708	28029	0.38
Run 12	14		44.12	0	5275	7177	9267	13689	16480	21340	24634	27986	0.38
Run 13	13		53.35	0	5341	7068	9161	13515	16268	21092	24306	27526	0.37
Run 14	14		51.39	0	5691	7516	9759	14331	17287	22406	25770	29202	0.40
Run 15	14		55.64	0	5499	7476	9704	14332	17242	22372	25751	29202	0.39
Run 16	15		42.65	0	6121	7774	10173	14875	17984	23297	26732	30406	0.41
Run 17	15		37.95	0	6142	7717	10024	14788	17832	23106	26667	30225	0.41
Run 18	16		44.45	0	6208	8353	10834	15987	19428	25057	28981	32820	0.44
Run 19	16		41.19	0	6424	8338	10847	16052	19245	24913	28689	32539	0.44
Run 20	16		47.41	0	6321	8556	11125	16356	19787	25605	29466	33432	0.45
Run 21	16		38.22	0	6645	8482	11077	16294	19634	25426	29355	33251	0.45
Run 22	17		38.96	0	6700	8844	11560	17095	20625	26656	30791	34958	0.47
Run 23	17		33.74	0	6818	8839	11476	17045	20554	26557	30747	34862	0.47
Run 24	18		34.86	0	7228	9726	12776	18880	22794	29411	33925	38661	0.51
Run 25	18		32.10	0	7426	9754	12658	18830	22678	29324	33856	38484	0.51
Run 26	19		32.13	0	7635	10275	12892	19750	23794	30854	35625	40509	0.54
Run 27	19		35.89	0	7869	10208	13306	19808	23854	30830	35490	40327	0.54
Run 28	20		38.02	0	7964	10576	13771	20480	24665	31737	36695	41457	0.56
Run 29	20		39.87	0	8148	10486	13716	20260	24408	31670	36562	41300	0.55
Run 30	21		59.52	0	8283	11219	14548	21626	26075	33725	38895	43429	0.59
Run 31	21		32.96	0	8504	11197	14611	21661	26187	33802	38689	44202	0.59
Run 32	23		33.55	0	9349	12400	16106	24069	29057	37520	43100	49019	0.65
Run 34	25		41.13	0	9847	13082	16959	25346	30530	39520	45537	51278	0.69
Run 35	24		37.14	0	9837	12863	17008	25330	30549	39645	45510	51813	0.68
Run 36	27		29.70	0	10391	14138	18381	27448	33140	42793	49301	56031	0.75
Run 37	26		39.48	0	10826	13547	17662	27468	33150	42741	49220	55894	0.71
Run 38	29		29.26	0	11201	15296	19878	29707	35853	46446	53456	60773	0.81

Glycerine 100% in 50 mm valve, 100% open (continued)

Date:	23/11/2004	
Valve Type:	Diaphragm	
Valve dimension[m]:	0.050	
Valve position:	Open	Area[m^2]
Pipe Diameter [m]:	0.0528	0.002189564

Material Type:	Glycerine 100%
Density[kg/m^3]:	1256
Concentration:	0
τ_y:	0
K:	0.8436
n:	1
PPT used:	101
Range selected:	0-130

		Axial distances [m]	-6.574	-3.526	-2.281	-1.031	1.2565	3.0115	5.6655	7.6655	9.6685
		Valve plane									
		Non-dim distances [L/D]:	-124.5075758	-66.78030303	-43.20075758	-19.52651515	23.79734848	57.03598485	107.3011364	145.1799242	183.1155303
		Distances[m]:	0	3.048	4.293	5.543	7.8305	9.5855	12.2395	14.2395	16.2425
Run #	Re_3		k_v	DP1	DP2	DP3	DP4	DP5	DP6	DP7	DP8	DP9	Average Q
				[Pa]	[Pa]	[Pa]	[Pa]	[Pa]	[Pa]	[Pa]	[Pa]	[Pa]	[l/s]
Run 39	29		19.53	0	11289	15279	19917	29736	35865	45889	53427	60480	0.81
Run 40	32		22.62	0	12793	17093	22080	33139	39961	51515	59413	67431	0.90
Run 41	32		26.78	0	12328	16917	22032	33118	39775	51358	59332	67244	0.89
Run 42	34		25.63	0	13450	17997	23466	35115	42421	54835	63196	71677	0.95
Run 43	34		25.37	0	13736	17963	23421	35082	42351	54642	63014	71309	0.95
Run 44	36		24.33	0	14166	18772	24297	36610	44215	57053	65580	74457	0.99
Run 45	35		18.94	0	13904	18592	24172	36309	43801	56428	65040	74146	0.98
Run 46	37		21.58	0	14458	19705	25438	38452	46219	59609	68724	78031	1.04
Run 47	37		22.60	0	14674	19658	25350	38354	46162	59630	68739	77936	1.04
Run 48	36		25.74	0	14257	19244	25013	38005	45605	58740	67720	76720	1.02
Run 49	36		27.44	0	13886	19145	24944	37776	45556	58656	67614	76664	1.01
Run 50	39		24.71	0	14857	20657	26852	40652	49080	63092	72860	82538	1.09
Run 51	39		27.64	0	15088	20620	26784	40775	48987	63131	72675	82214	1.09
Run 52	41		23.81	0	15935	21857	28396	43134	51924	66853	77065	87331	1.15
Run 53	41		26.67	0	15697	21745	28094	42953	51682	66699	76867	86954	1.15
Run 54	43		23.53	0	16284	22548	29211	44572	53653	68979	79469	90109	1.19
Run 55	43		25.48	0	16268	22472	29174	44451	53487	68945	79320	89881	1.19
Run 56	42		28.20	0	15847	22185	28886	44165	53102	68618	79070	89487	1.17
Run 57	42		21.78	0	16538	22329	28940	44215	53150	68343	78556	89327	1.18
Run 58	43		26.88	0	16816	22861	29749	45516	54688	70613	81310	91921	1.21
Run 59	43		22.95	0	17681	22795	29644	45449	54564	70399	80945	91754	1.20
Run 60	44		25.03	0	17189	23420	30383	46601	56013	72183	83278	94109	1.24
Run 61	44		22.99	0	17058	23484	30470	46605	56021	71974	82866	93969	1.24
Run 62	45		21.54	0	17416	23767	30883	47401	56920	73267	84370	95910	1.25
Run 63	45		23.94	0	17284	23827	30888	47397	56951	73298	84343	95628	1.26
Run 64	46		23.38	0	17500	24185	31298	48363	58068	74583	85990	97449	1.28
Run 65	46		23.65	0	17734	24155	31413	48180	57762	74294	85474	96836	1.27
Run 66	47		24.24	0	18329	24996	32384	50197	60225	77507	89141	101052	1.32
Run 67	48		23.36	0	18456	25108	32589	50174	60224	77457	89081	100938	1.32
Run 68	53		22.20	0	20301	28170	36545	56612	67854	87123	100272	113529	1.49
Run 69	53		20.21	0	20969	28121	36488	56330	67541	86798	99935	113158	1.48
Run 70	58		20.94	0	22430	30805	39967	62295	74469	95623	109929	124478	1.63
Run 71	58		20.14	0	22776	30779	39896	62079	74132	95395	109702	124179	1.62
Run 72	61		21.46	0	22861	32005	41609	64952	77438	99630	114623	129672	1.69
Run 73	61		21.76	0	22875	32013	41434	64858	77557	99509	114360	129360	1.69
Run 74	61		20.45	0	23244	32152	41709	65358	77820	99810	114734	129899	1.70
Run 75	61		20.59	0	23181	32072	41531	64944	77644	99657	114703	129747	1.69
Run 76	57		19.85	0	21584	29979	38844	59933	71766	91589	105551	119186	1.58

Glycerine 100% in 65mm valve, 100% open

Date:	24/11/2004	
Valve Type:	Diaphragm	
Valve dimension[m]:	0.065	
Valve position:	1	Area[m^2]
Pipe Diameter [m]:	0.06308	0.003125167

Material Type:	Glycerine 100%
Density[kg/m^3]:	1256
Concentration:	0
τ_y:	0
K:	0.837175
n:	1
PPT used:	101
Range selected:	0-130

		Axial distances [m]	-6.9735	-3.865	-2.885	-0.937	1.316	2.938	6.427	8.432	10.156	
		Valve plane										
		Non-dim distances [L/D]:	-110.5500951	-61.2714014	-45.73557387	-14.85415346	20.86239696	46.57577679	101.8864933	133.6715282	161.0019023	
		Distances[m]:	0	3.1085	4.0885	6.0365	7.9605	9.9115	**13.4005**	15.4055	17.1295	
Run #	Re_3		k_v	DP1	DP2	DP3	DP4	DP5	DP6	DP7	DP8	DP9	Average Q
				[Pa]	[Pa]	[Pa]	[Pa]	[Pa]	[Pa]	[Pa]	[Pa]	[Pa]	[l/s]
Run 1	13		76.40	0	3130	3775	5469	7276	9017	11537	13231	14901	0.43
Run 2	11		97.23	0	2646	3107	4496	5950	7341	9437	10775	12159	0.35
Run 3	10		83.60	0	2439	3041	4499	5997	7317	9344	10690	12062	0.35
Run 4	11		78.33	0	2450	3071	4368	5900	7299	9368	10693	12058	0.35
Run 5	13		60.40	0	2979	3759	5412	7287	8953	11516	13114	14817	0.43
Run 6	13		64.86	0	2921	3772	5405	7244	8916	11485	13149	14822	0.43
Run 7	16		53.90	0	3580	4519	6514	8911	10901	13991	16040	18088	0.51
Run 8	15		66.03	0	3628	4407	6543	8785	10901	13880	15985	18060	0.50
Run 9	18		51.01	0	4416	5338	7844	10430	12789	16589	19009	21461	0.61
Run 10	18		39.06	0	4376	5297	7804	10611	12939	16644	18976	21416	0.60
Run 11	22		34.77	0	5248	6268	9374	12429	15336	19747	22616	25441	0.71
Run 12	22		43.29	0	5233	6328	9278	12180	15152	19680	22422	25455	0.72
Run 13	24		38.79	0	6337	7080	10749	14572	17793	22908	26134	29692	0.80
Run 14	24		27.06	0	6265	7021	10479	14258	17655	22974	26165	29580	0.80
Run 15	29		30.33	0	6996	8304	11891	16298	20013	25998	29678	33548	0.94
Run 16	28		37.67	0	7007	8284	11855	16460	19865	25839	29590	33543	0.94
Run 17	30		29.07	0	7283	8731	12714	17359	21583	27607	31599	35743	0.99
Run 18	30		29.72	0	7244	8650	12611	17524	21212	27315	31558	35392	0.98
Run 19	33		23.55	0	7974	9631	14196	19113	23868	30731	35155	39764	1.09
Run 20	33		27.27	0	8159	9550	14213	19241	23863	30682	35114	39809	1.08
Run 21	40		22.24	0	9659	11619	17162	23271	28603	36774	42227	47674	1.32
Run 22	41		27.18	0	9925	11782	16952	23171	28648	36636	42004	47593	1.34
Run 23	45		19.82	0	10704	13120	18833	25926	31961	40975	47047	53060	1.49
Run 24	44		20.24	0	10810	12877	18900	25686	31761	40917	46865	53046	1.46
Run 25	48		19.87	0	11180	13982	20375	27652	34150	43861	50459	57056	1.59
Run 26	47		21.50	0	11147	13795	20366	27432	33888	43391	50076	56568	1.57
Run 27	50		14.35	0	11776	14515	21260	28872	35749	46168	52781	59665	1.65
Run 28	50		21.28	0	12261	14511	21358	28971	35938	45937	52784	59814	1.65
Run 29	55		14.75	0	13444	15988	23534	32057	39704	50986	58247	65943	1.82
Run 30	55		15.34	0	13575	15984	23457	31933	39542	50885	58064	65799	1.81
Run 31	59		15.45	0	14232	17063	24979	34328	42378	54284	62309	70467	1.94
Run 32	59		14.45	0	14282	17087	25106	34455	42225	54344	62173	70377	1.94
Run 33	60		13.23	0	14063	17581	25672	35170	43345	55734	63707	72244	2.00
Run 34	61		11.93	0	14376	17674	25891	35359	43837	56270	64335	72742	2.01
Run 35	61		13.28	0	14352	17647	25760	35042	43292	55612	63526	71920	2.00
Run 36	61		12.29	0	14306	17648	25881	35397	43701	56152	64264	72655	2.00
Run 37	63		12.14	0	14920	18298	26902	37560	45540	58432	66878	75673	2.08
Run 38	63		11.66	0	14654	18334	26728	36911	45215	58145	66619	75246	2.08
Run 39	62		10.71	0	14523	17907	26289	36195	44654	57386	65648	74152	2.03
Run 40	64		10.23	0	15003	18521	27233	37355	46374	59619	68277	77105	2.10

Glycerine 100% in 80 mm valve, 100% open

Date:	25/11/2004	
Valve Type:	Diaphragm	
Valve dimension[m]:	0.08	
Valve position:	Open	Area[m^2]
Pipe Diameter [m]:	0.08043	0.005080729

Material Type:	Glycerine 100%
Density[kg/m^3]:	1256
Concentration:	0
τ_y:	0
K:	0.698855
n:	1
PPT used:	101
Range selected:	0-130

Axial distances [m]	-6.413	-4.009	-2.408	-1.209	0.707	3.827	5.897	8.381	9.876		
Valve plane											
Non-dim distances [L/D]:	-79.73393013	-49.84458535	-29.93907746	-15.03170459	8.790252393	47.5817481	73.31841353	104.202412	122.7900037		
Distances[m]:	0	2.404	4.005	5.204	7.12	10.24	12.31	14.794	16.289		

Run #	Re_3	e	k_v	DP1	DP2	DP3	DP4	DP5	DP6	DP7	DP8	DP9	Average Q
				[Pa]	[Pa]	[Pa]	[Pa]	[Pa]	[Pa]	[Pa]	[Pa]	[Pa]	[l/s]
Run 1	29		24.35	0	1671	2778	3565	5453	7721	9131	10790	11874	1.02
Run 2	30		17.53	0	1740	2871	3639	5500	7741	9121	10775	11848	1.05
Run 3	22		23.76	0	1390	2072	2679	4018	5688	6706	7917	8720	0.76
Run 4	22		22.18	0	1384	2136	2723	4034	5711	6739	7933	8722	0.78
Run 5	31		26.18	0	1785	3015	3977	6038	8491	10080	11892	13106	1.11
Run 6	33		17.96	0	1899	3127	3990	6059	8522	10066	11895	13084	1.15
Run 7	35		19.19	0	2072	3384	4352	6628	9344	11045	13051	14343	1.24
Run 8	35		19.42	0	2093	3381	4349	6631	9342	11045	13041	14333	1.24
Run 9	39		17.61	0	2329	3748	4827	7386	10378	12264	14477	15918	1.38
Run 10	39		19.22	0	2291	3736	4820	7370	10372	12272	14482	15908	1.37
Run 11	43		16.76	0	2560	4135	5357	8238	11558	13641	16122	17720	1.52
Run 12	43		17.55	0	2597	4142	5357	8220	11558	13650	16097	17683	1.52
Run 13	46		16.65	0	2758	4431	5720	8838	12402	14635	17253	18967	1.63
Run 14	46		16.53	0	2701	4424	5724	8825	12376	14608	17252	18956	1.62
Run 15	50		15.86	0	2940	4782	6176	9594	13426	15834	18689	20528	1.75
Run 16	50		15.99	0	2910	4775	6166	9570	13410	15815	18666	20506	1.75
Run 17	67		14.47	0	3970	6434	8323	13262	18393	21652	25481	27951	2.36
Run 18	67		14.46	0	3889	6412	8314	13220	18300	21580	25408	27886	2.35
Run 19	53		16.29	0	3120	5085	6583	10281	14352	16965	20005	21965	1.87
Run 20	53		15.59	0	3164	5099	6601	10282	14360	16933	19976	21921	1.87
Run 21	59		15.97	0	3382	5616	7274	11457	15962	18819	22180	24333	2.06
Run 22	59		14.85	0	3550	5623	7276	11443	15944	18791	22148	24301	2.06
Run 23	61		14.84	0	3681	5883	7592	12041	16738	19715	23198	25478	2.16
Run 24	61		10.95	0	4573	5884	7606	12024	16712	19688	23169	25444	2.16
Run 25	64		15.50	0	3722	6147	7949	12665	17560	20680	24341	26687	2.26
Run 26	64		14.42	0	3909	6146	7930	12630	17495	20609	24248	26600	2.26
Run 27	67		14.57	0	4002	6441	8323	13342	18575	21691	25528	27988	2.36
Run 28	67		15.03	0	3865	6415	8301	13292	18393	21597	25403	27866	2.35
Run 29	71		14.01	0	4251	6785	8752	14075	19493	22892	26950	29525	2.49
Run 30	71		13.04	0	4525	6768	8732	14030	19398	22795	26798	29395	2.48
Run 31	76		15.39	0	4248	7240	9383	15162	20905	24637	28955	31687	2.66
Run 32	76		14.04	0	4421	7280	9360	15167	21042	24528	28877	31551	2.67
Run 33	77		13.03	0	4706	7423	9603	15569	21504	25229	29666	32565	2.72
Run 34	78		14.35	0	4582	7447	9585	15556	21469	25209	29659	32378	2.73
Run 35	86		15.04	0	4913	8279	10671	17588	24071	28393	33242	36345	3.04
Run 36	86		13.24	0	4830	8254	10656	17490	24043	28191	33150	36340	3.03
Run 37	90		15.15	0	5124	8591	11071	18485	25325	29940	35126	38397	3.15
Run 38	90		13.11	0	5398	8663	11172	18549	25397	29676	34780	38102	3.18
Run 39	94		15.98	0	5289	8974	11676	19632	26743	31427	36705	40124	3.29
Run 40	94		12.98	0	5836	9039	11578	19584	26622	31167	36570	39955	3.32
Run 41	95		14.10	0	5660	9078	11720	19909	26984	31538	36974	40373	3.33
Run 42	95		14.50	0	5337	9141	11790	20116	27162	31768	37253	40696	3.35
Run 43	97		13.62	0	5944	9299	11962	20452	27643	32348	37874	41410	3.41
Run 44	100		13.54	0	6044	9555	12207	21077	28428	33180	38931	42415	3.51
Run 45	99		13.08	0	6180	9505	12154	20975	28282	33011	38723	42250	3.49
Run 46	98		15.04	0	6027	9434	12221	21293	28664	33417	39157	42697	3.46
Run 47	101		14.43	0	6071	9697	12514	21903	29357	34182	40061	43688	3.56
Run 48	100		14.32	0	6670	9572	12542	21755	29174	34061	39830	43504	3.51

Glycerine 100% in 100 mm valve, 100% open

Date:	25/11/2004	
Valve Type:	Diaphragm	
Valve dimension[m]:	0.09	
Valve position:	1	Area[m^2]
Pipe Diameter [m]:	0.09717	0.007415736

Material Type:	Glycerine 100%
Density[kg/m^3]:	1
Concentration:	1256
τ_y:	0
K:	0.699
n:	1
PPT used:	101
Range selected:	0-40

		Axial distances [m]	-5.7395	-3.865	-2.885	-0.937	0.987	2.938	6.427	8.432	10.433	
		Valve plane										
		Non-dim distances [L/D]:	-59.06658434	-39.77565092	-29.69023361	-9.642893897	10.157456	30.23566945	66.14181332	86.77575383	107.3685294	
		Distances[m]:	0	1.8745	2.8545	4.8025	6.7265	8.6775	12.1665	14.1715	16.1725	
Run #	Re_3		k_v	PTT 1	PTT 2	PTT 3	PTT 4	PTT 5	PTT 6	PTT 7	PTT 8	PTT 9	Average Q
				[Pa]	[Pa]	[Pa]	[Pa]	[Pa]	[Pa]	[Pa]	[Pa]	[Pa]	[l/s]
Run 1	27		20.85	36983	36340	36025	35534	34758	34063	33305	32990	31032	1.19
Run 2	25		24.87	36083	35520	35181	34714	34026	33483	32756	32550	30721	1.12
Run 3	23		32.61	36005	35404	35184	34756	34027	33461	32760	32489	30720	1.02
Run 4	26		27.75	38193	37607	37251	36700	35772	35034	34292	33776	31715	1.17
Run 5	29		7.98	37926	37180	36893	36340	35460	34731	33919	33544	31540	1.29
Run 6	29		8.08	38123	37358	37071	36609	35686	34926	34196	33705	31780	1.31
Run 7	27		1.88	38011	37261	37048	36526	35681	34968	34048	33721	31792	1.20
Run 8	29		8.81	38854	38046	37833	37326	36341	35581	34671	34249	32174	1.27
Run 9	29		15.14	38768	37990	37716	37174	36248	35531	34630	34241	32103	1.31
Run 10	32		12.70	39777	39006	38646	38111	37073	36295	35368	34855	32617	1.41
Run 11	31		7.56	39687	38983	38588	38036	37016	36275	35294	34801	32622	1.37
Run 12	34		17.59	40347	39482	39148	38501	37457	36581	35761	35162	32785	1.49
Run 13	33		8.72	40314	39514	39126	38491	37423	36626	35627	35212	32832	1.48
Run 14	35		8.71	41378	40547	40125	39476	38383	37474	36425	35931	33426	1.56
Run 15	36		13.88	41322	40418	40038	39428	38342	37450	36386	35932	33347	1.60
Run 16	38		9.93	41777	40774	40427	39776	38616	37702	36649	36124	33515	1.68
Run 17	42		1.58	41549	40479	40034	39339	38181	37303	36164	35715	33075	1.89
Run 18	37		6.65	41118	40160	39803	39112	38132	37053	36048	35464	32961	1.64
Run 19	41		14.64	44267	43227	42814	42030	40692	39625	38394	37707	34648	1.81
Run 20	44		6.98	44185	43130	42632	41915	40532	39545	38298	37610	34666	1.94
Run 21	45		7.67	45378	44302	43776	42950	41465	40364	39023	38341	35127	2.00
Run 22	56		8.10	47024	45610	45019	44096	42273	41105	39672	38888	35088	2.50
Run 23	52		1.28	46565	45290	44726	43795	42158	40847	39254	38599	35028	2.29
Run 24	60		4.57	48918	47487	46786	45754	43877	42446	40702	39800	35693	2.66
Run 25	57		5.02	48477	47091	46457	45210	43282	41981	40292	39504	35380	2.52
Run 26	68		1.10	51061	49392	48626	47555	45245	43793	41877	40836	36413	3.03
Run 27	69		1.68	50888	49245	48437	47208	44877	43553	41618	40731	36174	3.05
Run 28	68		4.76	53193	51549	50781	49566	46920	45448	43434	42292	37413	3.00
Run 29	67		11.94	53246	51651	50870	49769	47244	45582	43690	42637	37468	2.96
Run 30	75		7.53	54772	53005	52083	51181	48618	46915	44988	43898	38739	3.35
Run 31	76		-0.28	56294	54670	53600	52165	49108	47243	44892	43736	38258	3.36
Run 32	73		3.13	55524	53731	52925	51497	48585	46808	44587	43424	38008	3.24

CMC 5%

CMC 5% in 40 mm valve, 100% open

Date:	22/10/2004	
Valve Type:	Diaphragm	
Valve dimension[m]:	0.04	
Valve position:	Open	Area[m^2]
Pipe Diameter [m]:	0.04212	0.00139337

Material Type:	CMC
Density[kg/m^3]:	1029
Concentration:	0.05
τ_y:	0
K:	0.204
n:	0.7924
PPT used:	101
Range selected:	0-130

			Axial distances [m]	-5.7395	-3.865	-2.885	-0.937	0.987	2.938	6.427	8.432	10.433
			Valve plane									
			Non-dim distances [L/D]:	-136.2654321	-91.76163343	-68.49477683	-22.24596391	23.43304843	69.75308642	152.5878443	200.1899335	247.697056
			Distances[m]:	0	1.8745	2.8545	4.8025	6.7265	8.6775	12.1665	14.1715	16.1725
Run #	Re_3		k_v	PTT 1	PTT 2	PTT 3	PTT 4	PTT 5	PTT 6	PTT 7	PTT 8	PTT 9
				[Pa]	[Pa]	[Pa]	[Pa]	[Pa]	[Pa]	[Pa]	[Pa]	[Pa]
Run 1	19		84.41	26854	26614	26312	26170	25852	25651	25208	24965	24730
Run 2	23		85.22	27208	26938	26546	26386	26006	25786	25298	25025	24750
Run 3	25		43.87	27304	27060	26637	26484	26108	25854	25349	25048	24759
Run 4	27		42.23	27551	27265	26838	26614	26213	25973	25412	25081	24770
Run 5	27		41.62	27549	27260	26814	26616	26233	25941	25412	25074	24770
Run 6	66		23.81	30048	29504	28714	28303	27555	27059	26062	25451	24887
Run 7	66		21.53	29978	29491	28711	28275	27573	27055	26055	25459	24889
Run 8	104		15.83	32004	31332	30233	29637	28599	27938	26562	25741	24957
Run 9	140		14.26	33772	32919	31559	30902	29447	28643	26983	25957	25013
Run 10	140		12.80	33715	32876	31539	30915	29490	28663	26983	25959	25011
Run 11	206		13.35	36570	35496	33704	32955	30821	29774	27608	26309	25090
Run 12	253		12.44	38529	37300	35296	34432	31717	30480	28038	26530	25140
Run 13	254		13.49	38583	37335	35398	34413	31671	30510	28016	26534	25139
Run 14	307		11.85	40497	39137	36932	35828	32607	31219	28441	26762	25184
Run 15	354		11.88	42240	40705	38208	37098	33306	31819	28729	26879	25164
Run 16	354		11.72	42192	40713	38330	36966	33297	31809	28736	26888	25179
Run 17	404		11.64	44117	42432	39757	38483	34025	32421	29090	27080	25210
Run 18	404		11.54	44147	42403	39784	38490	33987	32394	29094	27098	25206
Run 19	483		11.73	47003	45124	42192	40706	35088	33354	29591	27346	25272
Run 20	548		11.84	49376	47259	44040	42492	35876	33963	29935	27554	25280
Run 21	528		11.42	48664	46586	43485	41954	35680	33795	29887	27519	25302
Run 22	588		11.34	50796	48622	45270	43616	36497	34441	30243	27714	25345
Run 23	589		11.41	50800	48654	45253	43726	36459	34462	30238	27709	25346
Run 24	752		10.87	56673	54057	50129	48272	38468	36184	31197	28250	25466
Run 25	751		11.12	56677	54105	50162	48267	38543	36142	31165	28235	25466
Run 26	815		10.87	58834	56088	51974	50091	39147	36684	31487	28394	25494
Run 27	815		10.57	58780	56111	51980	50037	39247	36769	31538	28412	25498
Run 28	867		10.61	60682	57852	53634	51681	39911	37305	31792	28574	25534
Run 29	867		10.82	60829	58046	53664	51641	39814	37216	31824	28585	25571
Run 30	933		10.46	62992	60181	55646	53488	40703	37855	32166	28776	25601
Run 31	932		10.35	62957	60147	55763	53493	40633	37836	32165	28752	25582
Run 32	989		10.35	64895	61953	57286	54985	41095	38312	32451	28927	25664

CMC 5% in 40 mm valve, 100% open (continued)

Date:	22/10/2004	
Valve Type:	Diaphragm	
Valve dimension[m]:	0.04	
Valve position:	Open	Area[m^2]
Pipe Diameter [m]:	0.04212	0.00139337

Material Type:	CMC
Density[kg/m^3]:	1029
Concentration:	0.05
τ_y:	0
K:	0.204
n:	0.7924
PPT used:	101
Range selected:	0-130

			Axial distances [m]	-5.7395	-3.865	-2.885	-0.937	0.987	2.938	6.427	8.432	10.433	
			Valve plane										
			Non-dim distances [L/D]:	-136.2654321	-91.76163343	-68.49477683	-22.24596391	23.43304843	69.75308642	152.5878443	200.1899335	247.697056	
			Distances[m]:	0	1.8745	2.8545	4.8025	6.7265	8.6775	12.1665	14.1715	16.1725	
Run #	Re_3		k_v	PTT 1	PTT 2	PTT 3	PTT 4	PTT 5	PTT 6	PTT 7	PTT 8	PTT 9	Average Q
				[Pa]	[Pa]	[Pa]	[Pa]	[Pa]	[Pa]	[Pa]	[Pa]	[Pa]	[l/s]
Run 33	988		10.48	65134	62055	57325	55119	41178	38304	32441	28906	25627	2.02
Run 34	1038		10.44	66804	63627	58828	56642	41941	38803	32625	29013	25632	2.10
Run 35	1038		10.35	66700	63632	58825	56517	41706	38723	32579	29109	25574	2.10
Run 36	1107		10.46	69164	65802	60761	58412	42376	39189	32897	29180	25688	2.21
Run 37	1107		10.32	69009	65728	60777	58366	42324	39164	32915	29156	25698	2.21
Run 38	1169		10.25	71147	67821	62741	60237	42962	39687	33202	29355	25766	2.32
Run 39	1171		10.11	71166	67747	62703	60230	42927	39684	33217	29351	25733	2.32
Run 40	1219		10.01	72794	69510	64094	61603	43398	40102	33453	29441	25764	2.40
Run 41	1218		10.01	72793	69477	64062	61670	43429	40064	33490	29470	25810	2.40
Run 42	1291		9.89	75283	71748	66139	63838	44113	40618	33749	29658	25797	2.51
Run 43	1291		9.90	75347	71686	66323	63721	44127	40663	33757	29633	25814	2.52
Run 44	1345		9.89	77326	73589	67883	65398	44693	41048	33961	29759	25807	2.60
Run 45	1345		9.93	77261	73523	67896	65295	44669	41046	33945	29780	25832	2.60
Run 46	1406		9.69	79522	75808	69924	67285	45275	41582	34263	29894	25799	2.70
Run 47	1406		9.81	79502	75777	69994	67206	45279	41581	34210	29881	25816	2.70
Run 48	1470		9.81	82059	78270	72074	69311	45914	42008	34520	29992	25859	2.80
Run 49	1471		9.73	81976	78024	72170	69454	45998	42031	34553	30078	25907	2.80
Run 50	1528		9.81	84417	80248	74330	71377	46596	42507	34798	30228	25952	2.89
Run 51	1528		9.87	84435	80475	74219	71546	46586	42541	34793	30184	25941	2.89
Run 52	1617		9.69	87507	83274	77098	74027	47337	43143	35096	30367	25937	3.03
Run 53	1617		9.76	87460	83296	77011	73910	47164	42892	34816	30036	25625	3.03
Run 54	1658		9.61	88831	84514	78024	75179	47641	43423	35266	30358	25972	3.09
Run 55	1659		9.48	88721	84277	77819	74961	47416	43106	35265	30120	25908	3.10
Run 56	1729		9.22	91557	87237	80624	77327	48225	43539	35519	30270	25653	3.20
Run 57	1728		9.35	91359	87063	80248	77470	48246	43615	35525	30372	25816	3.20

CMC 5% in 50 mm valve, 100% open

Date:	22/10/2004	
Valve Type:	Diaphragm	
Valve dimension[m]:	0.04	
Valve position:	Open	Area[m^2]
Pipe Diameter [m]:	0.04212	0.00139337

Material Type:	CMC
Density[kg/m^3]:	1029
Concentration:	0.05
τ_y:	**0**
K:	**0.204**
n:	**0.7924**
PPT used:	101
Range selected:	0-130

			Axial distances [m]	-5.7395	-3.865	-2.885	-0.937	0.987	2.938	6.427	8.432	10.433
			Valve plane									
			Non-dim distances [L/D]:	-136.2654321	-91.76163343	-68.49477683	-22.24596391	23.43304843	69.75308642	152.5878443	200.1899335	247.697056
			Distances[m]:	0	1.8745	2.8545	4.8025	6.7265	8.6775	**12.1665**	14.1715	16.1725
Run #	Re_3		k_v	PTT 1	PTT 2	PTT 3	PTT 4	PTT 5	PTT 6	PTT 7	PTT 8	PTT 9
				[Pa]	[Pa]	[Pa]	[Pa]	[Pa]	[Pa]	[Pa]	[Pa]	[Pa]
Run 1	9		24.08	25572	25406	25352	25281	25167	25053	24909	24805	24697
Run 2	9		39.18	25582	25390	25356	25274	25153	25067	24904	24805	24692
Run 3	12		74.01	25847	25634	25541	25468	25343	25206	24999	24884	24741
Run 4	12		21.85	25852	25650	25557	25469	25321	25207	25006	24871	24736
Run 5	15		63.46	26116	25853	25769	25634	25434	25329	25083	24923	24769
Run 6	18		26.18	26279	26004	25887	25784	25572	25408	25153	24975	24799
Run 7	18		42.46	26270	25997	25893	25753	25563	25409	25145	24979	24799
Run 8	26		16.02	26758	26412	26288	26100	25837	25633	25298	25065	24837
Run 9	27		29.40	26768	26400	26268	26084	25827	25638	25292	25069	24837
Run 10	33		17.04	27105	26673	26534	26346	26026	25791	25400	25133	24867
Run 11	74		9.99	28862	28169	27868	27561	26980	26580	25905	25445	24987
Run 12	90		8.56	29448	28623	28322	27929	27293	26828	26063	25545	25017
Run 13	117		4.40	30309	29385	28984	28500	27762	27233	26319	25693	25063
Run 14	142		4.85	31047	29957	29554	29003	28162	27535	26515	25811	25107
Run 15	176		3.81	32002	30737	30239	29645	28664	27950	26779	25959	25152
Run 16	176		4.09	31979	30769	30256	29646	28672	27948	26771	25960	25152
Run 17	220		3.65	33073	31677	31130	30385	29201	28444	27057	26144	25200
Run 18	220		3.04	33068	31668	31097	30404	29239	28413	27066	26124	25195
Run 19	257		2.84	33980	32417	31764	30967	29704	28812	27313	26279	25243
Run 20	257		2.80	34011	32408	31798	31020	29728	28812	27321	26282	25244
Run 21	269		2.35	34209	32629	31962	31148	29852	28934	27386	26326	25255
Run 22	298		2.81	34837	33145	32458	31640	30181	29185	27529	26398	25276
Run 23	331		2.23	35544	33710	32999	32123	30501	29461	27742	26536	25324
Run 24	364		2.63	36311	34283	33520	32565	30841	29781	27908	26632	25339
Run 25	363		2.61	36224	34290	33514	32571	30852	29771	27896	26617	25346
Run 26	404		2.53	37066	34960	34085	33077	31260	30110	28121	26757	25395
Run 27	402		2.81	36997	34957	34046	33100	31258	30074	28088	26735	25388
Run 28	434		1.77	37574	35474	34595	33528	31574	30345	28277	26859	25399
Run 29	434		1.91	37595	35467	34584	33516	31561	30330	28281	26844	25408

CMC 5% in 50 mm valve, 100% open (continued)

Date:	22/10/2004	
Valve Type:	Diaphragm	
Valve dimension[m]:	0.04	
Valve position:	Open	Area[m^2]
Pipe Diameter [m]:	0.04212	0.00139337

Material Type:	CMC
Density[kg/m^3]:	1029
Concentration:	0.05
τ_y:	0
K:	0.204
n:	0.7924
PPT used:	101
Range selected:	0-130

			Axial distances [m]	-5.7395	-3.865	-2.885	-0.937	0.987	2.938	6.427	8.432	10.433	
			Valve plane										
			Non-dim distances [L/D]:	-136.2654321	-91.76163343	-68.49477683	-22.24596391	23.43304843	69.75308642	152.5878443	200.1899335	247.697056	
			Distances[m]:	0	1.8745	2.8545	4.8025	6.7265	8.6775	12.1665	14.1715	16.1725	
Run #	Re_3		k_v	PTT 1	PTT 2	PTT 3	PTT 4	PTT 5	PTT 6	PTT 7	PTT 8	PTT 9	Average Q
				[Pa]	[Pa]	[Pa]	[Pa]	[Pa]	[Pa]	[Pa]	[Pa]	[Pa]	[l/s]
Run 30	474		1.89	38315	36085	35173	34029	31945	30653	28476	26960	25455	1.61
Run 31	474		2.10	38398	36067	35140	34073	31959	30663	28466	26969	25437	1.61
Run 32	511		2.64	39078	36651	35673	34482	32318	30948	28608	27072	25484	1.72
Run 33	511		2.27	39103	36671	35708	34486	32319	30934	28639	27062	25478	1.72
Run 34	556		2.33	39873	37348	36313	35021	32722	31288	28828	27182	25518	1.84
Run 35	556		2.03	39829	37337	36283	35020	32707	31294	28839	27178	25511	1.84
Run 36	588		2.17	40396	37739	36711	35462	32988	31520	28977	27279	25555	1.93
Run 37	588		2.21	40443	37764	36680	35405	32976	31509	28972	27272	25538	1.93
Run 38	617		1.85	40740	38130	36980	35711	33131	31657	29056	27284	25520	2.01
Run 39	618		2.05	40770	38085	36950	35688	33137	31628	29044	27277	25524	2.01
Run 40	664		1.87	41531	38817	37579	36297	33506	31968	29244	27396	25547	2.13
Run 41	664		1.95	41595	38773	37638	36241	33518	31941	29242	27395	25543	2.13
Run 42	689		2.01	42074	39096	37957	36523	33690	32077	29352	27461	25564	2.20
Run 43	689		2.01	41999	39146	37959	36511	33663	32108	29341	27460	25570	2.20
Run 44	823		2.39	44537	41271	39958	38430	34955	33001	29905	27833	25698	2.54
Run 45	824		2.12	44514	41208	40010	38462	34979	33046	29933	27793	25685	2.55
Run 46	1030		2.30	47949	44232	42720	40955	36518	34259	30661	28254	25804	3.06
Run 47	1031		2.31	47944	44261	42730	40935	36548	34253	30644	28246	25786	3.06
Run 48	1134		2.15	49453	45618	44086	42124	37215	34842	31014	28434	25852	3.31
Run 49	1134		2.22	49564	45705	44047	42099	37215	34899	31038	28471	25871	3.31

CMC 5% in 65 mm valve, 100%

Date:	26/10/2004	
Valve Type:	Diaphragm	
Valve dimension[m]:	0.06	
Valve position:	1	Area[m^2]
Pipe Diameter [m]:	0.06308	0.003125167

Material Type:	CMC 5%
Density[kg/m^3]:	1026.5
Concentration:	0.0468
τ_y:	0
K:	0.380
n:	0.6877
PPT used:	101
Range selected:	0-130

		Axial distances [m]	-5.7395	-3.865	-2.885	-0.937	0.987	2.938	6.427	8.432	10.433	
		Valve plane										
		Non-dim distances [L/D]:	-90.98763475	-61.2714014	-45.73557387	-14.85415346	15.64679772	46.57577679	101.8864933	133.6715282	165.3931516	
		Distances[m]:	0	1.8745	2.8545	4.8025	6.7265	8.6775	**12.1665**	14.1715	16.1725	
Run #	Re_3		k_v	PTT 1	PTT 2	PTT 3	PTT 4	PTT 5	PTT 6	PTT 7	PTT 8	PTT 9	Average Q
				[Pa]	[Pa]	[Pa]	[Pa]	[Pa]	[Pa]	[Pa]	[Pa]	[Pa]	[l/s]
Run 1	309		0.37	33105	31721	31247	30419	29341	28400	27109	26253	25333	1.56
Run 2	334		0.07	33170	31786	31382	30437	29389	28465	27145	26259	25350	1.65
Run 3	359		0.42	33569	32033	31616	30692	29545	28608	27231	26314	25360	1.74
Run 4	360		0.14	33470	32051	31534	30673	29575	28636	27232	26324	25373	1.74
Run 5	395		0.33	33977	32468	32020	31016	29779	28847	27376	26376	25420	1.87
Run 6	395		0.83	34060	32526	31975	30959	29811	28820	27357	26397	25399	1.87
Run 7	413		0.04	34175	32595	32154	31113	29869	28923	27443	26443	25436	1.94
Run 8	413		0.26	34190	32599	32120	31184	29927	28885	27448	26403	25444	1.94
Run 9	468		0.35	34861	33207	32668	31642	30239	29186	27603	26577	25463	2.13
Run 10	469		0.16	34913	33188	32660	31633	30268	29203	27662	26579	25506	2.14
Run 11	514		0.22	35531	33684	33180	32040	30661	29470	27828	26694	25547	2.29
Run 12	516		0.91	35579	33691	33178	32091	30640	29500	27815	26702	25574	2.30
Run 13	583		0.82	36306	34281	33726	32529	30999	29807	28030	26852	25642	2.52
Run 14	584		0.22	36283	34315	33709	32666	31026	29851	28031	26873	25592	2.52
Run 15	626		0.02	36795	34830	34083	32843	31297	30063	28231	26940	25668	2.66
Run 16	627		0.25	36719	34857	34214	32880	31300	30080	28214	26932	25695	2.67
Run 17	708		0.48	37676	35576	34825	33520	31754	30461	28472	27115	25781	2.92
Run 18	706		0.33	37625	35391	34802	33492	31771	30451	28444	27176	25755	2.92
Run 19	768		0.32	38221	36012	35335	33980	32080	30680	28635	27222	25818	3.11
Run 20	770		0.37	38262	36020	35357	33919	32078	30680	28632	27239	25813	3.12
Run 21	811		0.45	38575	36286	35596	34190	32290	30814	28725	27314	25857	3.24
Run 22	810		0.32	38579	36314	35609	34209	32272	30839	28725	27305	25835	3.24
Run 23	880		0.43	39310	36988	36221	34758	32677	31129	28942	27453	25924	3.45
Run 24	876		0.52	39339	36920	36195	34779	32663	31124	28935	27452	25925	3.44
Run 25	960		0.76	40301	37829	37030	35426	33205	31511	29156	27591	25988	3.69
Run 26	955		0.75	40236	37823	37050	35518	33159	31509	29160	27603	26008	3.67
Run 27	1032		0.53	41261	38735	37900	36344	33820	31879	29478	27813	26084	3.90
Run 28	1036		1.01	41341	38680	37889	36203	33785	31977	29418	27765	26098	3.91
Run 29	1075		1.10	41917	39178	38327	36570	34080	32151	29566	27851	26152	4.02
Run 30	1073		0.60	41751	39182	38300	36625	34077	32182	29597	27812	26108	4.01
Run 31	1179		1.06	43062	40146	39375	37455	34630	32555	29863	28085	26235	4.31
Run 32	1167		0.95	42990	40135	39332	37529	34612	32567	29863	28035	26214	4.28
Run 33	1335		1.00	44838	41654	40846	38873	35517	33248	30331	28398	26360	4.74
Run 34	1343		0.94	44753	41588	40815	38712	35622	33183	30344	28341	26378	4.76
Run 35	1372		1.12	45142	42063	41040	38955	35824	33473	30397	28434	26403	4.84
Run 36	1542		1.28	46651	43160	42352	40106	36558	34015	30745	28715	26568	5.29
Run 37	1544		0.94	46642	43269	42296	40171	36614	33932	30863	28674	26560	5.30
Run 38	1703		1.28	48127	44706	43553	41312	37533	34520	31161	29055	26753	5.71
Run 39	618		2.05	40770	38085	36950	35688	33137	31628	29044	27277	25524	2.01
Run 40	664		1.87	41531	38817	37579	36297	33506	31968	29244	27396	25547	2.13
Run 41	664		1.95	41595	38773	37638	36241	33518	31941	29242	27395	25543	2.13
Run 42	689		2.01	42074	39096	37957	36523	33690	32077	29352	27461	25564	2.20
Run 43	689		2.01	41999	39146	37959	36511	33663	32108	29341	27460	25570	2.20
Run 44	823		2.39	44537	41271	39958	38430	34955	33001	29905	27833	25698	2.54
Run 45	824		2.12	44514	41208	40010	38462	34979	33046	29933	27793	25685	2.55
Run 46	1030		2.30	47949	44232	42720	40955	36518	34259	30661	28254	25804	3.06
Run 47	1031		2.31	47944	44261	42730	40935	36548	34253	30644	28246	25786	3.06
Run 48	1134		2.15	49453	45618	44086	42124	37215	34842	31014	28434	25852	3.31
Run 49	1134		2.22	49564	45705	44047	42099	37215	34899	31038	28471	25871	3.31

CMC 5% in 80 mm valve, 100% open

Date:	27/10/2004	
Valve Type:	Diaphragm	
Valve dimension[m]:	0.08	
Valve position:	1	Area[m^2]
Pipe Diameter [m]:	0.08043	0.005080729

Material Type:	CMC 5%
Density[kg/m^3]:	1027
Concentration:	0.0478
τ_y:	0
K:	0.342
n:	0.7161
PPT used:	101
Range selected:	0-130

		Axial distances [m]	-5.7395	-3.865	-2.885	-0.937	0.987	2.938	6.427	8.432	10.433	
		Valve plane										
		Non-dim distances [L/D]:	-71.36018898	-48.05420863	-35.86970036	-11.64988188	12.27154047	36.52865846	79.90799453	104.8365038	129.7152804	
		Distances[m]:	0	1.8745	2.8545	4.8025	6.7265	8.6775	**12.1665**	14.1715	16.1725	
Run #	Re_3	k_v	PTT 1	PTT 2	PTT 3	PTT 4	PTT 5	PTT 6	PTT 7	PTT 8	PTT 9	Average Q
			[Pa]	[Pa]	[Pa]	[Pa]	[Pa]	[Pa]	[Pa]	[Pa]	[Pa]	[l/s]
Run 1	89	9.71	27481	27269	27110	26767	26405	25951	25674	25323	25128	0.84
Run 2	89	15.78	27492	27262	27148	26782	26396	25971	25668	25325	25136	0.84
Run 3	97	11.63	27625	27413	27247	26886	26481	26015	25707	25360	25130	0.90
Run 4	120	8.48	27991	27700	27529	27142	26673	26172	25804	25444	25190	1.07
Run 5	121	6.67	27982	27692	27522	27122	26679	26168	25817	25435	25187	1.07
Run 6	130	8.84	28159	27878	27693	27266	26768	26244	25867	25478	25207	1.13
Run 7	130	7.83	28140	27885	27670	27244	26747	26230	25875	25462	25214	1.14
Run 8	145	7.20	28421	28126	27924	27471	26959	26369	25978	25536	25256	1.23
Run 9	165	11.10	28631	28349	28144	27628	27071	26462	26018	25594	25295	1.36
Run 10	150	6.61	28404	28094	27898	27452	26941	26325	25963	25537	25257	1.27
Run 11	173	5.98	28759	28467	28205	27722	27129	26504	26084	25609	25298	1.42
Run 12	208	6.80	29207	28830	28624	28060	27360	26693	26222	25702	25380	1.64
Run 13	223	5.80	29402	29023	28788	28221	27486	26794	26305	25759	25417	1.72
Run 14	248	6.37	29699	29358	29117	28515	27704	26939	26433	25858	25443	1.87
Run 15	250	4.76	29740	29332	29089	28480	27683	26958	26430	25839	25454	1.88
Run 16	269	4.69	30013	29590	29297	28663	27809	27047	26505	25845	25513	2.00
Run 17	305	6.35	30514	30101	29803	29136	28119	27220	26635	25998	25546	2.20
Run 18	337	5.11	30807	30346	29993	29316	28237	27281	26733	26026	25643	2.38
Run 19	386	5.13	31337	30875	30475	29782	28554	27554	26901	26115	25726	2.65
Run 20	439	4.21	31889	31408	30970	30191	28814	27768	27094	26252	25765	2.93
Run 21	439	5.35	31931	31376	31058	30254	28846	27758	27074	26310	25794	2.93
Run 22	469	4.74	32175	31599	31215	30405	29016	27850	27121	26275	25823	3.08
Run 23	470	3.87	32181	31550	31237	30417	29033	27878	27202	26354	25845	3.09
Run 24	508	4.24	32567	31955	31562	30726	29224	28045	27286	26389	25915	3.28
Run 25	507	4.38	32595	32014	31582	30724	29152	28011	27269	26402	25889	3.27
Run 26	531	4.33	32774	32269	31748	30926	29277	28097	27346	26467	25927	3.39
Run 27	627	3.76	33721	33037	32598	31696	29797	28489	27632	26659	26046	3.86
Run 28	625	3.81	33645	33020	32544	31616	29842	28434	27640	26680	26068	3.85
Run 29	670	3.38	34149	33478	32968	32077	30108	28618	27804	26760	26116	4.07
Run 30	671	3.75	34138	33464	32981	32051	30126	28623	27778	26775	26134	4.07
Run 31	720	4.03	34883	34123	33643	32625	30495	28909	27977	26951	26272	4.30
Run 32	725	3.54	34839	34151	33622	32586	30469	28932	28031	26947	26228	4.33
Run 33	806	4.00	35709	34977	34409	33314	30907	29260	28251	27125	26431	4.70
Run 34	871	4.30	36351	35623	34991	33831	31282	29439	28378	27251	26540	4.99
Run 35	871	3.61	36357	35552	34994	33800	31287	29483	28484	27236	26516	4.99
Run 36	959	3.61	37142	36327	35732	34511	31702	29763	28721	27447	26649	5.38
Run 37	1025	3.88	37842	37049	36401	35106	32073	30000	28889	27573	26761	5.66
Run 38	1078	3.75	38402	37552	36888	35552	32299	30254	29077	27710	26889	5.89
Run 39	1080	3.86	38385	37576	36910	35586	32327	30168	29077	27727	26894	5.90
Run 40	1142	3.64	38980	38112	37401	36048	32622	30422	29241	27857	26978	6.16
Run 41	1143	3.93	38781	38104	37371	36061	32638	30410	29252	27815	26987	6.16

CMC 5% in 100 mm valve, 75 % open

Date:	13/06/2005	
Valve Type:	Diaphragm	
Valve dimension[m]:	0.1	
Valve position:	¾ Open	Area[m^2]
Pipe Diameter [m]:	0.09717	0.007415736

Material Type:	CMC 5%
Density[kg/m^3]:	1020.3
Concentration:	0.05
τ_y:	0
K:	0.624
n:	0.7662
PPT used:	105
Range selected:	0-130

		Axial distances [m]	-5.7395	-3.865	-2.885	-0.937	0.987	2.938	6.427	8.432	10.433
		Valve plane									
		Non-dim distances [L/D]:	-59.06658434	-39.77565092	-29.69023361	-9.642893897	10.157456	30.23566945	66.14181332	86.77575383	107.3685294
		Distances[m]:	0	1.8745	2.8545	4.8025	6.7265	8.6775	12.1665	14.1715	16.1725
Run #	Re_3		k_v	PTT 1	PTT 2	PTT 3	PTT 4	PTT 5	PTT 6	PTT 7	PTT 8	PTT 9	Average Q
				[Pa]	[Pa]	[Pa]	[Pa]	[Pa]	[Pa]	[Pa]	[Pa]	[Pa]	[l/s]
Run 1	345		10.01	41139	39966	38886	38094	33598	33459	32916	31564	30833	6.02
Run 2	346		10.03	41185	39941	38983	38076	33695	33560	32986	31627	30939	6.03
Run 3	332		11.09	40723	39454	38530	37646	33340	33174	32609	31276	30660	5.84
Run 4	332		10.55	40631	39359	38426	37618	33310	33236	32615	31255	30634	5.84
Run 5	323		10.80	40387	39242	38269	37455	33229	33121	32508	31220	30534	5.71
Run 6	323		11.17	40301	39155	38189	37403	33141	33028	32410	31129	30487	5.72
Run 7	308		10.82	39646	38526	37567	36795	32781	32670	32095	30822	30161	5.49
Run 8	307		11.15	39561	38465	37526	36772	32774	32572	32069	30838	30197	5.48
Run 9	298		11.19	39239	38115	37173	36429	32576	32444	31931	30685	30083	5.35
Run 11	286		11.97	38855	37676	36719	35871	32351	32211	31681	30485	29888	5.17
Run 12	285		11.43	38732	37688	36782	36030	32283	32204	31694	30469	29900	5.16
Run 13	276		11.07	38161	37115	36205	35424	32064	31950	31446	30292	29684	5.03
Run 14	276		10.93	38156	37031	36161	35471	32007	31946	31466	30302	29708	5.02
Run 15	262		11.23	37548	36408	35590	34865	31744	31646	31149	30034	29459	4.82
Run 16	262		11.98	37727	36548	35616	34838	31690	31619	31164	30024	29471	4.82
Run 17	245		11.64	36905	35893	35055	34396	31392	31269	30832	29719	29204	4.56
Run 18	245		11.82	36901	35827	34946	34324	31345	31260	30816	29732	29197	4.57
Run 19	228		10.55	35828	34995	34246	33542	30915	30762	30392	29409	28836	4.30
Run 20	228		9.91	35876	35079	34263	33585	30941	30817	30416	29379	28799	4.30
Run 21	217		12.66	35707	34745	33948	33327	30701	30560	30187	29193	28687	4.13
Run 22	217		11.99	35593	34655	33938	33299	30560	30579	30163	29166	28661	4.13
Run 23	206		13.37	35247	34285	33523	32851	30348	30332	29919	28952	28482	3.96
Run 24	206		11.84	35226	34368	33566	32966	30405	30326	30001	28999	28505	3.97
Run 25	191		11.96	34454	33551	32892	32240	29922	29875	29570	28651	28146	3.73
Run 27	180		12.53	33884	33033	32330	31681	29635	29591	29266	28382	27920	3.55

CMC 5% in 100 mm valve, 75 % open (continued)

Date:	13/06/2005
Valve Type:	Diaphragm
Valve dimension[m]:	0.1
Valve position:	¾ Open
Pipe Diameter [m]:	0.09717

Area[m^2]
0.007415736

Material Type:	CMC 5%
Density[kg/m^3]:	1020.3
Concentration:	0.05
τ_y:	0
K:	0.624
n:	0.7662
PPT used:	105
Range selected:	0-130

Axial distances [m]	-5.7395	-3.865	-2.885	-0.937	0.987	2.938	6.427	8.432	10.433
Valve plane									
Non-dim distances [L/D]:	-59.06658434	-39.77565092	-29.69023361	-9.642893897	10.157456	30.23566945	66.14181332	86.77575383	107.3685294
Distances[m]:	0	1.8745	2.8545	4.8025	6.7265	8.6775	12.1665	14.1715	16.1725

Run #	Re_3		k_v	PTT 1	PTT 2	PTT 3	PTT 4	PTT 5	PTT 6	PTT 7	PTT 8	PTT 9	Average Q
				[Pa]	[Pa]	[Pa]	[Pa]	[Pa]	[Pa]	[Pa]	[Pa]	[Pa]	[l/s]
Run 29	168		12.06	33409	32489	31964	31385	29366	29341	28997	28120	27669	3.36
Run 30	168		15.07	33426	32554	31929	31322	29284	29285	28911	28121	27662	3.36
Run 31	158		14.26	32968	32208	31508	30956	29116	29046	28725	27910	27488	3.20
Run 32	157		13.57	32892	32085	31444	30938	29043	29043	28707	27888	27468	3.19
Run 33	145		13.38	32273	31529	30880	30465	28738	28664	28378	27522	27195	2.99
Run 34	144		15.43	32265	31512	30905	30435	28701	28664	28338	27532	27210	2.97
Run 35	136		15.47	31883	31125	30560	30082	28442	28405	28118	27405	27002	2.83
Run 36	134		14.65	31857	31279	30586	30061	28530	28399	28147	27368	27008	2.80
Run 37	122		18.35	31489	30737	30333	29932	28101	28070	27857	27150	26812	2.59
Run 39	111		25.00	31151	30500	29950	29526	27604	27644	27449	26795	26441	2.41
Run 41	100		27.86	30633	29888	29497	29079	27404	27366	27150	26530	26215	2.21
Run 42	100		27.63	30617	30004	29523	29110	27360	27362	27148	26523	26202	2.21
Run 43	85		31.13	29752	29175	28745	28381	26918	26920	26703	26188	25865	1.94
Run 44	85		27.81	29720	29189	28778	28314	26938	26920	26716	26144	25845	1.93
Run 45	76		24.40	29093	28631	28217	27877	26549	26506	26384	25848	25521	1.76
Run 47	68		30.33	28794	28260	27915	27579	26392	26388	26195	25671	25408	1.62
Run 48	68		29.95	28770	28274	27933	27594	26402	26379	26200	25707	25417	1.62
Run 49	60		38.73	28222	27732	27411	27148	26059	26044	25861	25449	25178	1.45
Run 50	60		37.15	28198	27737	27423	27130	26041	26044	25862	25434	25177	1.45
Run 51	51		40.10	27610	27193	26928	26640	25748	25676	25547	25133	24936	1.29
Run 52	51		31.37	27548	27129	26904	26640	25725	25697	25522	25136	24865	1.29
Run 53	41		58.26	26933	26565	26309	26101	25386	25304	25135	24802	24632	1.06
Run 55	33		97.96	26355	26008	25816	25610	24962	24923	24705	24524	24309	0.90
Run 56	33		47.23	26365	26009	25822	25503	25005	24990	24874	24564	24395	0.90

CMC 8%

CMC 8% in 40 mm valve, 100% open

Date:	05/11/2004	
Valve Type:	Diaphragm	
Valve dimension[m]:	0.4	
Valve position:	Open	Area[m^2]
Pipe Diameter [m]:	0.04212	0.00139337

Material Type:	CMC 8%
Density[kg/m^3]:	0.08
Concentration:	1040
τ_y:	0
K:	8.906
n:	0.415
PPT used:	105
Range selected:	0-130

		Axial distances [m]	-5.7395	-3.865	-2.885	-0.937	0.987	2.938	6.427	8.432	10.433	
		Valve plane										
		Non-dim distances [L/D]:	-136.2654321	-91.76163343	-68.49477683	-22.24596391	23.43304843	69.75308642	152.5878443	200.1899335	247.697056	
		Distances[m]:	0	1.8745	2.8545	4.8025	6.7265	8.6775	12.1665	14.1715	16.1725	
Run #	Re_3	k_v	PTT 1	PTT 2	PTT 3	PTT 4	PTT 5	PTT 6	PTT 7	PTT 8	PTT 9	Average Q
			[Pa]	[Pa]	[Pa]	[Pa]	[Pa]	[Pa]	[Pa]	[Pa]	[Pa]	[l/s]
Run 1	27	21.07	0	8925	23055	29875	41360	49256	66367	77041	86878	0.59
Run 2	28	34.59	0	9483	23168	29726	41198	49378	66676	76555	86308	0.60
Run 3	29	21.64	0	9571	23455	30032	41650	49886	67319	77929	87870	0.61
Run 4	29	27.24	0	9490	23279	30224	41953	49909	67397	78118	87816	0.62
Run 5	36	25.61	0	10605	25321	32567	45131	53747	72998	84485	94738	0.70
Run 6	36	26.63	0	10221	25206	32499	44582	54250	72706	84469	94361	0.71
Run 7	39	16.58	0	10457	25933	33462	45571	55830	74341	86067	97018	0.74
Run 8	39	22.38	0	10207	25075	33358	46124	54800	74437	85803	97308	0.74
Run 9	45	23.30	0	10950	27297	34914	48345	57580	78059	90402	100889	0.81
Run 10	45	12.08	0	10780	26731	34381	47941	58168	77976	89554	102272	0.81
Run 11	56	21.27	0	11581	28995	37269	52226	62571	84766	97960	109795	0.93
Run 12	56	18.87	0	12150	28706	37262	52310	62733	84363	97417	109618	0.93
Run 13	71	14.02	0	12327	29750	38234	54007	64964	87322	100553	113530	1.08
Run 14	71	16.44	0	12493	29674	38221	54200	64899	87237	100891	113061	1.08
Run 15	77	14.75	0	12313	30539	39290	55756	67083	90089	103655	116929	1.14
Run 16	77	13.09	0	12100	30590	39284	55625	66991	89757	103630	116764	1.14
Run 17	88	12.55	0	12914	31974	41086	58823	70313	94553	108800	122920	1.24
Run 18	94	13.18	0	12399	32451	41662	58718	70162	94447	108832	122008	1.29
Run 19	105	13.57	0	12455	32260	41562	60899	72568	97402	112557	126356	1.38
Run 20	105	14.77	0	12467	32339	41580	61056	72888	97869	112258	126514	1.39
Run 21	124	13.71	0	13288	34187	44056	65450	77823	104394	120290	134924	1.54
Run 22	125	12.72	0	13283	34105	44106	65492	77757	104295	120000	135163	1.54
Run 23	133	13.64	0	13478	34934	45098	67016	80087	107197	123452	138399	1.61
Run 24	133	14.34	0	13370	34661	45020	66997	79876	107141	123299	138261	1.61

CMC 8% in 40 mm valve, 100% open

Date:	12/11/2004	
Valve Type:	Diaphragm	
Valve dimension[m]:	0.04	
Valve position:	Open	Area[m^2]
Pipe Diameter [m]:	0.04212	0.00139337

Material Type:	CMC 8%
Density[kg/m^3]:	1040
Concentration:	0.08
τ_y:	0
K:	3.552
n:	0.6147
PPT used:	105
Range selected:	0-130

			Axial distances [m]	-5.7395	-3.865	-2.885	-0.937	0.987	2.938	6.427	8.432	10.433	
			Valve plane										
			Non-dim distances [L/D]:	-136.2654321	-91.76163343	-68.49477683	-22.24596391	23.43304843	69.75308642	152.5878443	200.1899335	247.697056	
			Distances[m]:	0	1.8745	2.8545	4.8025	6.7265	8.6775	**12.1665**	14.1715	16.1725	
Run #	Re_3		k_v	PTT 1	PTT 2	PTT 3	PTT 4	PTT 5	PTT 6	PTT 7	PTT 8	PTT 9	Average Q
				[Pa]	[Pa]	[Pa]	[Pa]	[Pa]	[Pa]	[Pa]	[Pa]	[Pa]	[l/s]
Run 1	33		14.32	0	9052	24980	31600	42949	51672	69692	80269	90779	0.66
Run 2	34		12.92	0	8201	24830	32000	42385	51058	69342	80368	90600	0.67
Run 3	28		41.45	0	8159	21759	28752	39253	46759	63785	73546	82664	0.58
Run 4	28		32.58	0	8656	21451	28323	39230	46508	63476	73224	82826	0.59
Run 5	23		39.87	0	8482	20032	26955	36394	43584	58944	68070	76752	0.52
Run 6	24		37.72	0	8078	19849	25724	36415	43546	58836	68067	76880	0.52
Run 7	19		20.15	0	7578	18401	23536	33054	39357	52956	61730	69630	0.44
Run 8	19		53.44	0	7738	18214	23925	32241	39502	53384	62048	69394	0.44
Run 9	15		26.28	0	6969	17556	21006	29475	35418	48398	56033	62957	0.37
Run 10	15		17.41	0	6854	17536	21629	30164	35742	48112	55956	62763	0.37
Run 11	12		42.01	0	5869	15558	19238	26599	32236	43833	50666	57180	0.32
Run 12	12		94.02	0	5843	14811	19563	27060	32452	43920	50721	57072	0.32
Run 13	8		77.47	0	5002	12881	16476	22544	27046	36809	42405	47995	0.24
Run 14	8		42.36	0	5078	12917	16477	22547	27060	36694	42464	48124	0.24
Run 15	6		99.61	0	4480	10938	14019	19253	23198	31314	36231	40922	0.18
Run 16	6		133.41	0	4533	10828	14037	19233	23122	31356	36245	40884	0.18
Run 17	3		253.81	0	3266	7755	9925	13591	16354	22097	25529	28769	0.10
Run 18	3		228.79	0	3291	7770	9958	13586	16342	22097	25616	28805	0.10
Run 19	1		393.15	0	2315	5142	6478	8839	10648	14362	16603	18695	0.05
Run 20	1		429.76	0	2248	5133	6507	8845	10646	14372	16633	18719	0.05

CMC 8% in 50 mm valve, 100%open

Date:	08/11/2004	
Valve Type:	Diaphragm	
Valve dimension[m]:	0.05	
Valve position:	1	Area[m^2]
Pipe Diameter [m]:	0.0528	0.002189564

Material Type:	CMC 8%
Density[kg/m^3]:	0.08
Concentration:	1040
τ_y:	0
K:	4.952
n:	0.5407
PPT used:	105
Range selected:	0-130

		Axial distances [m]	-5.7395	-3.865	-2.885	-0.937	0.987	2.938	6.427	8.432	10.433	
		Valve plane										
		Non-dim distances [L/D]:	-108.7026515	-73.20075758	-54.64015152	-17.74621212	18.69318182	55.64393939	121.7234848	159.6969697	197.594697	
		Distances[m]:	0	1.8745	2.8545	4.8025	6.7265	8.6775	12.1665	14.1715	16.1725	
Run #	Re_3		k_v	PTT 1	PTT 2	PTT 3	PTT 4	PTT 5	PTT 6	PTT 7	PTT 8	PTT 9	Average Q
				[Pa]	[Pa]	[Pa]	[Pa]	[Pa]	[Pa]	[Pa]	[Pa]	[Pa]	[l/s]
Run 1	11		19.60	0	7751	10466	14929	19208	23577	30505	35466	40309	0.45
Run 2	11		10.68	0	7740	10460	14889	19218	23637	30311	35493	40173	0.45
Run 3	13		28.72	0	8258	11190	15780	20493	25217	32563	37721	42787	0.50
Run 4	13		16.72	0	8167	11143	15830	20475	25145	32405	37868	42869	0.50
Run 5	15		31.44	0	8847	11700	16641	21518	26418	34388	39748	45074	0.55
Run 6	15		26.99	0	8853	11723	16635	21524	26470	34297	39835	45041	0.55
Run 7	17		30.50	0	9580	12316	17384	22747	27884	36418	41861	47593	0.60
Run 8	17		24.57	0	9801	12362	17409	22757	27898	36327	41910	47509	0.60
Run 9	22		43.57	0	10724	13666	19113	25218	30903	40853	46429	52695	0.72
Run 10	22		42.74	0	10314	13635	19073	25194	30925	40710	46384	52683	0.72
Run 11	26		37.78	0	11646	14646	20448	27178	33197	43968	49842	56633	0.82
Run 12	26		38.72	0	10779	14637	20468	27126	33163	43719	49846	56559	0.82
Run 13	31		31.81	0	12235	15610	21829	29102	35365	46900	53042	60475	0.92
Run 14	31		26.19	0	12403	15618	21831	28904	35414	46647	53155	60395	0.92
Run 15	37		7.43	0	11842	16669	22960	31691	37830	48720	56663	64509	1.04
Run 16	37		4.49	0	12038	16655	22982	31668	37855	48596	56862	64525	1.04
Run 17	42		9.02	0	12303	17320	23862	32808	39326	50681	59162	66970	1.12
Run 18	42		4.73	0	12363	17291	23828	32763	39365	50583	59142	67189	1.12
Run 19	47		8.83	0	12897	18141	24884	34394	41368	53308	61950	70363	1.22
Run 20	47		8.52	0	12981	18163	24943	34403	41295	53265	62000	70295	1.22
Run 21	52		10.15	0	12951	18029	24563	34080	41085	53282	61631	70049	1.30
Run 22	52		10.36	0	12872	18106	24664	34132	41089	53361	61664	70116	1.30
Run 23	58		11.01	0	13432	18873	25800	35684	42957	55740	64445	73047	1.40
Run 24	58		9.13	0	13375	18778	25719	35469	42759	55542	64203	73065	1.40
Run 25	65		8.08	0	14184	19614	26944	37175	44776	58012	67183	76267	1.51
Run 26	65		9.39	0	14050	19602	26856	37110	44699	58060	67048	76160	1.51
Run 27	72		7.75	0	14828	20414	27950	38609	46616	60406	69920	79317	1.62
Run 28	72		7.01	0	14824	20461	27977	38493	46639	60530	70019	79619	1.62
Run 29	77		6.63	0	15548	21010	28751	39735	48059	62352	72107	81930	1.71
Run 30	77		5.78	0	15733	21076	28878	39686	48123	62296	72084	81904	1.70
Run 31	84		7.28	0	15834	21746	29944	41301	49659	64706	74541	84855	1.81
Run 32	84		5.96	0	15872	21871	29931	41069	49651	64521	74748	84834	1.81
Run 33	90		6.28	0	16322	22494	30741	42380	51189	66642	76831	87465	1.90
Run 34	90		5.17	0	16676	22426	30634	42447	51234	66472	77033	87457	1.90
Run 35	101		6.29	0	16971	23504	32091	44413	53654	69643	80429	91283	2.05
Run 36	101		4.30	0	18208	23405	32026	44347	53605	69639	80508	91473	2.05
Run 37	106		5.38	0	17427	24017	32811	45344	54915	71208	82358	93518	2.13
Run 38	106		5.41	0	17678	23917	32636	45147	54683	71053	82187	93234	2.12
Run 39	118		4.51	0	18620	24928	33998	47090	57164	74135	85755	97369	2.28
Run 40	106		5.41	0	17678	23917	32636	45147	54683	71053	82187	93234	2.12
Run 41	118		4.51	0	18620	24928	33998	47090	57164	74135	85755	97369	2.28
Run 42	118		4.76	0	18226	24957	34034	47148	57090	74028	85649	97226	2.28
Run 43	117		4.23	0	18815	24803	33845	46838	56728	73667	85231	96723	2.27
Run 44	127		3.86	0	19343	25607	34961	48344	58628	76009	87827	99803	2.40
Run 45	127		3.81	0	19435	25580	34864	48179	58585	75998	87904	99810	2.40

CMC 8% in 65 mm valve, 100% open

Date:	08/11/2004	
Valve Type:	Diaphragm	
Valve dimension[m]:	0.05	
Valve position:	1	Area[m^2]
Pipe Diameter [m]:	0.0528	0.002189564

Material Type:	CMC 8%
Density[kg/m^3]:	0.08
Concentration:	1040
τ_y:	0
K:	6.147
n:	0.5161
PPT used:	105
Range selected:	0-130

Axial distances [m]		-6.413	-4.809	-3.61	-1.209	0.707	3.907	5.977	8.461	9.956	
Valve plane											
Non-dim distances [L/D]:		-79.73393013	-59.79112272	-44.88374984	-15.03170459	8.790252393	48.57640184	74.31306726	105.1970658	123.7846575	
Distances[m]:		0	1.604	2.803	5.204	7.12	10.32	12.39	14.874	16.369	
Run #	Re_3	k_v	DP1	DP2	DP3	DP4	DP5	DP6	DP7	DP8	DP9	Average Q
			[Pa]	[Pa]	[Pa]	[Pa]	[Pa]	[Pa]	[Pa]	[Pa]	[Pa]	[l/s]
Run1	4	27.54	0	1722	2812	5080	7304	10304	12246	14566	15984	0.50
Run2	4	3.21	0	1741	2838	5062	7267	10278	12194	14513	15940	0.50
Run3	6	16.77	0	2039	3349	5960	8607	12234	14485	17195	18882	0.68
Run4	7	22.30	0	2116	3449	6189	8966	12756	15109	17946	19712	0.72
Run5	7	4.56	0	2070	3420	6136	8878	12642	14971	17909	19657	0.73
Run6	8	19.36	0	2252	3643	6727	9599	13511	16025	19085	20914	0.82
Run7	8	7.53	0	2275	3729	6634	9456	13376	16014	19047	20883	0.80
Run8	8	4.92	0	2272	3625	6545	9356	13303	15811	18855	20707	0.82
Run9	8	2.27	0	2237	3675	6569	9431	13362	15882	18955	20792	0.81
Run10	12	7.30	0	2623	4266	7660	11025	15607	18538	22070	24215	1.04
Run11	12	9.96	0	2550	4235	7623	10990	15562	18476	22025	24139	1.03
Run12	17	11.21	0	2917	4734	8577	12325	17498	20837	24806	27177	1.29
Run13	17	11.69	0	2950	4725	8583	12348	17365	20799	24806	27106	1.29
Run14	20	12.52	0	2973	4973	8948	12965	18424	21950	26057	28593	1.45
Run15	20	7.88	0	3074	4939	8991	12968	18374	21865	26037	28591	1.45
Run16	23	6.68	0	3184	5229	9581	13923	19658	23322	27861	30585	1.62
Run17	23	5.51	0	3098	5249	9592	13776	19610	23240	27674	30491	1.62
Run18	28	4.26	0	3419	5708	10170	14831	21085	24994	29776	32693	1.85
Run19	28	5.98	0	3417	5625	10282	14785	21006	25008	29775	32749	1.85
Run20	32	4.50	0	3574	5947	10709	15415	21904	26037	31089	34012	2.00
Run21	32	12.14	0	3674	5736	10671	15379	21850	26114	30864	33976	2.00
Run22	37	7.10	0	3639	6086	11293	16349	23161	27474	32778	35966	2.23
Run23	37	3.41	0	3759	6203	11238	16337	23095	27378	32704	35859	2.23
Run24	40	6.34	0	3687	6363	11570	16817	23952	28228	33703	36839	2.36
Run25	40	6.75	0	3729	6365	11510	16779	23788	28304	33629	36920	2.35
Run26	44	4.90	0	3943	6493	11738	17328	24451	29076	34781	38052	2.51
Run27	44	7.20	0	4012	6469	11851	17428	24526	29217	34659	38102	2.51
Run28	47	5.46	0	3930	6619	12074	17707	24895	29763	35277	38949	2.60
Run29	47	4.13	0	3986	6629	12151	17663	25015	29605	35420	38777	2.60
Run30	54	3.82	0	4563	7030	12672	18664	26373	31236	37182	40723	2.85
Run31	54	5.52	0	4239	6901	12708	18399	26156	31246	37087	40833	2.85
Run32	62	4.54	0	4342	7194	13200	19343	27355	32537	38794	42558	3.15
Run33	62	5.30	0	4351	7187	13194	19431	27475	32591	38863	42553	3.15
Run34	67	5.42	0	4284	7413	13549	19950	28103	33514	39942	43723	3.31
Run35	67	3.22	0	4280	7417	13589	19920	28036	33490	39891	44002	3.30
Run36	69	4.01	0	4483	7545	13718	20184	28436	33930	40568	44351	3.39
Run37	69	5.04	0	4445	7524	13743	20318	28693	33993	40478	44337	3.39
Run38	75	4.54	0	4517	7640	14317	20820	29130	34896	41612	45662	3.57
Run39	75	4.06	0	4629	7820	14172	20881	29489	34959	41687	45568	3.58
Run40	81	4.98	0	4639	7928	14558	21458	30346	36065	42856	47011	3.77
Run41	81	5.56	0	4682	7870	14458	21590	30237	36129	42838	47077	3.76
Run42	89	3.61	0	4889	8268	14903	22307	31516	37345	44486	48775	4.02
Run43	90	5.54	0	4981	8233	15044	22623	31461	37605	44511	48799	4.03
Run44	97	3.33	0	5134	8403	15404	23001	32384	38417	45799	50274	4.25
Run45	97	3.45	0	5275	8380	15533	23069	32451	38469	45844	50321	4.24
Run46	108	3.36	0	5308	8779	16080	24123	33746	40092	47837	52372	4.57
Run47	108	2.67	0	5833	8825	15946	24081	33896	40150	47773	52425	4.57
Run48	118	4.11	0	6140	9085	16486	25053	35219	41847	49693	54251	4.85

CMC 8% in 80 mm valve, 100% open

Date:	10/11/2004	
Valve Type:	Diaphragm	
Valve dimension[m]:	0.08	
Valve position:	Open	Area[m^2]
Pipe Diameter [m]:	0.08043	0.005080729

Material Type:	CMC 8%
Density[kg/m^3]:	0.08
Concentration:	1040
τ_y:	0
K:	6.147
n:	0.5161
PPT used:	105
Range selected:	0-130

		Axial distances [m]	-6.413	-4.809	-3.61	-1.209	0.707	3.907	5.977	8.461	9.956	
		Valve plane										
		Non-dim distances [L/D]:	-79.73393013	-59.79112272	-44.88374984	-15.03170459	8.790252393	48.57640184	74.31306726	105.1970658	123.7846575	
		Distances[m]:	0	1.604	2.803	5.204	7.12	10.32	12.39	14.874	16.369	
Run #	Re_3	k_v	DP1	DP2	DP3	DP4	DP5	DP6	DP7	DP8	DP9	Average Q
			[Pa]	[Pa]	[Pa]	[Pa]	[Pa]	[Pa]	[Pa]	[Pa]	[Pa]	[l/s]
Run1	4	27.54	0	1722	2812	5080	7304	10304	12246	14566	15984	0.50
Run2	4	3.21	0	1741	2838	5062	7267	10278	12194	14513	15940	0.50
Run3	6	16.77	0	2039	3349	5960	8607	12234	14485	17195	18882	0.68
Run4	7	22.30	0	2116	3449	6189	8966	12756	15109	17946	19712	0.72
Run5	7	4.56	0	2070	3420	6136	8878	12642	14971	17909	19657	0.73
Run6	8	19.36	0	2252	3643	6727	9599	13511	16025	19085	20914	0.82
Run7	8	7.53	0	2275	3729	6634	9456	13376	16014	19047	20883	0.80
Run8	8	4.92	0	2272	3625	6545	9356	13303	15811	18855	20707	0.82
Run9	8	2.27	0	2237	3675	6569	9431	13362	15882	18955	20792	0.81
Run10	12	7.30	0	2623	4266	7660	11025	15607	18538	22070	24215	1.04
Run11	12	9.96	0	2550	4235	7623	10990	15562	18476	22025	24139	1.03
Run12	17	11.21	0	2917	4734	8577	12325	17498	20837	24806	27177	1.29
Run13	17	11.69	0	2950	4725	8583	12348	17365	20799	24806	27106	1.29
Run14	20	12.52	0	2973	4973	8948	12965	18424	21950	26057	28593	1.45
Run15	20	7.88	0	3074	4939	8991	12968	18374	21865	26037	28591	1.45
Run16	23	6.68	0	3184	5229	9581	13923	19658	23322	27861	30585	1.62
Run17	23	5.51	0	3098	5249	9592	13776	19610	23240	27674	30491	1.62
Run18	28	4.26	0	3419	5708	10170	14831	21085	24994	29776	32693	1.85
Run19	28	5.98	0	3417	5625	10282	14785	21006	25008	29775	32749	1.85
Run20	32	4.50	0	3574	5947	10709	15415	21904	26037	31089	34012	2.00
Run21	32	12.14	0	3674	5736	10671	15379	21850	26114	30864	33976	2.00
Run22	37	7.10	0	3639	6086	11293	16349	23161	27474	32778	35966	2.23
Run23	37	3.41	0	3759	6203	11238	16337	23095	27378	32704	35859	2.23
Run24	40	6.34	0	3687	6363	11570	16817	23952	28228	33703	36839	2.36
Run25	40	6.75	0	3729	6365	11510	16779	23788	28304	33629	36920	2.35
Run26	44	4.90	0	3943	6493	11738	17328	24451	29076	34781	38052	2.51
Run27	44	7.20	0	4012	6469	11851	17428	24526	29217	34659	38102	2.51
Run28	47	5.46	0	3930	6619	12074	17707	24895	29763	35277	38949	2.60
Run29	47	4.13	0	3986	6629	12151	17663	25015	29605	35420	38777	2.60
Run30	54	3.82	0	4563	7030	12672	18664	26373	31236	37182	40723	2.85
Run31	54	5.52	0	4239	6901	12708	18399	26156	31246	37087	40833	2.85
Run32	62	4.54	0	4342	7194	13200	19343	27355	32537	38794	42558	3.15
Run33	62	5.30	0	4351	7187	13194	19431	27475	32591	38863	42553	3.15
Run34	67	5.42	0	4284	7413	13549	19950	28103	33514	39942	43723	3.31
Run35	67	3.22	0	4280	7417	13589	19920	28036	33490	39891	44002	3.30
Run36	69	4.01	0	4483	7545	13718	20184	28436	33930	40568	44351	3.39
Run37	69	5.04	0	4445	7524	13743	20318	28693	33993	40478	44337	3.39
Run38	75	4.54	0	4517	7640	14317	20820	29130	34896	41612	45662	3.57
Run39	75	4.06	0	4629	7820	14172	20881	29489	34959	41687	45568	3.58
Run40	81	4.98	0	4639	7928	14558	21458	30346	36065	42856	47011	3.77
Run41	81	5.56	0	4682	7870	14458	21590	30237	36129	42838	47077	3.76
Run42	89	3.61	0	4889	8268	14903	22307	31516	37345	44486	48775	4.02
Run43	90	5.54	0	4981	8233	15044	22623	31461	37605	44511	48799	4.03
Run44	97	3.33	0	5134	8403	15404	23001	32384	38417	45799	50274	4.25
Run45	97	3.45	0	5275	8380	15533	23069	32451	38469	45844	50321	4.24
Run46	108	3.36	0	5308	8779	16080	24123	33746	40092	47837	52372	4.57
Run47	108	2.67	0	5833	8825	15946	24081	33896	40150	47773	52425	4.57
Run48	118	4.11	0	6140	9085	16486	25053	35219	41847	49693	54251	4.85

CMC 8% in 100 mm valve, 100% open: No data

CMC 8% in 100 mm valve, 75% open

Date:	16/06/2005	
Valve Type:	Diaphragm	
Valve dimension[m]:	0.1	
Valve position:	¾	Area[m^2]
Pipe Diameter [m]:	0.09717	0.007415736

Material Type:	CMC 8%
Density[kg/m^3]:	1040.7
Concentration:	0.08
τ_y:	0
K:	7.232
n:	0.5994
PPT used:	105
Range selected:	0-130

		Axial distances [m]	-5.55081	-4.55181	-2.03875	-0.69875	0.69975	1.50175	2.50175	3.50075	4.49875	
		Valve plane										
		Non-dim distances [L/D]:	-57.12472985	-46.84377894	-20.98126994	-7.191005454	7.201296697	15.4548729	25.74611506	36.02706597	46.29772564	
		Distances[m]:	0	0.999	3.51206	4.85206	6.25056	7.05256	**8.05256**	9.05156	10.04956	
Run #	Re_3		k_v	Pod 1	Pod 2	Pod 3	Pod 4	Pod 5	Pod 6	Pod 7	Pod 8	Pod 9	Average Q
				[Pa]	[Pa]	[Pa]	[Pa]	[Pa]	[Pa]	[Pa]	[Pa]	[Pa]	[l/s]
Run 1	38		18.73	87900	84891	77923	74151	66662	64324	61489	58633	55773	4.31
Run 2	38		17.74	88063	85191	78011	74307	66777	64459	61599	58671	55811	4.32
Run 3	36		15.94	86009	83211	76373	72650	65424	63213	60448	57610	54746	4.10
Run 4	36		16.80	85889	83143	76204	72561	65347	63170	60374	57524	54711	4.11
Run 5	34		17.76	84500	81700	74821	71356	64258	62106	59467	56647	53910	3.95
Run 6	34		20.49	84498	81786	75048	71567	64367	62215	59478	56827	54040	3.97
Run 7	32		16.97	82032	79573	73084	69693	62916	60797	58196	55418	52830	3.76
Run 8	32		21.02	82146	79486	72890	69669	62823	60640	58093	55399	52824	3.76
Run 9	29		21.88	80112	77613	71278	68088	61471	59439	56898	54343	51786	3.55
Run 10	29		27.89	80113	77635	71317	68034	61437	59375	56768	54358	51798	3.53
Run 11	28		17.65	78559	75988	69955	66766	60349	58437	55973	53469	50871	3.41
Run 12	27		23.11	78583	76009	70005	66854	60224	58290	55887	53395	50897	3.39
Run 13	25		19.74	76908	74583	68600	65472	59302	57337	54945	52526	49977	3.21
Run 14	25		22.69	76700	74183	68267	65152	59069	57096	54767	52386	49894	3.21
Run 15	23		23.28	75047	72729	66940	63966	58007	56146	53837	51469	49071	3.00
Run 16	23		24.77	75028	72681	66865	63915	57898	56096	53753	51408	49006	3.00
Run 17	21		27.97	73108	70881	65252	62379	56643	54835	52611	50312	48054	2.84
Run 18	21		23.82	72600	70428	64882	62077	56353	54627	52386	50115	47823	2.84
Run 19	19		29.98	70529	68339	62994	60324	54880	53196	51039	48878	46704	2.65
Run 20	19		30.36	70491	68375	63117	60351	54924	53200	51086	48949	46776	2.65
Run 21	18		25.15	68698	66561	61544	58930	53757	52104	50046	47971	45796	2.47
Run 22	18		25.85	68559	66477	61413	58732	53547	51910	49888	47785	45636	2.47
Run 23	16		39.82	66466	64481	59550	57060	52066	50518	48548	46638	44608	2.30
Run 24	16		32.57	66382	64287	59381	56942	52016	50456	48514	46491	44498	2.30
Run 25	14		34.14	64219	62156	57639	55225	50448	48987	47182	45288	43343	2.13
Run 26	14		41.64	63881	62072	57396	54975	50358	48920	47017	45163	43266	2.11
Run 27	12		51.06	61433	59684	55222	52863	48563	47142	45379	43724	41849	1.92
Run 28	12		34.54	61662	59913	55505	53235	48839	47375	45657	43845	41984	1.90
Run 29	11		58.93	58882	57060	52919	50804	46623	45130	43650	42035	40306	1.73
Run 30	11		40.38	58848	56996	53049	50900	46823	45483	43799	42083	40373	1.73
Run 31	9		31.82	56083	54700	50900	48740	45100	43776	42395	40820	39172	1.55
Run 32	9		56.38	56510	54996	51142	49146	45307	44065	42455	40927	39283	1.53
Run 33	8		56.33	54234	52792	49155	47301	43734	42539	41064	39645	38053	1.37
Run 34	8		56.42	54149	52674	49093	47217	43589	42495	41031	39505	38024	1.36
Run 35	6		59.68	51763	50419	47077	45348	41986	40924	39559	38148	36740	1.21
Run 36	6		52.67	51613	50266	46922	45163	41848	40786	39450	38064	36619	1.21
Run 37	5		64.66	48812	47560	44535	42943	39916	38895	37680	36381	35080	1.02
Run 38	5		52.34	48762	47578	44534	42939	39895	38911	37665	36368	35039	1.02
Run 39	4		81.89	46010	44870	42199	40809	38035	37156	36081	34950	33755	0.82
Run 40	4		49.30	46225	45080	42331	40935	38178	37283	36190	35013	33785	0.82

Kaolin 10%

Kaolin 10% in 40 mm valve, 100% open

Date:	06/08/2004	
Valve Type:	Diaphragm	
Valve dimension[m]:	0.05	
Valve position:	Open	Area[m^2]
Pipe Diameter [m]:	0.04212	0.00139337

Material Type:	Kaolin 10%
Density[kg/m^3]:	1168.2
Concentration:	10.19
τ_y:	3.255
K:	10.054
n:	0.16001
PPT used:	103
Range selected:	0-130

			Axial distances [m]	-6.298	-4.568	-2.932	-1.88	1.0755	3.8045	6.0455	8.0745	9.9745	
			Valve plane										
			Non-dim distances [L/D]:	-149.5251662	-108.4520418	-69.61063628	-44.63437797	25.53418803	90.32526116	143.5303894	191.7022792	236.811491	
			Distances[m]:	0	1.73	3.366	4.418	7.3735	10.1025	12.3435	14.3725	16.2725	
Run #	Re_3		k_v	PTT 1	PTT 2	PTT 3	PTT 4	PTT 5	PTT 6	PTT 7	PTT 8	PTT 9	Average Q
				[Pa]	[Pa]	[Pa]	[Pa]	[Pa]	[Pa]	[Pa]	[Pa]	[Pa]	[l/s]
Run 1	76		10.60	68206	64072	60433	57757	49944	43557	38246	33555	29039	0.61
Run 2	81		11.40	67766	63758	60030	57473	49667	43434	38101	33318	29095	0.63
Run 3	82		11.81	67643	63656	59937	57405	49679	43496	38049	33272	29081	0.63
Run 4	201		9.07	71617	67337	63394	60891	50756	44160	38599	33678	29017	1.02
Run 5	200		9.18	71586	67283	63396	60837	50723	44140	38558	33669	28958	1.02
Run 6	201		10.09	71420	67333	63345	60843	50721	44085	38468	33634	28940	1.02
Run 7	427		8.21	76584	72267	68019	65300	51530	44672	38981	33817	28757	1.54
Run 8	426		8.11	76586	72223	68044	65374	51631	44710	39018	33872	28754	1.54
Run 9	426		8.19	76423	71997	67953	65129	51499	44661	38976	33831	28756	1.54
Run 10	712		8.01	80700	76097	71930	69140	51338	44488	38821	33661	28717	2.02
Run 11	717		8.23	80443	75958	71855	69010	51408	44570	38778	33618	28799	2.03
Run 12	717		8.18	80244	75806	71727	69095	51335	44495	38786	33605	28812	2.03
Run 13	1115		7.06	84866	80423	76239	73654	51666	44882	38904	33730	28710	2.58
Run 14	1113		6.81	84792	80118	75975	73362	51710	44788	38864	33659	28617	2.58
Run 15	1109		7.07	84711	80524	76178	73302	51807	44761	38987	33566	28719	2.57
Run 16	1043		7.85	88815	83943	79365	76446	53488	45940	39806	34213	28965	2.49
Run 17	1045		7.92	88707	84025	79320	76115	53425	45983	39751	34172	28932	2.49
Run 18	1043		7.86	88454	83715	79066	76214	53346	45939	39697	34191	28936	2.49
Run 19	1480		7.03	93895	89116	84323	81045	53904	46163	39845	34054	28739	3.01
Run 20	1479		7.02	93680	89163	84073	81060	53790	46252	39769	34087	28719	3.01
Run 21	1478		7.06	93353	88351	84108	80902	53929	46070	39757	34023	28689	3.00
Run 22	2049		7.71	105210	99807	95635	93380	54286	46329	39760	33805	28349	3.58
Run 23	2049		7.93	105735	99848	96420	92588	54226	45932	39626	33662	28152	3.58
Run 24	2040		7.88	104804	101176	94978	91736	54306	46057	39526	33791	28394	3.57
Run 25	2563		8.50	115752	110535	106948	102739	54638	46045	39266	33278	27626	4.04
Run 26	2548		8.32	116249	111305	105760	101604	54500	45843	39099	33298	28012	4.03
Run 27	2553		7.90	116018	111373	105090	102530	54560	46115	39682	33525	28242	4.04
Run 28	2934		8.27	125694	119951	114673	109192	55105	46128	39309	33074	27218	4.35
Run 29	2938		8.24	126374	120263	115819	112276	54634	46662	40008	33145	27402	4.36
Run 30	2932		8.52	126063	121331	115225	113208	54911	46779	39085	34159	27272	4.35

Kaolin 10% in 40 mm valve, 100% open (continued)

Date:	11/08/2004	
Valve Type:	Diaphragm	
Valve dimension[m]:	0.04	
Valve position:	Open	Area[m^2]
Pipe Diameter [m]:	0.04212	0.00139337

Material Type:	Kaolin 10%
Density[kg/m^3]:	1172.4
Concentration:	0.1
τ_y:	3.6193
K:	9.8853
n:	0.15784
PPT used:	101
Range selected:	0-130

			Axial distances [m]	-6.298	-4.568	-2.932	-0.8315	1.0755	3.8045	6.0455	8.0745	9.9745
			Valve plane									
			Non-dim distances [L/D]:	-149.5251662	-108.4520418	-69.61063628	-19.74121557	25.53418803	90.32526116	143.5303894	191.7022792	236.811491
			Distances[m]:	0	1.73	3.366	5.4665	7.3735	10.1025	12.3435	14.3725	16.2725
Run #	Re_3		k_v	PTT 1	PTT 2	PTT 3	PTT 4	PTT 5	PTT 6	PTT 7	PTT 8	PTT 9	Average Q
				[Pa]	[Pa]	[Pa]	[Pa]	[Pa]	[Pa]	[Pa]	[Pa]	[Pa]	[l/s]
Run 1	1		1281.13	53930	51270	48722	45308	41755	35732	33770	30495	27805	0.06
Run 2	1		686.69	54061	51072	48686	45097	41768	35778	33668	30447	27464	0.06
Run 3	3		92.11	54554	51821	49122	45593	42206	36244	33991	30737	27432	0.10
Run 4	3		355.29	54599	51793	49198	45697	42313	35644	34064	30551	27870	0.10
Run 5	3		91.66	55623	52701	49963	46401	42897	36979	34402	30848	27697	0.11
Run 6	7		62.96	57165	54308	51330	47690	43870	38664	34883	31262	27806	0.16
Run 7	6		21.86	57564	54436	51421	47604	43974	38199	34954	31266	27820	0.15
Run 8	6		115.21	57582	54638	51608	47860	44037	37783	34952	31226	27972	0.15
Run 9	10		22.55	58730	55689	52380	48490	44693	39893	35298	31505	27921	0.20
Run 10	10		44.34	58825	55918	52604	48455	44701	38503	35329	31511	27909	0.20
Run 11	19		16.56	60420	57277	53872	49760	45693	40446	35822	31818	28019	0.29
Run 12	19		20.63	60588	57093	53876	49945	45731	39029	35841	31775	28235	0.29
Run 13	35		13.60	61698	58159	55154	50892	46521	39083	36173	31985	28009	0.40
Run 14	35		21.81	61817	58413	55226	50933	46400	39240	36165	31957	28170	0.40
Run 15	54		9.62	63108	59414	55934	51560	47011	39087	36321	32068	28100	0.50
Run 16	53		14.93	63182	59406	55994	51586	46987	38833	36348	32080	28349	0.49
Run 17	90		5.94	64411	60452	56854	52345	47426	38964	36538	32135	28119	0.65
Run 18	88		11.44	64435	60652	56975	52654	47411	38554	36555	32104	28394	0.65
Run 19	122		11.35	65592	61634	58142	53438	47664	38893	36708	32216	28327	0.77
Run 20	122		13.47	65391	61655	58203	53386	47712	38904	36695	32121	28322	0.77
Run 21	161		9.46	66772	62895	59207	54376	48021	39563	36854	32211	28077	0.90
Run 22	161		10.24	66802	62835	59158	54402	47963	40244	36787	32142	28169	0.90
Run 23	217		9.84	68220	64258	60490	55649	48310	39340	36903	32149	28056	1.05
Run 24	217		9.44	68127	64345	60376	55593	48215	39067	36925	32242	28059	1.05

Kaolin 10% in 50mm valve, 100% open

Date:	16/08/2004	
Valve Type:	Diaphragm	
Valve dimension[m]:	0.063	
Valve position:	1	Area[m^2]
Pipe Diameter [m]:	0.0528	0.002189564

Material Type:	Kaolin 10%
Density[kg/m^3]:	1163.4
Concentration:	0.1
τ_y:	3.9134
K:	9.3441
n:	0.15634
PPT used:	101
Range selected:	0-40

		Axial distances [m]	-6.574	-3.526	-2.281	-0.78	1.2565	3.0115	5.6655	7.6655	9.6685	
		Valve plane										
		Non-dim distances [L/D]:	-124.5075758	-66.78030303	-43.20075758	-14.77272727	23.79734848	57.03598485	107.3011364	145.1799242	183.1155303	
		Distances[m]:	0	3.048	4.293	5.794	7.8305	9.5855	12.2395	14.2395	16.2425	
Run #	Re_3		k_v	PTT 1	PTT 2	PTT 3	PTT 4	PTT 5	PTT 6	PTT 7	PTT 8	PTT 9	Average Q
				[Pa]	[Pa]	[Pa]	[Pa]	[Pa]	[Pa]	[Pa]	[Pa]	[Pa]	[l/s]
Run 1	1		693.02	46954	43437	42155	40401	37911	35768	32410	29600	27772	0.09
Run 2	1		1160.28	46986	43541	42129	40419	37813	35788	32386	29630	28034	0.09
Run 3	1		748.13	47555	43946	42587	40808	38225	36118	32570	29840	28013	0.11
Run 4	1		771.47	46537	43299	41939	40185	37741	35652	32385	29915	27756	0.08
Run 5	1		437.18	47557	44084	42529	40729	38273	36080	32634	29731	27812	0.11
Run 6	2		486.52	48011	44398	42811	41138	38479	36304	32638	29708	27876	0.12
Run 7	2		830.91	47910	44351	42959	41101	38504	36247	32617	29778	28126	0.12
Run 8	2		529.97	48415	44629	43145	41317	38602	36374	32626	29742	27895	0.13
Run 9	2		581.87	48270	44693	43140	41226	38620	36506	32773	29795	28059	0.13
Run 10	3		401.23	49023	45207	43790	41800	39000	36756	32898	30065	28051	0.17
Run 11	3		495.49	49082	45304	43854	41798	39075	36747	32879	29881	28105	0.16
Run 12	5		201.60	49937	45977	44357	42392	39489	37208	33195	30106	28009	0.20
Run 13	5		294.24	49963	46041	44320	42439	39479	37232	33189	30045	28305	0.21
Run 14	12		68.98	51409	47195	45359	43394	40274	37839	33671	30414	28166	0.33
Run 15	12		124.09	51427	47142	45458	43263	40201	37856	33469	30219	28236	0.33
Run 16	20		74.93	52287	47826	46240	43942	40920	38238	33669	30398	28224	0.44
Run 17	20		77.24	52517	47943	46135	43988	40916	38267	33558	30546	28241	0.43
Run 18	27		64.86	52681	48296	46462	44234	41120	38551	33652	30526	28282	0.51
Run 21	50		17.95	53113	48722	46796	44065	41274	38034	34324	29964	28320	0.72
Run 27	101		4.85	54760	50155	48205	45593	42258	39572	34860	31691	28353	1.05
Run 28	101		7.89	54540	50043	48090	45534	42058	39409	34792	31638	28525	1.05
Run 29	113		5.37	54812	50079	48089	45479	42060	39449	34733	31572	28382	1.12
Run 30	114		7.30	54871	50075	48125	45589	41991	39207	34703	31534	28524	1.12

Kaolin 10% in 65mm valve, 100% open

Date:	19/08/2004	
Valve Type:	Diaphragm	
Valve dimension[m]:	0.06	
Valve position:	Open	Area[m^2]
Pipe Diameter [m]:	0.06308	0.003125167

Material Type:	Kaolin 10%
Density[kg/m^3]:	1163.4
Concentration:	0.1
τ_y:	3.9134
K:	9.3441
n:	0.15634
PPT used:	101
Range selected:	0-130

			Axial distances [m]	-6.9735	-4.8855	-2.885	-0.937	0.987	1.968	2.938	3.916	4.858
			Valve plane									
			Non-dim distances [L/D]:	-110.5500951	-77.44927077	-45.73557387	-14.85415346	15.64679772	31.19847812	46.57577679	62.07989854	77.01331642
			Distances[m]:	0	2.088	4.0885	6.0365	7.9605	8.9415	**9.9115**	10.8895	11.8315
Run #	Re_3		k_v	PTT 1	PTT 2	PTT 3	PTT 4	PTT 5	PTT 6	PTT 7	PTT 8	PTT 9
				[Pa]	[Pa]	[Pa]	[Pa]	[Pa]	[Pa]	[Pa]	[Pa]	[Pa]
Run 1	125		1.75	53339	50428	47541	44807	41684	40325	38950	37581	36194
Run 2	124		3.24	53377	50463	47639	44779	41733	40320	38938	37553	36240
Run 3	153		2.52	53665	50622	47858	44919	41838	40449	39026	37681	36300
Run 4	156		1.11	53669	50704	47717	44923	41838	40499	39070	37611	36291
Run 5	183		2.25	53845	50917	48024	45129	42002	40586	39122	37705	36345
Run 6	177		2.30	53868	50890	47937	45081	41937	40555	39081	37654	36369
Run 7	222		2.10	54140	51124	48213	45358	41979	40640	39191	37850	36458
Run 8	221		1.34	54217	51205	48216	45268	42009	40601	39281	37837	36462
Run 9	256		1.70	54286	51311	48359	45449	42108	40756	39295	37837	36486
Run 10	248		1.77	54413	51312	48422	45464	42126	40715	39268	37908	36472
Run 11	287		1.46	54620	51521	48547	45608	42257	40841	39400	37925	36599
Run 12	289		1.45	54588	51521	48568	45739	42241	40813	39388	37955	36552
Run 13	338		1.23	54909	51770	48808	45837	42359	41015	39508	38067	36643
Run 14	340		1.82	54903	51644	48959	45845	42327	40956	39471	38069	36649
Run 15	379		2.12	55158	52013	49300	46083	42464	40995	39526	38117	36646
Run 16	384		1.13	55191	52077	49007	46290	42476	41037	39578	38101	36670
Run 17	425		1.76	55460	52198	49379	46278	42939	41354	39596	38192	36761
Run 18	423		1.22	55451	52314	49244	46269	42456	41076	39676	38188	36768
Run 19	472		1.42	55496	52423	49379	46288	42593	41240	39787	38214	36944
Run 20	467		1.31	55551	52306	49417	46358	42585	41162	39750	38208	36857
Run 21	525		1.16	55668	52517	49483	46514	42706	41253	39740	38265	36813
Run 22	522		1.13	55721	52579	49490	46507	42614	41191	39754	38273	36826
Run 23	573		1.04	55852	52677	49639	46687	42710	41306	39843	38338	36885
Run 24	586		1.12	55899	52711	49627	46663	42737	41283	39794	38255	36885
Run 25	644		1.12	56662	53433	50300	47275	43017	41512	40048	38515	36992
Run 26	648		1.26	56590	53504	50311	47237	42952	41494	40054	38510	37021
Run 27	703		1.53	57148	53935	50811	47726	43174	41682	40126	38610	37128
Run 28	708		1.50	57161	53912	50754	47691	43147	41626	40116	38601	37159
Run 29	756		1.47	57514	54240	51091	48019	43323	41764	40243	38713	37217
Run 30	760		1.50	57541	54268	51083	47962	43338	41799	40217	38697	37222

Kaolin 10% in 80 mm valve, 100% open

Date:	17/09/2004	
Valve Type:	Diaphragm	
Valve dimension[m]:	0.075	
Valve position:	1	Area[m^2]
Pipe Diameter [m]:	0.08043	0.005080729

Material Type:	Kaolin 10%
Density[kg/m^3]:	1168.8
Concentration:	0.1023
τ_y:	2.0681
K:	11.601
n:	0.13692
PPT used:	101
Range selected:	0-130

		Axial distances [m]	-6.413	-4.809	-3.61	-1.609	0.707	3.907	5.273	8.461	9.956		
		Valve plane											
		Non-dim distances [L/D]:	-79.73393013	-59.79112272	-44.88374984	-20.00497327	8.790252393	48.57640184	65.56011439	105.1970658	123.7846575		
		Distances[m]:	0	1.604	2.803	4.804	7.12	10.32	**11.686**	14.874	16.369		
Run #	Re_3		k_v	PTT 1	PTT 2	PTT 3	PTT 4	PTT 5	PTT 6	PTT 7	PTT 8	PTT 9	Average Q
				[Pa]	[Pa]	[Pa]	[Pa]	[Pa]	[Pa]	[Pa]	[Pa]	[Pa]	[l/s]
Run 1	0		4226.85	41042	39896	39039	37712	36065	33851	32994	30917	29854	0.06
Run 2	80		0.78	47498	45882	44679	41919	39731	36264	34800	31269	29661	2.18
Run 3	74		0.15	47273	45726	44490	41901	39600	36233	34734	31277	29679	2.10
Run 4	98		1.06	47744	46130	44812	42257	39767	36363	34921	31367	29742	2.42
Run 5	97		1.76	50420	48817	47507	44957	42506	39086	37608	34169	32494	2.41
Run 6	108		0.61	50383	48829	47504	44875	42565	39130	37733	34187	32549	2.55
Run 7	52		4.85	47469	45879	44547	42055	39959	36111	34809	31305	29665	1.73
Run 8	52		1.02	47419	45818	44577	42087	39854	36212	34803	31306	29657	1.73
Run 9	59		4.57	47615	45923	44737	42123	39927	36258	34764	31350	29730	1.85
Run 10	60		4.60	47658	45959	44731	42034	39943	36264	34758	31323	29712	1.87
Run 11	72		5.63	47879	46243	44909	42288	39992	36303	34797	31404	29723	2.06
Run 12	70		4.28	47801	46250	44965	42343	40037	36306	34857	31355	29734	2.03
Run 13	85		4.37	48044	46505	45118	42541	40090	36412	34849	31443	29735	2.25
Run 14	84		4.64	48078	46456	45176	42548	40069	36404	34881	31411	29772	2.24
Run 15	102		5.35	48249	46611	45370	42580	40101	36404	34972	31456	29836	2.48
Run 16	100		5.31	48366	46675	45269	42574	40114	36413	34902	31412	29743	2.46
Run 17	117		7.18	48434	46710	45375	42947	39767	36418	34836	31859	29798	2.67
Run 18	150		4.65	48758	46962	45645	43131	39908	36510	34980	31525	29841	3.05
Run 19	46		9.98	48895	47587	46347	44257	41909	38895	37548	34424	33112	1.62
Run 20	47		4.26	49019	47477	46345	44401	41940	38792	37541	34320	33023	1.63
Run 21	83		3.64	49377	47883	46697	44801	42277	39079	37771	34650	33252	2.21
Run 22	325		1.20	44723	43452	41881	39767	37587	33989	32556	29269	27879	4.58
Run 23	283		0.76	44912	43141	41938	40086	37525	34198	32564	29453	27946	4.25
Run 24	46		3.78	48895	47587	46347	44257	41909	38895	37548	34424	33112	1.62
Run 25	47		4.04	49019	47477	46345	44401	41940	38792	37541	34320	33023	1.63
Run 26	83		2.99	49377	47883	46697	44801	42277	39079	37771	34650	33252	2.21
Run 27	83		9.22	50069	47962	46702	44791	42300	39038	37799	34697	33321	2.21
Run 28	325		0.94	44723	43452	41881	39767	37587	33989	32556	29269	27879	4.58
Run 29	283		0.48	44912	43141	41938	40086	37525	34198	32564	29453	27946	4.25
Run 30	282		0.94	45143	42963	41789	39708	37723	34174	32771	29406	28122	4.25
Run 31	75		1.82	45586	44026	42876	40728	38408	35305	33854	30767	29300	2.10

Kaolin 10% in 100 mm valve, 75% open

Date:	29/04/2005	
Valve Type:	Diaphragm	
Valve dimension[m]:	0.1	
Valve position:	¾ Open	Area[m^2]
Pipe Diameter [m]:	0.09717	0.007415736

Material Type:	Kaolin 10%
Density[kg/m^3]:	1167.5
Concentration:	0.1015
τ_y:	6.0844
K:	5.1717
n:	0.2725
PPT used:	105
Range selected:	0-130

		Axial distances [m]	-5.55081	-4.55181	-2.54175	-1.03975	0.69975	1.50175	2.50175	3.50075	4.49875	
		Valve plane										
		Non-dim distances [L/D]:	-57.12472985	-46.84377894	-26.15776474	-10.70031903	7.201296697	15.4548729	25.74611506	36.02706597	46.29772564	
		Distances[m]:	0	0.999	3.00906	4.51106	6.25056	7.05256	8.05256	9.05156	10.04956	
Run #	Re_3		k_v	PTT 1	PTT 2	PTT 3	PTT 4	PTT 5	PTT 6	PTT 7	PTT 8	PTT 9	Average Q
				[Pa]	[Pa]	[Pa]	[Pa]	[Pa]	[Pa]	[Pa]	[Pa]	[Pa]	[l/s]
Run 1	248		8.17	54522	53484	51090	49262	43813	42930	41769	40573	39391	6.08
Run 2	248		8.69	54443	53455	51020	49252	43824	42896	41699	40586	39373	6.08
Run 3	203		8.91	54280	53145	50482	49042	43765	42849	41654	40498	39310	5.84
Run 4	226		8.23	54155	52982	50696	48881	43742	42849	41675	40503	39319	5.83
Run 5	208		7.71	53798	52559	50254	48455	43647	42762	41606	40453	39240	5.65
Run 6	179		8.15	53395	52365	49931	48245	43554	42647	41529	40340	39151	5.19
Run 7	144		8.97	52689	51589	49262	47474	43302	42431	41200	40142	38865	4.64
Run 8	122		5.44	52585	51190	48880	46600	43574	42500	41406	39900	38911	4.44
Run 9	100		9.35	52686	51290	48844	47044	43576	42367	41392	39982	39031	4.26
Run 10	86		10.50	51666	50572	48244	46290	43150	42196	41300	39888	39067	3.64
Run 11	57		12.47	51095	49674	47619	45892	42824	41899	40757	39378	38509	3.07
Run 12	54		9.09	50705	49544	47363	45653	42706	41805	40728	39581	38456	2.87
Run 13	46		11.19	50850	49564	47283	45585	42708	41757	40677	39518	38406	2.87
Run 14	43		1.59	50483	49263	47001	45251	42572	41707	40716	39458	38325	2.66
Run 15	46		3.95	49801	49023	46804	45123	42443	41631	40569	39441	38319	2.46
Run 16	41		2.33	50041	48870	46755	45095	42460	41583	40534	39380	38223	2.47
Run 17	34		6.32	49855	48847	46603	45001	42396	41492	40482	39347	38235	2.27
Run 18	31		4.43	49989	48887	46634	44969	42393	41447	40456	39308	38150	2.25
Run 19	28		2.13	49710	48695	46475	44859	42340	41422	40443	39256	38159	2.08
Run 20	29		1.56	49734	48728	46529	44815	42328	41436	40431	39215	38130	2.09
Run 21	23		0.02	49335	48408	46267	44614	42229	41316	40308	39148	38057	1.80
Run 22	21		2.01	49455	48440	46253	44658	42233	41307	40277	39135	38012	1.80
Run 23	17		6.92	49416	48296	46184	44532	42107	41284	40272	39112	37959	1.66
Run 24	17		1.02	49413	48355	46191	44551	42123	41255	40224	39062	37949	1.66
Run 25	12		6.95	49130	48075	45971	44376	41995	41124	40122	38952	37849	1.42
Run 26	12		0.77	49160	48084	45994	44385	41963	41123	40118	38984	37873	1.42
Run 27	9		12.77	48659	47787	45632	44066	41837	40980	39969	38831	37749	1.20
Run 28	9		14.93	48760	47884	45721	44143	41818	40962	39979	38821	37727	1.21
Run 29	8		38.06	48393	47604	45495	43913	41644	40839	39865	38678	37616	1.05
Run 30	7		26.48	48373	47608	45531	43926	41620	40806	39810	38700	37596	1.01

Kaolin 13%

Kaolin 13% in 40 mm valve, 100% open

Date:	28/09/2004	
Valve Type:	Diaphragm	
Valve dimension[m]:	0.05	
Valve position:	Open	Area[m^2]
Pipe Diameter [m]:	0.0528	0.002189564

Material Type:	Kaolin 13%
Density[kg/m^3]:	1214
Concentration:	0.1297
τ_y:	15
K:	15.035
n:	0.17031
PPT used:	101
Range selected:	0-130

			Axial distances [m]	-6.5744	-3.5264	-1.5314	-0.5274	1.2565	4.0125	5.6655	7.6655	9.6685
			Valve plane									
			Non-dim distances [L/D]:	-124.5151515	-66.78787879	-29.00378788	-9.988636364	23.79734848	75.99431818	107.3011364	145.1799242	183.1155303
			Distances[m]:	0	3.048	5.043	6.047	7.8305	10.5865	12.2395	14.2395	16.2425
Run #	Re_3		k_v	PTT 1	PTT 2	PTT 3	PTT 4	PTT 5	PTT 6	PTT 7	PTT 8	PTT 9	Average Q
				[Pa]	[Pa]	[Pa]	[Pa]	[Pa]	[Pa]	[Pa]	[Pa]	[Pa]	[l/s]
Run 1	15		55.78	97969	86275	78698	74499	67423	56684	48698	41285	33478	0.61
Run 2	16		104.01	97655	86178	78603	74328	67372	56629	48525	41211	34074	0.62
Run 3	23		33.51	99135	87292	79586	75251	68108	57323	49224	41611	33685	0.74
Run 4	22		86.22	99256	87143	79602	75401	68095	57284	48987	41612	34549	0.75
Run 5	31		33.16	100165	88066	80363	75937	68731	57734	49375	41873	33851	0.87
Run 6	32		53.73	99739	88098	80264	75516	68677	57589	48989	41861	34115	0.87
Run 7	40		40.45	100764	88840	80857	76368	68988	58003	49196	42017	34002	0.99
Run 8	40		50.99	100635	88243	80843	76389	68912	57825	49316	41929	34629	0.99
Run 9	46		43.38	101016	88654	80831	76620	69139	58046	48848	41950	33937	1.07
Run 10	48		49.80	100916	88842	80902	76589	68844	57909	49017	41940	34487	1.08
Run 11	70		23.87	101639	89058	81651	77226	69473	58420	49405	42209	34083	1.30
Run 12	100		3.52	101555	89432	81255	77155	69337	58223	50348	42158	33945	1.56
Run 13	100		6.93	101519	89395	81360	77115	69282	58217	50268	42084	34183	1.56
Run 14	112		10.82	102120	89886	81867	77344	69501	58354	50253	42238	34494	1.65
Run 15	119		0.19	102263	90018	81913	77339	69512	58442	50305	42185	33368	1.71
Run 16	118		8.04	102332	89997	81952	77461	69389	58483	50419	42216	34383	1.70
Run 17	160		5.48	103237	90872	82534	78250	70200	58957	50215	42383	33807	2.00
Run 18	157		12.36	103291	90842	82588	78170	70077	58990	49863	42293	34406	1.98
Run 19	230		3.70	101870	90333	82145	77140	69599	58560	50167	42409	34098	2.35
Run 20	277		3.26	102024	90932	82879	78369	70125	58809	50460	42542	34450	2.56
Run 21	278		6.44	102540	91340	83223	77910	70725	59045	50179	42568	34776	2.56
Run 22	336		3.03	101679	90545	81925	77558	68649	56860	48289	40108	31793	2.86
Run 23	348		5.26	100836	89845	82682	78334	68551	56641	47903	39932	32340	2.85
Run 24	379		3.59	101602	90260	81704	76842	68371	56672	47960	39704	31722	3.05
Run 25	440		4.66	102075	90768	82313	77804	68779	56422	47369	39558	31514	3.28
Run 26	450		6.30	101636	90685	82237	77770	68461	56515	47459	39451	32435	3.28

Kaolin 13% in 50mm valve, 100% open

Date:	28/09/2004	
Valve Type:	Diaphragm	
Valve dimension[m]:	0.05	
Valve position:	Open	Area[m^2]
Pipe Diameter [m]:	0.0528	0.002189564

Material Type:	Kaolin 13%
Density[kg/m^3]:	1214
Concentration:	0.1297
τ_y:	15
K:	15.035
n:	0.17031
PPT used:	101
Range selected:	0-130

		Axial distances [m]	-6.5744	-3.5264	-1.5314	-0.5274	1.2565	4.0125	5.6655	7.6655	9.6685	
		Valve plane										
		Non-dim distances [L/D]:	-124.5151515	-66.78787879	-29.00378788	-9.988636364	23.79734848	75.99431818	107.3011364	145.1799242	183.1155303	
		Distances[m]:	0	3.048	5.043	6.047	7.8305	10.5865	12.2395	14.2395	16.2425	
Run #	Re_3		k_v	PTT 1	PTT 2	PTT 3	PTT 4	PTT 5	PTT 6	PTT 7	PTT 8	PTT 9	Average Q
				[Pa]	[Pa]	[Pa]	[Pa]	[Pa]	[Pa]	[Pa]	[Pa]	[Pa]	[l/s]
Run 1	15		55.78	97969	86275	78698	74499	67423	56684	48698	41285	33478	0.61
Run 2	16		104.01	97655	86178	78603	74328	67372	56629	48525	41211	34074	0.62
Run 3	23		33.51	99135	87292	79586	75251	68108	57323	49224	41611	33685	0.74
Run 4	22		86.22	99256	87143	79602	75401	68095	57284	48987	41612	34549	0.75
Run 5	31		33.16	100165	88066	80363	75937	68731	57734	49375	41873	33851	0.87
Run 6	32		53.73	99739	88098	80264	75516	68677	57589	48989	41861	34115	0.87
Run 7	40		40.45	100764	88840	80857	76368	68988	58003	49196	42017	34002	0.99
Run 8	40		50.99	100635	88243	80843	76389	68912	57825	49316	41929	34629	0.99
Run 9	46		43.38	101016	88654	80831	76620	69139	58046	48848	41950	33937	1.07
Run 10	48		49.80	100916	88842	80902	76589	68844	57909	49017	41940	34487	1.08
Run 11	70		23.87	101639	89058	81651	77226	69473	58420	49405	42209	34083	1.30
Run 12	100		3.52	101555	89432	81255	77155	69337	58223	50348	42158	33945	1.56
Run 13	100		6.93	101519	89395	81360	77115	69282	58217	50268	42084	34183	1.56
Run 14	112		10.82	102120	89886	81867	77344	69501	58354	50253	42238	34494	1.65
Run 15	119		0.19	102263	90018	81913	77339	69512	58442	50305	42185	33368	1.71
Run 16	118		8.04	102332	89997	81952	77461	69389	58483	50419	42216	34383	1.70
Run 17	160		5.48	103237	90872	82534	78250	70200	58957	50215	42383	33807	2.00
Run 18	157		12.36	103291	90842	82588	78170	70077	58990	49863	42293	34406	1.98
Run 19	230		3.70	101870	90333	82145	77140	69599	58560	50167	42409	34098	2.35
Run 20	277		3.26	102024	90932	82879	78369	70125	58809	50460	42542	34450	2.56
Run 21	278		6.44	102540	91340	83223	77910	70725	59045	50179	42568	34776	2.56
Run 22	336		3.03	101679	90545	81925	77558	68649	56860	48289	40108	31793	2.86
Run 23	348		5.26	100836	89845	82682	78334	68551	56641	47903	39932	32340	2.85
Run 24	379		3.59	101602	90260	81704	76842	68371	56672	47960	39704	31722	3.05
Run 25	440		4.66	102075	90768	82313	77804	68779	56422	47369	39558	31514	3.28
Run 26	450		6.30	101636	90685	82237	77770	68461	56515	47459	39451	32435	3.28

Kaolin 13% in 65mm valve, 100% open

Date:	23/09/2004	
Valve Type:	Diaphragm	
Valve dimension[m]:	0.065	
Valve position:	1	Area[m^2]
Pipe Diameter [m]:	0.06308	0.003125167

Material Type:	Kaolin 13%
Density[kg/m^3]:	1219.9
Concentration:	0.1333
τ_y:	18
K:	17.123
n:	0.16791
PPT used:	101
Range selected:	0-130

			Axial distances [m]	-6.9735	-4.8855	-2.885	-0.937	0.987	2.938	3.916	8.432	10.156	
			Valve plane										
			Non-dim distances [L/D]:	-110.5500951	-77.44927077	-45.73557387	-14.85415346	15.64679772	46.57577679	62.07989854	133.6715282	161.0019023	
			Distances[m]:	0	2.088	4.0885	6.0365	7.9605	9.9115	10.8895	15.4055	17.1295	
Run #	Re_3		k_v	PTT 1	PTT 2	PTT 3	PTT 4	PTT 5	PTT 6	PTT 7	PTT 8	PTT 9	Average Q
				[Pa]	[Pa]	[Pa]	[Pa]	[Pa]	[Pa]	[Pa]	[Pa]	[Pa]	[l/s]
Run 1	14		57.26	96407	88689	81998	74975	67657	60713	57241	43109	36270	0.88
Run 2	14		53.68	96226	88769	81653	74986	67580	60730	57289	43215	36285	0.89
Run 3	21		38.66	96380	89520	82170	75238	67929	60799	57430	43117	36317	1.03
Run 4	21		30.11	96287	89312	82156	75172	67908	60945	57605	43136	36351	1.02
Run 5	26		33.90	96978	89584	82551	75501	68170	61125	57594	43328	36457	1.15
Run 6	26		25.57	96844	89821	82490	75509	68257	61127	57852	43421	36482	1.15
Run 7	27		29.68	96676	89594	81947	75445	68200	61003	57635	43650	36518	1.22
Run 8	28		42.28	96524	89570	82117	75334	68429	60927	57220	43645	36588	1.21
Run 9	35		30.25	97166	90134	82426	75836	68522	61237	57660	43821	36676	1.36
Run 10	34		38.10	97313	90170	82670	75854	68698	61185	57407	43825	36688	1.35
Run 11	43		27.96	97561	90219	83206	76263	68692	61601	57761	43975	36870	1.47
Run 12	41		25.59	97716	90539	83096	76069	68958	61761	57998	44058	36886	1.46
Run 13	48		26.46	98132	90708	83528	76391	68771	61975	57961	44184	37039	1.58
Run 14	47		23.27	98361	90391	83564	76316	69111	61997	58157	44250	37021	1.58
Run 15	54		19.57	97312	89998	82818	75398	68420	61525	57609	43706	36525	1.66
Run 16	55		20.96	97454	90221	83097	75671	68346	61373	57589	43621	36559	1.66
Run 17	65		14.05	97573	90096	82831	75433	68292	61545	57821	43643	36507	1.84
Run 18	61		14.29	97708	89889	82573	75812	68134	61376	57795	43596	36396	1.82
Run 19	69		13.14	97514	90329	83082	76164	68419	61513	57872	43839	36509	1.87
Run 20	68		15.63	98109	90441	83443	76298	68434	61532	57876	43808	36580	1.88
Run 21	88		10.77	96187	88331	81301	73800	66224	58915	55502	40869	33825	2.15
Run 22	86		10.97	96220	88648	81237	73944	66342	59216	55559	41076	33818	2.14
Run 23	97		12.08	96200	88559	81412	73868	66248	59089	55236	41007	33725	2.25
Run 24	92		17.84	96422	88626	81161	73956	66225	59229	54989	41039	34247	2.24
Run 25	130		14.44	96466	88659	81479	73945	66481	59148	54462	40788	33686	2.61
Run 26	127		20.98	96516	88933	81438	73923	66400	59093	53973	40286	34483	2.58
Run 27	204		6.42	97568	90069	82299	74890	66864	59613	55468	41150	33530	3.32
Run 28	197		7.49	98342	90123	82792	74966	67011	59802	55606	40920	33894	3.29

Kaolin 13% in 80 mm valve, 100% open

Date:	05/10/2004	
Valve Type:	Diaphragm	
Valve dimension[m]:	0.08	
Valve position:	1	Area[m^2]
Pipe Diameter [m]:	0.08043	0.005080729

Material Type:	Kaolin
Density[kg/m^3]:	1209.1
Concentration:	0.13
τ_y:	20
K:	11.5
n:	0.17031
PPT used:	101
Range selected:	0-130

			Axial distances [m]	-6.413	-4.809	-3.61	-1.609	0.707	3.907	5.273	8.461	9.956
			Valve plane									
			Non-dim distances [L/D]:	-79.73393013	-59.79112272	-44.88374984	-20.00497327	8.790252393	48.57640184	65.56011439	105.1970658	123.7846575
			Distances[m]:	0	1.604	2.803	4.804	7.12	10.32	11.686	14.874	16.369
Run #	Re_3		k_v	PTT 1	PTT 2	PTT 3	PTT 4	PTT 5	PTT 6	PTT 7	PTT 8	PTT 9
				[Pa]	[Pa]	[Pa]	[Pa]	[Pa]	[Pa]	[Pa]	[Pa]	[Pa]
Run 1	4		17.41	69761	66281	63744	59345	53949	47047	44101	37177	33911
Run 2	10		6.34	69909	66469	63924	59653	54123	47117	44250	37397	34011
Run 3	12		19.51	69880	66578	63918	59631	54092	47140	44151	37461	34015
Run 4	11		13.54	70145	66640	64109	59660	54205	47252	44256	37334	34032
Run 5	14		33.13	70217	66553	64120	59511	54087	47042	44015	37156	34012
Run 6	14		49.12	69849	66378	63779	59476	54145	46749	44146	36750	34669
Run 7	18		17.15	70484	66975	64250	59873	54269	47177	44370	37015	34307
Run 8	22		9.78	70309	66864	64095	59411	54260	46920	44050	37383	33672
Run 9	38		4.43	70131	66664	64000	59563	53773	46716	43671	36695	33196
Run 10	37		5.24	70216	66654	64002	59580	53730	46708	43649	36654	33171

Date:	08/10/2004	
Valve Type:	Diaphragm	
Valve dimension[m]:	0.080	
Valve position:	Open	Area[m^2]
Pipe Diameter [m]:	0.08043	0.005080729

Material Type:	Kaolin 13%
Density[kg/m^3]:	1210.2
Concentration:	0.13
τ_y:	20
K:	7.0867
n:	0.24955
PPT used:	101
Range selected:	0-130

			Axial distances [m]	-6.012	-4.809	-3.61	-1.609	0.707	3.907	5.273	8.461	9.956	
			Valve plane										
			Non-dim distances [L/D]:	-74.74822827	-59.79112272	-44.88374984	-20.00497327	8.790252393	48.57640184	65.56011439	105.1970658	123.7846575	
			Distances[m]:	0	1.203	2.402	4.403	6.719	9.839	11.205	14.393	15.888	
Run #	Re_3		k_v	PTT 1	PTT 2	PTT 3	PTT 4	PTT 5	PTT 6	PTT 7	PTT 8	PTT 9	Average Q
				[Pa]	[Pa]	[Pa]	[Pa]	[Pa]	[Pa]	[Pa]	[Pa]	[Pa]	[l/s]
Run 1	7		26.01	67947	65766	63173	58783	53458	46614	43671	36991	33709	0.95
Run 2	9		23.26	68344	65989	63453	59099	53647	46766	43825	37123	33820	1.09
Run 3	14		14.06	68498	66242	63637	59120	53791	46900	43951	37279	33863	1.27
Run 4	24		5.97	69061	66870	64234	59340	54301	47361	44332	37406	34103	1.56
Run 5	32		7.21	68325	65958	63399	58423	53298	46424	43299	36427	33045	1.83
Run 6	102		3.25	70754	68203	65494	60645	54529	47472	44418	37037	33777	3.35
Run 7	105		7.97	71590	69014	66206	61362	55110	48035	44557	37641	34182	3.51
Run 8	126		3.85	71454	68753	66064	61152	54643	47568	44341	37027	33550	3.80
Run 9	163		3.56	72050	69724	66590	61695	55115	47719	44609	37197	33741	4.33
Run 10	130		4.39	72942	70035	67069	62340	55040	47858	44588	37010	33605	4.46
Run 11	168		1.92	73164	69740	67359	62754	55364	48011	45001	37218	33755	4.81
Run 12	211		3.87	73303	70200	67671	63040	55389	47962	44720	37452	33761	5.08
Run 13	247		2.73	74200	71547	68498	63572	55202	48222	45074	37323	33690	5.53

Kaolin 13% in 100 mm valve, 100% open

No data

Appendix H

Comparison with Hooper (1981) and ESDU (2004) at 75% opening position

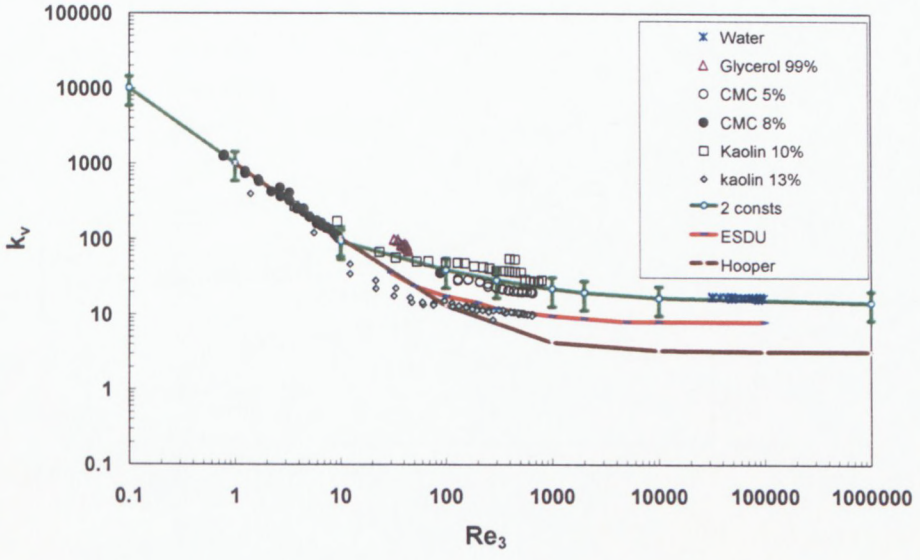

Figure H.1: Comparison of models for 40mm valve, ¾ open

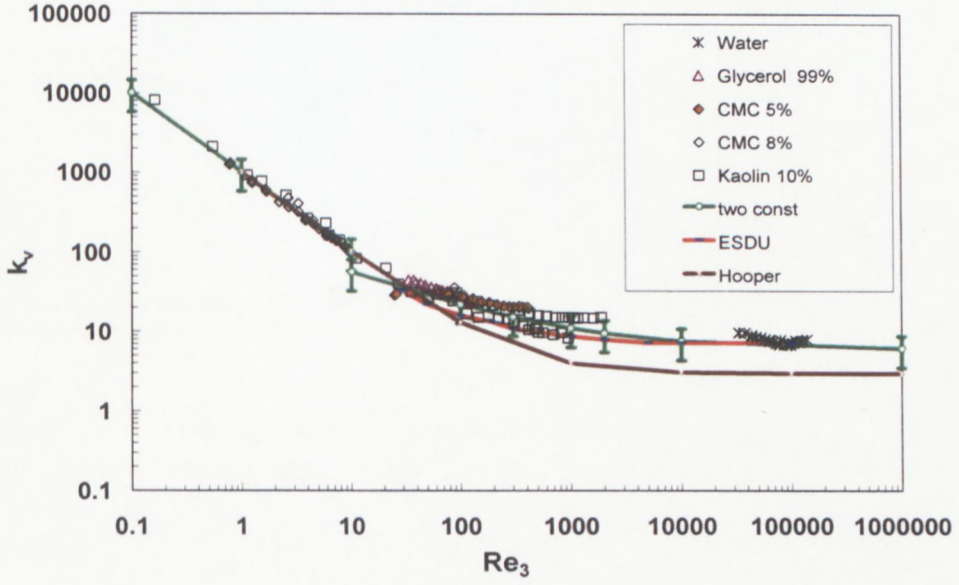

Figure H.2: Comparison of models for 50 mm valve, ¾ open

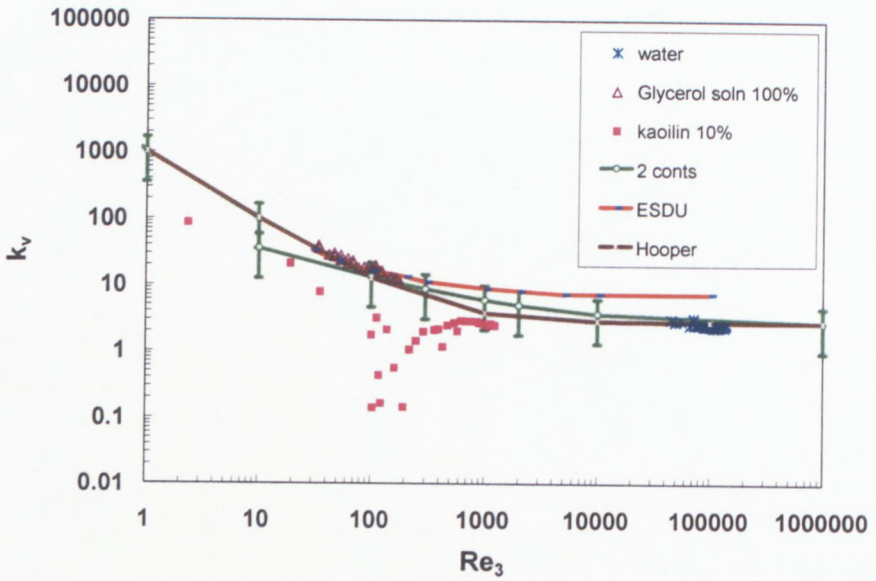

Figure H.3: Comparison of models for 65 mm valve, ¾ open

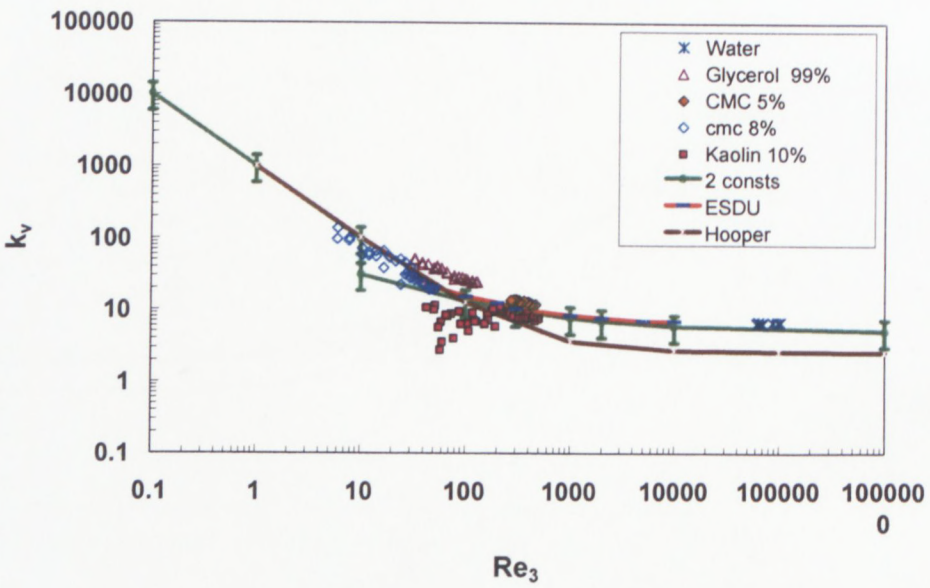

Figure H.4: Comparison of models for 80 mm valve, ¾ open

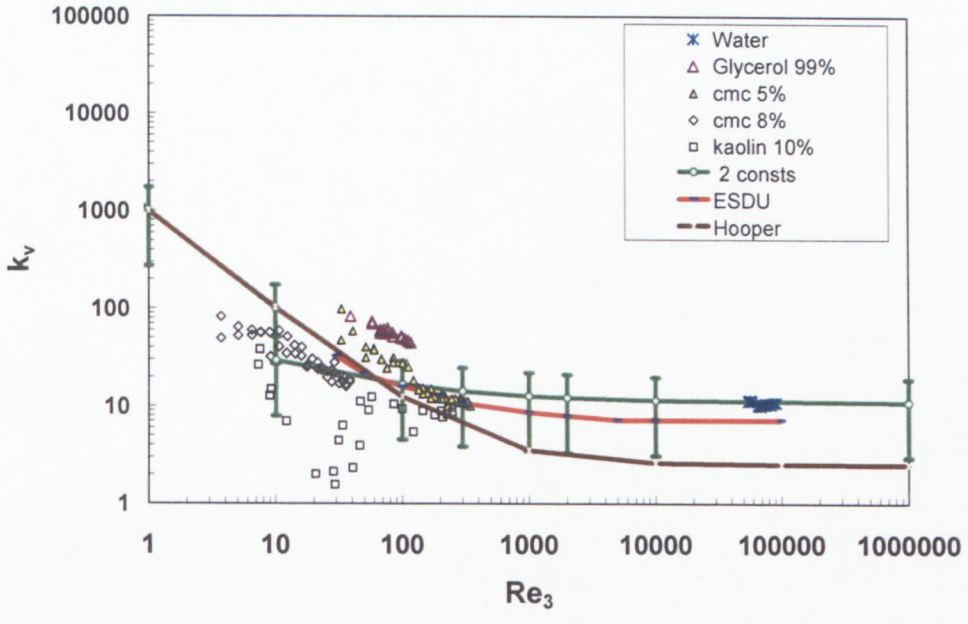

Figure H.5: Comparison of models for 100 mm valve, ¾ open

Comparison with Hooper (1981) and ESDU (2004) at 25 % opening position [2]

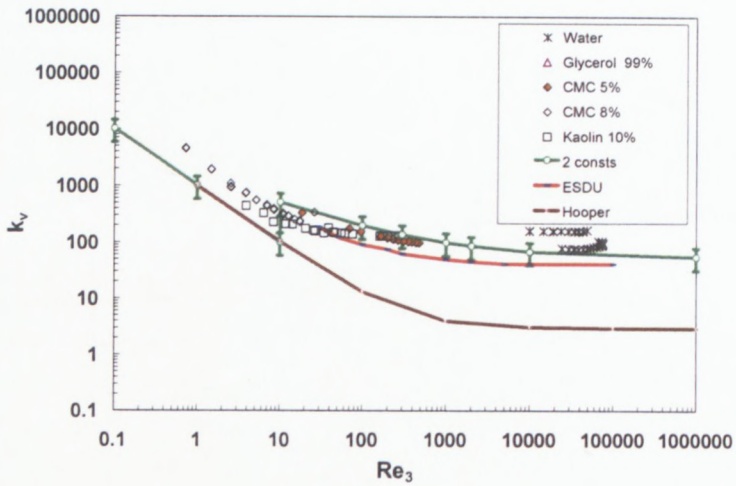

Figure H.6: Comparison of models for 50mm valve, ¼ open

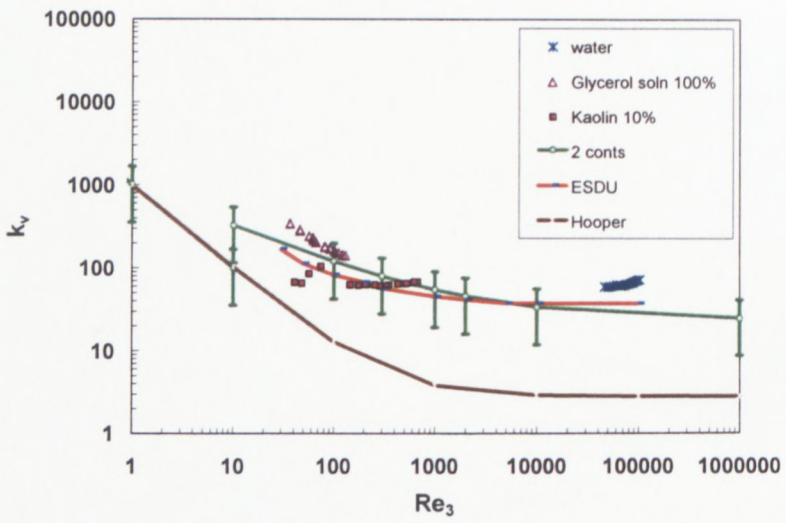

Figure H.7: Comparison of models for 65 mm valve, ¼ open

[2] There was not enough data for comparison in 40mm valve ¼ open

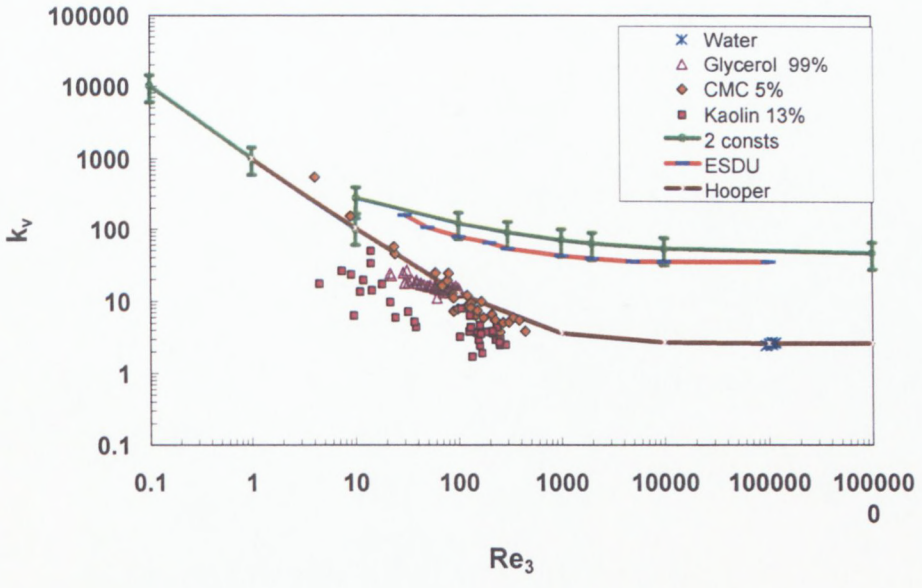

Figure H.8: Comparison of models for 80 mm valve, ¼ open

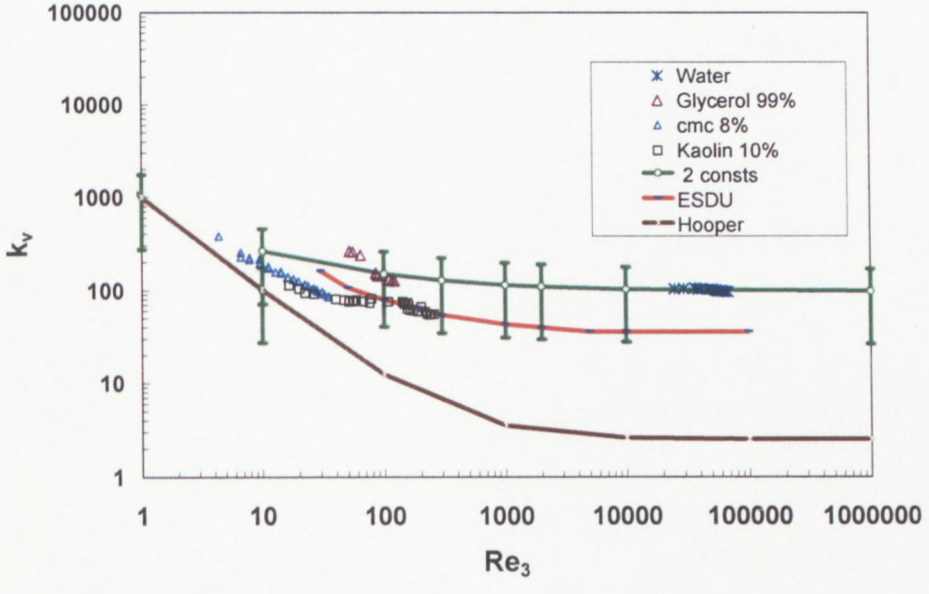

Figure H.9: Comparison of models for 100 mm valve, ¼ open